



<https://theses.gla.ac.uk/>

Theses Digitisation:

<https://www.gla.ac.uk/myglasgow/research/enlighten/theses/digitisation/>

This is a digitised version of the original print thesis.

Copyright and moral rights for this work are retained by the author

A copy can be downloaded for personal non-commercial research or study, without prior permission or charge

This work cannot be reproduced or quoted extensively from without first obtaining permission in writing from the author

The content must not be changed in any way or sold commercially in any format or medium without the formal permission of the author

When referring to this work, full bibliographic details including the author, title, awarding institution and date of the thesis must be given

Enlighten: Theses

<https://theses.gla.ac.uk/>
research-enlighten@glasgow.ac.uk

STRUCTURAL REQUIREMENTS FOR CONFORMATIONAL
CHANGES AND SUBSTRATE BINDING OF
THE HUMAN FACILITATIVE
GLUCOSE TRANSPORTER-GLUT3

A thesis submitted to the
FACULTY OF SCIENCE
for
the degree of
DOCTOR OF PHILOSOPHY

BY

LISA MARIE PORTER

Division of Biochemistry & Molecular Biology
Institute of Biomedical & Life Sciences
University of Glasgow

April 1997

ProQuest Number: 10391272

All rights reserved

INFORMATION TO ALL USERS

The quality of this reproduction is dependent upon the quality of the copy submitted.

In the unlikely event that the author did not send a complete manuscript and there are missing pages, these will be noted. Also, if material had to be removed, a note will indicate the deletion.



ProQuest 10391272

Published by ProQuest LLC (2017). Copyright of the Dissertation is held by the Author.

All rights reserved.

This work is protected against unauthorized copying under Title 17, United States Code
Microform Edition © ProQuest LLC.

ProQuest LLC.
789 East Eisenhower Parkway
P.O. Box 1346
Ann Arbor, MI 48106 – 1346

Abstract

The role of proline residues in transport catalysis mediated by GLUT3 has been investigated using site-directed mutagenesis. PCR methodology was used to construct a series of eight mutant GLUT3 cDNAs in which individual proline residues were replaced with alanine. Heterologous expression of the GLUT3 Pro-Ala mutants in *Xenopus laevis* oocytes was achieved by microinjection of *in vitro* transcribed mRNA and has enabled an extensive analysis of the kinetic properties of these mutants. K_m values for the zero-*trans* influx of 2-deoxy-D-glucose into mutant-injected oocytes have been determined, and compared to the values obtained for wild type GLUT3 expressed in the same system. The effect of each proline substitution on the integrity of the exofacial and endofacial binding sites was investigated by determining K_i values for the inhibition of 2-deoxy-D-glucose zero-*trans* influx by maltose and cytochalasin B, respectively. Although no individual proline residue was observed to be absolutely essential for GLUT3 catalytic activity, mutation of Pro²⁰⁶, Pro³⁸¹, Pro³⁸⁵ and Pro⁴⁵¹ to alanine resulted in an increase in the K_i for maltose. Replacement of prolines at positions 381, 383 and 385, located within putative transmembrane helix 10 of GLUT3, resulted in a reduction in the K_i for cytochalasin B. The small but significant changes observed in the nature of exofacial substrate binding indicate that proline residues are important for transporter function. In addition, the prolines located within helix 10 are important in the conformational changes of the protein.

Measurement of transporter turnover numbers in *Xenopus* oocytes has not previously been possible due to the lack of an accurate and reproducible method for the isolation of a pure plasma membrane fraction. In order to further characterise the kinetics of the Pro-Ala mutants, a protocol was designed, based on a number of previous attempted methods, for the isolation of a clean plasma membrane fraction from *Xenopus* oocytes. Results from dot blot and Western blot analysis of plasma membrane fractions isolated from GLUT3-expressing oocytes, indicated that the preparation of a plasma membrane fraction free from other cellular contaminants was extremely problematic, despite various attempts at optimisation. This was attributed to the abundance of glutinous yolk protein and to the extremely fragile nature of the plasma membrane of the oocyte. Consequently, it was

concluded that this methodology was not suitable for the accurate quantitation of cell surface transporters and the subsequent determination of turnover numbers in this system.

To address the problem of quantitation of cell surface transporters, stable expression of GLUT transporters in a mammalian cell-culture line was investigated as an alternative to expression in oocytes. Simple and reproducible subcellular fractionation procedures are available for this cell line which would enable measurement of transporter turnover numbers. Additionally, this system is more convenient for use in photolabelling studies using ATB-BMPA and cytochalasin B, since large amounts of plasma membranes from cultured mammalian cells can be easily obtained without the need for repeated mRNA injections.

Acknowledgements

I would like to acknowledge the following people, all of whom have contributed to this **delightful** experience in their own unique way.

Special thanks to Gwyn, my supervisor, for giving me the opportunity to come to Glasgow in the first place, and for his much appreciated patience, encouragement and guidance. I can only say that I am truly sorry for attenuating the bald patch, but Susie started it!

I extend my thanks to: all the oocytes Mikey, Fiona, Margaret and Susie, for providing me with endless frog eggs and for generating such stimulating conversation which helped to while away all those weary hours!; Others members of Lab C36, past and present, for providing such a great atmosphere in which to work in....well most of the time anyway! The Fo and The Grandma whose manic expressions helped me to believe.....well, I'm lost for words there really!; and to all the proof-readers who helped me to put this thesis together.

Special thanks to my not-so-practically-dead mate...Susie, for *endless* chat, be(e)er and crisps, for discovering my rather embarrassing spoon-playing ability, and for helping me out in so many ways; to Colin, Di and especially to Jo (my most favourite flat mate!) who provided some of the more entertaining out-of-work moments of this PhD; to the hardcore T-in-the-Parkers, Ali-B and especially Tommywhat can I say guys? I'm not sure words can describe those experiences or that the rest of the world should hear about them either! However, your taste in music is awful....!!

Finally I would like to acknowledge my Mom (and her intoxicating cake mix), Patrick, John, Sharon and the Sprogg-Danielle, Roman & Tereja, Aunty Chris and Nan F for their continuous belief, support and encouragement throughout all the studious years.

I dedicate this Thesis to you all....CHEERS!

Abbreviations

Ac	Acetate
Amp	Ampicillin
ASA-BMPA	2- <i>N</i> -(4-azidosalicyl)-1,3-bis(D-mannos-4-xyloxy)propyl-2-amine
ATB-BMPA	2- <i>N</i> -[4-azi-2,2,2-trifluoroethyl)benzoyl]-1,3-bis(D-mannos-4-xyloxy)-2-propylamine
ATP	adenosine 5'-triphosphate
BGH	bovine growth hormone
BMPA	1,3-bis(D-mannos-4-xyloxy)-2-propylamine
bps	base pairs
BSA	bovine serum albumin
C-1	carbon position number 1
cDNA	complementary deoxyribonucleic acid
CD	circular dichroism
CIP	calf intestinal alkaline phosphatase
CMV	cytomegalovirus
cpm	counts per minute
CTP	cytidine 5'-triphosphate
DeGlc	deoxyglucose
DFP	Diisopropylfluorophosphate
DMSO	dimethyl sulfoxide
DNA	deoxyribonucleic acid
dsDNA	double-stranded deoxyribonucleic acid
dNTPs	deoxyribonucleic nucleoside 5'-triphosphate
dTTP	deoxyribonucleic thymidine 5'-triphosphate
DIT	dithiothreitol
ECL	enhanced chemiluminescence
EDTA	Diaminoethanetetra-acetic acid, disodium salt
FDNB	1-fluoro-2,4-dinitrobenzene
FTIR	fourier-transform infra-red

g_{av}	average gravitational force
GLUT	glucose transporter
GTP	guanosine 5'-triphosphate
HB	homogenisation buffer
HEPES	<i>N</i> -2-hydroxyethylpiperazine- <i>N'</i> -2-ethane sulphonic acid
IAPS-forskolin	iodo-4-azidophenylethylamido-7- <i>O</i> -succinyldeacetyl forskolin
IgG	Immunoglobulin gamma
IR	infra-red
K_{cat}	turnover number per unit time
K_i	inhibitory affinity constant
K_m	affinity constant
KRP	Krebs ringer phosphate
LB	Luria-Bertani
min	minutes
MOPS	3'-(<i>N</i> -morpholino)propanesulphonic acid
mRNA	messenger ribonucleic acid
NHS-biotin	<i>N</i> -hydroxysuccinimidobiotin
NHS-LC-biotin	sulfosuccinimidyl 6-(biotinamido) hexanoate
NIDDM	non-insulin-dependent diabetes mellitus
NMR	nuclear magnetic resonance
OD	optical density
PBS	phosphate buffered saline
pCMBS	<i>p</i> -chloro-mercuribenzenesulphonate
PCR	polymerase chain reaction
PEG	polyethylene glycol
PEP	phospho-enol-pyruvate
RNA	ribonucleic acid
RNase A	ribonuclease A
rNTPs	ribonucleoside 5'-triphosphates
rpm	revolutions per minute
sec	seconds

SD	standard deviation
SDS-PAGE	sodium dodecyl sulphate polyacrylamide gel electrophoresis
SGLT1	sodium-glucose-linked transporter 1
ssDNA	single-stranded deoxyribonucleic acid
STE	saline-Tris-EDTA
sulfo-NHS-biotin	sulfosuccinimidobiotin
SV40	simian virus 40
TACS	terminator ammonium cycle sequencing
TAE	Tris-acetate-EDTA
TBE	Tris-borate-EDTA
TE	Tris-EDTA
TEMED	<i>N,N,N',N'</i> -tetramethylenediamine
TMH	transmembrane helix
Tris	tris(hydroxymethyl)aminoethane
rUTP	uridine 5'-triphosphate
UTR	untranslated region
V_{\max}	theoretical maximum velocity
v/v	volume/volume ratio
w/v	weight/volume ratio

Contents

	Page
Title	i
Abstract	ii
Aknowledgements	iv
Abbreviations	v
Contents	viii
List of Figures	xxi
List of Tables	xxv

Chapter 1. Introduction.

1.1	General Background.	2
1.2	Tissue-Specific Distribution of the Facilitative Glucose Transporters.	5
1.2.1	Introduction.	5
1.2.2	GLUT1.	5
1.2.3	GLUT2.	7
1.2.4	GLUT3.	9
1.2.5	GLUT4.	11
1.2.6	GLUT5.	12
1.2.7	GLUT6.	14
1.2.8	GLUT7.	14
1.3	Homologous Transporters in Other Organisms.	15
1.4	Structure of Mammalian Facilitative Glucose Transporters.	17
1.4.1	Introduction.	17
1.4.2	Sequence Alignments and General Topology.	17

1.4.3	Spectroscopic Techniques.	20
1.5	Dynamics of Glucose Transport.	22
1.5.1	Introduction.	22
1.5.2	Transport Studies.	22
1.5.2a	Zero- <i>trans</i> Entry.	23
1.5.2b	Zero- <i>trans</i> Exit.	23
1.5.2c	Equilibrium Exchange.	23
1.5.2d	Kinetic Properties of GLUT1.	24
1.5.3	Models for the Mechanism of D-Glucose Transport.	25
1.5.3a	Introduction.	25
1.5.3b	The Single Site Alternating Conformer Model.	25
1.5.3c	Measurement of Individual Kinetic Parameters Governing Transport.	26
1.5.3d	Multiple Site Models.	28
1.6	Conformational Changes.	29
1.6.1	Introduction.	29
1.6.2	Detection of GLUT1 Conformational Changes by Intrinsic Fluorescence.	30
1.6.3	Sensitivity of Transporter Conformations to Chemical Inactivation.	31
1.6.4	Susceptibility of GLUT1 Conformational States to Proteolysis.	32
1.7	Location of the Substrate-Binding Site(s).	34
1.7.1	Introduction.	34
1.7.2	Affinity Labelling at the Endofacial D-Glucose Binding Site.	34
1.7.3	Affinity Labelling at the Exofacial D-Glucose Binding Site.	36
1.7.4	Role of the N- and C-Terminal Domains in Formation of the Exo- and Endofacial Substrate Binding Sites.	37
1.7.4a	Contribution of the C-Terminus to Substrate Binding.	38

1.7.4b	Contribution of the N-Terminus to Substrate Binding.	40
1.8	Mutagenesis.	41
1.9	Tertiary Structure of GLUT1.	41
1.10	Oligomerisation of GLUT1.	43
1.11	Aims of this Study.	45

Chapter 2. Materials and Methods.

1 - Molecular Biology and Use of *Xenopus laevis* Oocytes.

2.1	Materials.	65
2.2	Recombinant Polymerase Chain Reaction.	67
2.2.1a	Synthesis of Oligonucleotides.	67
2.2.1b	Precipitation of Oligonucleotides.	67
2.2.1c	Quantitation of Oligonucleotides.	68
2.2.2	Primary Polymerase Chain Reactions Using <i>Taq</i> DNA Polymerase.	68
2.2.2a	Reaction Conditions.	68
2.2.2b	Thermal Cycling.	69
2.2.3	Secondary Polymerase Chain Reactions Using <i>Taq</i> DNA Polymerase.	70
2.2.3a	Reaction Conditions.	70
2.2.3b	Thermal Cycling.	71
2.2.4	Primary Polymerase Chain Reactions Using <i>Pfu</i> DNA Polymerase.	72
2.2.4a	Reaction Conditions.	72

2.2.4b	Thermal Cycling.	72
2.2.5	Secondary Polymerase Chain Reactions Using <i>Pfu</i> DNA Polymerase.	74
2.2.5a	Reaction Conditions.	74
2.2.5b	Thermal Cycling.	74
2.2.6	Purification of PCR Fragments.	75
2.2.6a	Separation of PCR Fragments by Agarose Gel Electrophoresis.	75
2.2.6b	Elution of DNA Fragments from Agarose Gel Slices by Electrophoresis.	75
2.2.6c	Preparation of Dialysis Tubing for Electroelution.	75
2.2.6d	Purification of DNA Using Elutip-D Affinity Columns.	76
2.3	General Techniques Used for Manipulation of cDNA.	76
2.3.1	Plasmid Constructs.	76
2.3.2	Agarose Gel Electrophoresis.	77
2.3.3	Alcohol Precipitation of DNA	78
2.3.4	Restriction Digestion of DNA.	78
2.3.5	Dephosphorylation of Double Stranded DNA using Calf Intestinal Phosphatase (CIP).	79
2.3.6	Ligation of Double-Stranded cDNA.	79
2.3.7	Preparation of Competent <i>E.coli</i> (JM109) Cells.	79
2.3.8	Transformation of Competent <i>E.coli</i> (JM109) Cells.	80
2.3.9	Transformation of Ultracompetent <i>E.coli</i> (JM109) Cells.	80
2.3.10	Preparation of Small Quantities of Plasmid DNA	81
2.3.11	Restriction Digestion Analysis of Small-Scale Plasmid cDNA Preparations.	81
2.3.12	Large Scale Preparation of Plasmid DNA using QIAGEN QIAprep Plasmid Maxi Preparation Kits.	82
2.3.13	Large Scale Preparation of Plasmid cDNA.	84
2.3.14	Calculation of Plasmid DNA Concentration and Purity.	85

2.4	<i>Taq</i> DyeDeoxy™ Terminator Cycle Sequencing Protocol.	86
2.4.1a	Kit Reagents.	86
2.4.1b	Other Reagents.	86
2.4.2	Preparation of Templates and Sequencing Reactions.	87
2.4.3	Thermal Cycling.	88
2.4.4	Acrylamide Gel Preparation.	88
2.4.4a	Preparing the Gel Plates.	88
2.4.4b	Casting the Gel.	89
2.4.5	Setting Up for a Sequencing Run.	89
2.4.6	Sample Extraction and Precipitation.	90
2.4.7	Preparing and Loading Samples.	90
2.4.8	Analysis of Samples.	90
2.5	<i>In vitro</i> synthesis of mRNAs from Plasmid cDNA.	91
2.6	Use of <i>Xenopus laevis</i> Oocytes for Heterologous Expression of GLUT Constructs.	92
2.6.1	Housing of <i>Xenopus laevis</i> .	92
2.6.2	Chemical Anaesthesia.	93
2.6.3	Surgery.	93
2.6.4	Oocyte Isolation and Injection.	93
2.7	Sugar Transport in <i>Xenopus</i> Oocytes.	95
2.7.1	Transport Assay Conditions.	95
2.7.2	Collagenase Treatment of Oocytes.	96
2.8	Subcellular Fractionation of <i>Xenopus laevis</i> Oocytes.	105
2.8.1	Oocyte Isolation and Injection.	105
2.8.2	Transport Assays.	105
2.8.3	Subcellular Fractionation of Oocytes - Method 1.	105

2.8.3a	Reagents.	106
2.8.3b	Biotinylation of Intact Oocytes.	106
2.8.3c	Fractionation of Oocytes	106
2.8.3d	Lowry Protein Determination Microassay.	107
2.8.3e	Detection and Quantitation of Plasma Membranes Using ^{125}I -Streptavidin.	108
2.8.4	Subcellular Fractionation of Oocytes - Method 2.	108
2.8.4a	Reagents.	109
2.8.4b	Biotinylation of Intact Oocytes.	109
2.8.4c	Fractionation of Oocytes.	109
2.8.4d	Protein Concentration Determination Using the Quantigold Assay.	110
2.8.4e	Detection of GLUT3 Transporters by Immunoprecipitation.	110
2.8.5	Assessment of the Relative Enrichment of Oocyte Fractions.	111
2.8.5a	Reagents.	111
2.8.5b	$5'$ Nucleotidase Assays.	111

2 - Cell Culture.

2.9	Cell Culture Materials.	112
2.10	Growth and Storage Media.	112
2.10.1	Chinese Hamster Ovary (CHO-) Cell Growth Media.	112
2.10.2	Freeze media.	113
2.11	Long Term Storage of Cells.	113
2.11.1	Preparation of Cells for Frozen Stocks.	113
2.11.2	Resurrection of Frozen Cell Stocks from Liquid Nitrogen.	113
2.12	Trypsinisation of Cells.	114

2.13	Transfection of CHO-Cells Using Calcium Phosphate.	114
2.13.1	Preparation of Cells for Transfection.	114
2.13.2	Transfection and Selection Protocol.	114
2.13.3	Isolation and Propagation of Individual Clones.	115
2.14	Identification of GLUT-Transfected Clones.	115
2.14.1	Preparation of CHO-Cells for Western Blotting.	115
2.15	Measurement of [^3H]2-Deoxy-D-Glucose Uptake by CHO-Cells.	116
2.15.1	Reagents.	116
2.15.2	Preparation of Cells for Transport Assays.	116
2.15.3	Transport Assays.	116

3 - Western Blotting and Immunodetection of Proteins.

2.16	Materials.	117
2.17	Immunodetection of GLUT2 and GLUT3 Proteins.	117
2.17.1	SDS/Polyacrylamide Gel Electrophoresis (SDS /PAGE).	117
2.17.2	Western Blotting of Proteins.	118
2.17.3	Blocking of Nitrocellulose Membranes and Probing with Anti-GLUT2 and Anti-GLUT3 Antibodies.	119
2.17.4	Immunodetection of Proteins by Autoradiography.	119
2.17.5	Detection of Immunoprecipitated Proteins using Enhanced Chemiluminescence (ECL).	119

Chapter 3. Construction and Sequencing of Pro-Ala Mutants of the Brain-Type Glucose Transporter-GLUT3.

3.1	Aims	123
-----	------	-----

3.2	Structure-Function Studies of GLUT Isoforms using Mutagenic Techniques.	124
3.2.1	Introduction.	124
3.2.2	Substitution of Conserved Polar Residues.	125
3.2.3	Substitution of Conserved Tryptophan Residues.	128
3.2.4	Substitution of Proline Residues.	130
3.2.5	Mutation of Cysteine Residues of GLUT1.	131
3.2.6	Point Mutations in the N-Terminus.	132
3.2.7	Substitution of Extramembraneous Residues.	133
3.2.8	Generation and Characterisation of Chimeric Transporter Proteins.	133
3.3	Role of Transmembrane Proline Residues in Membrane Transport Proteins.	136
3.3.1	Introduction.	136
3.3.2	Characteristics of Proline Residues.	137
3.3.2a	General Properties.	137
3.3.2b	Transmembrane Proline Residues Cause Kinks in Helices.	138
3.3.2c	Accommodation of a <i>Cis</i> -Proline in Transmembrane Helices.	138
3.3.3	Mutation of Proline Residues in the <i>lac</i> Permease of <i>E.coli</i> .	139
3.3.4	Mutation of Proline Residues in the Phosphate-Specific Transporter of <i>E.coli</i> .	140
3.3.5	Role of Transmembrane Proline Residues in Bacteriorhodopsin.	141
3.3.6	Mutation of Proline Residues in GLUT1.	142
3.3.7	Mutation of Proline Residues in GLUT3.	143
3.4	Mutagenesis, Subcloning and Sequencing of GLUT3 cDNAs.	153
3.4.1	Introduction.	153
3.4.2	Vectors.	153
3.4.3	Recombinant Polymerase Chain Reaction.	153
3.4.3a	Primary PCR Reactions.	154

3.4.3b	Secondary PCR Reactions.	154
3.4.3c	Results using <i>Taq</i> DNA Polymerase.	155
3.4.3d	Results using <i>Pfu</i> DNA Polymerase.	156
3.4.4	Sequencing of Subclones.	157
3.5	Discussion.	175
3.6	Summary.	177
 Chapter 4. Functional Studies of Heterologously Expressed Pro-Ala Mutants in <i>Xenopus laevis</i> Oocytes.		
4.1	Aims	179
4.2	Introduction.	180
4.2.1	General Information Regarding GLUT Tertiary Structure.	180
4.2.2	Conclusions from Previously Investigated Proline Residues of GLUT1.	181
4.2.3	Use of Site Specific Ligands as Transport Inhibitors.	182
4.3	Heterologous Expression of Proteins in <i>Xenopus laevis</i> Oocytes.	183
4.3.1	Use of <i>Xenopus laevis</i> Oocytes.	183
4.3.2	Expression of Glucose Transporter Isoforms.	184
4.4	Results.	192
4.4.1	Transport of 2-Deoxy-D-Glucose by GLUT3 Pro-Ala Mutants into <i>Xenopus</i> Oocytes.	192
4.4.2	Determination of K_i Values for Cytochalasin B Inhibition of 2-Deoxy-D-Glucose Zero- <i>trans</i> Uptake.	193
4.4.3	Determination of K_i Values for Maltose Inhibition of 2-Deoxy-D-Glucose Zero- <i>trans</i> Uptake.	194

4.5	Conclusions.	194
4.5.1	Expression of Pro-Ala GLUT3 Mutant Transporters and Their Ability to Transport 2-Deoxy-D-Glucose in <i>Xenopus</i> Oocytes.	194
4.5.2	Kinetics of 2-Deoxy-D-Glucose Transport Mediated by Pro-Ala Mutants and Wild Type GLUT3.	195
4.5.3	Competitive Inhibition of 2-Deoxy-D-Glucose <i>Zero-trans</i> Influx by Maltose.	195
4.5.4	Non-Competitive Inhibition of 2-Deoxy-D-Glucose <i>Zero-Trans</i> Influx by Cytochalasin B.	196
4.6	Discussion.	222
4.6.1	Location of GLUT3 Proline Residues and Mutation to Alanine.	222
4.6.2	Proline Residues and GLUT3 Function.	223
4.6.3	Effects of Pro-Ala Mutations Mediated at the Exofacial Binding Site.	224
4.6.4	Effects of Pro-Ala Mutations Mediated at the Endofacial Binding Site.	227
4.6.5	Problems with this Study.	228
4.7	Summary.	237
Chapter 5	Isolation of Plasma Membrane Fractions from <i>Xenopus</i> Oocytes.	
5.1	Aims.	240
5.2	Introduction.	241
5.2.1	Use of <i>Xenopus</i> Oocytes for Kinetic Studies.	241
5.2.2	Measurement of Turnover Numbers.	241
5.3	Subcellular Fractionation of <i>Xenopus</i> Oocytes.	243

5.4	Methods.	244
5.4.1	Cell Surface Labelling of Oocytes by Biotinylation.	244
5.4.2	Subcellular Fractionation Procedures.	244
5.4.3	Dot Blot Analysis.	245
5.4.4	Quantitative Immunoblotting.	245
5.4.5	Plasma Membrane Marker Assay.	245
5.5	Results.	248
5.5.1	2-Deoxy-D-Glucose Zero- <i>trans</i> Influx Mediated by GLUT3 Expressing Oocytes.	248
5.5.2	Surface Labelling and Fractionation of Oocytes.	248
5.5.3	Activity of Plasma Membrane 5'Nucleotidase in <i>Xenopus</i> Oocyte Fractions.	250
5.5.4	¹²⁵ I-Dot Blot Analysis of Oocyte Fractions.	250
5.5.5	Western Blot Analysis of Oocyte Fractions.	250
5.6	Discussion.	264
 Chapter 6 Construction of GLUT2/GLUT3 Chimeric Glucose Transporters.		
6.1	Aims.	267
6.2	Introduction.	268
6.2.1	Regions Involved in Substrate Selectivity.	269
6.2.2	Expression and Characterisation of GLUT2/GLUT3 Chimeras.	270
6.3	Methodology Used to Generate GLUT2/GLUT3 Chimeric Transporters.	275
6.3.1	Recombinant PCR Reactions.	275
6.3.2	Cloning Procedures.	276

6.3.3	Expression of GLUT2/GLUT3 Chimeras in <i>Xenopus</i> Oocytes.	277
6.4	Results.	283
6.4.1	PCR Using Vent Polymerase.	283
6.4.2	Subcloning of Chimeric Constructs.	283
6.4.3	<i>In Vitro</i> Synthesis of mRNA from G2(7St) and G2(10Ed) Constructs.	284
6.4.4	Measurement of 2-Deoxy-D-Glucose Zero- <i>Trans</i> Influx Mediated by G2(7St) and G2(10Ed) Expressing Oocytes.	284
6.5	Discussion.	293
Chapter 7	Expression of GLUT2 and GLUT3 in CHO-Cells.	
7.1	Aims	297
7.2	Introduction.	298
7.2.1	Heterologous Expression of Proteins in Mammalian Cell-Culture Lines.	298
7.2.2	Further Characterisation of GLUT3 Pro-Ala Mutants and the GLUT3 Series Chimeras in CHO-Cells.	298
7.3	Methods.	300
7.3.1	Expression Vectors.	300
7.3.2	Subcloning of GLUT3/GLUT2 Chimeras for Expression In CHO-Cells.	300
7.3.3	Transfection of CHO-Cells and Selection of Stable Transfectants.	301
7.3.4	Western Blotting and Immunodetection of GLUT2 and GLUT3.	301
7.3.5	Functional Studies in CHO-Cells.	302
7.4	Results.	309

7.4.1	Restriction Digestion Analysis of pcDNA3-G3/G2 Constructs.	309
7.4.2	Immunoblotting of Lysates Prepared from GLUT2-Transfected CHO-Cells.	309
7.4.3	Immunoblotting of Lysates Prepared from GLUT3-Transfected CHO-Cells.	309
7.4.4	Immunoblotting of Lysates Prepared from GT3/GT2-Transfected CHO-Cells.	310
7.4.5	Transport Measurements in Transfected and Non-Transfected CHO-Cells.	310
7.5	Discussion.	321
Chapter 8. Discussion.		323
References.		329

List of Figures

Figure 1.1	Interaction of β -D-glucose at the Exofacial Binding Site of GLUT1.	48
Figure 1.2	Topological Model of the Mammalian Facilitative Glucose Transporters.	50
Figure 1.3	Single-Site Alternating Conformation Model for GLUT1-Mediated D-Glucose Influx.	52
Figure 1.4	King-Altman Representation of the Glucose Transport Cycle.	54
Figure 1.5	Structures of Cytochalasin B and ATB-BMPA.	56
Figure 1.6	Diagram Showing Regions of Importance in the Transporter Structure.	58
Figure 1.7	Speculative Model for the Arrangement of Transmembrane α -Helices in GLUT1.	60
Figure 1.8	Diagram Showing the Proposed Model for GLUT1 Oligomerisation.	62
Figure 2.1	Diagram of a GLUT cDNA Cloned Into the pSP64T Vector.	100
Figure 2.2	1% Agarose Gel Showing the Restriction Digestion Analysis of GLUT3 Pro-Ala Mutant cDNAs.	102
Figure 2.3	1% Agarose Gel of <i>In Vitro</i> Synthesised mRNA.	104
Figure 3.1	Structure and Isomerisation of a Xaa-Pro Peptide Bond.	146
Figure 3.2	Comparison of Amino Acid Sequences in Putative Transmembrane Helices 6, 10 and 12 of the Human and Rat Facilitative Glucose Transporters.	148
Figure 3.3	Location of Proline Residues Targeted for Mutagenesis.	150
Figure 3.4	Diagrammatic Representation of pSPGT3 Showing the Binding Positions of the PCR Primers.	159
Figure 3.5	Generation of GLUT3 Pro-Ala Mutant cDNAs by Recombinant PCR Reactions.	163

Figure 3.6	1% Agarose Gel of PCR Products and Vectors Used for Cloning of GLUT3 Pro-Ala Mutants.	165
Figure 3.7	Subcloning of Secondary PCR Products into pSPGT3.	167
Figure 3.8	Diagram of the Binding Positions of Sequencing Oligonucleotides in the GLUT3 cDNA.	170
Figure 3.9	ABI Trace of GLUT3 Sequence Showing the Pro ³⁸¹ Ala Mutation.	172
Figure 3.10	ABI Trace of Wild Type GLUT3 Sequence in the Region of Pro ³⁸¹ .	174
Figure 4.1	Models of the Interaction of β -D-Glucose with GLUTs 1 and 3.	188
Figure 4.2	Structure of β -D-Glucose and β -D-Maltose.	190
Figure 4.3	Lineweaver-Burk Plot of 2-Deoxy-D-Glucose Transport by GLUT3 Injected Oocytes.	199
Figure 4.4	Lineweaver-Burk Plot of 2-Deoxy-D-Glucose Transport by P451A Injected Oocytes.	201
Figure 4.5	Lineweaver-Burk Plot of 2-Deoxy-D-Glucose Transport by P206A Injected Oocytes in the Presence and Absence of Cytochalasin B.	203
Figure 4.6	Lineweaver-Burk Plot of 2-Deoxy-D-Glucose Transport by P381A Injected Oocytes in the Presence and Absence of Cytochalasin B.	205
Figure 4.7	Lineweaver-Burk Plot of 2-Deoxy-D-Glucose Transport by P383A Injected Oocytes in the Presence and Absence of Cytochalasin B.	207
Figure 4.8	Lineweaver-Burk Plot of 2-Deoxy-D-Glucose Transport by P385A Injected Oocytes in the Presence and Absence of Cytochalasin B.	209
Figure 4.9	Lineweaver-Burk Plot of 2-Deoxy-D-Glucose Transport by GLUT3 Injected Oocytes in the Presence and Absence of Maltose.	211
Figure 4.10	Lineweaver-Burk Plot of 2-Deoxy-D-Glucose Transport by P206A Injected Oocytes in the Presence and Absence of Maltose.	213

Figure 4.11	Lineweaver-Burk Plot of 2-Deoxy-D-Glucose Transport by P381A Injected Oocytes in the Presence and Absence of Maltose.	215
Figure 4.12	Lineweaver-Burk Plot of 2-Deoxy-D-Glucose Transport by P383A Injected Oocytes in the Presence and Absence of Maltose.	217
Figure 4.13	Lineweaver-Burk Plot of 2-Deoxy-D-Glucose Transport by P385A Injected Oocytes in the Presence and Absence of Maltose.	219
Figure 4.14	Lineweaver-Burk Plot of 2-Deoxy-D-Glucose Transport by P451A Injected Oocytes in the Presence and Absence of Maltose.	221
Figure 4.15	King-Altman Diagram Showing the Competition of 2-Deoxy-D-Glucose and Maltose at the Exofacial Binding Site of the Transporter.	232
Figure 4.16	Predicted α -Helical Structure of GLUT3 Transmembrane Helix 12.	234
Figure 4.17	Predicted α -Helical Structure of GLUT3 Transmembrane Helix 10.	236
Figure 5.1	Reaction of NHS-Biotin and Sulfo-NHS-Biotin with Protein Amines.	247
Figure 5.2	Measurement of the 5'Nucleotidase Activity of Oocyte Fractions.	254
Figure 5.3	5'Nucleotidase Activities in Oocyte Membrane Fractions.	256
Figure 5.4	Specific Recovery of ^{125}I -Streptavidin Associated With Oocyte Fractions.	258
Figure 5.5	Recovery of ^{125}I -labelled Biotinylated Plasma Membranes from Oocytes.	260
Figure 5.6	Western Blot Analysis of Oocyte Fractions Expressing GLUT3.	263
Figure 6.1	Junction Points of the GLUT2/GLUT3 Chimeric Transporters.	273
Figure 6.2	Generation of GLUT2/GLUT3 Chimeras Using Recombinant PCR Reactions.	280
Figure 6.3	Restriction Digestion of pSPGT4 with <i>Sal</i> I and Cloning of GLUT2/GLUT3 Chimeric cDNAs.	282

Figure 6.4	GLUT2/GLUT3 PCR Products Generated Using Vent DNA Polymerase.	286
Figure 6.5	Restriction Digestion Analysis of GLUT2/GLUT3 Constructs.	288
Figure 6.6	1% Agarose Gel of <i>In Vitro</i> Synthesised mRNA.	290
Figure 6.7	Measurement of 2-Deoxy-D-Glucose Uptake by Oocytes Expressing GLUT2, GLUT3, G2(7St) and G2(10Ed).	292
Figure 7.1	Schematic Representation of pLK444 Containing the Human GLUT2 cDNA.	304
Figure 7.2	Schematic Representation of pCMV-4 Containing the Human GLUT3 cDNA.	306
Figure 7.3	Schematic Representation of pcDNA3.	308
Figure 7.4	Subcloning of the GLUT3 Series of Chimeras into pcDNA3.	312
Figure 7.5	Restriction Digestion Analysis of pcDNA3-G3/G2 Constructs.	314
Figure 7.6	Immunological Detection of GLUT2 and G3(7St) in Lysates Prepared from CHO-Cells Individually Transfected with GLUT2 and G3(7St).	316
Figure 7.7	Measurement of 2-Deoxy-D-Glucose Transport in GLUT3-Transfected CHO-Cells.	318
Figure 7.8	Measurement of 2-Deoxy-D-Glucose and D-Fructose Transport in GLUT2-Transfected CHO-Cells.	320

List of Tables

Table 1.1	Conserved Motifs Present in the Mammalian Facultative Glucose Transporters.	63
Table 2.1	Solutions and Buffers Used for DNA Manipulation.	97
Table 2.2	Table of Buffers.	98
Table 2.3	SDS-PAGE and Western Blotting Buffers.	121
Table 3.1	Distribution of Proline Residues in Human GLUTs 1-5 and Rat GLUT7.	151
Table 3.2	Summary of the Distribution of Proline Residues in Human GLUTs 1-5 and Rat GLUT7.	152
Table 3.3	Mutagenesis Oligonucleotides.	160-161
Table 3.4	Sequencing Oligonucleotides.	168
Table 4.1	Summary of the Kinetic Data Available for Human GLUT1 Proline Mutants.	186
Table 4.2	Kinetic Parameters of the Glucose Transporter Isoforms Expressed in Oocytes.	191
Table 4.3	Kinetic Parameters of GLUT3 Wild-Type and Pro-Ala Mutants Expressed in <i>Xenopus</i> Oocytes.	197
Table 5.1	Protein Yields of Oocyte Fractions.	252
Table 5.2	Data obtained from a Typical Dot Blot Analysis.	261
Table 6.1	Kinetic Parameters for Transport of Substrates by GLUT2/GLUT3 Chimeras.	274
Table 6.2	Sequences of Oligonucleotide Primers Used to Generate GLUT2/GLUT3 Chimeric Transporters.	278

CHAPTER 1

Introduction

1.1 General Background.

Glucose is possibly the most abundant biological molecule on earth. It is a basic source of energy and, together with other sugars, it represents a very important nutrient for many cells types, not only in mammals and other higher organisms, but also in microbes. Glucose metabolism in mammalian cells provides ATP under both aerobic and anaerobic conditions. Its importance as a cellular metabolite is exemplified in certain tissues such as brain which is almost entirely dependent upon glucose as an energy source. A variety of mechanisms have naturally evolved to enable cells to selectively catalyse the movement of molecules and ions, including glucose, across their plasma membrane (reviewed in Carruthers, 1991).

Mammalian cell plasma membranes possess two general mechanisms by which glucose can enter the cell. The first is a protein mediated event which is not coupled to an energy requiring component such as ATP hydrolysis or a H^+ gradient. Transport is driven only by the concentration gradient and can be bidirectional. It is therefore referred to as facilitative diffusion and is possible due to the maintenance of a relatively constant high physiological blood glucose concentration of 5-10mM which is achieved by complex homeostatic mechanisms. A second distinctive transport mechanism exists in those cells that require movement of glucose against its concentration gradient, for example the transepithelial cells of the kidney and small intestine. Here transport is mediated by the Na^+ /glucose cotransporter that utilizes a Na^+ gradient to couple the transport of glucose against its concentration gradient. Active transporters are also found in many bacterial systems which may need to take up sugars that are present at very low concentrations. Like their mammalian counterparts, these active sugar transporters are symport or antiport systems that exploit the electrochemical gradient of H^+ or Na^+ across the membrane.

In 1952, Widdas, investigating the nature of glucose transport in human erythrocytes and sheep placenta, demonstrated that the mechanism conformed to simple Michaelis-Menton kinetics (Widdas, 1952). This important discovery suggested that the catalytic properties of the glucose transport system were comparable to those of enzyme-mediated reactions in which the transporter acts as an enzyme and D-glucose acts as the substrate at

the exofacial side of the membrane and the product at the endofacial side (or vice versa). Saturation of the transport system can occur indicating that the erythrocyte contains a finite number of transport sites. A further observation stemming from this study was that different tissues displayed distinct kinetics of sugar uptake, alluding to the possibility that tissue specific transporter isoforms may exist.

The first evidence locating the glucose transport system to the erythrocyte plasma membrane was provided by Jung in 1971. Bilayers formed from purified erythrocyte lipids were demonstrated to be incapable of catalysing glucose transport, whereas lipid membranes made from crude total lipid extracts (erythrocyte ghosts, largely devoid of intracellular material) were approximately 100 times more permeable to glucose, possibly due to protein contaminants present in the crude lipid preparation (Jung, 1971). In addition to confirming the location of the transport system, this study also provided evidence that the movement of glucose across membranes was facilitated by a protein moiety. Further evidence in support of this view came from the demonstration that glucose transport could be inhibited by very low concentrations of cytochalasin B and phloretin. These compounds act at the intracellular and extracellular moieties of the transport system respectively to inhibit transport with apparent K_i values of ~ 140 and 200nM (Bloch, 1973, LeFevre, 1961, Zoccoli *et al.*, 1978).

Due to the easy availability of red blood cells and the fact that they are replete with glucose transporters, constituting approximately 5% of the total membrane protein (Allard & Lienhard, 1985), much of the early work to determine the structural requirements and kinetics of glucose binding to its carrier protein were carried out using the erythrocyte system. Several studies from the early 1970's predicted that D-glucose binds to its carrier via hydrogen bonding. Inhibition of the stereospecific uptake of D-glucose by various derivatives identified the pyranose ring oxygen and the hydroxyl groups at the C1, C3 and C4 positions of D-glucose to be important in the formation of hydrogen bonds between glucose and the transporter protein (Barnett *et al.*, 1973, Kahlenberg & Dolansky, 1972). Based on these studies a model was proposed for the formation of a glucose-carrier complex in human erythrocytes (Figure 1.1).

Purification of the erythrocyte transporter protein was achieved independently by two research groups. The first group used reconstitution of D-glucose transport activity as an

assay to identify an active protein extracted from detergent solubilised erythrocyte membranes (Kasahara & Hinkle, 1977). The second approach relied upon an assay for the binding of cytochalasin B as a tool for purification (Baldwin *et al.*, 1979). Both methods identified one major protein with an apparent molecular mass of 55kDa as determined by SDS-polyacrylamide gel electrophoresis. Treatment with endoglycosidase F₁ reduced the apparent molecular mass to 46kDa revealing that the protein is heterogeneously glycosylated. Reconstituted purified protein exhibited a dissociation constant for cytochalasin B that was comparable to that of the native protein in erythrocytes and was later found to bind cytochalasin B with a stoichiometry of 1:1 (Baldwin & Lienhard, 1989). When reconstituted into liposomes, the purified transporter exhibited the same kinetic parameters as observed in the native red blood cell system (Wheeler, 1981). Thus, purification of the transporter protein represented a key advance in the characterisation of this important system and subsequently led to the elucidation of partial protein sequence information enabling the generation of specific antibody probes. The use of specific antisera revealed that membranes from a variety of cell types contained similar immunoreactive proteins, consistent with the hypothesis that a number of cell types contain structurally similar, but distinct glucose transporter proteins. This would account for the differences observed in glucose transport capacity between cell types. Availability of antibody probes and partial sequence information led to the isolation of a cDNA clone from human HepG2 hepatoma cells in 1985 ((Mueckler, 1985) and to the subsequent isolation of the gene (Fukumoto *et al.*, 1989, Williams & Birnbaum, 1988). The availability of GLUT1 cDNA clones has led to the rapid identification of homologous isoforms in other mammalian tissues through low-stringency screening of appropriate cDNA libraries. A further six isoforms have been identified, five of which are functional facilitative transporters. They have been named GLUTs 2-7 according to the terminology introduced by Fukumoto and co-workers in 1989, based on the chronological identification of their cDNAs.

1.2 Tissue-specific Distribution of the Facilitative Glucose Transporters.

1.2.1 Introduction.

The specific requirements of different mammalian tissues for glucose is reflected in the complexity of the facilitative glucose transport system. This family of transport proteins constitutes, to date, six structurally related proteins exhibiting different kinetic and biochemical properties with overlapping, but distinct, tissue distributions. Such diversity presumably exists to allow for the precise disposal of glucose under varying physiological conditions and efficient cellular uptake of glucose in the presence of a concentration gradient. Individual tissues may express more than one facilitative glucose transporter isoform and, in some cases, may also express the Na⁺/glucose cotransporter, SGLT1.

1.2.2 GLUT1.

The GLUT1 isoform is commonly referred to as the erythrocyte/brain or HepG2 transporter. This is due to the initial isolation of clones encoding GLUT1 by screening human hepatocellular carcinoma cell line (HepG2) and rat brain cDNA libraries with antibodies generated against the human erythrocyte glucose transporter. Comparison of the predicted amino acid sequence of the HepG2 glucose transporter with partial amino acid sequence obtained for the erythrocyte transporter revealed that these proteins were in fact identical. Isolation of the protein in the early 1980's represented a major advance in the elucidation of the glucose transport mechanism (Baldwin *et al.*, 1981; Baldwin *et al.*, 1982). GLUT1 transporters of humans, rats (Birnbaum, 1989), mice (Kaestner *et al.*, 1989), rabbits (Asano *et al.*, 1988) and pigs (Weiler-Guttler *et al.*, 1989) are all proteins of 492 amino acids in length and are more than 97% identical in sequence.

Kinetic studies of the purified protein in defined lipid environments and also in the native human erythrocyte revealed that GLUT1 has a very broad substrate specificity (reviewed in LeFevre, 1961), transporting a range of hexoses and pentoses. However,

GLUT1 has a very low affinity for the metabolically important ketose, fructose, with a K_m of approximately 1.5M. The implications are that GLUT1 is not the normal route of fructose uptake and that other isoforms mediate its transport (sections 1.2.3 and 1.2.6).

With the purified protein and cDNA leading to the generation of antibody probes, many studies have demonstrated that the GLUT1 protein and its mRNA are widely distributed in many tissue types (Flier *et al.*, 1987a). It is especially abundant in foetal heart, liver and brown fat (Asano *et al.*, 1988, Santalucia *et al.*, 1992). These tissues in adults however, possess only small levels of GLUT1 with highest levels occurring in erythrocytes (Allard & Lienhard, 1985). The K_m for zero-*trans* uptake (section 1.5.2) of D-glucose by GLUT1 at 37°C is approximately 7mM which is close to physiological blood-glucose concentrations. At plasma glucose concentrations of 5mM, the maximum transport capacity is 12,000 times the rate of cellular glucose utilisation. The red blood cells of most foetal animals have a similar transport capacity which is soon lost after birth (Widdas, 1955). The physiological importance of this high transport capacity is unclear. It is possible that the intracellular space of mammalian foetal erythrocytes available for distribution of glucose, facilitates its transfer across the placenta and that this occurs to a lesser extent across the blood-tissues barriers in adult primates (Jacquez, 1984), however, conclusive evidence for this theory is lacking. Interestingly, GLUT1 has been identified in muscle and fat tissue which exhibit acute insulin-stimulated glucose transport (Flier *et al.*, 1987b), however, the predominant transporter expressed in these tissues is GLUT4. Only very low levels were detected in the liver, the other major tissue involved in regulation of whole body glucose homeostasis. Immunocytochemical studies show an abundance of GLUT1 in endothelial and epithelial cells that form the blood-brain and blood-nerve barriers, various blood-eye barriers and the placental syncytiotrophoblast. It may be that the kinetic properties of GLUT1 have evolved to facilitate transendothelial and transepithelial transport.

All cell culture lines exhibit pronounced elevation of GLUT1 protein and mRNA levels upon transformation. Most mitogens result in stimulation of GLUT1 transcription and glucose starvation is reported to stimulate GLUT1 expression. A potential explanation of the cell increasing GLUT1 levels may be related to the kinetic asymmetry of this isoform (Craik & Elliott, 1979, Diamond & Carruthers, 1993) described in section 1.5.2d, and the

observation that asymmetry appears to be allosterically regulated by the binding of intracellular metabolites. Intracellular ATP is known to allosterically inhibit GLUT1 function in human erythrocytes and AMP and ADP are competitive inhibitors of ATP inhibition of transport (Diamond & Carruthers, 1993). This may allow GLUT1 to function as a unidirectional transporter when the extracellular glucose concentration is low and the intracellular demand for glucose is high, e.g. glucose starvation of cells in culture.

1.2.3 GLUT2

The liver plays a crucial role in the maintenance of blood glucose homeostasis. Large amounts of glucose are taken up by the liver after feeding for conversion into glycogen stores. These stores are subsequently broken down and glucose is released into the blood. The liver can also form glucose *de novo*. So, the fact that GLUT1 is detected only at very low levels in hepatocytes, in addition to the distinct glucose transport kinetics observed in these cells, led to the proposal that a distinct transporter is expressed in hepatocytes. For example, the reported dissociation constant for cytochalasin B, and the apparent K_m for glucose transport mediated by the liver-type glucose carrier is approximately 10-fold greater than those observed in erythrocytes (Axelrod & Pilch, 1983). Availability of the GLUT1 cDNA enabled its use as a probe to screen cDNA libraries from hepatocytes, among other cell types, under low stringency conditions in order to identify GLUT1-like cDNAs. Two groups independently isolated such a cDNA from human (Thorens, 1988) and rat (Fukumoto *et al.*, 1988) hepatocytes. Analysis of the predicted amino acid sequences revealed high homology to GLUT1. Hydropathy analyses of the predicted sequences gave virtually superimposable plots and therefore, the two isoforms are predicted to adopt a similar topology in the membrane. cDNA clones encoding GLUT2, the liver-type transporter, have been isolated from human, rat and mouse cDNA libraries. The proteins are 522, 523 and 524 amino acid residues in length respectively and share 80% homology. Human GLUT2 has 55% sequence identity to GLUT1. Most of the sequence divergence occurs at the extreme C-terminus and in the extracellular loop connecting putative transmembrane helices 1 and 2. In GLUT2 this loop is 64 amino acids long compared to 32

amino acids in GLUT1, and shares no sequence identity. The only similarity between the two isoforms in this region of the proteins is an *N*-linked glycosylation site. Expression of the liver transporter cDNA in *E.coli* mutants defective in glucose uptake revealed that the encoded protein was incorporated into the bacterial membrane. Glucose uptake was increased as a result and transport was shown to be stereospecific for D-glucose and inhibited by phloretin and Mercury Chloride (Thorens, 1988).

GLUT2 is kinetically quite distinct from GLUT1. It does not appear to bind forskolin (Hellwig & Brown, 1992) and only weakly binds cytochalasin B with a K_d of approximately $1\mu\text{M}$ (Axelrod & Pilch, 1983, Ciaraldi *et al.*, 1986), an order of magnitude higher than the same parameters determined in previous studies of facilitative glucose transport. Equilibrium exchange studies for 3-*O*-methyl-D-glucose reveal that this transporter has a K_m of 42mM when expressed in *Xenopus laevis* oocytes (Gould *et al.*, 1991). This supra-physiological value agrees with the high K_m of 66mM reported previously in oocytes, (Elliott & Craik, 1983), and is significantly higher than the normal blood glucose concentration, and also the value of approximately 7mM reported for zero-*trans* entry by GLUT1 at 37°C in the human erythrocyte. The physiological role of glucose transport in the liver is different from most other tissues as this organ participates in both uptake and release of glucose to maintain normal blood glucose levels. The presence of a high capacity and high K_m transporter in hepatocytes would allow rapid glucose efflux following gluconeogenesis. In addition, GLUT2 is abundant in these cells increasing their transport capacity such that the actual transport process is not the rate-limiting step in either metabolism or supply of glucose to the blood. The fact that transport mediated by this isoform is symmetrical and is characterised by a high K_m will no doubt reflect its specific location to the liver, allowing glucose transport into and out of the hepatocyte to respond linearly to changes in glucose concentration.

There are other sites of high GLUT2 expression including the islets of Langerhans of the pancreas, where expression is exclusive to the β -cells (Orci, 1989, Thorens, 1988), the basolateral surfaces of the kidney and the small intestine epithelia. GLUT2 expression therefore seems to be restricted to tissues involved in net release of glucose during fasting (liver), glucose sensing (β -cells) and transepithelial transport (kidney and small intestine).

Pancreatic β -cells are the site of insulin production, which depends upon the uptake and metabolism of glucose. Glucose concentrations in the range of 5-15mM stimulate insulin secretion. At these concentrations it is the metabolism of glucose by the high K_m enzyme (~6mM) glucokinase rather than the transport of glucose across the plasma membrane that is the rate-limiting step. The high K_m of GLUT2 therefore allows glucokinase to effectively act as a glucose sensor by ensuring that the intracellular glucose concentration changes rapidly in response to the extracellular levels. Carruthers pointed out that the key to rapid equilibration of the cytosol with interstitial sugar is a high capacity of transport rather than a low affinity. A study in 1990 illustrated the importance of GLUT2 expression where glucose-induced insulin secretion occurs, and involved the use of two mouse insulinoma cell lines. One line expresses GLUTs 1 and 2 at high levels whereas the other only expresses GLUT2. Only the later was found to exhibit glucose-induced insulin secretion compared to normal mouse islet cells (Miyazaki *et al.*, 1990).

Glucose transport in the kidney and small intestinal epithelial cells is a two step process. The Na^+ -linked glucose transporter located on the apical side of the small intestine mediates active glucose accumulation against its concentration gradient by cotransporting Na^+ inward down its electrochemical gradient. GLUT2 present at the basolateral surfaces of the transepithelial cells of the intestine and of the proximal tubule of the kidney facilitate its subsequent release into the capillaries, thus playing a specific role in glucose absorption and reabsorption (Hediger *et al.*, 1987). In addition, this isoform is also predicted to mediate the exit of fructose from the basolateral membrane of enterocytes

1.2.4 GLUT3.

Application of the low-stringency hybridisation approach to other tissues as a method for detecting glucose transporter cDNAs resulted in the isolation of a novel cDNA, GLUT3, from a human foetal muscle library (Kayano *et al.*, 1988; Nagamatsu, 1992). Northern blot analysis yielded the rather surprising observation that GLUT3 is barely detectable in human adult skeletal muscle but is abundant in the brain, with lower levels of expression in fat, kidney, liver and muscle. GLUT3 cDNA clones have, to date, been isolated from humans,

monkeys, rabbits, rats and mice - in addition to an avian homologue. In monkeys, rabbits, rats and mice, GLUT3 mRNA is expressed exclusively in the brain (Maher *et al.*, 1992; Nagamatsu, 1992; Yano, 1991) whereas in humans GLUT3 protein can be immunologically detected at highest levels in the brain, with lower levels in the liver, heart, kidney and placenta ((Kayano *et al.*, 1988). It is not, however, detectable in three different muscle groups:- soleus, vastus lateralis and psoas major (Shepherd, 1992a). The lack of any immunological detection of GLUT3 in these tissues does not agree with the levels of mRNA which can be detected by Northern blot analysis. For example, mRNA levels in kidney and placenta are 50% of that detected in brain, but the level of GLUT3 protein in these tissues is much lower. So, there seems to be some disparity between the levels of GLUT3 mRNA and protein. One possible explanation may be the presence of significant neural contamination in the tissue preparations used for the Northern analysis. Alternatively, it is possible that these tissues exhibit negative post-transcriptional regulation of GLUT3.

Human GLUT3 shares 64% and 52% identity with human GLUT1 and GLUT2 respectively, and some 83% amino acid sequence identity with its mouse counterpart. As in the case with GLUT2, the GLUT3 sequence is not as highly conserved among species as the GLUT1 sequence. Portions of the transporter containing the regions of most sequence divergence occur within the large extracellular loop and the intracellular C-terminal domain.

When expressed in *Xenopus* oocytes GLUT3 exhibits a substantially lower K_m (about 10mM) for 3-*O*-methyl-D-glucose exchange transport than GLUT1 (Colville *et al.*, 1993b; Gould *et al.*, 1991). The observation that GLUT3 is expressed at high levels in the brain indicates a requirement for two facilitative glucose transporter isoforms to mediate glucose uptake and disposal across the blood-brain barrier. Since GLUT1 is the major isoform expressed at the blood-nerve and blood-brain barrier, it is likely that GLUT3 mediates glucose uptake into neuronal cells which lie beyond the GLUT1-enriched blood-tissue barriers of the brain and peripheral nerve. Comparison of the kinetic parameters for these two isoforms is compatible for a role for both GLUTs 1 and 3. Under normal conditions in the brain, the capacity of hexokinase for its preferred energy source, glucose, is much greater than the capacity of the glucose transport system and so transport is rate limiting. Under hypoglycaemic conditions, the expression of a low capacity, high affinity

transporter ensures successful utilisation of low blood sugar concentrations. In fact GLUT3 has the lowest K_m for hexoses of all the isoforms of the family. Thus, co-expression of GLUT3 with GLUT1 in the brain allows a high efficiency of glucose transport over the entire physiological range of blood glucose concentrations, with GLUT1 working at maximum capacity at high blood glucose levels, and GLUT3 mediating efficient transport at lower levels.

1.2.5 GLUT4.

The observation that GLUT3 mRNA levels are relatively low in adult muscle, coupled to the realisation that this isoform is not the major protein responsible for glucose uptake by this tissue, led to the exciting possibility of an additional isoform to add to the expanding family of GLUTs. Furthermore, fat and muscle were observed to exhibit insulin-responsive glucose transport properties, thus leading to an extensive effort to identify the insulin-responsive glucose transporter. In 1989, five separate reports of cloning and sequencing of GLUT4 were published (Birnbaum, 1989; Charron *et al.*, 1989; Fukumoto *et al.*, 1989; James *et al.*, 1989; Kaestner *et al.*, 1989). A monoclonal antibody that specifically recognised GLUT4 revealed that this isoform is specific to muscle and adipose tissue (James *et al.*, 1988). mRNA levels were found to be highest in brown and white adipose tissue in addition to cardiac and skeletal muscle, i.e. tissues that are regulated by insulin (James *et al.*, 1989).

The cDNA for human GLUT4 was found to encode a protein of 509 amino acids in length which shared 65%, 54% and 58% identity with human GLUTs 1, 2 and 3 respectively, with 95% and 96% sequence identity between the human and rat or mouse proteins. Major differences in sequence are found at the N-terminal hydrophilic region, which has an additional twelve amino acids compared to GLUT1, the central cytoplasmic loop and the C-terminus.

Studies on rat adipocytes reported a 20- to 30-fold increase in D-glucose uptake upon insulin stimulation, while rat muscle cells exhibited a 7-fold increase (Ploug, 1987). The effect observed in human skeletal muscle cells and human adipocytes in response to insulin

was even lower, with a 2-fold (Dohm *et al.*, 1988) and 2- to 4-fold (Pederson & Gliemann, 1981) increase in glucose uptake. In terms of the kinetics, the increase in transport capacity observed in these cells in response to insulin is a result of an increase in the V_{\max} and not a change in the K_m (Holman *et al.*, 1990; May & Mikulecky, 1982; Simpson & Cushman, 1986; Taylor & Holman, 1981; Whitesell & Gliemann, 1979). There is some speculation as to whether this increase in V_{\max} is a result of intrinsic activation of the transporter protein. However, it is now largely established that the increase in transport capacity is achieved by recruitment of a large number of transporters to the plasma membrane from an intracellular pool in response to insulin. The exact nature of the intracellular pool remains unknown at present. This has been demonstrated to occur in both fat (Cushman & Wardzala, 1980; Suzuki & Kono, 1980) and skeletal muscle (Hirshman *et al.*, 1990; Klip *et al.*, 1987).

Kinetically, GLUT4 differs substantially from GLUT1 in that it appears symmetrical and does not exhibit *trans*-acceleration, (Taylor & Holman, 1981; Whitesell & Gliemann, 1979) described in section 1.5.2d. Under equilibrium exchange conditions for 3-*O*-methyl-D-glucose transport, K_m values of 1.8mM (Keller *et al.*, 1989) and 4.3mM (Nishimura, 1993) have been reported in oocytes, compared to the value of 26.2mM obtained for GLUT1 (Nishimura, 1993). This would indicate that at low substrate concentrations, GLUT4 would be responsible for the majority of glucose uptake in human tissues. Upon insulin stimulation, the number of GLUT4 transporters at the plasma membrane increases resulting in an increase in the transport capacity of the cell.

1.2.6 GLUT5.

The most divergent member of the facilitative glucose transporter family, GLUT5, is a 501 amino acid residue protein that exhibits only 40% sequence identity to GLUT1. This isoform is expressed at high levels in the small intestine, as revealed by Northern blot analysis (Kayano *et al.*, 1990), and studies using human small intestine have shown that the protein is located in the brush-border membrane (Davidson *et al.*, 1992). Obviously, the small intestine is an important site for hexose transport, making a significant contribution to maintaining whole body glucose homeostasis. It is not so surprising, then, to find a

facilitative glucose transporter system located in this important tissue. What is surprising however is the exclusive localisation of GLUT5 to the apical brush border of the luminal side of epithelial cells (Davidson *et al.*, 1992), considering that under normal circumstances glucose transport is mediated by SGLT1, the Na⁺-dependent glucose transporter. The rationale for the presence of a passive transporter in addition to an active transporter is unclear, especially since GLUT5 has been demonstrated to be a relatively poor glucose transporter (Kayano *et al.*, 1990). One possible explanation has been provided by the demonstration that GLUT5 is a high affinity D-fructose transporter. When expressed in *Xenopus* oocytes, GLUT5 transports D-fructose with a K_m of 6mM, i.e. with a much higher affinity than for D-glucose and its analogues (Burant *et al.*, 1992). Therefore its primary role at the luminal surface of the small intestine could be the uptake of dietary fructose. In fact, fructose has been recommended as a substitute for glucose and sucrose in the diets of both diabetic and obese people as it is sweeter, more soluble and less glycogenic. The adaptation of intestinal fructose transport in response to diabetes has been largely neglected with studies mainly concentrating on glucose adaptation. A recent study in rat small intestine was undertaken to address this aspect of diabetes (Corpe *et al.*, 1996). In this study it was concluded that adaptation to diabetes involved significant enhancement in levels of GLUT5 and GLUT2 at their specific sites of expression. Also, the intrinsic activity of GLUT5 was diminished. Thus, the regulation of fructose transport is clearly an important aspect of diabetes.

Northern and immunoblot analyses reveal that GLUT5 is expressed in a range of other human tissues including muscle (all major types), brain, adipose tissue and testis (Burant *et al.*, 1992; Kayano *et al.*, 1990; Shepherd, 1992b). Again, GLUT5 may act to provide these tissues with fructose. It is unknown at present if other fructose transporters exist in addition to GLUT5 and it seems unlikely that this transporter undergoes insulin-stimulated translocation. This is consistent with the lack of insulin-stimulated fructose transport observed in human adipocytes (Shepherd, 1992b).

1.2.7 GLUT6

The extensive application of the homology screening approach to many tissues identified a further transporter-like sequence that appeared to be ubiquitously distributed. Further analysis of the base sequence revealed a high level of identity to GLUT3 (~80%). The cDNA was however found to contain multiple frame shifts and stop codons and so is unlikely to encode a functional transporter. The extent of the sequence identity suggests that the transcript may have arisen by insertion of a reverse-transcribed copy of GLUT3 into a non-coding region of a ubiquitously expressed gene (Kayano *et al.*, 1990).

1.2.8 GLUT7

The most recent member of the GLUT family to be identified is GLUT7 which exhibits 68% amino acid sequence identity to GLUT2. Interestingly these two isoforms are virtually identical throughout the first four transmembrane domains and also in the region of helices 9 and 10. In fact, the GLUT7 sequence is 100% identical to that of GLUT2 at three locations. These regions do not coincide with the intron/exon boundaries ((Bell *et al.*, 1990)) and so it is unlikely that GLUT7 is a splice variant of GLUT2. One important difference in the sequences of GLUTs 2 and 7 is the presence of an additional six amino acids at the C-terminus of GLUT7. This sequence contains a consensus motif, (KKMKND) for the retention of transmembrane proteins in the endoplasmic reticulum (ER). GLUT7 is a 528 amino acid residue protein that, so far, has only been cloned from the rat (Waddell, 1992). Western blotting experiments show that it is located in the microsomal fraction of the rat liver, unlike GLUT2 which is located at the plasma membrane (Waddell *et al.*, 1991). In fact, GLUT7 is localised to the endoplasmic reticulum hence the presence of the ER targeting motif.

In mammals, the regulation of blood glucose levels is achieved by balancing the rate of glucose uptake by all tissues with the rate of release of glucose produced from gluconeogenesis and glycogenolysis in the liver. As already mentioned, GLUT2 plays an important role in mediating both efflux and influx of glucose across the hepatocyte plasma

membrane. The terminal step in glucose production by gluconeogenesis and glycogenolysis is the removal of the phosphate group from glucose-6-phosphate. This reaction is catalysed by glucose-6-phosphatase, a multi-enzyme complex located in the lumen of the endoplasmic reticulum. In order for glucose to be exported from the liver it must first cross the membrane of the endoplasmic reticulum before being transported across the hepatocyte plasma membrane by GLUT2. Thus, it has been proposed that GLUT7 mediates the initial transport stage and therefore works in conjunction with GLUT2 to achieve hepatic release of glucose (Waddell, 1992).

However, given that there is a surprising lack of base drift in the third position of the codons over the GLUT2 and GLUT7 sequences, the existence of GLUT7 as a separate isoform awaits confirmation from other sources.

1.3 Homologous Transporters in Other Organisms.

For many years, little information was available regarding the primary structure of integral membrane proteins that transport small molecules such as sugars, ions and antibiotics across the cell membrane. These proteins are difficult to study because of their low abundance and hydrophobic nature. The advent of recombinant DNA technology enabled the cloning and sequencing of many genes encoding membrane transport proteins thus facilitating their study. From the DNA sequence, the order of amino acids can be deduced and sequence alignments have revealed that many membrane transporters comprise a highly homologous family extending from cyanobacteria, yeasts, algae and protozoa, plants, fungi and mammals including rat, mouse and man.

In 1987, the primary sequences of the arabinose/H⁺ and xylose/H⁺ transporters of *E.coli* were determined from their complementary cDNAs (Maiden *et al.*, 1987). Sequence alignments revealed that, not only are these proteins homologous with each other, but they also share high homology with the human hepatoma and rat brain glucose transporters. All four proteins displayed sequence similarities with the *E.coli* citrate transporter. Conserved amino acid sequences identified by sequence alignment of homologous sugar transporters were also found to occur in the Tet A, B and C proteins which mediate tetracycline export in

gram-negative bacteria, in addition to those of gram positive bacteria, Tet L and K. A rigorous analysis of such proteins was undertaken revealing that although transport proteins exhibit differences in substrate selectivity (e.g. antibiotics, antiseptics, carboxylates and sugars), direction of transport (influx versus efflux) and mechanism of transport (H^+ -dependent symports, antiports and uniports, active and passive transporters), they are all derived from a common ancestor. Several highly conserved motifs have been identified and despite differences in sequence lengths of these transporters, all are predicted to have the same membrane topology, spanning the membrane twelve times with a large cytoplasmic loop linking helices 6 and 7 (reviewed in Henderson *et al.*, 1992).

Four families of related transporter proteins have been identified within the larger "superfamily" of homologous proteins. The mammalian GLUT isoforms constitute part of the larger family. Other members of this group include AraE, the H^+ /L-arabinose symporter of *E.coli* ; Xyl E the H^+ /D-xylose symporter of *E.coli* and GalP, the galactose transporter of *E.coli* . These share 23%, 27% and 25% sequence identity with GLUT1 respectively. GalP and AraE both bind cytochalasin B and GalP can bind forskolin with a similar affinity to that of GLUT1. Furthermore, proteolytic digestion of GalP photolabelled with cytochalasin B yields fragments of similar size to those obtained from digestion of labelled GLUT1.

Interestingly, the mammalian Na^+ -linked glucose transporters and the bacterial ATP- and PEP-utilising active transporters are not included in the superfamily. It is uncertain if the lac permease of *E.coli* is a member as it displays little sequence identity to GLUT1. It is however, thought to adopt a similar transmembrane topology, having twelve transmembrane α -helices which, in the case of the lac permease, are proposed to be arranged in a bilobular structure (Li & Tooth, 1987). In addition, it possesses many of the conserved motifs identified within this superfamily.

1.4 Structure of Mammalian Facilitative Glucose Transporters.

1.4.1 Introduction.

The last 10-15 years have seen technological advances in gene cloning and molecular biology that have facilitated the investigation of the relationship between glucose transporter structure and function. Of the mammalian family, GLUT1 is the only isoform that is currently available in a purified and functional form and therefore is being studied extensively to elucidate the glucose transport mechanism. Its cloning and expression in 1985 therefore represents a significant advance in this field (Mueckler *et al.*, 1985). In addition, the availability of the GLUT1 cDNA led to the subsequent identification of the other isoforms through low stringency hybridisation techniques.

Today a whole range of techniques are being applied to the investigation of the GLUT isoforms, and these range from the use of spectroscopic techniques to analyse secondary structure to the use of antibodies, proteases, affinity labels and group-specific chemical reagents to elucidate the membrane topology. Sequence alignments have revealed the presence of conserved motifs that have been probed further by mutagenesis to map sequences involved in substrate binding and conformational changes.

1.4.2 Sequence Alignments and General Topology.

The GLUT1 cDNA was initially isolated from human HepG2 cells (Mueckler *et al.*, 1985). An open reading frame encoding a 492 amino acid residue polypeptide was identified and from this the amino acid sequence was deduced. Isolation of a cDNA clone from rat brain in 1986 revealed that the GLUT1 protein sequence was highly conserved with 98% sequence identity between the two species (Birnbaum *et al.*, 1986). Such a high degree of sequence conservation implies that all regions of the GLUT1 transporter are functionally important.

Based on the deduced primary sequence, a hydropathy analysis led to a speculative model for the topology of GLUT1 in the membrane (Figure 1.2). Computer and graphical

analyses of the protein sequence along with proteolytic studies of the native membrane-bound transporter support this model. A highly hydrophobic protein is predicted such that approximately 50% of the protein lies within the membrane bilayer. The transporter consists of twelve transmembrane segments each of about 21 amino acids predicted to form α -helices. These are linked by short hydrophilic extramembraneous regions of 7-14 residues that may form β -turns. Loops at the cytoplasmic surface are very short, typically eight residues long and this is a highly conserved feature throughout the wider transporter family. Severe constraints are placed on the possible tertiary structure as a consequence, suggesting a closely packed helical structure at the inner surface of the protein. The loops at the extracellular surface are generally longer and more varied in terms of length and sequence identity. Helical packing is likely to be less compact at this side of the protein.

Tryptic digestion of intact erythrocytes and sealed ghosts suggests the presence of an extremely hydrophilic loop of 65 residues on the cytoplasmic side that connects helices 6 and 7, effectively dividing the transporter into N- and C-terminal domains. The extramembraneous N- and C-terminal segments are both hydrophilic and are also cytoplasmic, confirmed by the use of anti-peptide antibodies that react only when the inner surface of the transporter is accessible, for example in inverted vesicles (Davies *et al.*, 1987; Haspel *et al.*, 1988). A large extracellular loop of 33 residues connects helices 1 and 2 and contains a potential site for N-linked glycosylation at Asn⁴⁵. Another potential glycosylation site is located within helix 11 (Asn⁴¹¹) and is therefore unlikely to be modified. This is consistent with proteolytic studies in which the transporter was cleaved at cysteine residues to yield a large fragment of 31kDa corresponding to residues 133-428 and a short N-terminal fragment. The large fragment encompasses Asn⁴¹¹ but was not found to contain carbohydrate (Cairns *et al.*, 1984), thus Asn⁴⁵ is assigned as the glycosylation site. In addition, mRNA derived from the first N-terminal 40 amino acids can be translated in a reticulocyte cell-free system to produce a truncated protein that is inserted into the membrane of the endoplasmic reticulum and glycosylated at the same site as the full length protein.

Some of the transmembrane helices contain several serine, threonine, glutamine and asparagine residues. These polar residues are predicted to lie on the same face of an α -helix and therefore helices 3, 5, 7, 8 and 11 are suggested to be amphipathic. Hydroxyl and amide

side chains of such residues in a transmembrane helix may line a channel or pore and partake in transient H-bond formation as the substrate translocates through the channel of the transporter across the membrane.

The other members of the mammalian facilitative transporters are of a similar size to GLUT1 (~500 amino acids) and are predicted to share the same membrane topology including : twelve transmembrane α -helices, a large extracellular loop connecting helices 1 and 2 which contains a single site for N-linked glycosylation, a large hydrophilic loop between helices 6 and 7, and cytoplasmically located N- and C-termini. Despite such similarity in both structure and function, there is still quite a high degree of sequence divergence within the family. There is 39-65% sequence identity and 50-76% sequence similarity between isoforms, 26% of the residues are absolutely conserved in all isoforms and a further 13% of the residues are conservative substitutions.

Sequence alignments have revealed that there are several conserved motifs present throughout the glucose transporters (Table 1.1). These include GRR(K) located between helices 1 and 2 in the N-terminus and, correspondingly, between helices 7 and 8 in the C-terminus; EXXXXXXR between helices 4 and 5 in the N-terminus and 10 and 11 in the C-terminal half; PESPR in the cytoplasmic loop connecting helices 6 and 7 paralleled by the PETKG motif in the C-terminal cytoplasmic loop. These motifs may have been conserved to maintain conformational stability and may be involved in the formation of salt bridges. Repetition of these sequences suggests that duplication of an ancestral gene encoding a six transmembrane helical protein may have given rise to the twelve transmembrane helical structure that is so highly conserved throughout the glucose transporter family (Baldwin & Henderson, 1989; Maiden *et al.*, 1987). The conformational constraints imposed by the short cytoplasmic loops make it unlikely that the protein is composed of a single group of twelve transmembrane α -helices. It is more likely that the protein adopts a bilobular structure involving six closely packed helices of the N- and C-terminal domains similar to that which is reported in low resolution electron microscopic images of the *E.coli* lactose permease (Li & Tooth, 1987). Recently, two three-dimensional structural models were proposed for the arrangement of helices in the protein tertiary structure (Zeng *et al.*, 1996). Both models are based on the prediction that an aqueous channel is formed from five amphipathic α -helices.

The helices are arranged in bundles of four, and in both models the N-terminus contributes two helices that participate directly in channel formation (section 1.9). Other models have suggested alternative helical packing schemes (Baldwin, 1993), however the precise arrangement of the transmembrane segments of the transporter and the relative contributions made by the N- and C-termini are as yet unclear. Evidence from photolabelling studies and proteolytic digestion suggest that the glucose binding sites are located in the C-terminal domain of GLUT1 and so transport occurs in this region. However the N-terminal domain may also play a role (section 1.7.4b).

1.4.3 Spectroscopic Techniques.

The model for the topological arrangement of GLUT1 and the other isoforms in the lipid bilayer was based mainly on theoretical structural analysis such as hydropathy plots. The protein is strongly hydrophobic and is predicted to span the membrane twelve times. Other analyses evaluate the probability of α -helices or β -sheet configurations. Confirmation of the predicted secondary structure has been obtained from various spectroscopic techniques. UV circular dichroism (CD) spectroscopy yields information regarding the extent of α -helical, β -sheet or random coil structures that are present in proteins. Spectra have been obtained from proteins that contain either pure α -helices, β -sheet or random coil structures or known quantities of these various secondary structural motifs. These reference spectra can then be used to estimate the percentage of each type of secondary structure in a new protein. GLUT1 is estimated to contain 82% α -helix, 10% β -turn and 8% random coil structure. No β -sheet structure was detected using this technique (Chin *et al.*, 1987).

Infrared (IR) spectroscopy has proven to be an important tool for elucidating protein secondary structure, particularly in the last 5-10 years. An empirical correlation exists between the frequency of the amide I and II absorption bands and the secondary structural motifs present within a protein. The amide I and II absorptions are influenced by the strength of hydrogen bonds involving amide C=O and N-H groups. As each secondary structural motif (i.e. α -helix, β -sheet, β -turn and random coil) has a characteristic hydrogen bonding pattern involving amide C=O and N-H groups, they each give rise to distinct amide I and II

absorptions. It is the separation of these absorption bands that allows the determination of protein secondary structure by IR spectroscopy. Fourier Transform methods of data acquisition (FTIR) enable the structural analysis of large proteins in aqueous media by deconvolution of spectra. Application of this technique to purified GLUT1, reconstituted into erythrocyte lipids in H_2O , revealed that the protein adopts a mainly α -helical structure. Vibrational frequencies corresponding to β -strand and random coil structure were also detected from deconvoluted spectra (Alvarez *et al.*, 1987). However, the presence of β -turns is uncertain in this study due to difficulties in resolving the appropriate absorption bands in this region of the spectrum. Chin and co-workers in 1986 predicted the presence of α -helical structure in extramembraneous domains (Chin *et al.*, 1986). The first direct evidence for this came from FTIR analysis of GLUT1 before and after proteolytic digestion (Cairns *et al.*, 1987). Extramembraneous, cytoplasmic domains of the transporter removed by trypsin were found to contain α -helical structure. The observation that the transmembrane domain contains some β -structure (Alvarez *et al.*, 1987) was also corroborated in this study.

FTIR spectroscopy has also been employed to assess the orientation of the glucose transporter in the membrane bilayer. A spin drying technique has been used to obtain orientated multilamellar films of reconstituted GLUT1 (Chin *et al.*, 1986). Linear dichroism of the IR spectra reveal that the α -helices are orientated perpendicular to the plane of the membrane with an average tilt angle of less than 38° from the membrane normal. This is comparable to the membrane orientation reported for rhodopsin and bacteriorhodopsin. The application of FTIR was then extended to assess the possibility that certain α -helices are arranged within the membrane to form a water-filled channel. Hydrogen-deuterium exchange of reconstituted GLUT1 incubated in 2H_2O resulted in band shifts in the amide II region of the IR spectrum. It was estimated that 70-80% of the amide hydrogens are accessible to solvent water. In addition, hydrogen-tritium exchange also corroborated these results. 25-30% of hydrogens exchange very rapidly and these are suggested to be in direct contact with solvent. Based on the fact that most of the protein mass is transmembrane, these results strongly suggest the presence of an aqueous channel. Furthermore, the presence of D-glucose and cytochalasin B drastically altered the kinetics of these rapidly exchangeable hydrogens indicating significant conformational changes in the protein (Jung *et al.*, 1986).

FTIR spectroscopy has been applied to investigate other aspects of GLUT1 structure and function including substrate induced conformational changes. Intrinsic tryptophan fluorescence has also been correlated with conformational changes resulting from ligand or substrate binding and has been used to resolve the dynamics of these events. A more detailed review of these studies are given in the appropriate section. In conclusion, the application of chemical and physical techniques described give a consistent picture of a transmembrane structure containing an aqueous pore through which substrate can pass. Large conformational changes occur such that the transporter reorientates the substrate binding site to the exo- and endofacial surfaces of the protein.

1.5 Dynamics of Glucose Transport.

1.5.1 Introduction

Most kinetic, thermodynamic and ligand binding studies of glucose transport have been carried out using erythrocytes. They are simple cells, available in large quantities and thus the erythrocyte transporter, GLUT1, is assumed as the prototypic model for such studies. Based on the structural similarity between the GLUT isoforms, many of the properties determined for GLUT1 will most likely apply to the other family members. However, the isoforms do exhibit differences in sugar specificity, kinetic parameters, ligand binding, targeting patterns, tissue expression and hormonal regulation which can be both acute and chronic.

1.5.2 Transport Studies

There are a variety of methodologies which have been used to measure glucose transport by GLUT1 in erythrocytes. The most widely employed is the use of radiolabelled sugars which act as tracers for sugar movement. Other methods include chemical analyses of cellular sugar content, spectrophotometric monitoring of cell volume changes induced by glucose transport or coupling of transport to a secondary enzyme-linked assay to detect

changes in intracellular sugar levels. In addition, a variety of different assay conditions have been used to measure distinct parameters of the transport process and each are explained in turn below. The terminology is such that the *cis* -side of the membrane refers to the side from which transport occurs and the *trans* -side is the opposite side.

1.5.2a Zero-*trans* Entry.

This is the simplest study and involves the measurement of uptake of trace amounts of radiolabelled D-glucose into cells. Prior to assay, cells are stored in a glucose-free medium for a certain period of time to ensure that the cytosolic sugar concentration is as low as possible. External sugar concentrations are varied with each measurement. Initial transport of glucose into the cell should be linear since the cytosolic sugar concentration is zero. Measurements are therefore recorded during this initial time period before reverse-flow of sugar occurs. The parameters which are determined are the affinity of the exofacial binding site for sugar (K_m outside) and the maximum velocity of sugar entry under conditions of infinitely high sugar concentrations (V_{max} entry).

1.5.2b Zero-*trans* Exit.

Cells are pre-incubated with varying sugar concentrations plus tracer until equilibrium is reached. The external medium is rapidly replaced with one without sugar. Initial rates of sugar exit are determined by measurement of radioactivity levels in the external medium. Parameters determined from this type of assay are the affinity of the endofacial binding site for sugar (K_m inside) and the V_{max} for sugar efflux.

1.5.2c Equilibrium Exchange.

In this case intra- and extracellular sugar concentrations are identical and the unidirectional flow of radiolabelled sugar is measured in either direction. Values are obtained for the K_m and V_{max} for sugar exchange. This is the most common type of assay.

1.5.2d Kinetic Properties of GLUT1.

Many transport assays using erythrocytes under various assay conditions have been performed by different groups. A summary of the kinetic parameters outlined above, determined for D-glucose transport at 0°C and at 20-25°C, is reviewed by Carruthers (1990). All transport profiles show simple, hyperbolic Michaelis-Menton kinetics and several important features of the transport process in erythrocytes are noted from the presented data. The kinetic parameters of glucose transport mediated by GLUT1 are very temperature dependent with K_m and V_{max} values generally lower at subphysiological temperatures. Also, very different values for these parameters are obtained depending on the assay conditions used. For example, at 0°C under zero-*trans* entry conditions, the K_m and V_{max} values were approximately 0.15-0.2mM and 0.0035-0.0055mMs⁻¹ respectively whereas under zero-*trans* exit conditions these values are 1.64-3.4mM and 0.071-0.092mMs⁻¹ respectively. Thus, the kinetic values for zero-*trans* exit are 12-fold greater than those for zero-*trans* entry at 0°C. This asymmetry of transport is somewhat reduced at 20-25°C to a 3-fold difference in kinetic parameters for entry and exit. One physiological significance of the observed GLUT1 asymmetry would be to allow it to act effectively as a unidirectional transporter under conditions in which D-glucose concentrations on one side of the membrane are low and the demand on the other side is high, e.g. transport across the blood-brain barrier under hypoglycaemic conditions.

The kinetic parameters determined under equilibrium exchange conditions are substantially greater than those determined under zero-*trans* exit conditions. This observation can be explained in terms of a phenomenon known as *trans* -acceleration. This describes the effect of the presence of sugar on one side of the membrane on the rate of unidirectional transport from the opposite side, for example, intracellular D-glucose stimulates D-glucose uptake and vice versa. This results in lower than expected initial transport rates under zero-*trans* conditions. Assuming that the rate limiting step for net transport is the reorientation of the unloaded carrier, under exchange conditions the transporter will bind a second sugar molecule before it reorients, effectively bypassing this slow step. This is not the case under zero-*trans* conditions due to the initial absence of sugar on one side of the membrane.

1.5.3 Models for the Mechanism of D-Glucose Transport.

1.5.3a Introduction

Glucose transport is characterised by a number of properties: 1) transport of glucose occurs more rapidly than can be accounted for by simple diffusion across the lipid bilayer; 2) transport displays simple Michaelis-Menton saturation kinetics; 3) the rate of transport is proportional to the number of transporter proteins; 4) transport of sugars is stereospecific and there is competition between sugars for transport; 5) the transport capacity of cells can be regulated by endocrine and metabolic factors. Such properties liken the mechanism of glucose transport with those of enzyme-catalysed reactions.

1.5.3b The Single Site Alternating Conformer Model.

In 1952, Widdas proposed a simple, symmetric carrier model for glucose transport (Widdas, 1952) from which a kinetic model that can account both for transport asymmetry and for *trans*-acceleration arose. The model is known as the single site alternating conformation model (Figure 1.3).

The transporter is described as a simple asymmetric carrier that can alternate between two conformational states such that a single D-glucose binding site is sequentially and alternately exposed to either the cytoplasm (T_i) or the extracellular medium (T_o). So, at any point in time, a carrier can be available for either sugar efflux or influx, but not for both simultaneously. When sugar binds to one of these sites to form a carrier-sugar complex (T_iG or T_oG), a conformational change is induced such that the sugar is presented at the other side of the membrane. The re-orientation event may involve the substrate binding site or a larger portion of the transporter (Hodgson *et al.*, 1992). Dissociation of the sugar occurs and the transporter is then available to bind a further sugar molecule for transport in the opposite direction, or it can isomerise back to its original state in the absence of sugar. Thus, re-orientation of the carrier can occur in the presence or absence of D-glucose. The dissociation constants for sugar binding at the endofacial (K_{si}) and exofacial (K_{so}) sites are not

necessarily equal, and the rate constants governing the re-orientation of the loaded carrier (k_1 and k_{-1}) are greater than those relating to the movement of the unloaded carrier (k_2 and k_{-2}). Rates of association and dissociation of glucose from the transporter are also much greater than the rates of re-orientation and therefore the latter is the rate-limiting factor in the transport cycle (Figure 1.4). Indeed evidence has been obtained from an NMR study in support of this (Wang, 1986). Therefore under zero-*trans* conditions, unidirectional flux of D-glucose is retarded by the slow re-orientation rate of the unloaded carrier, a situation which does not prevail under equilibrium exchange conditions since D-glucose dissociation is rapidly followed by D-glucose association.

1.5.3c Measurement of Individual Kinetic Parameters Governing Transport.

Individual rate constants and activation energies that govern re-orientation of the loaded and unloaded carrier have been determined under zero-*trans* entry, exit and equilibrium exchange conditions for transport of radiolabelled D-glucose in erythrocytes by exploiting the temperature dependence of the transport process (Lowe & Walmsley, 1986). Pre-steady state values for the rates of interconversion from T_1 to T_0 were determined spectroscopically by monitoring the intrinsic protein fluorescence in the presence and absence of D-glucose. Intrinsic fluorescence altered in a time dependent manner when purified GLUT1 reconstituted in unscaled membranes was mixed with 4,6-*O*-ethylidene-D-glucose at 10°C. This is a non-transported glucose analogue that preferentially binds to the T_0 conformation. Incubating the transporter at saturating concentrations of this analogue causes a rapid, first-order quenching of the intrinsic protein fluorescence as a result of the conversion of T_1 to T_0 . The transporter is then trapped in the T_0 EGlc complex. This methodology has enabled single half-turnover events to be measured. This approach was expanded to the determination of rate constants governing the conformational change in the opposite direction i.e. T_0 to T_1 , made possible with the use of *n*-propyl- β -D-glucopyranoside which binds preferentially to the T_1 conformer (Barnett *et al.*, 1975), complexing at least 90% of the transporter in this conformation at equilibrium. Fluorescence was monitored in

the presence and absence of D-glucose allowing determination of single "half turnovers" (Appleman & Lienhard, 1989).

The values obtained for each individual rate constant under both steady-state and equilibrium exchange conditions are in good agreement and support the existence of the alternating conformer model. Values are quoted in the legend to Figure 1.4 and to summarise, the relative rate constants are $k_2 > k_{-2} > k_1 > k_{-1}$.

The dissociation constants for substrate at the exofacial and endofacial binding sites can be calculated from the rate constants for transporter re-orientation and the transport kinetics. Values calculated for the exofacial binding site, K_{so} , were found to remain constant at ~10mM over a range of temperatures between 0°C to 37°C. Over the same temperature range, values for the endofacial binding site K_{si} , increased from 13mM to 23mM. Thus, at low temperatures, the dissociation constants for the glucose-carrier complex on either side of the membrane are similar despite large differences between individual rate constants. This is in sharp contrast to the measured 10-fold lower affinity (K_m) of the endofacial site at 0°C. It is likely that the large asymmetries in the zero-*trans* Michaelis constants observed at low temperatures arise from the differences in individual rate constants for transporter re-orientation and not from large changes in the affinity for glucose at the two sites. Consequently there is an asymmetric distribution of exo- and endofacial conformations of loaded and unloaded transporter at 0°C. In the absence of glucose, only 6% and 7.5% of the unloaded and loaded transporter is in the exofacial conformation. This distribution changes in response to temperature such that at 37°C, 40% and 60% of the unloaded and loaded transporters are outwardly orientated (Walmsley, 1987).

Thermodynamic analysis show that the temperature distribution may arise as a result of endothermic enthalpy and positive entropy changes associated with re-orientation of the transporter from an endofacial to an exofacial conformation. It has been suggested that such changes emanate from the increased stability of the inward-facing conformation due to salt bridges present in the hydrophilic cytoplasmic domain of the transporter (Walmsley, 1987). Glucose binding to the transporter is probably dependent on the dissociation of water molecules from both the transporter and glucose molecule, followed by the subsequent formation of hydrogen bonds between glucose and the transporter at the binding site. This

may provide a kinetic means by which glucose can accelerate the interconversion of the two conformational states.

1.5.3d Multiple Site Models.

The single site alternating conformer model accounts for the majority of kinetic data obtained from transport studies in erythrocytes. This includes discrepancies between kinetic parameters for net entry and exit and an exchange rate that is more rapid than net flux. However, there are some discrepancies between observed and predicted values derived from integrated rate equations for certain parameters and these have led to the proposal of alternative transport models. Carruthers has proposed several alternatives including the fixed site carrier models in which the carrier consists of two subunits that each act by alternating between two conformational states. The mechanism of transport is such that sugar binding at one site of a subunit induces its reorientation to the *trans* side of the membrane. This conformational change is coupled to the simultaneous re-orientation of the binding site of the second subunit in the opposite direction. The basic tenet of this model is similar to that of the alternating-conformer model but it also allows for the simultaneous existence of exofacial and endofacial binding sites that may act co-operatively when both occupied. A second fixed site model envisages the existence of a two-site aqueous channel. When both sugar binding sites are occupied, a conformational change occurs that stabilises the channel in an opened state that is sufficiently wide to allow the simultaneous translocation of two sugar molecules in opposite directions. Due to the complex nature of these fixed site models, they are less amenable to analysis by steady-state methods.

Experimental evidence has been obtained that supports the simultaneous presence of exo- and endofacial binding sites. Erythrocyte transporters have been shown to bind the endofacial ligand, cytochalasin B and also an exofacial ligand such as maltose, phloretin or 4,6-*O*-ethylidene-D-glucose simultaneously (Helgersson & Carruthers, 1987). The effect of each of these ligands on the inhibition of D-glucose uptake by the other ligand suggests that these simultaneously occupied sites exhibit negative co-operativity (Carruthers & Helgersson, 1991). Also, glucose-induced fluorescence quenching has been shown to consist of two

saturable components of low and high dissociation constants suggesting the presence of multiple substrate binding sites (Carruthers, 1986).

Perhaps the most direct evidence to support the single site alternating conformation model over the fixed site model came from the demonstration of a single half-turnover of the transporter. Erythrocyte transporters incubated with maltose, a non-transporter exofacial ligand, are effectively pulled into the outward facing conformation. Rapid dilution of maltose by the simultaneous addition of D-glucose allows a portion of the outwardly orientated transporters to bind D-glucose and undergo conformational changes, producing an initial burst of glucose uptake and a change in intrinsic fluorescence corresponding to formation of the inward-facing conformation (Lowe & Walmsley, 1987). No such intrinsic fluorescence change would be predicted in a two site model since an outward-facing binding site is always exposed. Consequently, maltose would not have the effect of re-orientating the transporter.

1.6 Conformational Changes.

1.6.1 Introduction.

Although the mechanism of transport mediated by GLUT1 is still unclear and the distinct number of binding sites is still unresolved, there is little doubt that the transporter alternates between two different conformational states. The first piece of compelling evidence for this came from the demonstration that glucose derivatives with large bulky substituents at the C-4 or C-6 position such as maltose or 4,6-*O*-ethylidene-D-glucose were not transported but inhibited sugar transport when present only at the outside of the erythrocyte (Baker & Widdas, 1973, Barnett *et al.*, 1975). These ligands were therefore proposed to bind at the extracellular binding site, in contrast to endofacial ligands such as n-propyl- β -D-glucopyranoside which has a large substituent at the C-1 position and inhibits transport only when present inside the cell. The orientation of the sugar is preserved at each side of the membrane such that binding at the exofacial site is via the C-1 position whereas binding at the endofacial site is via the C-4 and C-6. Transport is therefore inhibited not by

lack of sugar binding, but by steric prevention of the subsequent conformational changes that mediate substrate translocation.

1.6.2 Detection of GLUT1 Conformational Changes by Intrinsic Fluorescence.

Monitoring intrinsic protein fluorescence and measurement of the relative abilities of external hydrophilic molecules to quench protein fluorescence in the presence of various ligands has provided evidence for the occurrence of apparent conformational or positional changes during substrate translocation. GLUT1 contains six tryptophan residues throughout its 492 amino acid sequence and the intrinsic fluorescence of the transporter due to these residues report on the overall tertiary protein structure and its relationship to the bilayer. Quenchers such as potassium iodide (KI) and acrylamide can be used to determine which tryptophan(s) are accessible to a hydrophilic environment. A maximum peak at 336nm in the fluorescence emission spectrum indicates the location of tryptophan in both polar and apolar environments. Fluorescence quenching by KI and acrylamide indicate that not all tryptophans are located within the hydrophobic interior of the protein or the lipid bilayer (Pawagi & Deber, 1990).

Both D-glucose and transport inhibitors such as maltose, 4,6-*O*-ethylidene-D-glucose, phloretin, cytochalasin B and forskolin quench the fluorescence, with this effect strongest at longer wavelengths, indicating the involvement of one or more tryptophans exposed to a polar environment, possibly at the substrate binding site(s) (Chin *et al.*, 1992; Gorga & Lienhard, 1982). Individual replacement of Trp⁴¹² and Trp³⁸⁸ to leucine by site directed mutagenesis leads to decreased transport activity and perturbed cytochalasin B binding (Garcia *et al.*, 1992; Katagiri *et al.*, 1991). These residues are predicted to lie approximately opposite to one another within transmembrane segments 10 and 11. Trp³⁸⁸ is located within an optimally dynamic segment which undergoes movement from an accessible aqueous environment to a less accessible environment as a result of ligand binding. As mutation of this residue results in markedly reduced cytochalasin B binding, it is proposed that Trp³⁸⁸ is involved in ligand binding at the endofacial site. Changes in the accessibility

of certain groups as a result of ligand binding is also likely to be involved in the quenching mechanism. Indeed, it has been observed that the exofacial conformation of the unloaded carrier is 20% less fluorescent than the endofacial conformation (Appleman & Lienhard, 1989) as already described.

1.6.3 Sensitivity of Transporter Conformations to Chemical Inactivation.

1-fluoro-2,4-dinitrobenzene (FDNB) is an amino-group modifying agent that can irreversibly inactivate GLUT1, with the endofacial and exofacial conformations exhibiting different reactivities toward this compound. Rates of inactivation increased in the presence of extracellular D-glucose but were reduced in the presence of intracellular glucose (Edwards, 1973). Also, there is a direct correlation of protection with binding of non-transported ligands to the outside of the transporter and inactivation with binding at the inner side. For example, the presence of n-propyl- β -D-glucopyranoside accelerates GLUT1 inactivation by FDNB. Protection from inactivation occurs in the presence of extracellular maltose, 4,6-O-ethylidene-D-glucose, phloretin (Baker & Widdas, 1973; Krupka, 1971) and 6-O-alkyl-D-galactoses (Barnett *et al.*, 1975). Although the precise mechanism of inactivation by FDNB is unknown, the results suggest that FDNB, which can rapidly penetrate membranes and is therefore present on both sides, acts only when the transporter is in the endofacial orientation. It may be that this reagent does not act directly at the binding site but modifies a reactive group that becomes exposed upon binding of endofacial ligands. The apparently anomalous observation that intracellular D-glucose protects against inactivation can be explained by an increased rate of re-orientation to the outward-facing conformation in the presence of glucose (Barnett *et al.*, 1973; Edwards, 1973).

Another conformationally sensitive sulphydryl group has been identified as the sole exofacial cysteine residue located at residue 429 of GLUT1. This group can be modified by impermeant sulphydryl group modifying reagents such as bis-(maleimidomethyl)-ether-L-[^{35}S]cysteine, glutathione-maleimide and p-chloromercuri-benzenesulphonate (pCMBS), resulting in transporter inactivation (May *et al.*, 1990; Wellner *et al.*, 1992). Modification by these compounds is increased in the presence of ligands that interact at the exofacial binding

site such as maltose and phloretin. In each case, cytochalasin B protects against modification by stabilising the inward-facing conformation. The Cys⁴²⁹ is probably located at a site that is structurally distinct from the substrate binding site since ligands that bind to the exofacial binding site actually increase the sensitivity of this residue to modification.

Cys⁴²⁹ is predicted to lie at the extracellular end of helix 12 in the C-terminal half of the transporter. Evidence also exists to suggest that in addition to the C-terminal half, the N-terminal domain also takes part in conformational changes associated with substrate translocation across the bilayer. Inhibition of transport by N-ethylmaleimide correlates with modification of a sulphhydryl group located in the N-terminus (May, 1989). Cytochalasin B binding protects the transporter from modification and this is likely to be due to steric hindrance.

1.6.4 Susceptibility of GLUT1 Conformational States to Proteolysis.

Data obtained from fluorescence spectroscopy and chemical modification studies most likely reflect the conformational states of the hydrophobic membrane spanning regions of the transporter. Studies assessing the susceptibility of the hydrophilic cytoplasmic domains to proteolysis reveal that these regions are also affected by conformational changes associated with substrate translocation. Trypsin and thermolysin cleave GLUT1 at sites within the large, central hydrophilic loop and the C-terminal sequence yielding two large fragments. The reversible binding of exofacial ligands such as maltose, phloretin and 4,6-*O*-ethylidene-D-glucose substantially reduce the rate of proteolytic cleavage (Gibbs *et al.*, 1988; King *et al.*, 1991). Photoaffinity-labelling of GLUT1 at the exofacial site by the bis-mannose derivative ATB-BMPA, provides almost complete protection from proteolysis (Clark & Holman, 1990). As the cleavage sites are cytoplasmic, such effects are not likely to be a result of steric hindrance between exofacial ligand binding and proteases. Exofacial ligands stabilise the outward facing conformation thereby providing indirect protection of the cytoplasmic domains from proteolysis by causing them to adopt an orientation that is less accessible to proteinase.

As would be expected, binding of reversible endofacial ligands such as n-propyl- β -D-glucopyranoside increase the rate of cleavage, presumably due to increased steady-state levels of the transporter in a proteolytically-sensitive orientation. A somewhat surprising observation, however, is that cytochalasin B binding has no effect on the rate of tryptic or thermolytic cleavage (Gibbs *et al.*, 1988; King *et al.*, 1991). It is possible that cytochalasin B stabilises a conformation that is distinct from those induced by binding of other ligands. Intracellular D-glucose increases the rate of proteolysis. This can be explained in terms of the asymmetric carrier model since kinetic theory predicts a modest increase in the steady-state proportion of outward-facing transporters in the presence of glucose (Lowe & Walmsley, 1986). Increased sensitivity to proteolysis may also occur during the transport process itself.

The observation that trypsinised GLUT1 is still capable of subsequently binding cytochalasin B, but has reduced affinities for the exofacial ligand, ATB-BMPA, suggests that the proteolysed transporter is locked in an inward-facing conformation (Cairns *et al.*, 1984; Clark & Holman, 1990; Karim *et al.*, 1987). Similar characteristics are exhibited by a C-terminally truncated mutant of GLUT1 lacking 37 C-terminal amino acid residues (Oka, 1990). Conversely, a mutant truncated by removal of only 12 C-terminal residues does not display such characteristics. Thus, removal of residues 455-480 produces a transport-deficient protein that is locked in an inward-facing conformation.

Taken together, results obtained from the application of chemical and physical methodologies to the study of glucose transport, particularly by GLUT1, have given a consistent picture of a transmembrane protein that mediates substrate translocation by alternating between two conformational states. The process is dynamic and involves movement of at least some transmembrane helices and the cytoplasmic loops. A putative mode of operation of the GLUT1 transporter has been proposed based on molecular dynamics and molecular modelling studies (Hodgson *et al.*, 1992). Conformational changes are proposed to occur in the region of transmembrane helix 10 enabling the transporter to adopt two distinct glucose binding conformations. Modelling predicts that proline and glycine residues located within this helix may provide the flexibility required for such positional changes to take place. The role of membrane-buried proline residues in the conformational changes required for substrate translocation is discussed in Chapters 3 and 4.

1.7 Location of the Substrate-Binding Site(s).

1.7.1 Introduction.

Identification of the substrate-binding site(s) of GLUT1 has been greatly facilitated by the availability of specific inhibitors of transport that bind with greater affinity than D-glucose. Some of these inhibitors can be covalently attached to their binding sites on the protein by photoactivation using ultraviolet irradiation. Limited proteolysis of the photolabelled transporter using radiolabelled photoaffinity ligands should reveal the approximate position of the substrate binding site(s). Interpretation of such studies depends upon the assumption that the site of photoaffinity labelling does not sterically hinder glucose binding either directly or by inducing an altered conformational state. In addition, the site of photolabelling and that of reversible inhibition of glucose transport are assumed to be the same.

1.7.2 Affinity Labelling at the Endofacial D-Glucose Binding Site.

Cytochalasin B is a naturally occurring fungal metabolite that acts as a high affinity inhibitor of sugar transport mediated by both mammalian and bacterial facilitated diffusion sugar transporters (Basketter & Widdas, 1978; Krupka & Deves, 1986). Cytochalasin B has been demonstrated to bind to various symporters of *E.coli* including the galactose/H⁺ symporter, GalP and AraE, the arabinose/H⁺ symporter. The xylose/H⁺ symporter, XylE, does not bind cytochalasin B (Henderson *et al.*, 1992).

With regard to the mammalian GLUT isoforms, cytochalasin B was found to bind exclusively at the inner surface of GLUT1 in a D-glucose inhibitable manner with a stoichiometry of one molecule per polypeptide chain (Baldwin & Lienhard, 1989) and a K_d of 120nM (Zoccoli *et al.*, 1978). The binding is quantitative and is therefore used as an assay for GLUT1 activity in purified preparations. The inhibitor binds to GLUT2 (Axelrod & Pilch, 1983) and GLUT7 (Waddell *et al.*, 1991) with much lower affinities, (K_d of ~1μM for GLUT2) and does not appreciably bind to GLUT5 (Burant *et al.*, 1992).

A more precise location of the cytochalasin B binding site has emanated from the use of photolabelling in conjunction with proteolysis. Tryptic removal of hydrophilic, cytoplasmic domains of GLUT1 leaves membrane embedded portions of the protein that retain the ability to bind cytochalasin B (Cairns *et al.*, 1984; Karim *et al.*, 1987). Photolabelling with [^3H]cytochalasin B after tryptic cleavage yields a C-terminal 18kDa fragment corresponding to amino acid residues 265-456. This region has been resolved further by extensive cleavage of photolabelled GLUT1 with trypsin, thermolysin, 2-nitro-5-thiocyanobenzoic acid (2-NTCB) and *N*-bromosuccinimide (NBS). A 3kDa NBS cleavage fragment corresponding to amino acid residues 388-412 comprising the loop connecting transmembrane helices 10 and 11, and helix 11 itself was identified as the D-glucose inhibitable cytochalasin B binding site (Holman & Rees, 1987). The endofacial glucose binding site is therefore mapped to this region of GLUT1. Derivatives of cytochalasin B and forskolin are proposed to bind at this endofacial site since the oxygen atoms of these molecules are superimposable with those of D-glucose and therefore, are capable of forming equivalent hydrogen bonds with residues at the binding site. A recent observation that GLUT1 is capable of simultaneously binding cytochalasin B and 4,6-*O*-ethylidene-D-glucose casts some doubt on the accuracy of the single-site alternating conformer model (Carruthers & Helgerson, 1991).

Forskolin is a diterpene toxin that competitively inhibits both 3-*O*-methyl-D-glucose transport and cytochalasin B binding (Sergeant & Kim, 1985; Shanahan *et al.*, 1987). It therefore binds to the endofacial side of the transporter in close proximity to the site of interaction with cytochalasin B and D-glucose. The 3-[^{125}I]iodo-4-azidophenethylamido-7-*O*-succinyldeacetyl (IAPS) derivative of forskolin is a high affinity photolabel of glucose transporters (Wadzinski *et al.*, 1987; Wadzinski *et al.*, 1988). In contrast to cytochalasin B, some disagreement exists as to the exact location of the forskolin and IAPS-forskolin labelling site(s). Forskolin photolabelling has been located to the same 18kDa C-terminal tryptic fragment as cytochalasin B while IAPS-forskolin labelling has been mapped to amino acid residues 369-389 within helix 10 of GLUT1 ((Wadzinski *et al.*, 1990) and helix 9 of GLUT4 (Hellwig & Brown, 1992). Since labelling is inhibited in the presence of cytochalasin B, this sequence may also comprise part of the endofacial D-glucose binding

site. Other derivatives include the iodinated 7-aminoalkylcarbamate form of forskolin that has a very high affinity (IC_{50} of 200nM) for the brain and erythrocyte isoforms (Morris *et al.*, 1991). GalP has also been reported to bind [3H]IAPS-forskolin with inhibition of sugar transport (Henderson *et al.*, 1992).

Recently, a transportable diazirine derivative of D-glucose, 3-deoxy-3,3-azido-D-glucopyranose (3-DAG) has been demonstrated to be rapidly transported by GLUT1 into erythrocytes and resealed ghosts at a rate comparable to that of 3-O-methyl-D-glucose, in a cytochalasin B inhibitable manner (Lachaal *et al.*, 1996). Upon UV irradiation, 3-DAG can be covalently incorporated into purified GLUT1, reconstituted into liposomes. Proteolysis of 3-DAG-labelled GLUT1 revealed that sequences within both the N- and C-terminal regions interacted with this substrate analogue and are therefore most likely to contribute to channel formation. However, definitive assignment of 3-DAG labelling to individual transmembrane helices and amino acids was not possible in this study. Involvement of the N-terminal half in channel formation is consistent with the proposal that the glucose channel is formed at the interface between the N- and C-terminal domains involving five amphipathic helices of either 3, 4, 7, 8 and 11 or 2, 5, 7, 8 and 11 (section 1.9). Identification of the individual 3-DAG-labelled amino acids would no doubt contribute to a more compelling map of the contact sites of D-glucose within the channel.

Other known photoaffinity labels of GLUT1 include the naturally occurring steroid, androstenedione which acts as a potent competitive inhibitor of 3-O-methyl-D-glucose uptake. Cytochalasin B binding is also inhibited and photo-incorporation has been mapped to the 18kDa tryptic fragment of erythrocyte ghosts ((May, 1988).

1.7.3 Affinity Labelling at the Exofacial D-Glucose Binding Site.

Several attempts have been made to synthesise an impermeant, exofacial photoaffinity label to facilitate mapping of the exofacial D-glucose binding site. A series of bis-hexoses have been designed by Holman and colleagues, based on the rationale that these would bind to the exofacial D-glucose binding site (Clark & Holman, 1990; Holman & Karim, 1988; Holman *et al.*, 1986). Identification of an impermeant bis-mannose core as a

photolabile substituent has made possible the synthesis of a number of photoactivatable compounds that have an affinity for GLUT1. These include the bis-hexoses 2-*N*-(4-)-1,3-bis(D-mannos-4-yloxy)propyl-2-amine (ASA-BMPA), and 2-*N*-[4-azi-2,2,2-trifluoroethyl)benzoyl]-1,3-bis(D-mannos-4-yloxy)-2-propylamine (ATB-BMPA). Each compound was found to bind exofacially to GLUT1 and was displaced by D-glucose, 4,6-*O*-ethylidene-D-glucose and cytochalasin B binding. Similar to cytochalasin B labelling, photolabelling of GLUT1 with these compounds followed by tryptic cleavage of the native membrane-bound transporter yields a labelled 18kDa fragment. ASA-BMPA labelling has been localised to a region between amino acid residues 347-388, probably at the extracellular end of helix 9 (Holman & Rees, 1987). ATB-BMPA, which exhibits better selectivity, is suggested to label at a site located within helix 8, between residues 301 and 330 (Baldwin, 1993; Saravolac & Holman, 1997). ATB-BMPA-labelled fragments were identified in this study by their pattern of recognition by site-directed anti-peptide antibodies.

Thus, transmembrane helices 8 and 9 may contribute to the exofacial substrate binding site whereas the endofacial site is composed of helices 10 and 11. This implies some structural separation of the endo- and exofacial binding sites.

1.7.4 Role of the N- and C-Terminal Domains in Formation of the Exo- and Endofacial Substrate Binding Sites.

Various studies in which GLUT1 has been photolabelled by cytochalasin B, bis-mannose derivatives and forskolin derivatives (as outlined above), and proteolysis, suggest that the six transmembrane α -helices of the C-terminal domain contain both the endo- and exofacial D-glucose binding sites. Ligand binding sites are also located within this region. Site-directed mutagenesis has identified several key amino acid residues that are involved in the binding sites and, interestingly, all but one of these residues are located in the C-terminal domain of the transporter (i.e. from the start of helix 7 to the end of the cytoplasmic C-terminal tail). There are three predicted amphipathic helices within this domain, helices 7, 8 and 11, that are particularly rich in conserved polar residues that could participate in transient hydrogen-bond formation with D-glucose during translocation through an aqueous channel

lined by these helices. Such residues have also been targeted for mutagenesis, and roles for these helices in the transport mechanism and formation of the substrate binding sites have been implicated. Similar studies have also implicated helices 9 and 10 as important regions.

Data supporting a function for the N-terminal domain presents a much less clear picture. Lack of information regarding this region of the transporter prompted a study in which the individual stability of the N- and C-terminal domains of GLUT1 were investigated (Cope *et al.*, 1994). Truncated GLUT1 constructs encoding either the N-terminal or C-terminal domains were heterologously expressed in Sf9 cells. Surprisingly, when expressed separately, both constructs were targeted with high efficiency to the plasma membrane but neither were capable of binding the site specific ligands ATB-BMPA or cytochalasin B. Simultaneous expression of both constructs, however, resulted in restoration of the ligand-binding capacity of the C-terminal domain. Thus, both domains are sufficiently stable to be targeted correctly to the plasma membrane and to recognise the other domain. It is possible that the N-terminal domain permits the C-terminus to bind ligands by providing a packing surface against which the C-terminal helices can arrange themselves for correct and stable exposure of the ligand binding sites. It is unlikely that the N-terminus provides amino acid side chains that participate directly in ligand binding since the N-terminal half is not labelled by active site ligands.

1.7.4a Contribution of the C-Terminus to Substrate Binding.

Residues thought to participate in hydrogen bond formation with sugars can be divided into those important for binding inside-specific ligands, and those that are important for outside specific ligands. It is possible using mutagenesis to target such residues resulting in disruption of either binding site without affecting the other. The first demonstration, using site-directed mutagenesis, that helix 7 constitutes part of the exofacial ligand binding site was carried out in 1992. Replacement of Gln²⁸²-Leu in helix 7 perturbs exofacial binding of ATB-BMPA without any detectable disruption of cytochalasin B binding (Hashiramoto *et al.*, 1992). In contrast, the mutation Tyr²⁹³-Ile resulted in a transporter that had approximately a 300-fold reduction in affinity for cytochalasin B at the endofacial site whilst

its ability to bind D-glucose and ATB-BMPA was unaffected (Mori *et al.*, 1994). Thus, the Gln²⁸²-Leu and Tyr²⁹³-Ile mutants are conformationally locked in an inward or outward-facing state respectively. Both studies provide additional evidence supporting the structural separation of the exo- and endofacial binding sites. It was concluded that Gln²⁸² and Tyr²⁹³ are both essential for hydrogen bonding to D-glucose and are involved in closing the exofacial binding site during substrate translocation. Since Gln²⁸² is predicted to lie in the centre of helix 7, it is suggested that this helix moves up in the membrane to accept exofacial ligands (Figure 1.6). This may involve some unfolding of the helical structure at the endofacial end (Hashiramoto *et al.*, 1992). Proteolytic studies also support this upward helical movement.

C-terminal deletion analysis of rabbit GLUT1, (Oka *et al.*, 1990), has provided compelling evidence that the cytoplasmic C-terminal domain is required for formation of the exofacial binding site (Figure 1.6). Truncation of 37 of the 42 intracellular C-terminal amino acid residues results in a conformationally locked protein that is transport deficient and unable to bind exofacial ligands. However, the protein retains the ability to bind endofacial ligands. In addition, a mutant lacking twelve amino acids from the C-terminus retains wild-type expression levels and transport activity (Lin *et al.*, 1992). Similar studies have been undertaken with human GLUT1, yielding a similar pattern of inhibition. Deletion of C-terminal 40, but not 21 amino acids, virtually abolishes transport activity (Due *et al.*, 1995).

In order to determine the point at which conformational locking is localised, sequential truncations of the GLUT1 C-terminal tail were performed. Removal of up to 24 amino acids was without significant effect on transport activity or endo- and exofacial ligand binding. Deletion of 25-27 amino acids resulted in loss of transport activity associated with reduced ATB-BMPA labelling but normal levels of cytochalasin B labelling (Muraoka *et al.*, 1995). It was demonstrated that Gly⁴⁶⁶ and Phe⁴⁶⁷ are not specifically required at position 26 and 27 (from the C-terminal end), respectively, since point mutations at these sites do not affect the proteins ability to transport 2-deoxy-D-glucose. Therefore the minimum structure at the C-terminus that allows correct formation of the exofacial binding site requires all but the last 24 amino acids. The significance of the C-terminus regarding transport activity was further demonstrated by revealing that C-terminal deletions alter the turnover number for 3-

O-methyl-D-glucose transport mediated by both murine GLUT1 and GLUT4 (Dauterive *et al.*, 1996).

1.7.4b Contribution of the N-Terminus to Substrate Binding.

The only residue located outwith the C-terminal domain that seems to affect ligand-binding is Gln¹⁶¹ (Figure 1.6). Mutagenic studies in which this residue was replaced with leucine or asparagine resulted in a 50-fold and 10-fold reduction in transport activity respectively (Mueckler *et al.*, 1994a). This was attributed to a 7.5-fold reduction in the catalytic turnover number and not due to reduced affinity for substrate since the K_m for zero-*trans* influx of 2-deoxy-D-glucose was unaffected by substitution of Gln¹⁶¹ with aspartate. The ability of this mutant to bind the exofacial ligand 4,6-*O*-ethylidene-D-glucose was also reduced. The data, combined with the high degree of conservation of this residue within the twelve helix membrane spanning hexose transporters, is consistent with Gln¹⁶¹ constituting part of the exofacial binding site. In addition, this residue is likely to be involved in events subsequent to substrate binding, such as conformational changes since mutation affected the turnover number of the transporter (Figure 1.6)

Mutation of Tyr¹⁴³ in GLUT4 to phenylalanine resulted in a 70% reduction in transport activity (Wandel *et al.*, 1994) when expressed in COS-7 and LTK cells. This residue is located within helix 4 and is highly conserved among all GLUT isoforms. It was concluded that the hydroxyl group of this residue could provide a hydrogen bond for the formation of the pore-forming complex of helices. Alternatively, it could represent a contact site for the substrate during translocation. Helix 4 contains the highly conserved motif **VPMY¹⁴³XGEX** (where X represents V or I) of which only Tyr¹⁴³ of GLUT4 has been investigated. This helix has been included as a possible channel-forming helix in the speculative models proposed (Zeng *et al.*, 1996) and discussed in section 1.9, however, the precise role of residues within helix 4 of the N-terminal domain remains unclear.

1.8 Mutagenesis.

The common features revealed by alignment and analysis of the amino acid sequences of the mammalian glucose transporters and the wider superfamily of sugar transporters have been outlined previously in section 1.4.2. There are a number of highly conserved regions, ranging from single residues to various sequence motifs (Table 1.1). It was also mentioned in section 1.4.2 that the repetition of such sequences in the N- and C-terminal domains may represent the occurrence of an ancient gene duplication event. Such high conservation of these motifs suggest that they may be involved in transporter function, thus making them obvious targets for mutagenesis. A number of strategies have been employed ranging from substitution of individual residues to replacement or removal of entire domains and construction of chimeric transporters. Such efforts to elucidate the relationship between transporter structure and function has produced a whole range of phenotypic effects which will be discussed in the relevant chapters of this thesis.

1.9 Tertiary Structure of GLUT1.

As described, there is much evidence in support of the occurrence of large conformational changes in transporter structure as a consequence of ligand binding and transport catalysis. Such structural alterations are too large to be accounted for by the localised movement of amino acid side chains. Various molecular modelling and molecular dynamics techniques have been applied to assess the conformational flexibility of GLUT1 (Hodgson *et al.*, 1992). Such theoretical studies have highlighted transmembrane helix 10 as containing a Pro-Gly rich, flexible region which may act as a pivotal point around which helices can pack to alternately expose the endofacial and exofacial binding sites (Gould & Holman, 1993).

It has been suggested that the cytoplasmic region at the base of helix 12 packs against the bottom of helix 10. This blocks the cytochalasin B binding site and exposes the exofacial binding site comprising helices 7, 8 and 9. Conversely in the endofacial conformation, the cytoplasmic tail at the base of helix 12 is predicted to move away from the

base of helix 10, thus enabling cytochalasin B to bind to this conformation. This model is consistent with conclusions drawn from the C-terminally truncated GLUT1 study in which the mutant was found to be locked in an endofacial conformation (Oka *et al.*, 1990). It would also explain why the length of the cytoplasmic tail appears to be critical for correct formation of the exofacial binding site. In the truncated mutant, the tail is not long enough to pack against the endofacial binding site, which consequently remains exposed.

In the absence of any three-dimensional crystallographic structural data, the arrangement of the transmembrane α -helices in GLUT1 remains to be elucidated. Several hypothetical models have been predicted but, unfortunately, none are entirely consistent with the mutagenic, structural and kinetic data. The most recent attempts have made use of computer modelling and recent advances in protein structure prediction algorithms to generate low-resolution structural models of the transmembrane domains of GLUT1. Two models have been proposed which seem to fit many of the biochemical and biophysical observations made with this protein. Several criteria are considered including the physical dimensions and water-accessibility of the channel, lengths of loops connecting helices, macrodipole orientation in a four-helix bundle motif and the helical packing energy. Five transmembrane helices are predicted to line a channel and the remaining helices pack around them (Figure 1.7). The channel is lined either by helices 3, 4, 7, 8 and 11 (model 1) or helices 2, 5, 7, 8 and 11 (model 2). It is interesting to note that helices 7, 8 and 11, which are predicted to be highly amphipathic, are predicted to line the channel in both models. The other two helices are provided by the N-terminal domain. In addition, in both models, the helices that are frequently labelled, helices 8-10, are proposed to lie adjacent to one another. Although these models are consistent with much of the mutagenic data, they are purely speculative in the absence of any crystal structures. They do, however, provide a template for the design of further biochemical and biophysical studies to probe the structure and function of these proteins.

1.10 Oligomerisation of GLUT1.

GLUT1 protein recovered from erythrocytes by cholate solubilisation of membranes and purified by size exclusion chromatography and sucrose gradient ultracentrifugation can be reconstituted in proteoliposomes. The resulting protein complex displays transport activity and D-glucose inhibitable cytochalasin B binding (Herbert & Carruthers, 1991). Analysis of the particle size of these complexes by target size analysis of radiation-inactivation of GLUT1, indicate that, under different reducing conditions, the transporter can exist as dimeric or tetrameric assemblies of a 55kDa monomer. Hydrodynamic studies of cholate solubilised GLUT1, the use of conformationally specific antibodies and chemical cross-linking of membrane resident GLUT1 suggest that the native transporter exists as a tetramer (Herbert & Carruthers, 1992). In this state, the GLUT1 complex can bind one molecule of cytochalasin B per two molecules of GLUT1 and presents at least two binding sites to D-glucose. Upon reduction to the dimeric form, cytochalasin B binds with a stoichiometry of 1 molecule per GLUT1 molecule and a single population of glucose binding sites are presented.

A model has been proposed for the interaction of monomeric subunits in the dimeric and tetrameric forms (Figure 1.8). In the dimer, the monomers can isomerise between the exofacial and endofacial conformations independently of each other. Cytochalasin B binds to the endofacial conformation and gives rise to the observation that cytochalasin B binds to GLUT1 with a stoichiometry of 1:1 in this state. In the tetramer, conformationally active parts of each monomer are constrained by the interaction of the subunits. This results in coupling of the isomerisation events between the exofacial and endofacial conformations in the two dimers that constitute the tetramer. Therefore, each dimer presents an exofacial and endofacial binding site simultaneously with an antiparallel arrangement, i.e. isomerisation of one subunit from an exofacial to endofacial conformation induces reorientation of the adjacent subunit in the opposite direction.

Carruthers suggested that the major physiological form of GLUT1 in erythrocytes is the tetramer, and that this isoform is 2- to 8-fold catalytically more active than the dimer. This model is consistent with most of the kinetic data on substrate binding (Herbert &

Carruthers, 1992). A physiological advantage of this system is that the rate-limiting step in the transporter turnover cycle, i.e. reorientation of the unloaded carrier, is accelerated due to the coupled isomerisation events between the subunits. The differences observed between the kinetics of purified and reconstituted GLUT1 and the native GLUT1 in intact erythrocytes can also be rationalised by this model. The catalytic turnover (k_{cat}) of the reconstituted protein is 20-fold lower than that of the native transporter in erythrocytes (Connolly *et al.*, 1985; Herbert & Carruthers, 1992; Wheeler and Hinkle, 1981)

The presence of a single intramolecular disulphide bridge between Cys³⁴⁷ and Cys⁴²¹ has been proposed to stabilise the tetramer (Zottola *et al.*, 1995). This observation is somewhat questionable due to the finding that a GLUT1 Cys-less mutant displays wild type kinetics and is capable of accelerated exchange (Due *et al.*, 1995a). Thus, the role of a putative disulphide bond in facilitating accelerated exchange is unclear.

Several studies have been undertaken to address the question as to whether the other GLUT isoforms are capable of forming oligomeric structures. Such studies have made use of mutagenic techniques and heterologous expression systems. For example, the possibility of interactions between GLUT1 and GLUT4 was investigated by engineering two GLUT1/GLUT4 chimeric proteins which were expressed in CHO cells. The chimeras consisted of N-terminal GLUT1 sequence with the C-terminal 29 or 294 amino acids replaced with those of GLUT4. Both mutants co-immunoprecipitated with native GLUT1 using an anti-GLUT4 C-terminal peptide antibody. The N-terminal 199 residues of GLUT1 were concluded to contain the sequence governing subunit interactions. No co-immunoprecipitation of native GLUT1 and GLUT4 was detected in 3T3-L1 cells using the same antibody, suggesting that GLUT1 can form homodimers but not heterodimers *in vivo* (Pessino *et al.*, 1991).

GLUT2 and GLUT3 can be heterologously expressed in *Xenopus* oocytes where they exhibit distinct kinetic profiles (Burant & Bell, 1992; Colville *et al.*, 1993b). Simultaneous expression of the two isoforms in oocytes results in a kinetic pattern that can be separated into two components attributable to each isoform. Thus, in this system at least, GLUT2 and GLUT3 do not interact to form heterodimers. Further evidence supporting the occurrence of monomeric GLUT3 comes from a study in which wild-type GLUT3 was

heterologously co-expressed with a transport-deficient GLUT3 mutant. The observed kinetics were indistinguishable from those exhibited by wild-type GLUT3, even when a 3-fold excess of the mutated mRNA was injected (Burant & Bell, 1992).

1.11 Aims of this Study.

The basis of this study, initially, is to investigate the role of proline residues in GLUT3 transporter function. All members of the mammalian GLUT isoforms contain several highly conserved proline residues, and many of these are located within putative transmembrane segments of the protein. Transmembrane proline residues are of particular interest because they are proposed to have a characteristic structural and/or dynamic role in the function of various membrane transport proteins. Isomerisation of the peptide bonds formed by this unique imino acid has been suggested to endow regions of proteins with conformational flexibility which may be crucial for transporter function. Since this isomerisation event is unique to Xaa-Pro peptide bonds, then replacement of the proline residue of interest should, in effect, remove the flexibility around this peptide bond. Proline residues of interest will be replaced by alanine by site directed mutagenesis utilising mutagenic oligonucleotides and recombinant PCR methodology. Transmembrane proline residues of helix 10 will be targeted for mutagenesis in addition to other proline residues that are located close to the endofacial side of the membrane within highly conserved motifs. Heterologous expression in the *Xenopus laevis* oocyte system will enable kinetic characterisation of the transporters. Two such studies investigating the role of transmembrane proline residues of GLUT1 have recently been reported. However, an extensive kinetic characterisation of the Pro-Ala mutants generated in these studies was not carried out and it is therefore possible that subtle structural effects caused by the mutations have been overlooked. GLUT3 Pro-Ala mutants generated in this study will be investigated with the use of site-specific ligands to highlight effects mediated at the exofacial and endofacial substrate binding sites.

In an effort to further characterise the kinetics of the GLUT3 Pro-Ala mutants, a protocol will be designed for the isolation of plasma membranes from *Xenopus* oocytes.

This will enable quantitation of the transporter proteins expressed at the plasma membrane, thus enabling turnover numbers to be calculated. This is an important and useful parameter to measure when characterising mutant transporter proteins, since the effect of the mutation can be manifested in aspects of the transport cycle other than the substrate binding events. The isolation of pure plasma membrane fractions in this laboratory (and others), has previously proved to be problematic, mainly due to the nature of the oocyte which contains a high amount of glutinous yolk proteins. Subcellular fractionation of oocytes expressing GLUT3, in combination with quantitative immunoblotting against membrane fractions expressing known amounts of GLUT3, will be used in an attempt to quantify the heterologously expressed glucose transporters at the plasma membrane.

GLUT2 and GLUT3 have previously been demonstrated to exhibit differential substrate specificities and isoform specific kinetics. In an effort to address the structural basis of substrate selectivity, a series of GLUT2/GLUT3 chimeric transporters have previously been constructed in this lab (Dr.M.Arbuckle, Glasgow University). The partial kinetic characterisation of the GLUT3-series of chimeric transporters expressed in oocytes has already been reported (S.Kane, Ph.D. Thesis, 1997, Glasgow University). However, expression of the entire GLUT2 series was not achieved due to expression problems encountered for two of the chimeras in this series. In an effort to address this problem, the relevant chimeras will be regenerated, sequenced and subcloned into vectors suitable for expression in oocytes.

The use of an alternative expression system for a more detailed analysis of the various mutants will be investigated. The establishment of stable cell lines expressing GLUT2, GLUT3 and the GLUT3 chimeras will be undertaken. Simple and reproducible protocols for subcellular fractionation of CHO-cells are available, thus enabling quantitation of transporters expressed at the plasma membrane and therefore measurement of turnover numbers. This system is also more convenient for photolabelling of transporters with cytochalasin B and ATB-BMPA. Thus, establishment of stable cell lines expressing wild type and mutant transporter proteins will provide a useful system in which to extend the studies that are not possible utilising the oocyte system.

Figure 1.1

Interaction of β -D-glucose at the Exofacial Binding Site of GLUT1.

This diagram shows the hydrogen bonding interactions formed between β -D-glucose and the exofacial binding site of GLUT1, and is based on a model proposed by Barnett *et al.* Hydrogen bonds form between the transporter and the sugar hydroxyls of carbons C-1, C-3 and C-4. The ring oxygen of the sugar is also involved. Possible hydrophobic interactions between the transporter and the sugar at the C-6 position have also been suggested (Barnett *et al.*, 1973). Hydrogen bonds are represented by dotted lines, and the C-6 hydrophobic interactions are illustrated as a dashed area.

Figure 1.1

Interaction of D-Glucose at the Exofacial Binding Site of GLUT1.

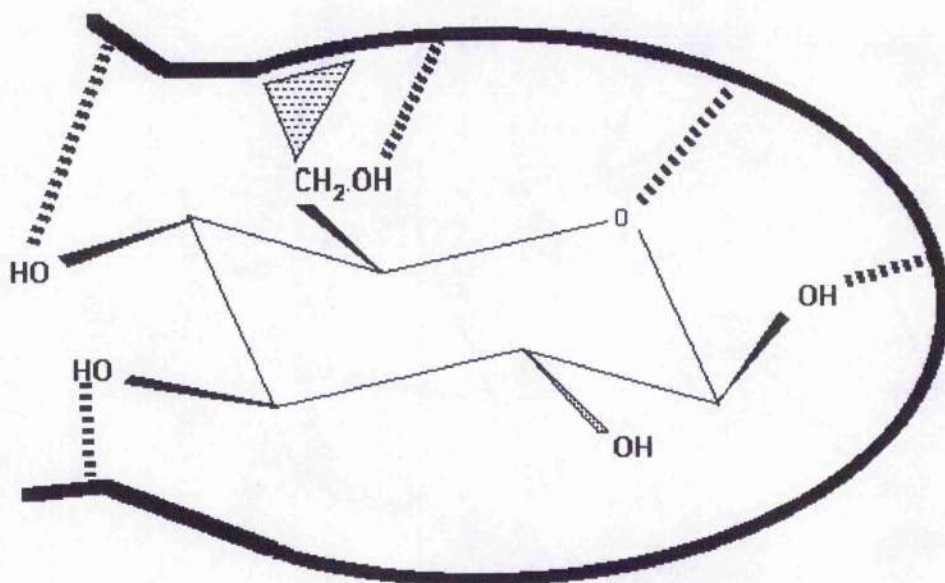


Figure 1.2

Topological Model of the Mammalian Facilitative Glucose Transporters.

This model is based on the results of hydropathy analysis of GLUT1 (Mueckler *et al.*, 1985), and has been confirmed by glycosylation scanning mutagenesis. Since the hydropathy plots of GLUT1 and GLUTs 2, 3, 4, and 5 are virtually superimposable, it is assumed that the model is applicable to all the isoforms in the glucose transporter family. The diagram shows the twelve predicted transmembrane helices as boxes, numbered 1-12. The amino- and carboxy-termini (labelled NH₂ and COOH respectively) are located on the cytoplasmic side of the membrane. The N- and C-terminal "halves" of the structure are separated by the large central cytoplasmic loop between helices 6 and 7. The large loop connecting helices 1 and 2 is exofacial and contains a site for *N*-linked glycosylation. This site is labelled "CHO" in the diagram. Invariant residues are shown by their single letter abbreviations.

Topological Model of the Mammalian Facilitative Glucose Transporters.



Figure 1.3

Single-Site Alternating Conformation Model for GLUT1-Mediated D-Glucose Influx.

The diagram is a schematic representation describing the conformational changes associated with transport of D-glucose mediated by GLUT1 and the other isoforms. Glucose binds at an exofacial site on the transporter which induces a conformational change such that D-glucose is presented at the endofacial side of the transporter. Dissociation of glucose from the endofacial binding site is followed by the substrate-independent re-orientation of the carrier such that the binding site is once again exposed to the exofacial side of the transporter.

Figure 1.3
Single-Site Alternating Conformation Model for GLUT1-Mediated D-Glucose Influx.

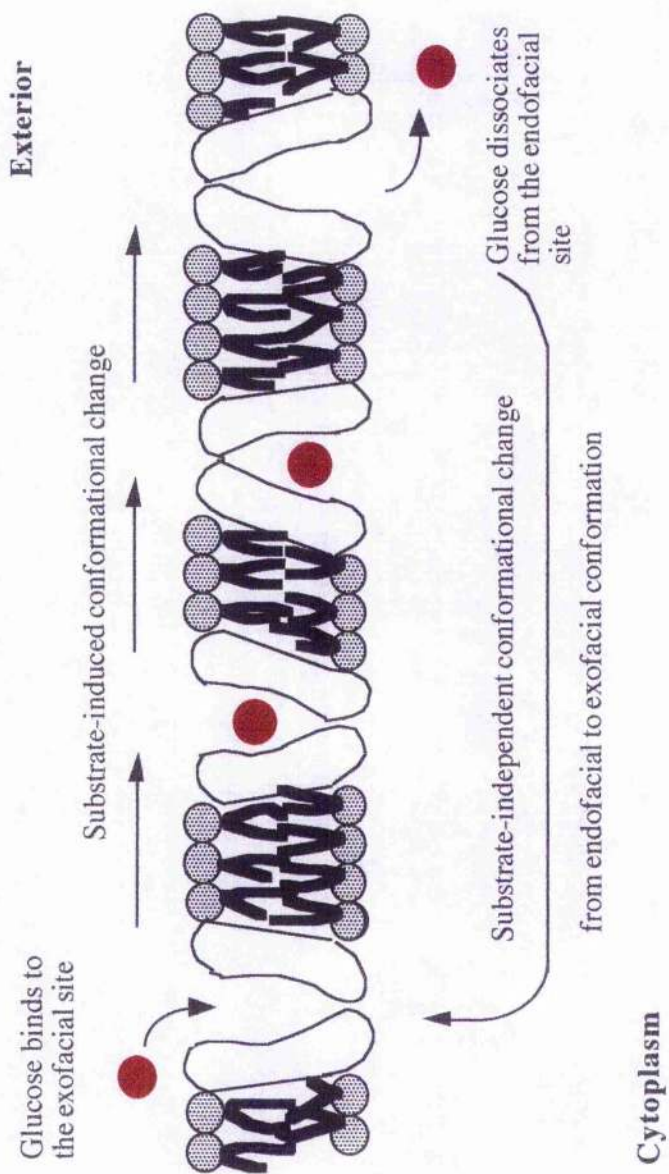


Figure 1.4

King-Altman Representation of the Glucose Transport Cycle.

This figure shows a King-Altman diagram of the alternating conformation model of GLUT1. T_O represents the transporter in the outward-facing conformation, in the absence of substrate. T_OS represents the transporter in the outward-facing conformation, in the presence of substrate. T_i and T_iS represent the transporter in the inward-facing conformation, in the absence and the presence of substrate, respectively. K_{SO} and K_{Si} represent the dissociation constants of substrate (i.e. D-glucose), at the exofacial and endofacial binding sites, respectively. The rate constant for the re-orientation of the unloaded transporter from the outward-facing conformation to the inward-facing conformation is denoted as k_1 . Re-orientation of the empty carrier from the inward-facing conformation to the outward-facing conformation is denoted as k_{-1} . The rate constants for the movement of loaded transporter from the outward-facing conformation to the inward-facing conformation and back again, are denoted as k_2 , and k_{-2} , respectively. The values of these constants, measured for GLUT1 at 0 °C are shown below (Lowe & Walmsley, 1986).

Rate Constant	Value at 0 °C (s ⁻¹)
k_1	12.1 ± 0.98
k_{-1}	0.726 ± 0.498
k_2	1113 ± 498
k_{-2}	90 ± 3.47

Figure 1.4

King-Altman Representation of the Glucose Transport Cycle.

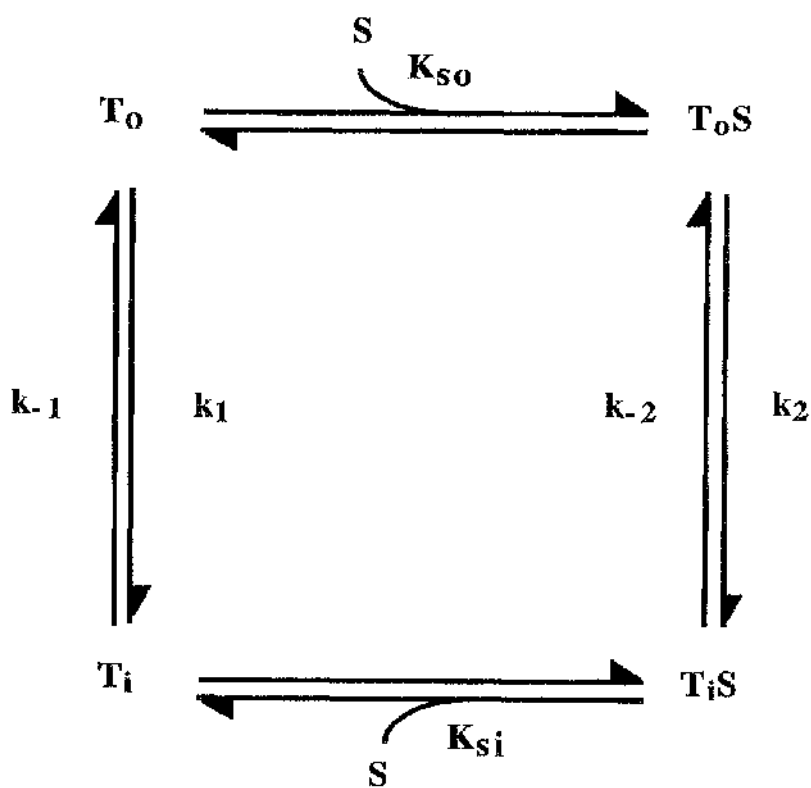


Figure 1.5

Structures of Cytochalasin B and ATB-BMPA.

The structures of the site-specific inhibitors cytochalasin B and ATB-BMPA are shown. These compounds interact competitively with glucose at the endofacial and exofacial binding sites, respectively. They are reported to bind to the transporter specifically at these sites and, upon exposure to ultra-violet illumination, can be covalently attached.

Figure 1.5

Structures of Cytochalasin B and ATB-BMPA.

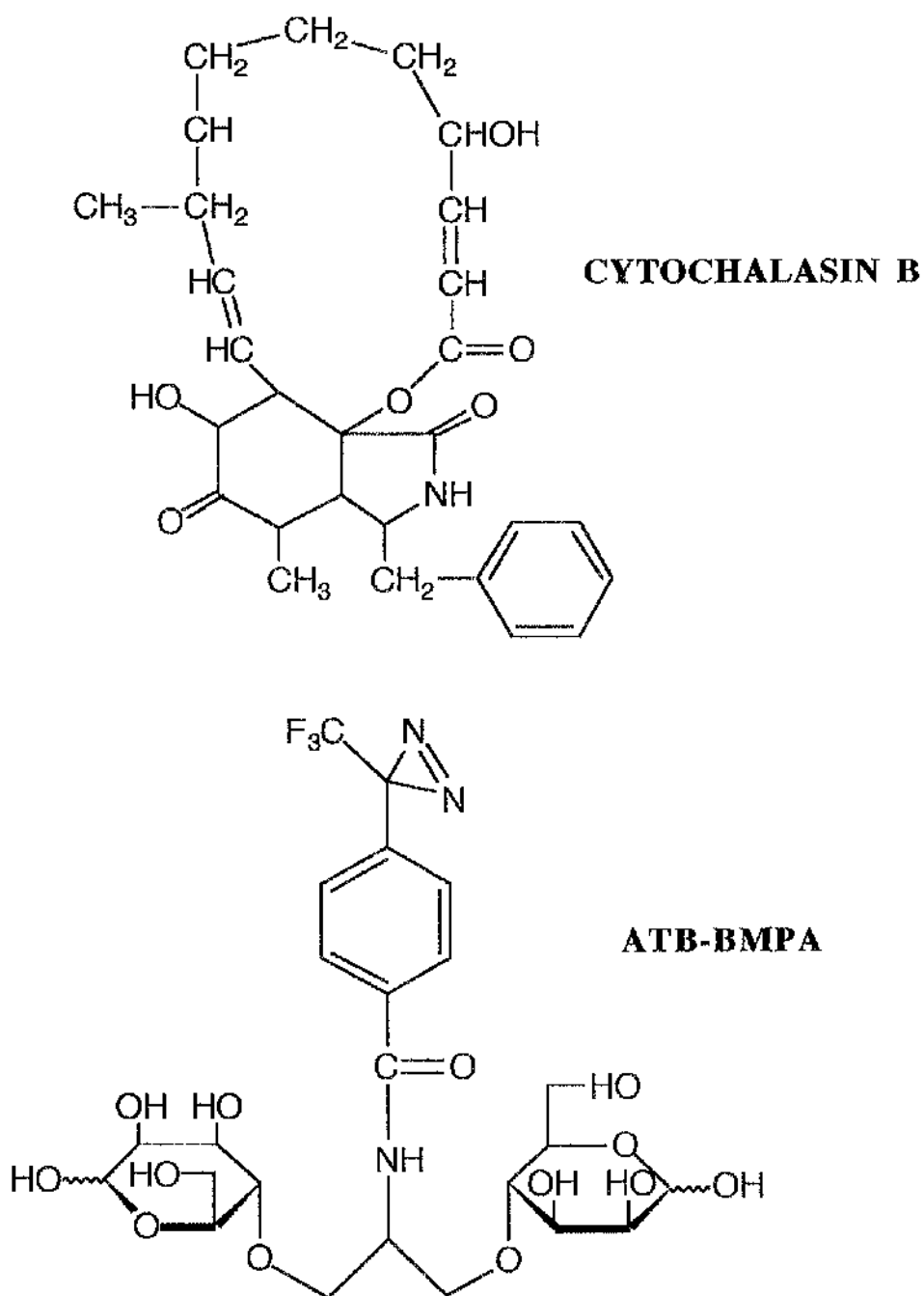


Figure 1.6

Diagram Showing Regions of Importance in the Transporter Structure.

This diagram shows regions of the transporter which have been reported to be involved in formation of the exofacial and endofacial binding sites, as demonstrated by studies using conformational-specific ligands ATB-BMPA, forskolin, and cytochalasin B. Also shown are regions important in the ability of the transporter to undergo conformational changes.

Figure 1.6
Diagram Showing Regions of Importance in the Transporter Structure.

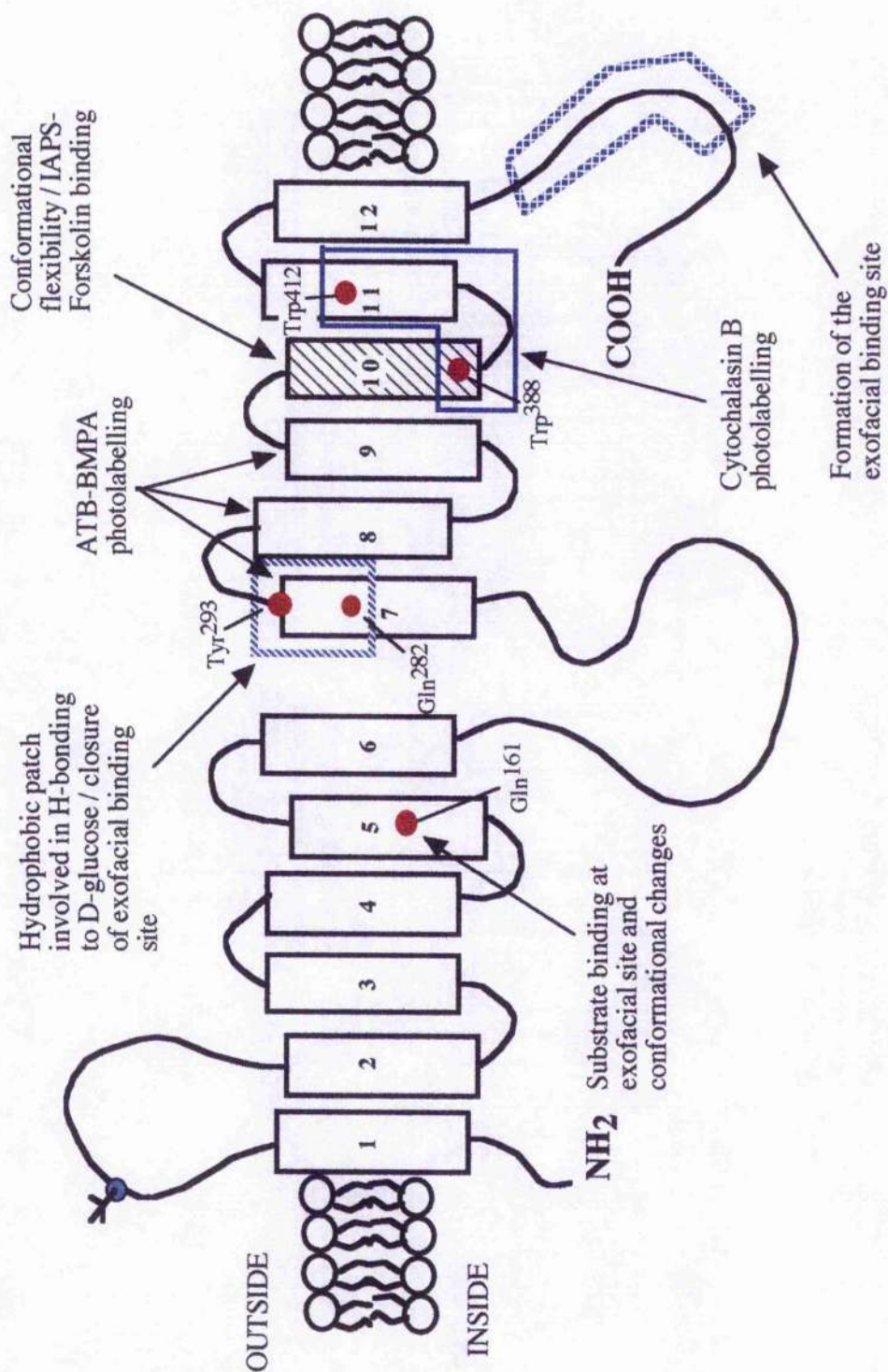


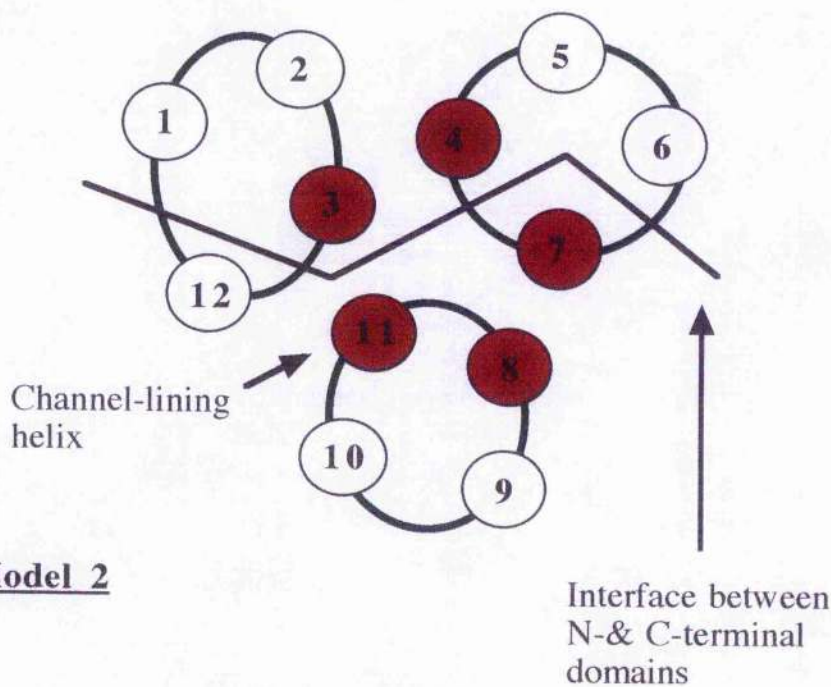
Figure 1.7

Speculative Model for the Arrangement of Transmembrane α -Helices in GLUT1.

This is a diagrammatic representation of the exoplasmic view of two proposed models for the tertiary structure of GLUT1 in the membrane. Both models fit many of the biophysical and biochemical data available for this protein. Model 2 incorporates a structural role for the large central cytoplasmic loop which serves to locate helix 7 near to helices 1 and 2 on the far side of the protein relative to helix 6. It also has a bilobular symmetry, as reflected in the hydropathy profile, and is consistent with that proposed for the *lac* permease of *E.coli*. The models emphasise the physical dimensions and water accessibility of the channel, loop lengths between transmembrane helices, macrodipole orientation in the 4-helix bundle motifs, and helical packing energy. Both models predict that the channel is lined by five helices (shown in red), either helices 3, 4, 7, 8 and 11 in model 1 or 2, 5, 11, 8 and 7 in model 2. The remaining helices surround the channel forming helices and provide a packing surface for their arrangement. Each model is composed of three 4-helix bundles (shown in green) which assemble together to form the aqueous channel for glucose passage. The bundle formation is different in the 2 models- in model 1 adjacent helices in sequence form the bundles whereas in the second model, helices far apart in sequence form bundles, with helix 5 and helix 11 occurring in two bundles.

Figure 1.7
Speculative Model for the Arrangement of Transmembrane α -Helices in GLUT1.

Model 1



Model 2

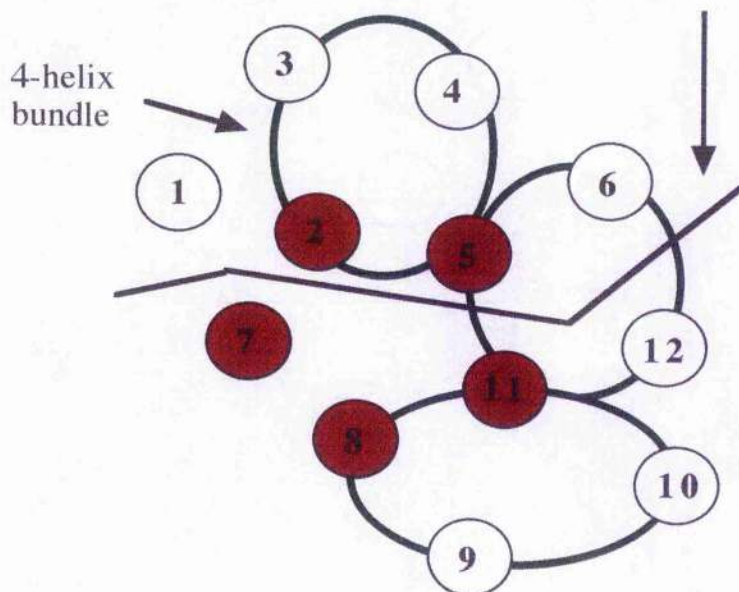


Figure 1.8

Diagram Showing the Proposed Model for GLUT1 Oligomerisation.

This diagram shows a representation of the two oligomeric structures that GLUT1 can exist in, as described in the model proposed by Carruthers. GLUT1 can exist as a dimer or a tetramer. Each of the two molecules of GLUT1 that exist in the dimer can isomerise independently of the other. Hence in this situation, both transporters can be outward-facing or inward-facing at the same time. Alternatively, one may be outward-facing whilst the other is inward-facing. In the tetrameric form however, the subunits are conformationally linked. The tetramer is effectively composed of two dimers of GLUT1, but the subunits of these dimers are coupled so that isomerisation of one subunit results in the isomerisation of the adjacent subunit. Therefore, in the tetramer, two of the GLUT1 subunits will be outward-facing, and two will be inward-facing. Glucose binding to any of these subunits will induce conformational changes in that subunit, and also in the adjacent subunits. The result of this is that every re-orientation of a GLUT1 subunit from the outward-facing conformation to the inward-facing conformation is accompanied by the linked movement of another subunit into the outward-facing conformation. The diagram indicates that from the evidence put forward by Carruthers, tetrameric GLUT1 can be converted to dimeric GLUT1 under reducing conditions.

Figure 1.8
Diagram Showing the Proposed Model for GLUT1 Oligomerisation.

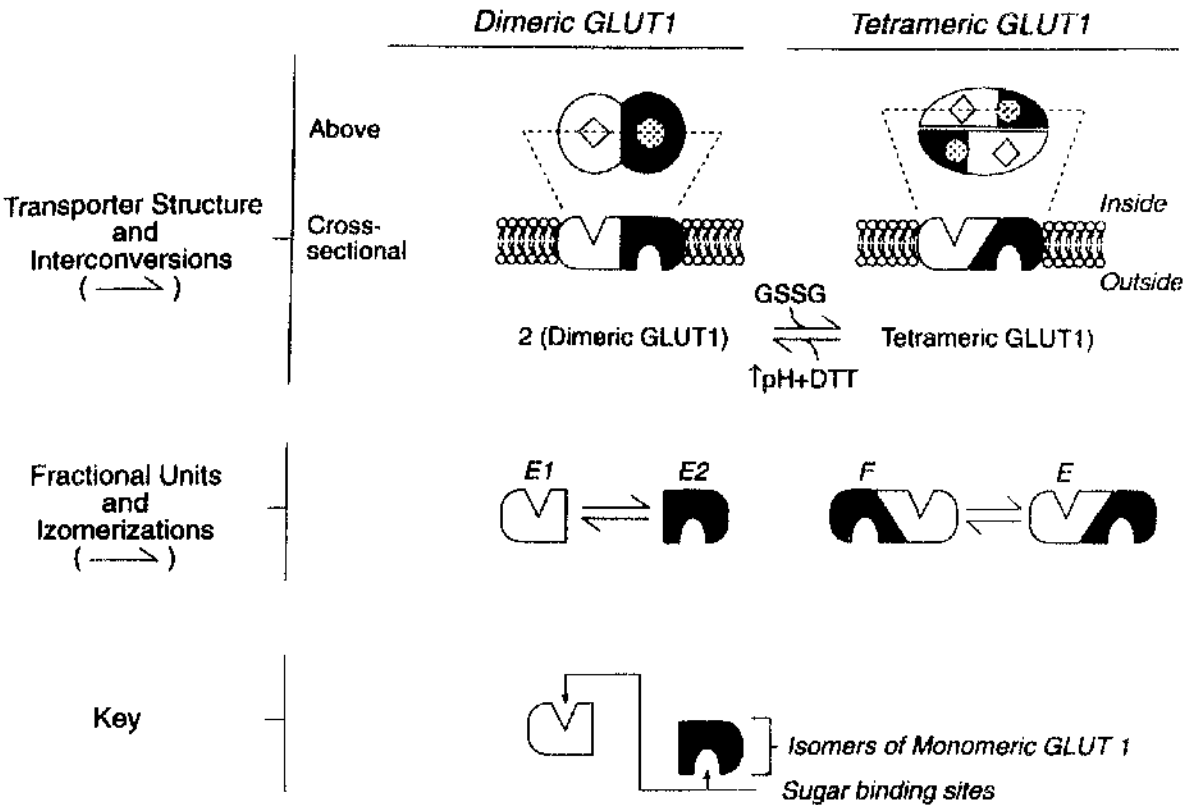


Table 1.1

Conserved Motifs Present in the Mammalian Facilitative Glucose Transporters.

Motif	Location	Function
GRRK	Intracellular loops connecting TM2-3 and TM7-8	Conformational stability
EXXXXXXR	Intracellular loops connecting TM4-5 and TM10-11	Conformational stability and salt bridging between helices
PESPR	Intracellular loop at the base of TM6	Conformational stability
QQXS GXNXXY	TM7	Exofacial substrate binding and closure of exofacial binding site
VPETKG	C-terminal cytoplasmic loop	Conformational stability
GPGPIP	TM10	Conformational flexibility

CHAPTER 2

Materials and Methods

1 - Molecular Biology and Use of *Xenopus laevis* Oocytes.

2.1 Materials.

Adult female *Xenopus laevis* were obtained from either Blades Biologicals, Edenbridge, Kent, UK, or directly from South Africa, (African *Xenopus* Facility, PO Box 118, Noordhoek, Republic of South Africa). "Frog Brittle" was also obtained from Blades Biologicals.

Tricaine Methane Sulphonate, MS222 was supplied by Thompson & Joseph Ltd., Norwich, UK.

Chromic sterile catgut® was supplied by Ethicon Ltd., London, UK.

2-deoxy-D-glucose, β -D-fructose, maltose, phloretin, kanamycin, ampicillin, tetracycline, dithiothreitol, collagenase, cytochalasin B, were supplied by Sigma Chemical Company, Poole, Dorset, UK.

Ammonium formate, and chloroform (Analytical Reagent) were supplied by BDH, Poole, UK.

Bacto®-tryptone, Bacto®-agar and Bacto®-yeast extract were supplied by Difco, East Molesey, Surrey, UK.

Tris was supplied by Boehringer Mannheim GmbH., Lewes, East Sussex, UK.

Agarose (electrophoresis grade), DNA ligase and 5x ligase buffer were supplied by Gibco BRL, Paisley, UK.

Lambda ladder (*Bst*E II digested) and ribonuclease A were supplied by New England Biolabs, Hitchin, Herts, UK.

Sequencing grade urca, Tris, EDTA, de-ionised formamide, and TEMED were obtained from International Biotechnologies Inc. Ltd. (IBI), Cambridge, UK.

National Diagnostics Sequagel-6™ 6% sequencing gel solution and Sequagel™ Complete Buffer Reagent were obtained from BS&S, Edinburgh, UK.

Ultima-flo AF scintillant was obtained from Canberra Packard Ltd., Pangbourne, Berks., UK.

Taq DyeDeoxy™ Terminator Cycle Sequencing kits and sequencing-grade phenol/chloroform/H₂O (68:18:14) was obtained from Applied Biosystems Inc. (ABI), Warrington, Cheshire, UK.

Plasmid Maxi Preparation Kits were supplied by QIAGEN, UK.

Elutip-D DNA purification columns (Schleicher & Schuell) were obtained from Anderman Ltd, London, UK.

Permacel™ tape was obtained from Genetic Research Instruments, Dunmow, Essex, UK.

Alconox™ detergent was supplied by Aldrich Chemical Company Ltd., Gillingham, Dorset, UK.

'Native' *Pfu* DNA polymerase and 'Native' *Pfu* polymerase 10x buffer were obtained from Stratagene, Cambridge, UK.

Vent DNA Polymerase was supplied by New England Biolabs Inc., Beverly, M.A.

All restriction enzymes and corresponding 10x buffers, *Taq* DNA polymerase with supplied 10x buffer and MgCl₂, calf intestinal alkaline phosphatase and 10x buffer, polynucleotide kinase and polynucleotide kinase 10x buffer, rNTPs, dNTPs, nuclease-free H₂O, 5x transcription buffer, dithiothreitol (DTT), RNasin, RNA ladder (360-9,490 bases) and SP6 RNA polymerase were supplied by Promega, Southampton, UK.

[2,6-³H]2-deoxy-D-glucose, [U-¹⁴C]D-fructose and [U-³H]D-galactose were supplied by DuPont NEN, Stevenage, Herts, UK.

Dialysis tubing (Visking size 1-8/32") was supplied by Medicell International Ltd, London, UK.

Sterile Acrodisc® 0.2 µm filters were supplied by Gelman Sciences Ltd., Northampton, UK.

Sodium diguanosine triphosphate, GpppG (5' Cap) was supplied by Pharmacia, Milton Keynes, UK.

All oligonucleotides (Tables 3.3 and 3.4) were synthesised by Dr. V. Math, Department of Biochemistry, University of Glasgow.

NHS-LC-biotin and sulfo-NHS-biotin were supplied by Pierce and Warriner (U.K.) Limited, Chester.

2.2 Recombinant Polymerase Chain Reaction.

2.2.1a Synthesis of Oligonucleotides.

Oligonucleotides (15'mers) with identical sequence to GLUT3 in the region of the proline residue of interest were synthesised (Dr. V. Math, Department of Biochemistry, University of Glasgow). The oligonucleotides were designed such that the base triplet encoding the proline contained a single base change such that alanine was incorporated in its place (Table 3.3). This base change was located towards the centre of the oligonucleotide. Pairs of oligonucleotides were constructed encoding the same codon change: one sequence representing the sense strand and another the complementary strand. These oligonucleotides will subsequently be referred to as internal mutagenic primers. In addition, an oligonucleotide (37'mer) was constructed which had positive polarity and a sequence complementary to the 5' untranslated region of GLUT3. An antisense oligonucleotide complementary to the 3' untranslated end of GLUT3 was synthesised (Figures 3.4-3.5). Both of these oligonucleotides, referred to as external primers G3-start and G3-end respectively, incorporated a *Sal* I restriction site at their 5' end for cloning purposes (Table 3.3).

2.2.1b Precipitation of Oligonucleotides.

Oligonucleotides (stored in 0.88M aqueous NH_4OH) were prepared for use in PCR reactions by ethanol precipitation. 360 μl of the oligonucleotide was added to an Eppendorf tube containing 40 μl 3M sodium acetate, pH5.5 and 1.2mls ice cold absolute ethanol. The solutions were mixed thoroughly before incubation at -20°C for at least 1 hour. The DNA was pelleted by centrifugation at 16,000 $\times g_{av}$ in a microfuge for 30 mins. The pellet was washed with 70% ethanol, dried in air for 5 mins and resuspended in 100-250 μl sterile H_2O , depending on the yield.

2.2.1c Quantitation of Oligonucleotides.

The OD_{260nm} was determined for each oligonucleotide. From this value the concentration of the solution can be calculated, since an OD_{260nm} of 1 is equal to 33.3mg/ml. Measurement of the OD_{280nm} value allows an estimation of the purity of the solution from the OD₂₆₀/OD_{280nm} ratio (the closer the ratio is to 2, the more pure the solution is).

2.2.2 Primary Polymerase Chain Reactions Using *Taq* DNA Polymerase.

2.2.2a Reaction Conditions.

1.6μg	"internal" primer
1.6μg	"external" primer
100ng	template pSPGT3 dsDNA
1μl	dNTPs (20mM dATP, 20mM dCTP, 20mM dGTP, 20mM dTTP)
10μl	10x <i>Taq</i> DNA polymerase buffer (Mg ²⁺ -free)
6μl	25mM MgCl ₂
2.5 units	<i>Taq</i> DNA polymerase
sterile water to a final volume of 100μl	

Two identical primary PCR reactions were carried out using either the internal primer corresponding to the antisense strand in conjunction with G3-start, or the internal primer corresponding to the sense strand in conjunction with G3-end. Reactions were carried out in 0.5ml microfuge tubes and components were added in the above order, adding *Taq* DNA polymerase last. Upon completion of the thermal cycling program (see below), 20μl of 5x DNA gel loading buffer was added to each reaction and mixed, before loading the entire reaction volume onto a 1.6% agarose gel. Following electrophoresis (section 2.2.6a), cDNA bands were identified by size and excised from the gel, electro-cluted (section 2.2.6b),

purified (section 2.2.6d) and precipitated (section 2.3.3). DNA solutions obtained from 3 reactions were combined and passed through the same Elutip-d column (section 2.2.6d) and the final DNA pellet was resuspended in a volume of 60 μ l of sterile H₂O. 3 μ l of this was analysed by 1% agarose gel electrophoresis to assess the yield of the primary PCR product.

2.2.2b Thermal Cycling.

Tubes were placed in a Techne PHC-3 Thermal Cycler with a heated lid. The machine was programmed as follows: -

Initial Melt	95°C	3 min
--------------	------	-------

Cycling- (30 cycles total, with a ramp rate of 1°C/sec)

Separation	95°C	1 min
------------	------	-------

Primer Annealing	X°C	30 secs
------------------	-----	---------

Extension	72°C	2 min
-----------	------	-------

Final Extension	72°C	2 min
-----------------	------	-------

Soak	4°C	Hold
------	-----	------

"X" = 0-5°C below the melting temperature of the oligonucleotide having the lower melting temperature.

2.2.3 Secondary Polymerase Chain Reactions Using *Taq* DNA Polymerase.

2.2.3a Reaction Conditions.

1.6 μ g	G3-start (external primer)
1.6 μ g	G3-end (external primer)
100ng	template (5' primary product)
100ng	template (3' primary product)
1 μ l	dNTPs (20mM dATP, 20mM dCTP, 20mM dGTP, 20mM dTTP)
10 μ l	10x <i>Taq</i> DNA polymerase buffer (Mg ²⁺ -free)
6 μ l	25mM MgCl ₂
2.5 units	<i>Taq</i> DNA polymerase
sterile water to a final volume of 100 μ l	

Secondary PCR reactions were carried out using a similar procedure as described for the primary reactions, except that the two primary products both act as templates in a single secondary PCR reaction. G3-start and G3-end are the primers used to amplify the full-length secondary product. During the first few cycles of the chain reaction, the two primary products denature and re-anneal at their complementary sequences, i.e. the 3' end of the 5' primary product (encoding the N-terminal portion of GLUT3) anneals to the 5' end of the 3' primary product (encoding the 3' portion of GLUT3) (Figure 3.5). Following 3' extension from the annealing site, using the other strand as a template for this extension, the strands denature and associate with the external primers for amplification of the full-length product. The thermal cycling parameters were modified to include a lower annealing temperature for the first 3 reaction cycles. Six identical reactions were carried out for each mutant to obtain enough secondary product to carry out the subsequent cloning procedures.

Upon completion of the thermal cycling program, the reaction products were treated in exactly the same way as described for the primary fragments, except that the final purified product was resuspended in a total volume of 20 μ l.

2.2.2b Thermal Cycling.

Tubes were placed in a Techne PHC-3 Thermal Cycler with a heated lid. The machine was programmed as follows:-

Initial Melt	95°C	3 min
--------------	------	-------

Cycling- (3 cycles total, with a ramp rate of 1°C/sec)

Separation	95°C	1 min
Primer Annealing	37°C	30 secs
Extension	72°C	2 min

Cycling- (27 cycles total, with a ramp rate of 1°C/sec)

Separation	95°C	1 min
Primer Annealing	X°C	30 secs
Extension	72°C	2 min

Final Extension	72°C	5 min
Soak	4°C	Hold

"X" = 0-5°C below the melting temperature of the oligonucleotide having the lower melting temperature.

2.2.4 Primary Polymerase Chain Reactions Using *Pfu* DNA Polymerase.

2.2.4a Reaction Conditions.

1.6 μ g	"internal" primer
1.6 μ g	"external" primer
10ng	template pSPGT3 dsDNA
1 μ l	dNTPs (20mM dATP, 20mM dCTP, 20mM dGTP, 20mM dTTP)
10 μ l	10x <i>Pfu</i> DNA polymerase reaction buffer
2.5 units	<i>Pfu</i> DNA polymerase
sterile water to a final volume of 100 μ l	

Oligonucleotide primers used were identical to those described for use with *Taq* DNA polymerase. Reaction components were added to sterile 0.5ml microfuge tubes in the above order, adding the polymerase after the initial 10 min separation step (see below). This is referred to as "Hot Start PCR". Tubes were vortexed briefly to mix their contents and placed in a Techne PHC-3 Thermal Cycler with a heated lid. On completion of the thermal cycling programme (section 2.2.4b), 20 μ l of 5x DNA gel loading buffer was added to each reaction. The entire reaction volume was loaded onto a 1.6% agarose gel (section 2.2.6a). Following electrophoresis, cDNA bands were visualised under ultra-violet illumination, appropriate bands located and excised from the gel, electro-eluted (section 2.2.6b) and purified by passing through an Elutip-d column (section 2.2.6d) followed by ethanol precipitation (section 2.3.3). DNA solutions obtained from 3-6 reactions were combined and passed through the same Elutip-d column, and the final DNA pellet was resuspended in a volume of 60 μ l of sterile H₂O. 3 μ l of the final primary PCR product was further analysed by 1% agarose gel electrophoresis to assess the recovery of the purified product.

2.2.4b Thermal Cycling.

Tubes were placed in a Techne PHC-3 Thermal Cycler with a heated lid. The machine was programmed as follows:-

Initial Melt	95°C	10min
--------------	------	-------

Addition of Pfu DNA polymerase

Cycling- (3 cycles total, with a ramp rate of 1°C/sec)

Separation	95°C	1 min
------------	------	-------

Reannealing	40°C	5 min
-------------	------	-------

Extension	72°C	5 min
-----------	------	-------

Cycling- (27 cycles total, with a ramp rate of 1°C/sec)

Separation	95°C	1 min
------------	------	-------

Reannealing	X°C	2 min
-------------	-----	-------

Extension	72°C	5 min
-----------	------	-------

Final extension	72°C	10 min
-----------------	------	--------

Soak	4°C	Hold
------	-----	------

"X" = 0-5°C below the melting temperature of the oligonucleotide having the lower melting temperature.

The main difference between the protocols used for *Taq* DNA polymerase and *Pfu* DNA polymerase is the stage at which the enzyme is added to the reaction mixture. With the later protocol, the enzyme is added after the initial melt and this is referred to as "Hot Start PCR" (section 3.4.3d).

2.2.5 Secondary Polymerase Chain Reactions Using *Pfu* DNA Polymerase.

2.2.5a Reaction Conditions.

1.6 μ g	G3-start (external primer)
1.6 μ g	G3-end (external primer)
1 μ l	template (5' primary product)
1 μ l	template (3' primary product)
1 μ l	dNTPs (20mM dATP, 20mM dCTP, 20mM dGTP, 20mM dTTP)
10 μ l	10x <i>Pfu</i> DNA polymerase reaction buffer
2.5 units	<i>Pfu</i> DNA polymerase
sterile water to a final volume of 100 μ l	

Secondary reactions were carried out as described for the primary reactions with the exception that the two primary PCR products, one 5' and one 3' product, were used as templates in the secondary reaction. The templates encode the N- and C-terminal portions of GLUT3 respectively and they are single-stranded, complementary and overlapping (Figure 3.5). Prior to addition of the two templates to the reaction mix, their relative concentrations were assessed by 1% agarose gel electrophoresis. The more concentrated template, usually the smaller fragment, was diluted to an approximately equal concentration as the other template such that approximately equimolar ratios were added in the secondary PCR reaction. This was found to be important in determining the overall yield of the secondary PCR reaction.

2.2.5b Thermal Cycling.

Thermal cycling parameters for the secondary PCR reaction were identical to those used for the primary PCR reactions.

2.2.6 Purification of PCR Fragments.

2.2.6a Separation of PCR Fragments by Agarose Gel Electrophoresis.

20 μ l of 5x DNA gel loading buffer was added to the PCR reaction mixture and mixed on completion of the cycling procedure. The entire reaction volume was loaded onto a 1.6 % agarose gel alongside a lambda ladder marker (section 2.3.2). A current of 100mA was applied until the dye front had migrated a suitable distance to obtain sufficient resolution of PCR fragments to enable excision from the gel with minimal contamination of non-specific products (Figure 3.6).

2.2.6b Elution of DNA Fragments from Agarose Gel Slices by Electrophoresis.

DNA fragments to be isolated were identified by size on the agarose gel under ultra-violet illumination. A gel slice containing the DNA band was excised from the gel and transferred to a piece of dialysis tubing, prepared as described in section 2.2.6c, sealed at one end using a clip. 1ml of 1x TAE buffer was added to the tubing which was then sealed at the other end. The tubing was transferred to an electrophoresis tank containing 1 litre of 1x TAE buffer (Table 2.1). A weight (e.g. a gel comb) was applied to ensure that the gel slices were completely submerged in the buffer. 150V was applied for 2 hours. The direction of the current flow was reversed for approximately 30 secs before transferring the DNA solution to a sterile eppendorf tube. At this point, the DNA solution was either stored frozen at -20°C or was passed through an Elutip-d column to further purify the DNA (section 2.2.6d).

2.2.6c Preparation of Dialysis Tubing for Electroelution.

Approximately 10g of dialysis tubing (Visking, size 2 Inf Dia 18/32") was cut into pieces of 3-4cm in length and transferred to a 500ml glass beaker. 500ml of 2% NaHCO₃, 10mM EDTA was added and the tubing was incubated in the boiling solution for 10mins.

After washing with distilled water, the tubing was stored in 50% ethanol, 50% water containing 1mM EDTA at 4°C. Prior to use the tubing was boiled in distilled water for 10 mins.

2.2.6d Purification of DNA Using Elutip-D Affinity Columns.

The DNA to be purified was extracted from the gel into 1x TAE buffer as described in section 2.2.6b. An Elutip-d affinity column was firstly prepared by gently forcing 1-2ml of high salt solution (Table 2.1) into the column. This serves to pre-wash the column matrix. A second syringe (5, 10 or 20ml depending on the sample size) was loaded with 5ml of low salt solution (Table 2.1) and this was passed through the column to ensure that all the high salt solution had been removed from the matrix before application of the DNA sample. The same syringe was loaded with the DNA sample and this, together with a 0.4 μ m cellulose acetate Elutip prefilter was attached to the column. Use of the filter ensures the removal of any particulates from the sample. All of the sample was forced through the filter and column at a flow rate of 1-2ml/min to ensure complete adsorption of the DNA to the column matrix. The same syringe was loaded with 2-3ml of low salt solution which was passed through the column, washing any remaining DNA sample from the filter and syringe into the column. 0.4ml of high salt solution was then passed through the column without the filter attached to elute the DNA from the matrix. The eluate was collected in a 1.5ml Eppendorf tube, and the DNA further concentrated by alcohol precipitation, as described in section 2.3.3.

2.3 General Techniques Used for Manipulation of cDNA.

2.3.1 Plasmid Constructs.

Human glucose transporter cDNAs encoding GLUTs 2 and 3 have been cloned into pSP64T as described previously (Krieg & Melton, 1984) to form pHTL217 and pSPGT3, respectively (Figures 2.1 and 3.4). These constructs contain the protein coding region of the

cDNAs and various amounts of the 5'- and 3'- untranslated regions. The cDNA sequences are flanked by 89bp of 5'- and 141bp of 3'- untranslated regions of the β -globin gene of *Xenopus laevis* (Kayano *et al.*, 1990). The plasmids contain an SP6 RNA Polymerase promoter located 5' to the transporter sequence and a gene conferring ampicillin resistance.

2.3.2 Agarose Gel Electrophoresis.

Various agarose concentrations, gel volumes and combs were used for the separation of DNA fragments. The number of samples and the degree of separation required between DNA fragments determined the gel volume. The choice of comb was governed by the sample volume. Differing degrees of band separation was achieved by varying the agarose concentration. High molecular weight species are separated better at low agarose concentrations whereas lower molecular weight bands are resolved better at higher concentrations. 1.0% and 1.6% (w/v) are typical agarose concentrations used.

Example: For a 100ml 1.0% agarose gel, 1g of agarose was dissolved in 100ml distilled water by heating in a microwave until boiling point was reached. On cooling, 2ml 50x TAE buffer (Table 2.1) was added and the solution was mixed before pouring on to an appropriate gel base sealed with tape. A comb was inserted and the gel was left to set at room temperature for approximately 15 mins. The tape was removed from the gel base before transferring the gel and gel base to the electrophoresis tank containing 1 litre of 1x TAE buffer, sufficient to completely cover the gel and fill the sample wells on removal of the comb. The samples to be loaded were prepared by addition of approximately 1/4 volume of 5x DNA loading buffer (Table 2.1). This serves to ensure that the samples sink to the bottom of the wells as loading buffer is more dense than the electrophoresis buffer due to the presence of glycerol. Samples were mixed and loaded directly into the wells by pipetting. 10 μ l of loading buffer containing 25 μ g/ml *Bst*E II-cut lambda DNA ladder was loaded into a well adjacent to the samples. 50 μ l of 10mg/ml ethidium bromide was added to the electrophoresis buffer and the electrodes were connected such that the negative electrode was connected to the well-end of the gel. Samples were electrophoresed at 50-100mA using an

1.KB 2197 power supply until the dye front had migrated to the appropriate distance, usually approximately two thirds the length of the gel. DNA was visualised under ultra-violet light using an ultra-violet transilluminator. Correctly sized DNA species were identified by their migration relative to the Lambda ladder markers. A gel photograph was taken using a Mitsubishi video copy processor.

2.3.3 Alcohol Precipitation of DNA

0.2 volumes of 100% ethanol, stored at 4°C, was added to the DNA sample in a 1.5ml Eppendorf tube. After vortexing, the solution was incubated at -20°C for at least 1 hour, or at -80°C for 30 mins. DNA was pelleted by centrifuging at 16,000 x g_{av} for 30 mins. The supernatant was removed and the pellet washed with 300-500 μ l of 70% ethanol, centrifuging at 16,000 x g_{av} for 15 mins to re-pellet the DNA. The supernatant was removed and the pellet allowed to dry in air for 10 mins before resuspending in an appropriate volume of sterile water.

2.3.4 Restriction Digestion of DNA.

Restriction digestion of cDNA and plasmid DNA was performed by the addition of the restriction enzyme(s) to the DNA in an appropriate buffer containing the optimum salt concentration and pH for the individual enzyme. When DNA was to be cleaved with two enzymes, the digests were carried out simultaneously if both enzymes had the same buffer requirements. Alternatively, the DNA was first digested with the enzyme requiring the buffer of lowest ionic strength and/or temperature, and then the appropriate amount of sodium chloride and the second enzyme added. A typical reaction contained 0.5-10 μ g of DNA in a reaction volume of 10 μ l per 1 μ g of DNA. 1 volume of the appropriate 10x buffer was added to 9 volumes of the reaction volume before addition of the restriction enzyme. This was mixed and incubated for 3 hours at 37°C (unless otherwise stated, depending on the particular enzyme). Reactions were terminated by addition of 1/4 volume of 5x DNA loading buffer and the reaction volume loaded onto an agarose gel for analysis by electrophoresis.

Any bands of interest were excised from the gel and the DNA purified and concentrated as described (sections 2.2.6a-d).

2.3.5 Dephosphorylation of Double Stranded DNA using Calf Intestinal Phosphatase (CIP).

CIP catalyzes the removal of 5' phosphate groups from DNA fragments to prevent religation. Plasmid DNA was cleaved with the appropriate restriction enzyme(s) for 3 hours and then treated with RNase A for 15 mins at 37°C. The reaction volume was made up to 100 μ l by addition of dephosphorylation buffer (provided with the enzyme), 10 units of CIP and the appropriate volume of sterile water. Reactions were carried out at 37°C for 2 hours. DNA was isolated from the enzymes by passing through an Elutip-d column and alcohol precipitation as described (sections 2.2.6b-d).

2.3.6 Ligation of Double-Stranded cDNA.

cDNA fragments were ligated into pSPGT3 backbone vector that had been restricted to remove a *Bst*X I-*Eco*R V fragment of the wild type GLUT3 cDNA sequence (sections 2.3.4). In order to increase the efficiency of ligation, an insert:vector molar ratio of approximately 10:1 was used. cDNA fragments and 100ng of vector DNA (10:1) were incubated overnight at 16°C in the presence of 3 units of T4 DNA ligase in ligation buffer. Ligation reactions were stored at -20°C. A 5-10 μ l aliquot was used to transform competent *E.coli* cells as described (sections 2.3.7-2.3.9).

2.3.7 Preparation of Competent *E.coli* (JM109) Cells.

10 μ l of a frozen stock of JM109 cells were used to streak an LB plate. After incubation at 37°C for 12-16 hours, a single colony was used to inoculate 3ml of sterile LB medium which was incubated for 12-16 hours at 37°C with shaking. 500 μ l of this starter culture was transferred to a 1 litre flask containing 50mls of sterile LB. The cells were grown

at 37°C with shaking for 2 hours before being harvested by centrifugation at 6000 x g_{av} at 4°C for 5 mins in a Beckman CPR benchtop centrifuge. The supernatant was discarded and the cell pellet resuspended in 20mls of ice-cold 100mM CaCl₂ solution. The suspension was incubated on ice for 20 mins before harvesting the cells as previously described. The cell pellet was resuspended in 4mls of ice-cold 100mM CaCl₂ solution and incubated at 4°C for at least 1 hour. (NB/ Cells remained competent at 4°C for up to 24 hours).

2.3.8 Transformation of Competent *E.coli* (JM109) Cells.

200µl of competent cells (section 2.3.7) were transferred to a pre-chilled 13.5ml Falcon tube to which 5-10µl of the ligation mix is added. The tubes are incubated on ice for 40 mins to allow uptake of the DNA by the competent cells. Transformation is terminated by heat-shocking the cells at 42°C for 45 secs, followed by incubation on ice for 5 mins. 0.8mls of sterile LB is then added and the cells incubated at 37°C with shaking for 1 hour. After centrifugation at 6000 x g_{av} for 5 mins at 4°C, 0.9mls of the supernatant was discarded and the cells were resuspended in the remaining 100µl which was plated out immediately onto LB agar plates containing 50µg/ml ampicillin. The plates were inverted and incubated at 37°C for 12-16 hours.

2.3.9 Transformation of Ultracompetent *E.coli* (JM109) Cells.

Ultracompetent cells were purchased from Promega and stored at -70°C. Cells were thawed by incubating in an ice-bath for 5 mins and mixed by flicking the tube. A 100µl aliquot (pcr transformation) was transferred to a pre-chilled 13.5ml Falcon tube. 5-10µl of the ligation mixture was added to the cells which were mixed gently and immediately incubated on ice for 10 mins. The transformation was terminated by heat-shocking the cells at 42°C for 45 secs, and incubating on ice for 2 mins. 900µl of SOC medium (Table 2.1) was added and the cells were grown for 1 hour at 37°C with shaking at 225rpm. 100µl of the transformation mixture was plated onto LB plates containing 50µg/ml ampicillin. The remaining 900µl was centrifuged at 6000 x g_{av} for 10 mins to pellet the cells. 800µl of the

medium was removed and the cells resuspended in the remaining 100 μ l which was also plated as described. The plates were incubated at room temperature for 15 mins to dry before inverted and incubated at 37°C for 12-16 hours.

2.3.10 Preparation of Small Quantities of Plasmid DNA

Colonies were picked from LB agar-ampicillin plates (50 μ g/ml) and used to inoculate 1.5mls of sterile LB. Cells were incubated at 37°C for 12-16 hours with shaking, centrifuged at 4°C for 5 mins at 6000 x g_{av} , and gently resuspended in 100 μ l glucose buffer (Table 2.1). The cell suspension was incubated on ice for 5 mins, 200 μ l 0.2M NaOH, 1% SDS added, and the cells returned to 4°C for 10 mins. 300 μ l 3M potassium/5M acetate was added. After a 5 min incubation at 4°C, the cells were centrifuged at 16,000 x g_{av} in a microfuge. 600 μ l of the supernatant was transferred to a sterile Eppendorf tube, 4 μ l RNase A (10mg/ml stock) was added and the tubes were incubated at 37°C for 30 mins. The DNA was extracted once with phenol:chloroform (1:1) and twice more with chloroform. 0.1 volumes of 3M NaOAc and 2 volumes of absolute ethanol (4°C) was added, the solutions mixed thoroughly and incubated at -20°C overnight (or at -70°C for 30 mins). After centrifugation at 16,000 x g_{av} in a microfuge for 30 mins, followed by a 70% ethanol rinse, the DNA pellet was air-dried and resuspended in a volume of 60 μ l of sterile H₂O. A 5 μ l aliquot was analysed by 1% agarose gel electrophoresis (section 2.3.2) along with a suitable undigested plasmid as a size standard.

2.3.11 Restriction Digestion Analysis of Small-Scale Plasmid cDNA

Preparations.

For initial identification of Pro-Ala mutant pSPGT3 constructs, a small scale preparation of plasmid DNA was carried out as described above. Typically, 5 μ l of the DNA sample (depending on the yield, as assessed by agarose gel electrophoresis) was analysed by restriction digestion to identify clones that contained the *Bst*XI-*Eco*RV insert. Digestions were carried out as described in section 2.3.4 in a reaction volume of 25 μ l, and the reaction

terminated by addition of 5 μ l of 5x DNA gel loading buffer. The resulting digestion pattern was analysed by 1% agarose gel electrophoresis. Positive clones were identified by the presence of a band of 4825bps, corresponding to the backbone pSPGT3 vector, and a second band of 871bps, corresponding to the *Bst*XI-*Eco*RV insert (Figure 2.2). Large scale plasmid preparations (sections 2.3.12 and 2.3.13) of any positive clones were carried out such that sufficient quantities of plasmid DNA were obtained for full sequencing of the constructs (section 2.4).

2.3.12 Large Scale Preparation of Plasmid DNA using QIAGEN QIAprep Plasmid Maxi Preparation Kits.

This method of plasmid preparation is based on the modified alkaline lysis procedure and on the adsorption of DNA onto an anion-exchange resin in the presence of low salt. The kits contain various buffer solutions and columns and the protocols are designed for purification of up to 500 μ g of plasmid DNA from an appropriate volume of an overnight culture of *E.coli* cells in LB medium.

Components (supplied with kits):-

<u>Buffer P1 (Resuspension Buffer):</u>	50mM Tris-HCl, pH8.0; 10mMEDTA; 100 μ g/ml RNase A, stored at 4°C.
<u>Buffer P2 (Lysis Buffer):</u>	200mM NaOH; 1% SDS.
<u>Buffer P3 (Neutralization Buffer):</u>	3.0M KOAc, pH5.5; stored at 4°C.
<u>Buffer QBT (Equilibration Buffer):</u>	750mM NaCl; 50mM MOPS, pH7.0; 15% ethanol; 0.15% Triton X-100.
<u>Buffer QC (Wash Buffer):</u>	1.0M NaCl; 50mM MOPS, pH7.0; 15% ethanol.
<u>Buffer QF (Elution Buffer):</u>	1.25M NaCl; 50mM Tris-HCl, pH8.5; 15 % ethanol.

TE:

10mM Tris-HCl, pH8.0; 1mM EDTA.

STE:

100mM NaCl; 10mM Tris-HCl, pH8.0;

1mM EDTA.

Plasmid Maxi Preparation Protocol:-

A colony of cells containing the plasmid to be purified was used to inoculate 3ml of sterile LB containing the appropriate antibiotic(s). This was incubated with shaking at 37°C for 12-16 hours. From this starter culture 0.5ml was transferred to 300ml of sterile LB plus antibiotic(s) which was then incubated shaking at 37°C for a further 12-16 hours. Cells were harvested by centrifugation at 4,000 x g_{av} for 10 mins at 4°C, and the bacterial pellet resuspended in 10ml of Buffer P1. The pellet was resuspended completely such that no cell clumps remained. 10ml of Buffer P2 was added and the solution mixed gently by inverting the tube 4-6 times. After incubating at room temperature for 5 mins, 10ml of chilled Buffer P3 was added, the tubes were mixed gently and incubated on ice for 20 mins. After centrifugation at 20,000 x g_{av} for 30 mins at 4°C in a Beckman JA-20.1 rotor, the supernatant was promptly transferred to clean tubes and recentrifuged for a further 15 mins. The supernatant was removed promptly and transferred to a QIAGEN-tip 500 equilibrated with 10ml of Buffer QBT. The QIAGEN-tip was then washed with 2 x 30ml of Buffer QC. Plasmid DNA was eluted by application of 15ml of Buffer QF to the tip, which was allowed to empty by gravity. DNA was precipitated with 0.7 volumes of room-temperature isopropanol followed by immediate centrifugation at 15,000 x g_{av} for 30 mins at 4°C. The supernatant was carefully removed and the DNA pellet washed with 5ml of 70% ethanol, recentrifuged, air-dried for 5 mins at room-temperature and redissolved in a suitable volume of sterile H₂O. A sample of the plasmid solution was analysed by agarose gel electrophoresis (section 2.3.2).

2.3.13 Large Scale Preparation of Plasmid cDNA.

Solutions:-

<u>Buffer 1:</u>	50mM glucose 10mMEDTA 25mM Tris, pH8.0
<u>Buffer 2*:</u>	1% SDS 0.2M NaOH
<u>Buffer 3:</u>	60 ml 5M KOAc 11.5 ml acetic acid 28.5ml st.H ₂ O
<u>PEG:</u>	20% PEG (Mol.wt 6000) 2.5M NaCl
<u>Other Soutions:</u>	TE Buffer 5MLithium Chloride 3M NaOAc

*Solution 2 was made up fresh on the day of use.

All procedures following initial cell harvesting were carried out on ice.

Protocol:-

A colony of cells containing the plasmid to be purified was used to inoculate 3ml of sterile LB containing the appropriate antibiotic(s). This was incubated shaking at 37°C for 12-16 hours. From this starter culture 0.5ml was transferred to 500ml of sterile LB plus antibiotic(s) which was then incubated shaking at 37°C for a further 12-16 hours. Cells were harvested by centrifugation at 4°C for 10 mins at 4,000 x g_{av} in a Beckman centrifuge. The resulting supernatant was carefully decanted from the pellet which was resuspended completely in 25 ml of Buffer 1. 25 ml of Buffer 2 was slowly added whilst swirling the solution on ice. To this, 25 ml of Buffer 3 was added followed by thorough mixing.

Centrifugation at 4°C for 10 mins at 4,000 x g_{av} resulted in a clear supernatant which was transferred to clean 250ml Beckman centrifuge tubes by filtering through a double thickness of fine muslin. 100ml of isopropanol (room temperature) was added and mixed thoroughly before incubating at -20°C for 15 mins. The DNA was precipitated by centrifugation at 4°C for 10 mins at 4,000 x g_{av}, and the resulting supernatant discarded. The pellet obtained from the entire 500ml culture was resuspended in 7.5ml TE buffer and transferred to 50ml Beckman centrifuge tubes to which 10ml of 5M lithium chloride solution was added. After incubating on ice for 2-5 mins, the solution was centrifuged at 4°C for 10 mins at 4,000 x g_{av} in a JA-20 rotor. The resulting supernatant was retained and transferred to a clean tube. 2 volumes of ice-cold absolute ethanol was added, the DNA solution was incubated at -20°C for 20 mins, and precipitated by centrifugation as described for 20 mins. The resulting pellet was rinsed with 70% ethanol and air-dried before resuspension in 0.5ml TE buffer. RNase A was added to 40µg/ml and the tubes incubated at 37°C for 15 mins. 0.5 volumes of PEG solution was added, followed by an incubation period of 15 mins on ice. After centrifugation, the resulting pellet was resuspended in 0.6 ml TE buffer and the DNA extracted once with phenol:chloroform and twice more with chloroform. 0.1 volumes of 3M NaOAc and 2 volumes of ice-cold absolute ethanol was added to the final extract, the solutions mixed thoroughly and incubated at -20°C overnight. After centrifugation at 16,000 x g_{av} in a microfuge for 30 mins, followed by a 70% ethanol rinse, the DNA pellet was air-dried and resuspended in a volume of 100-200µl of sterile H₂O, depending on the size of the pellet. The purity and yield of the plasmid was determined as described in section 2.3.14.

2.3.14 Calculation of Plasmid DNA Concentration and Purity.

Absorbance at 260nm of 1.0 = 50µg / ml dsDNA.

Absorbance at 260nm of "a" = "a" x 50µg / ml dsDNA.

Absorbance at 260nm = "b"

Absorbance at 280nm

DNA has a lower protein concentration and a higher purity when the value of "b" is nearer to 2.0.

2.4 Taq DyeDeoxy™ Terminator Cycle Sequencing Protocol.

This protocol was used with the Applied Biosystems Taq DyeDeoxy™ Terminator Cycle Sequencing Kit, in conjunction with the Applied Biosystems Model 373A Automated Sequencer.

2.4.1a Kit Reagents.

100 µl	G DyeDeoxy™ Terminator
100 µl	A DyeDeoxy™ Terminator
100 µl	T DyeDeoxy™ Terminator
100 µl	C DyeDeoxy™ Terminator
100 µl	dNTP mix- (750 µM dGTP, 150 µM dATP, 150 µM dTTP, 50 µM dCTP)
400 units	AmpliTaq® DNA Polymerase, 8 units/µl
400 µl	5x Terminator Ammonium Cycle Sequencing (TACS) Buffer- (400 mM Tris-HCl, 10 mM MgCl ₂ , 100 mM (NH ₄) ₂ SO ₄ pH 9.0)
6 µg	pGEM®-3Zf(+) double-stranded DNA Control Template, 0.2 µg/µl
50 µl	-21M13 Forward Primer, 0.8 pmoles/µl

2.4.1b Other Reagents.

Distilled water

De-ionised formamide

Phenol/H₂O/Chloroform (68:18:14, v/v/v)

Alconox™ detergent

Ethanol

Gel Reagents-	Sequagel-6™ 6% Sequencing Gel Solution
	Sequagel™ Complete Buffer Reagent
	10% Ammonium persulphate solution
	TEMED

2.4.2 Preparation of Templates and Sequencing Reactions.

pSPGT3 dsDNA was prepared from colonies as described previously (section 2.3.12). The quantities of template and sequencing oligonucleotide primer used per reaction were 2 µg dsDNA template and 35 ng of primer. The primers used are listed in Table 3.4. The combined volume of template and primer did not exceed 10.5 µl since 9.5 µl of reaction premix was added to bring the final volume to 20 µl. The total volume was adjusted to 20 µl by the addition of sterile water. A reaction premix sufficient for 20 reactions consisted of:-

Reagents:-

5x TACS Buffer	80 µl
dNTP mix	20 µl
DyeDeoxy™ A Terminator	20 µl
DyeDeoxy™ T Terminator	20 µl
DyeDeoxy™ G Terminator	20 µl
DyeDeoxy™ C Terminator	20 µl
AmpliTaq® DNA Polymerase	10 µl

The reagents were mixed in a 0.5 ml microfuge tube-

Reaction Premix	9.5 µl
Template DNA (0.4mg/ml)	5.0 µl
Primer (7ng/µl)	5.0 µl
dH ₂ O	<u>0.5 µl</u>
Final volume	20 µl

2.4.3 Thermal Cycling.

The tubes were placed in a Techne PHC-3 Thermal Cycler with a heated lid. The following parameters were programmed into the machine:-

Initial Melt	96°C	3 min
--------------	------	-------

Cycling- (30 cycles total, with a ramp rate of 1°C/sec)

Separation	96°C	30 sec
------------	------	--------

Reannealing	50°C	15 sec
-------------	------	--------

Extension	60°C	4 min
-----------	------	-------

Soak	4°C	Hold
------	-----	------

2.4.4 Acrylamide Gel Preparation.

The gel required a minimum period of 2 hours for polymerisation before pre-running so the gel was prepared whilst the reactions underwent thermal cycling.

2.4.4a Preparing the Gel Plates.

The plates, spacers and comb were washed with AlconoxTM and dH₂O. Only the plates were then wiped with absolute ethanol. The plates were aligned with the spacers between them along the outside of the longer edges and clamped into position. PermacelTM tape was applied along the short bottom edges of the plates and the lower ends of both longer edges so that the corners were covered and a seal was formed. The plates were balanced on a rest so that the open top was raised and the angle between the plane of the plates and that of the desktop surface was 30-45°.

2.4.4b Casting the Gel.

60ml of Sequagel-6™ 6% Sequencing Gel Solution was mixed with 15ml of Sequagel™ Complete Buffer Reagent and 0.6ml of 10% ammonium persulphate solution was added while stirring. 60μl of TEMED was added, the solutions were mixed and the gel was immediately poured between the glass plates up to the top edge of the notched plate with the aid of a 60ml syringe. All air bubbles were removed with the aid of a Promega "Bubble Hook". The plates were lowered so that they were lying flat on the bench and the gel casting comb was carefully inserted, the comb was secured by clamping the top of the gel with two binder clamps and the well was topped up with gel solution. The gel was then incubated at room temperature until complete polymerisation was achieved.

2.4.5 Setting Up for a Sequencing Run.

All the clamps and tape were removed from the gel plates and the casting comb carefully taken out. Excess acrylamide was cleaned off the plates which were then washed with Alconox™, distilled water and ethanol making sure that the plates were especially clean in the region where the laser read (about a third of the way from the bottom of the plates). A 24-well-shark's tooth comb was carefully placed on the gel surface so that it indented the gel but did not puncture it. The 373A DNA Sequencer and the Macintosh IIfx computer were switched on. The gel was placed onto the lower buffer chamber and the beam-stop rack locked. The gel plates were scanned for the presence of dirt particles by initiating a pre-run scanning program. If the baselines were flat, then there was judged to be no dirt on the plates- if they were not then the plates were cleaned again. 1.5 litres of 1x TBE buffer (Table 2.1) was prepared and about half added to the upper buffer chamber and the remainder poured into the bottom chamber. The wells were rinsed with a syringe fitted with a 18-gauge needle containing 1x TBE buffer. The gel was left to pre-run for approximately 30-40 mins, during which time the gel was equilibrated at 40°C.

2.4.6 Sample Extraction and Precipitation.

After the cycling (section 2.4.3) was complete, 80 μ l of sterile water was added to each reaction mixture. 100 μ l of phenol/water/chloroform (68:18:14, v/v/v) was added to each tube and vortexed for at least 1 min, and then centrifuged for 2 min in a microfuge. The upper aqueous phase was retained, discarding the lower organic phase. This process was repeated. The extracted aqueous phase was transferred to a fresh microfuge tube and precipitated by the addition of 15 μ l of 2 M sodium acetate and 300 μ l of absolute ethanol (stored at -20°C). Tubes were vortexed to mix the contents and then placed at -20°C for 30 min to ensure complete precipitation. The tubes were centrifuged in a microfuge for 15 min to pellet the cDNA, the pellets washed in 70% ethanol, and dried in air for 5-10 mins.

2.4.7 Preparing and Loading Samples.

4 μ l of de-ionised formamide/10 mM EDTA was added to each of the samples and mixed well. Samples were then heated at 90°C for 2 min, and placed onto ice immediately. The wells of the gel (section 2.4.5) were flushed out with 1x TBE and 4 μ l of each odd-numbered sample added to its corresponding well in the gel. The sequencing program was initiated and left for 10 mins to allow these samples to enter the gel. The program was then interrupted and the wells of the gel rinsed again before loading the remaining samples into their corresponding wells. The sequencer was restarted and the collect program initiated.

2.4.8 Analysis of Samples.

The samples were electrophoresed at a constant temperature of 40°C for 12 hours, passing through the "read window" area of the gel where laser light was periodically passed along this area of the gel. The resulting fluorescence emitted by the DyeDeoxyTM Terminator dyes over a period of time were measured by the 373A

sequencer and incorporated by the ABI Data Collection Program on the Macintosh IIci computer. After the data was collected, it was analysed by the ABI Data Analysis Program. Sequences were determined by use of this program. When different sequences were generated by the use of various sequencing primers (Table 3.4) with the same template cDNA, these were compared using the GeneJockey II (Biosoft) program.

2.5 *In vitro* synthesis of mRNAs from Plasmid cDNA.

All work with mRNA was conducted wearing gloves with sterile solutions and equipment, since ribonucleases which can degrade mRNA can be found on the skin and elsewhere. All reagents were thawed on ice. A nucleotide stock (2.5mM rATP, 2.5mM rCTP, 2.5mM rUTP and 0.5mM rGTP) was made up from 100mM stock solutions of each ribonucleotide. The diguanosine triphosphate (5' cap analogue) was prepared at 10mM in RNase-free water. Reagents were added to a sterile Eppendorf tube in the following order:-

- 75 μ l ribonuclease-free H₂O
- 40 μ l 5x transcription buffer
- 20 μ l 100mM dithiothreitol (DTT)
- 40 μ l nucleotide mix (see above)
- 10 μ l GpppG (5' Cap) (25 units/100 μ l)
- 10 μ l linearised plasmid cDNA (~ 1 μ g/ml;)
- 2.5 μ l SP6 polymerase (25 units)

This gave a total volume of 200 μ l. The tube was placed in a 37°C water bath for 1 hour, after which a further 0.5 μ l of SP6 polymerase was added, mixed and incubated at 37°C for 30 min. At this point the reaction was centrifuged in a microfuge to collect the condensate and then 1 volume of phenol/chloroform [1:1 (v/v)] added. This was vortexed for 1 min and centrifuged in a microfuge for a further 1 min. The upper aqueous phase, which contained both mRNA and cDNA, was carefully collected into a clean tube. 100 μ l of chloroform was added to the solution, before vortexing.

centrifuging, and again collecting the aqueous phase. This procedure was repeated, before finally adding 0.3 volumes of 5 M potassium acetate and 2.5 volumes of ice-cold absolute ethanol to precipitate the nucleic acid. The reaction was mixed and incubated at -20°C for approximately 1 hour, then centrifuged in a microfuge for 30 min. The pellet was washed with 0.5ml 70% ethanol and centrifuged as above. All traces of ethanol were removed from the pellet by drying under vacuum. The pellet was resuspended in 40µl of ribonuclease-free H₂O. 3µl of this was mixed with 3µl of 5x DNA gel loading buffer (Table 2.1) and loaded into a 1% agarose gel immersed in 1x TAE running buffer (Table 2.1) to assess the integrity of the mRNA. 5µl of 100 µg/ml *Bst* E II-cut lambda ladder DNA was loaded into an adjacent well and the current adjusted to 50 mA so that negatively charged ribonucleic acids migrated toward the positive electrode. Electrophoresis was carried out until the dye-front was half to two thirds across the gel, then 20µl of 10 mg/ml ethidium bromide added per litre of running buffer. The bands were visualised by viewing the gel under ultra-violet light, and the size of any mRNA bands checked by its relative migration to the lambda ladder. A typical photograph of mRNA on a 1% agarose gel can be seen in Figure 2.3. mRNA used for injection appeared on a gel as a distinct band with no evidence of smearing.

2.6 Use of *Xenopus laevis* Oocytes for Heterologous Expression of GLUT Constructs.

2.6.1 Housing of *Xenopus laevis*.

Adult female *Xenopus laevis* (average length of 15cm) were kept in an aquarium maintained at a constant water temperature of 16-18°C on a 12 hour day/night cycle. 2-4 animals were housed per tank containing 6in of distilled water located in a quiet environment. The animals were fed on a weekly basis on a diet of raw chopped sheep heart or "frog brittle" obtained from Blades Biologicals. The water was changed the day after feeding to remove undigested or decomposed food. Each animal was maintained in such an environment for at least one month prior to operating to allow for acclimatisation.

2.6.2 Chemical Anaesthesia.

The animal to be operated on was placed in a tank containing 500ml of distilled water and 0.75g Tricane Methane Sulphonate (MS222) supplemented with 25ml 0.5M sodium bicarbonate. MS222 has a low pH and is thus an irritant to amphibian skin. The use of the bicarbonate raises the pH to neutrality making it acceptable for the animal. Anaesthesia is rapid resulting in a state of unconsciousness within about 5-10 mins such that when the animal is placed on its back, it is completely immobile.

2.6.3 Surgery.

This procedure requires both Home Office Project and Individual Animal Handling Licenses. The anaesthetised animal is placed on her back and a small incision made (~1cm) in the lower third of the abdominal wall followed by a further incision in the inner body cavity. Oocyte lobes are removed using fine watchmakers forceps and fine scissors and are transferred to a universal tube containing Barths solution. A single stitch in the abdominal wall is made using chronic sterile catgut, followed by 2 stitches in the dermis. The animal was then rinsed with distilled water and placed in a recovery tank containing 2-3mm of distilled water until consciousness was completely regained. Animals were returned to their housing tanks within 2 hours of surgery and kept for at least 3 months before a second operation performed.

2.6.4 Oocyte Isolation and Injection.

Oocyte lobes were removed from the adult female *Xenopus laevis* as described. Before beginning individual isolation, the oocytes were inspected closely under a microscope. Only healthy oocytes at the correct stage of development, stage IV or V, are suitable for injection. These are characterised by several important criteria such as a distinct boundary between the animal (dark brown) and vegetal (pale green/yellow) poles. They are the largest oocytes and should exhibit a uniform pigmentation of the dark pole, i.e. no spots

or mottling. Oocytes that do not meet these criteria were not suitable for injection and were therefore discarded.

Individual oocytes are attached via a translucent vein and connective tissue to the central artery. They can be stripped from the central artery using fine watchmaker's forceps. This delicate procedure is carried out in a petri dish containing Barths solution and with the aid of a binocular dissecting microscope. Isolated oocytes were then transferred to a 50ml Sterilin vial containing Barths for storage. Damaged oocytes were periodically removed from the petri -dish and the Barths solution was changed regularly to remove endogenous oocyte proteases released throughout the isolation procedure. The number of oocytes isolated was generally 2-3 times the number required for microinjection so as to take into account the percentage of cells expected to die during the 48 hour incubation prior to assay.

The injection apparatus consisted of a 0-10 μ l micro-injector (Drummond Scientific Co.), 6 inch capillary tubes, a micro-manipulator (Narshige, Japan), a PUL-1 needle puller (World Precision Instruments), a Nikon SMZ-2B binocular microscope (10x23 eyepieces) and swan-necked fibre-optic lamp unit, a petri-dish fitted with a Spectramesh grid (Fischer), paraffin oil and a syringe. Gloves were worn throughout the injection procedure to prevent contamination of mRNA with ribonuclease present on the fingertips. A capillary tube was secured in the needle pulling unit, which uses a combination of heat and a pulling motion to produce needles with a bore size of about 2 μ m. The tip of the needle was then broken off with forceps and filled with paraffin oil with the aid of a syringe and a 25 gauge needle. The barrel of a 0-10 μ l micropipette (set at 1.5 μ l) was carefully inserted into the end of the oil-filled needle, avoiding air bubbles. The micropipette was then secured in the micromanipulator. The mRNA to be injected was pulsed briefly (20 secs) in a microfuge, to pellet any debris, and about 8 μ l of the supernatant was transferred to a sterile microfuge tube lid under the microscope. The micropipette was lowered such that the tip of the needle was submerged in the mRNA droplet, and the mRNA was drawn slowly up into the needle. Oocytes, submerged in Barths in a petri dish, were aligned on a SpectraMesh grid. The needle was introduced into the vegetal pole of the oocyte by applying a gentle downward force using the micromanipulator. 50nl of mRNA was expelled into the oocyte cytoplasm, and the needle was slowly removed. Oocytes were stored in Barths medium at 18-20°C for

48 hours, transferring to fresh Barths medium every 12 hours. Oocytes were then ready for assay.

2.7 Sugar Transport in *Xenopus* Oocytes.

2.7.1 Transport Assay Conditions.

Groups of 7 oocytes were incubated in 0.45ml Barths medium (Table 2.2) in 13.5ml centrifuge tubes at room temperature. Transport (zero-*trans* entry) was initiated by the addition of 50 μ l of [2,6-³H]2-deoxy-D-glucose or [U-³H]D-fructose to give a specified final sugar concentration with an activity of $\sim 1\mu$ Ci / ml. After a designated time period, usually 30 mins or 60 mins for 2-deoxy-D-glucose and D-fructose transport respectively, the media was aspirated from the oocytes and the transport quenched by three washes with ice-cold 1x PBS (Table 2.2) containing 0.1mM phloretin (a potent transport inhibitor). Oocytes were individually dispensed into scintillation vials using a P200 Gilson pipette and tip with the end cut off. 1ml 1% SDS was added to the oocytes which were incubated overnight, before addition of 4ml scintillation fluid and subsequent measurement of radioactive uptake by a scintillation counter. For each group of injected oocytes assayed, non-injected oocytes were assayed in parallel under identical conditions to determine the endogenous transport levels under the specified assay conditions. Subtraction of these rates from those obtained from injected oocytes yields the specific rates mediated by the heterologously expressed transporter.

Transport rates measured over a range of external sugar concentrations enabled Lineweaver-Burk plots to be constructed by a double reciprocal plot of the measured rates (y-axis) vs the concentration of external sugar (x-axis). K_m values were calculated from such plots.

To investigate the inhibitory effects of maltose and cytochalasin B on 2-deoxy-D-glucose transport by GLUT3 and mutant GLUT3 transporters, oocytes were incubated in the presence of these inhibitors prior to initiation of radiolabelled sugar uptake. Oocytes were incubated in 0.45ml of 50mM maltose in Barths medium at room temperature for 15 mins

prior to assay. Use of cytochalasin B however, required pre-treatment of the oocytes with collagenase solution (section 2.7.2). Collagenase treated oocytes were then incubated in 0.45ml 2 μ M cytochalasin B for 15 mins prior to assay. Again, transport rates were measured over a range of external sugar concentrations and construction of Lineweaver-Burk plots enabled calculation of K_i values. Non-injected oocytes were assayed in parallel under identical conditions as described above.

2.7.2 Collagenase Treatment of Oocytes.

Both injected and non-injected oocytes to be assayed in the presence of cytochalasin B were pre-treated with collagenase solution to facilitate removal of the follicular cell layer of the oocyte. A 2mg/ml solution of collagenase (Sigma, Type II) was prepared in Barths medium. Oocytes were incubated in 10mls of collagenase solution in a petri dish for 30 mins at room temperature with gentle agitation. Collagenase was then removed by washing 3-4 times with 15ml Barths medium. Oocytes were then incubated in the presence of 2 μ M cytochalasin B prior to assay as described in section 2.7.1.

Table 2.1**Solutions and Buffers Used for DNA Manipulation.**

Solution	Constituents
50x Tris-acetate (TAE) buffer	242g Tris base; 57.1ml glacial acetic acid, 100ml 0.5M EDTA, pH 8.0
High salt solution	1M NaCl; 20mM Tris, pH 7.4; 1mMEDTA
Low salt solution	0.2M NaCl; 20mM Tris-HCl, pH 7.4; 1mMEDTA
10x Tris-borate (TBE) buffer	108g Tris base; 55g Boric acid; 40ml 0.5M EDTA, pH 8.0
TE buffer (pH 8.0)	10mM Tris-HCl, pH 8.0, 1mM EDTA, pH 8.0
5x DNA gel-loading buffer	0.25% (w/v) bromophenol blue; 30% (w/v) glycerol in water
SOC medium - per 100mls	2g Tryptone (Bactotryptone); 0.5g Yeast extract; 1ml 1M NaCl; 0.25ml 1M KCl; 1ml 2M Mg^{2+} stock; 1ml 2M glucose
Glucose buffer	50mM glucose; 10mM EDTA; 25mM Tris- HCl, pH8.0
Luria-Bertani medium (LB) - per litre	10g Tryptone (Bactotryptone); 5g Yeast extract; 10g NaCl
LB plates - per litre	10g Tryptone (Bactotryptone); 5g Yeast extract; 10g NaCl, 15g Agar

Table 2.2**Table of Buffers.**

Buffer	Constituents
Barths buffer	88mM NaCl; 1mM KCl; 2.4mM NaHCO ₃ ; 0.82mM MgSO ₄ ; 0.41mM CaCl ₂ ; 0.33mM Ca(NO ₃) ₂ ; 5mM HEPES-NaOH, pH 7.6.
10x Phosphate Buffered Saline (PBS)	1.37M NaCl; 26.8mM KCl; 43mM Na ₂ HPO ₄ ; 14.7mM KH ₂ PO ₄ , pH 7.4
Krebs ringer phosphate buffer (KRP)	1.28M NaCl; 47mM KCl; 50mM Na ₂ HPO ₄ ; 12.5mM MgSO ₄ ; 12.5mM CaCl ₂ ; final pH7.4 at 37°C
2x HEPES Buffered Saline (HBS)	50mM Hepes, pH7.1; 280mM NaCl; 1.5mM Na ₂ HPO ₄ ;
Homogenisation buffer (HB)	0.25M sucrose; 10mM HEPES, pH7.4; 1mMEGTA; 2mMMgCl ₂

Figure 2.1

Diagram of a GLUT cDNA Cloned Into the pSP64T Vector.

The GLUT2 cDNA was ligated to *Bgl* II DNA linkers and cloned into the untranslated regions of the *Xenopus* β -globin gene, which had previously been cloned into the multiple cloning site of pSP64 (Krieg and Melton, 1984). The GLUT3 cDNA was cloned into the pSP64T construct as a *Bgl* II/*Bam* HI fragment into the untranslated regions of the *Xenopus* β -globin gene. The 5' untranslated region (UTR) is 89 bp long and the 3' untranslated region is 141 bp long. The GLUT cDNA and its flanking sequences are located 3' of the SP6 polymerase promoter.

Figure 2.1

Diagram of a GLUT cDNA Cloned into the pSP64T Vector.

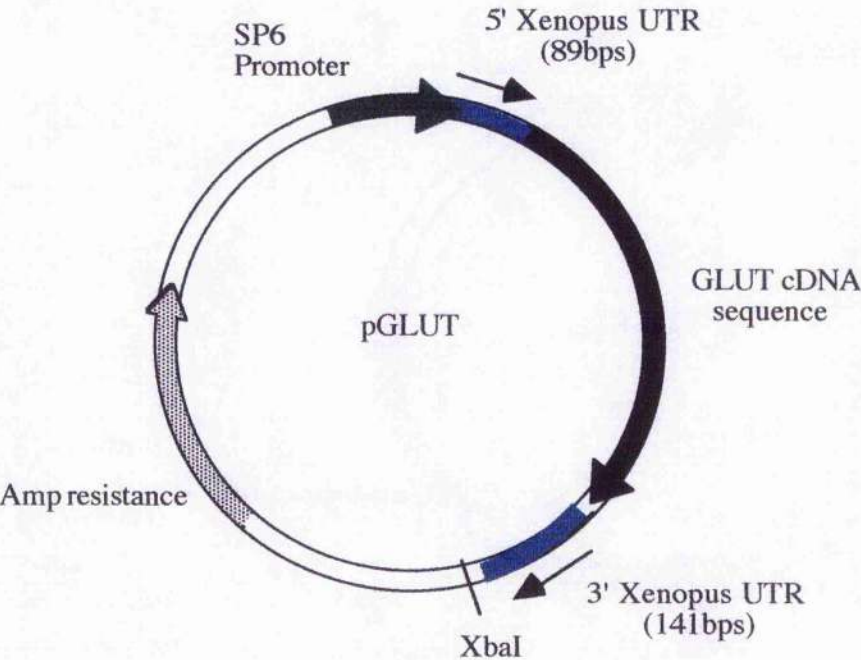


Figure 2.2

1% Agarose Gel Showing the Restriction Digestion Analysis of GLUT3 Pro-Ala Mutant cDNAs.

Small scale plasmid preparations were isolated from transformed *E.coli* cells and were subjected to restriction digestion analysis. Restriction of plasmids containing GLUT3 Pro-Ala mutants with *BstX* I and *EcoR* V yields a large fragment of 4825 bps corresponding to the backbone vector and a smaller fragment of 871 bps corresponding to the *BstX* I/*EcoR* V fragment of GLUT3 that contains the point mutation.

Figure 2.2

1% Agarose Gel Showing the Restriction Digestion Analysis of GLUT3 Pro-Ala Mutant cDNAs.

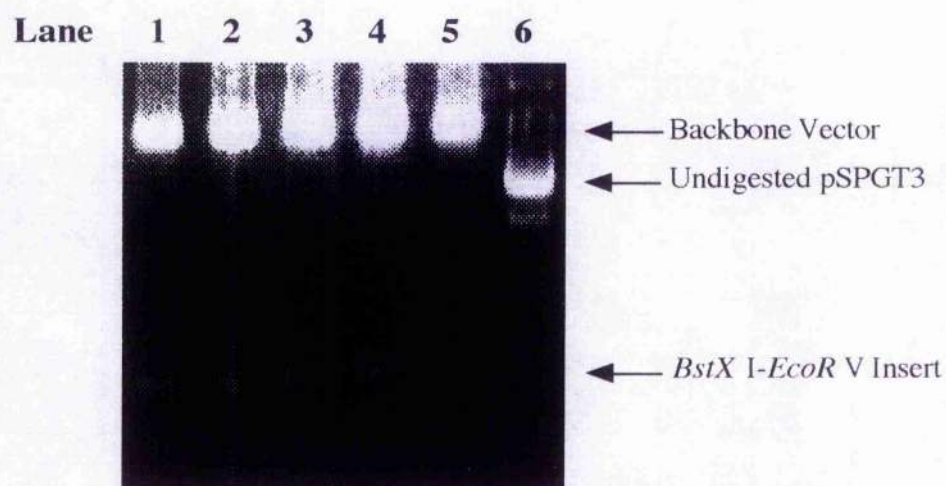


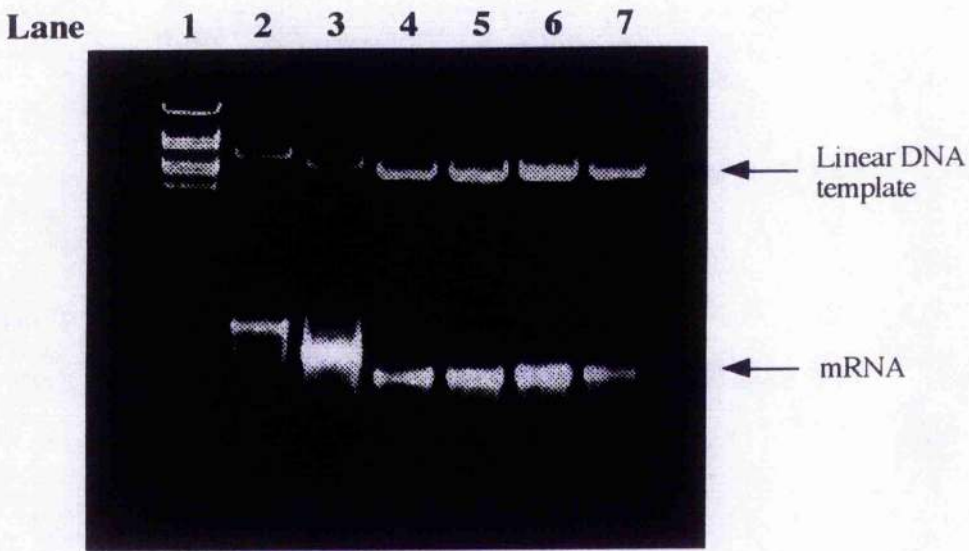
Figure 2.3

1% Agarose Gel of *In Vitro* Synthesised mRNA.

3 μ l samples of *in vitro* synthesised mRNA (from a total of 40 μ l) were subjected to 1% agarose gel electrophoresis and stained with ethidium bromide. DNA markers are loaded in Lane 1 (not applicable to RNA sizes), Lanes 2 and 3 contain GLUT2 and GLUT3 mRNA, and Lanes 4-7 contain mRNA synthesised from Pro²⁰⁶, Pro³⁸¹, Pro³⁸³ and Pro⁴⁵¹ linear DNA templates.

Figure 2.3

1% Agarose Gel of *In Vitro* Synthesised mRNA.



2.8 Subcellular Fractionation of *Xenopus laevis* Oocytes.

2.8.1 Oocyte Isolation and Injection.

Oocytes were isolated from adult female *Xenopus laevis* as described in section 2.6.4 GLUT3 mRNA was synthesised as described in section 2.5 from pSPGT3 linearised with *Xba* I. Oocytes were subsequently injected with 50nl mRNA and incubated for 48 hours at 18-20°C in Barths medium before they were fractionated or assayed for transport activity.

2.8.2 Transport Assays.

Prior to subcellular fractionation of oocytes to obtain a plasma membrane fraction, oocytes were first checked for expression levels of GLUT3 by measurement of the rates of [2,6-³H]2-deoxy-D-glucose transport into oocytes. Oocytes that express GLUT3 at the plasma membrane exhibited elevated rates of transport over non-injected control oocytes. 10 GLUT3 injected oocytes or 5 non-injected oocytes were incubated in 0.45ml Barths medium in a 13.5ml Falcon tube at room temperature. Transport was initiated by the addition of 50µl Barths medium containing [2,6-³H]2-deoxy-D-glucose with an activity of 1µCi/ml and a final sugar concentration of 0.1mM. After a 30 min incubation period, transport was terminated as described in section 2.7, and the amount of radioactive tracer accumulated in individual oocytes measured by scintillation counting. Oocytes exhibiting transport rates of 3-5pmoles/min/oocyte were suitable for subcellular fractionation.

2.8.3 Subcellular Fractionation of Oocytes - Method 1.

This method for the preparation of plasma membranes from oocytes was based on the method described by Wall and Patel in 1989.

2.8.3a Reagents.

Barths medium

NHS-LC-biotin dissolved in a minimum volume of DMSO

20mg/ml L-lysine solution made up in Barths medium

Homogenisation buffer containing the following protease inhibitors:-

100 μ M diisopropylfluorophosphate

1 μ g/ml aprotinin

2 μ M pepstatin A

2.8.3b Biotinylation of Intact Oocytes.

100 GLUT3 injected oocytes were transferred to a glass tube containing 3mls Barths medium and were incubated on ice for 15 mins. 10mgs NHS-LC-biotin was dissolved in the minimum volume of DMSO, 1ml Barths medium was added and this solution was mixed with the oocytes. After incubating on ice for 15 mins with gentle shaking, the biotin solution was removed by aspiration, the oocytes were washed with 3x 3ml Barths medium, to ensure removal of excess biotin, and 1ml of a 20mg/ml L-lysine solution in Barths was added. The oocytes were incubated on ice for a further 15 mins with gentle mixing. The L-lysine was removed by aspiration and the oocytes washed with 3x 3ml Barths medium before addition of 1ml homogenisation buffer (HB Buffer) containing protease inhibitors.

2.8.3c Fractionation of Oocytes

The biotinylated oocytes were transferred to a 1ml Dounce homogeniser and were carefully disrupted with 6-7 strokes using a loose-fitting pestle. This process produced large plasma membrane sheets (PM) with adherent pigment granules and other organelles which were allowed to settle to the bottom of the vessel by gravity over a period of 5-10 mins. The supernatant fraction was removed from the pellet and retained as the initial supernatant fraction (S_{initial} , consisting mainly of yolk protein). The pellet containing the PM sheets was

gently resuspended in 6mls HB+protease inhibitors (Table 2.2) using a glass pasteur pipette. Note, from here on the same pipette was used throughout the procedure : to minimise loss of PM fragments. Again the PM sheets were allowed to settle by gravity to the bottom of the vessel and the resulting supernatant removed and retained as the wash fraction (S_{wash}). The resuspension, gentle disruption and settling procedure was repeated a further 4-5 times until a clear PM fraction was obtained, each time removing the supernatant and pooling with the previously removed wash. The final PM fraction contained large translucent plasma membrane sheets that were clearly visible by eye. The final PM fraction along with the $S_{initial}$ and S_{wash} fractions were subjected to centrifugation at $66,700 \times g_{av}$ at $4^{\circ}C$ for 1 hour in a Beckman Ultracentrifuge, and the resulting pellets resuspended in a suitable volume of 1x PBS (depending on the pellet size) and snap frozen in liquid nitrogen for storage at $-70^{\circ}C$.

2.8.3d Lowry Protein Determination Microassay.

- Solution 1** - (a) 500mg $CuSO_4 \cdot 5H_2O$
 1g potassium tartrate
 250ml H_2O
- (b) 50g Na_2CO_3
 250ml H_2O
 Slowly add solution (b) to solution (a).

Solution 2 - 10% (w/v) SDS

Solution 3 - 0.8N sodium hydroxide

Reagent 1: Mix 25ml of solutions 1, 2 and 3 with 25ml H_2O

Reagent 2: Mix 25ml Folin-Ciocateau with 100ml H_2O
 (stored at $4^{\circ}C$ in a brown bottle)

Precipitants: 0.15% (w/v) deoxycholate (DOC)
 72% (w/v) trichloroacetic acid (TCA)

Standards: 0, 4, 8, 12, 16, 20 μ g BSA

The sample volume was adjusted to 0.5ml with H₂O. 100 μ l 0.15% (w/v) DOC was added, the solutions mixed and incubated at room temperature for 10mins. 100 μ l (w/v) TCA was added and the solutions were mixed and centrifuged at 16,000 x g_{av} for 10 mins. The supernatant was discarded and the volume of the pellet was resuspended in 0.2mls H₂O by vortexing. 200 μ l of reagent A was added, mixed and incubated at room temperature for 10 mins before addition of 100 μ l of reagent B, mixing immediately. After an incubation of 30 mins at room temperature, the A_{750nm} was measured, using 1x PBS as the blanking solution. A standard curve was constructed from the BSA absorbances from which the protein concentration of each sample was determined.

2.8.3e Detection and Quantitation of Plasma Membranes Using ¹²⁵I-Streptavidin.

Samples were diluted to a suitable and equal concentration in 1x PBS. 10-20 μ l aliquots were spotted onto nitrocellulose membrane squares and allowed to dry before addition of the next aliquot. Typically, a volume of 50 μ l was spotted in total. The squares were left to completely dry before being transferred to a petri dish containing 15mls of 3% (w/v) BSA in 1x PBS. The membrane squares were incubated in this blocking solution for a period of 2 hours at room temperature with gentle agitation. Excess BSA was removed from the membranes by rinsing with 1x PBS. ¹²⁵I-Streptavidin (0.5mCi/ml, ~10⁶ cpm) was added to 10 mls 1x PBS and the membranes were incubated in this solution for 3 hours with gentle agitation. The membranes were washed thoroughly with 1x PBS, placed between 2 pieces of wet phosphocellulose sheets and dried for 30 mins using a hair dryer. The phosphocellulose sandwich was placed in a developing cassette and stored at -20°C for a suitable time period before developing using a Kodak X-OMAT processor Model MF3.

2.8.4 Subcellular Fractionation of Oocytes - Method 2.

This method was based on that described previously with modifications to improve the yield of PM fraction obtained during the homogenisation procedure. A water soluble

form of Biotin was used to avoid the use of DMSO. In addition to the dot blot analysis of the oocyte fractions, GLUT3 was detected by immunoprecipitation (section 2.17).

2.8.4a Reagents.

Barths medium

sulfo-NHS-biotin dissolved in Barths medium

20mg/ml L-lysine solution made up in Barths medium

Homogenisation buffer containing the following protease inhibitors:-

100 μ M diisopropylfluorophosphate

1 μ g/ml aprotinin

2 μ M pepstatin A

2.8.4b Biotinylation of Intact Oocytes.

The biotinylation procedure was exactly as described in section 3.8.3b, except that a 10mg/ml solution of sulfo-NHS-biotin was made up in Barths and then added to the oocytes. The labelling and quenching procedures were identical in all other aspects.

2.8.4c Fractionation of Oocytes.

Oocytes were disrupted by gentle pipetting using a P200 Gilson pipette with the tip cut to approximately the diameter of an oocyte (~1-2mm). The glass tube containing the homogenate was placed on ice and the PM sheets were allowed to settle to the bottom of the tube by gravity. After approximately 10 mins, the majority of the supernatant, containing predominantly yolk protein, was removed from the pellet and transferred to an Eppendorf tube. The tube was centrifuged at 1000 x g_{av} for 5 mins to remove contaminating yolk granules, and the supernatant transferred to another tube. The disruption and centrifugation steps were repeated, typically 6-8 times depending on the oocytes, until all contaminating yolk and pigment granules had been removed from the supernatant. Yolk pellets obtained at

each centrifugation step were resuspended in 50 μ l 1x PBS and combined to form the yolk fraction (Y). The resulting supernatant was transferred to a Ti-50 centrifuge tube and was centrifuged at 204,000 \times g_{av} at 4°C for 1 hour in a Benchtop Beckman Ultracentrifuge. The resulting supernatant was removed (and retained) from the plasma membrane pellet which was resuspended in 200 μ l of 1x PBS (S_{wash} fraction). Thus, a total of 3 final fractions were obtained by this procedure referred to as the Y (yolk), PM (plasma membrane) and S (supernatant) fractions. These were then snap frozen in liquid nitrogen and stored at -70°C until further analysis.

2.8.4d Protein Concentration Determination Using the Quantigold Assay.

This is a faster, alternative method to the Lowry assay described in section 2.8.3d, and allows detection of as little as 5ng of protein. BSA standards were prepared in the range of 0-200ng BSA/10 μ l. Various dilutions of the protein samples to be measured were made. 800 μ l of the Quantigold reagent was added to disposable 1ml micro-assay cuvettes and these were equilibrated to room temperature. 10 μ l of each protein sample or standard samples were added to the appropriate cuvettes which were mixed immediately. After a 40-60 min incubation at 37°C, the OD_{595nm} was measured for each sample, using 10 μ l of water in 800 μ l of Quantigold as the blanking reagent.

2.8.4e Detection of GLUT3 Transporters by Immunoprecipitation.

Oocyte fractions were separated by SDS/polyacrylamide gel electrophoresis (section 2.17.1). The gels were removed from the plates and were assembled in a Bio-Rad mini trans-blot electrophoretic transfer cell. The proteins were transferred to nitrocellulose membrane by application of a constant current of 275mA for 3 hours at room temperature (section 2.17.2). Non-specific binding sites on the nitrocellulose membrane were blocked (section 2.17.3) and the membranes were probed with a rabbit polyclonal antiserum (1 in 250 dilution) raised against a synthetic peptide corresponding to the C-terminal 14 amino

acids of human GLUT3. ^{125}I -labelled goat anti-rabbit IgG ($1\mu\text{Ci}/20\text{ml}$) was used for detection by autoradiography (section 2.17.4)

2.8.5 Assessment of the Relative Enrichment of Oocyte Fractions.

2.8.5a Reagents.

<u>Buffer A:</u>	150mM KCl 20mM Hepes, pH 7.2 2mM MgCl_2 (stored at 4°C)
<u>Reaction Mix:</u>	50-100 μl of sample to be assayed 0.3% (v/v) TX-100 5mM 2'3'-AMP (10x stock stored at -20°C) 0.2mM 5'-AMP (10x stock stored at -20°C) 2 μCi $[^3\text{H}]5'$ -AMP
<u>Precipitants:</u>	0.25M $\text{Zn}(\text{SO}_4)_2$ (stored at room temperature) 0.125M BaCl_2

2.8.5b 5'Nucleotidase Assays.

To an Eppendorf tube 100 μl each of TX-100, 2'3'-AMP, 5'-AMP; 2 μl of $[^3\text{H}]5'$ -AMP and 648 μl of Buffer A was added. The solutions were mixed and incubated at 37°C for 5 mins to equilibrate before addition of 50 μl of the protein sample at $T=0$. Immediately, 2 x 5 μl aliquots were removed from each tube and transferred to separate tubes containing 50 μl of 0.25M $\text{Zn}(\text{SO}_4)_2$. Further aliquots in duplicate were removed from the reaction tubes at 15, 30, 60, 90 and 120 mins. At the end of the incubation period, 100 μl of 0.125M BaCl_2 solution was added to the tube containing the 5 μl aliquots and the $\text{Zn}(\text{SO}_4)_2$. The solutions were mixed and incubated on ice for 10 mins, centrifuged for 10 mins in a microfuge, and 200 μl of the resulting supernatant was transferred to a scintillation vial. 4mls scintillation

fluid was added to each vial and the amount of radioactivity measured by scintillation counting. The 5'nucleotidase activity associated with each oocyte fraction was calculated and plotted as a function of time. Comparison of the gradients of the resulting lines gives an estimate of the fold enrichment of enzyme activity associated with each fraction relative to another.

In addition, 10 non-injected oocytes were extensively homogenised in 0.7 ml PBS using a 0.1ml Dounce homogeniser to obtain a total protein sample.

2 - Cell Culture.

2.9 Cell Culture Materials.

Nutrient Mixture F-12 (HAM) with L-Glutamine, Non-essential amino acids and Foetal Calf Serum were supplied by Gibco Life Technologies LTD, Paisley, Scotland.

Trypsin-EDTA and Penicillin/streptomycin were supplied by Sigma Chemical Company, Poole, Dorset, UK.

Calcium phosphate transfection kit was supplied by Invitrogen, The Netherlands

CalPhos Maximizer was supplied by Clontech Laboratories, USA.

Geneticin (G418-sulphate) was supplied by Calbiochem-Novabiochem LTD, Nottingham (U.K.).

Ciproxin was obtained from the Western Infirmary, Glasgow, U.K.

Cell culture plasticware was purchased from NUNC and Falcon (Beckton Dickson) unless otherwise stated.

2.10 Growth and Storage Media.

2.10.1 Chinese Hamster Ovary (CHO-) Cell Growth Media.

Ham's F12 media was supplemented with 10% (v/v) Foetal Calf Serum, 200 IU penicillin, non-essential amino acids and 200 μ g streptomycin / 500ml.

2.10.2 Freeze media.

Ham's F12 media supplemented with 10% (v/v) Foetal Calf Serum, 200 IU penicillin, non-essential amino acids and 200 μ g streptomycin/500ml, 10% (v/v) sterile glycerol and equilibrated at 37°C.

2.11 Long Term Storage of Cells.

2.11.1 Preparation of Cells for Frozen Stocks.

CHO cells were grown in supplemented Ham's F12 medium in 25ml flasks until 95% confluent. Growth media was aspirated from the cells which were then trypsinised (section 2.12) and transferred to a 13.5ml falcon tube containing 1-2mls of quenching media (section 2.10.1). Cells obtained from 1-2 flasks were pooled at this stage. Centrifugation at 1,000 rpm for 2 mins at room temperature resulted in a cell pellet which, after removal of the supernatant, was resuspended in 2.5mls of filtered cell freeze-down media (section 2.10.2). Aliquots were transferred to cryo-tubes, incubated at -80°C for 12-16 hours and then transferred to liquid nitrogen for long term storage.

2.11.2 Resurrection of Frozen Cell Stocks from Liquid Nitrogen.

A vial containing the frozen cell stock was removed from the liquid nitrogen and rapidly thawed by incubating in a 37°C water bath. An aliquot from the vial was then transferred to a 75ml flask containing 14ml of normal growth media supplemented with Ciproxin (5ml/500ml media). Cells were incubated at 37°C in a 10% CO₂ incubator.

2.12 Trypsinisation of Cells.

Media was aspirated from the cells which were then rinsed with 1ml of trypsin-EDTA. This was quickly removed from the cells and a further 2-4mls trypsin-EDTA added. After incubation at 37°C for 2-5 mins in a 10% CO₂ incubator the cells began to lift from the surface of the plate/flask. The reaction was terminated by addition of 10mls of growth medium and the cell suspension washed over the growth surface of the plate/flask using a pipette to aid resuspension. Growth media was added to obtain the required dilution factor and the cells were transferred to fresh flasks/plates.

2.13 Transfection of CHO-Cells Using Calcium Phosphate.

2.13.1 Preparation of Cells for Transfection.

CHO cells were plated at a density of 10⁴/cm² (approximately 7 x 10⁵ cells/10cm plate) in Ham's F12 media supplemented with 10% (v/v) fetal calf serum. The cells were cultured overnight at 37°C in 10% CO₂. 3-4 hrs prior to transfection fresh media was added to the dishes.

2.13.2 Transfection and Selection Protocol.

5-20µg of DNA was added to a sterile 13.5ml falcon tube. To this, 36µl of 2M CaCl₂ was added and the final volume made up to 300µl with sterile H₂O. This solution was slowly added dropwise using a pasteur pipette to another tube containing 300µl 2x HEPES Buffered Saline (HBS- Table 2.2) whilst bubbling air through the solution using another pipette. This process was performed over 1-2 mins. After incubation at room temperature for 30 mins, a fine precipitate forms which is then added dropwise to cells in 10cm plates. Cells are maintained at 37°C in a 10% CO₂ incubator for 6-12 hours before removal of the precipitate by washing the cells twice with 1x PBS. Media is aspirated from the plates and 3ml of a fresh solution of 1x PBS/10% (v/v) DMSO was added. Cells were

then incubated at room temperature for 2.5 mins before removal of the DMSO solution and replacement with fresh growth media. The cells were incubated under normal growth conditions for a further 24-48 hours. At this point, the selection reagent, G418 at 600 μ g/ml was added to the media which was subsequently changed every 2 days to remove cell debris and to allow resistant cells to grow. This process was carried out for 7-14 days post transfection until colonies appeared under the microscope. Individual colonies were isolated and cultured for further analysis.

2.13.3 Isolation and Propagation of Individual Clones.

Media was aspirated from the cells. A sterile cloning ring was then placed over an individual colony of cells and secured to the plate using sterile vaseline. 200 μ l of trypsin-EDTA solution was added and after 2-3 mins the cells began to lift from the plate aided by gentle titration using a P200 Gilson pipette. The cells were then transferred to a 6cm plate containing 5mls normal growth media supplemented with G418 (150 μ /ml). Cells were propagated under these conditions, with frequent media changes until confluent. At this point cells could be split and grown for transport assays or frozen down in liquid nitrogen for long term storage (Section 2.11).

2.14 Identification of GLUT-Transfected Clones.

2.14.1 Preparation of CHO-Cells for Western Blotting.

Cells were grown on 6cm plates until nearly confluent. They were then washed with 3x 5ml of 1x PBS and 1ml of SDS sample buffer was added (Table 2.3). Cells were scraped from the plate, resuspended in the sample buffer and transferred to an Eppendorf tube. Disruption of the cells was achieved by passing them through a 1ml syringe fitted with a 25 gauge needle several times. The samples were then incubated in a boiling water bath for 2-3 mins before either storage at -20°C or analysis by SDS-PAGE (section 2.17.1) and Western blotting (section 2.17.2).

2.15 Measurement of [^3H]2-Deoxy-D-Glucose Uptake by CHO-Cells.

2.15.1 Reagents.

1x KRP Solution (stored at 4°C).

1x KRP containing BSA at 1mg/ml.

10 μM cytochalasin B in 1x KRP solution.

1% (w/v) TX-100.

1x PBS Solution (stored at 4°C).

Sugar stocks made up in 1x KRP containing BSA at 1mg/ml.

2.15.2 Preparation of Cells for Transport Assays.

CHO-cells were grown as described and were split into 6-well plates. Growth media was aspirated from cells that were 70-80% confluent, and replaced by serum-free Ham's F12 media containing non-essential amino acids. After an incubation period of 2 hours at 37°C in a CO₂ incubator, the cells were ready for analysis of transport activity.

2.15.3 Transport Assays.

Cells were rinsed with 3x 3ml KRP (Table 2.2) at 37°C. 950 μl of KRP/BSA solution was added to each well. For measurement of basal transport levels, 950 μl of KRP/BSA containing 10 μM cytochalasin B was added. The cells were incubated at 37°C on a hot plate for 15 mins. Transport was initiated by the addition of a 50 μl aliquot containing a final concentration of 0.1mM 2-deoxy-D-glucose and 0.25 μCi [^3H]2-deoxy-D-glucose to each well. Transport activity was terminated after an incubation period of 3 or 10 mins at 37°C by flipping the contents out of the wells and immersing the plates in 2 litres of ice-cold 1x PBS solution. Excess PBS was removed from the cells by inverting the plates and 1ml of 1% Triton X-100 was added to each well. Plates were left at room temperature overnight on a rotating platform before the solubilised cells were transferred to scintillation vials,

scintillation fluid was added and the amount of radioactivity measured by scintillation counting.

3 - Western Blotting and Immunodetection of Proteins.

2.16 Materials.

ECL Western blotting detection reagents supplied by Amersham Life Science, U.K.

Broad range molecular weight markers were supplied by BioRad Labs, BioRad House, Herts, U.K.

Acrylamide and bisacrylamide were supplied by BDH, Merck Ltd, Hunter Boulevard, Magna Park, Leics, U.K.

Aprotinin, diisopropylfluorophosphate, pepstatin A and Kodak film were supplied by Sigma Chemical Company, Poole, Dorset, UK.

Nitrocellulose (Schleicher & Schuell) was supplied by Anderman Ltd, London, UK.

Goat anti-rabbit IgG was supplied by Amersham

Anti-GLUT2 and anti-GLUT3 antibodies were generated by Dr. Gwyn Gould and the animal house technical staff and purified by Dr. Jacqueline Rice, Department of Biochemistry, IBLS, University of Glasgow, U.K.

GLUT3 rat brain and GLUT2 rat liver standards were provided by Ian Campbell, Glasgow University, U.K.

2.17 Immunodetection of GLUT2 and GLUT3 Proteins.

2.17.1 SDS/Polyacrylamide Gel Electrophoresis (SDS /PAGE).

SDS polyacrylamide gels were prepared using either Bio-Rad mini-Protean II or Hoefer large gel units. Typically a 10% (w/v) resolving gel was used consisting of 0.383M Tris-HCl, pH8.8; 10% acrylamide/bisacrylamide and 0.1% SDS; polymerised with 0.1% (w/v) ammonium persulphate and 0.001% (v/v) TEMED. Stacking gels were typically 2 and

3cm for mini- and large gels respectively and consisted of 0.135M Tris-HCl, pH8.8; 5% acrylamide/bisacrylamide; 0.1% SDS polymerised with 0.1% (w/v) ammonium persulphate and 0.001% (v/v) TEMED.

Protein samples to be analysed were solubilised in 1x sample buffer (Table 2.3) containing 1 μ g/ml aprotinin, 100 μ M diisopropylfluorophosphate and 2 μ M pepstatin A, and stored at -20°C until required.

The gel apparatus was assembled and the gels immersed in 1x electrode buffer (Table 2.3). Prestained broad range molecular weight markers (Bio-Rad, ranging between 202-6.9kDa) were loaded followed by the protein samples. Mini-gels were electrophoresed at 150V until the tracking dye front reached the bottom of the gel and good separation of the prestained molecular weight markers was obtained. Large gels were run at 40V overnight.

2.17.2 Western Blotting of Proteins.

Proteins were separated by SDS-PAGE as previously described (section 2.17.1). The gels were removed from the plates and rinsed with 1x transfer buffer (Table 2.3). Each gel was placed onto a blotting cassette on top of a piece of Whatman 3mm blotting paper soaked in transfer buffer. Nitrocellulose membrane (0.45 μ M pore size, Schleicher and Schuell) was cut to the same size as the gel, pre-soaked in transfer buffer and placed on top of the gel. Pre-soaked blotting paper was placed on top of the nitrocellulose and all air bubbles were removed from the "sandwich". The cassette was secured and placed into the blotting tank containing transfer buffer. Transfer was performed using a Bio-Rad mini trans-blot electrophoretic transfer cell at a constant current of 275mA for 3 hours at room temperature. Large gels were transferred to nitrocellulose in much the same way using larger cell units and at 40mA overnight. On removal of the nitrocellulose membrane from the blotting apparatus the efficiency of transfer was qualitatively determined by the presence and intensity of the pre-stained molecular weight markers.

2.17.3 Blocking of Nitrocellulose Membranes and Probing with Anti-GLUT2 and Anti-GLUT3 Antibodies.

Non-specific binding sites on the nitrocellulose membranes were blocked by shaking for 1-3 hours in 1st wash buffer (Table 2.3) containing 5% (w/v) non-fat milk (Marvel, Premier Brands U.K.). The nitrocellulose was then rinsed with 1st wash buffer to remove excess blocking solution and transferred to 1st wash buffer containing 1% (w/v) BSA and primary antibody at the appropriate dilution, typically 1:100 to 1:250 dilution. The membrane was incubated with primary antibody overnight in a sealed bag with shaking at room temperature before being washed extensively with 1st wash buffer over a period of 1 hour, changing the buffer every 10 mins.

GLUT2 and GLUT3 antibodies were generated by immunising a rabbit with synthetic peptides corresponding to the C-terminal 14 amino acids of human GLUT2 and GLUT3 isoforms.

2.17.4 Immunodetection of Proteins by Autoradiography.

Membranes probed with antisera to GLUT2 or GLUT3 were incubated in 1% Marvel/1st wash buffer containing $1\mu\text{Ci}/20\text{ml}$ ^{125}I -labelled goat anti-rabbit IgG. After incubation at room temperature for 3 hours, the membranes were washed four times at 10 min intervals with 2nd wash buffer, draining off the final wash. The membranes were then dried overnight between two sheets of Bio-Rad cellophane, assembled in a developing cassette and exposed to Kodak X-OMAT S 100 film for 12-24 hours at -80°C . The film was developed using an X-OMAT processor.

2.17.5 Detection of Immunoprecipitated Proteins using Enhanced Chemiluminescence (ECL).

Washed membranes prepared as described above were transferred to a clean container and excess buffer drained from them. An equal volume of detection solutions 1 and 2

(obtained from Amersham Life Sciences) were mixed to produce a final volume sufficient to cover the membrane ($0.125\text{ml}/\text{cm}^2$). Membranes were immersed in the detection solution mixture for 1 min before decanting the solutions off. The membranes were wrapped in cling-film and exposed using Kodak X-OMAT S 100 film for varying time periods depending on the relevant band intensities and the background signal. Films were developed using an X-OMAT processor.

Table 2.3**SDS-PAGE and Western Blotting Buffers.**

Solution	Constituents
1x Electrode buffer	120mM Tris-HCl, pH8.3; 40mM glycine; 0.1% (v/v) SDS
1x Sample buffer	93mM Tris-HCl, pH6.8; 2% (w/v) SDS; 10% (v/v) glycerol; 10mM Na ₂ EDTA; 0.002% (w/v) bromophenol blue
Transfer buffer	25mM sodium phosphate buffer, pH6.5
1st Wash buffer	1x PBS, pH7.4; 0.1% (V/V) Triton X-100; 1mMEDTA
2nd Wash buffer	9g NaCl per 250mls 1st Wash buffer

CHAPTER 3

Construction and Sequencing of Pro-Ala **Mutants of the Brain-Type Glucose** **Transporter-GLUT3.**

3.1 Aims

1. To construct a series of eight mutated GLUT3 cDNAs using recombinant PCR technology. These mutants will contain single base changes such that the proline residue of interest is replaced by alanine. Proline residues targeted for mutation are highly conserved in GLUTs 1-5 and are located within or near the start/end of a putative transmembrane helix.
2. Mutated cDNAs will be subcloned into the vector pSPGT3 to form a series of constructs that can be used as templates for *in vitro* synthesis of mRNA for subsequent heterologous expression in *Xenopus laevis* oocytes.
3. pSPGT3 cDNA clones will be screened by automated DNA sequencing to confirm the presence of the desired mutation. Positive constructs will then be fully sequenced on both strands to ensure that no sequence errors were incorporated during the PCR reactions and subcloning procedures.

3.2 Structure-Function Studies of GLUT Isoforms using Mutagenic Techniques.

3.2.1 Introduction.

Recent advances in recombinant molecular biological techniques and the availability of cloned cDNAs for each of the glucose transporters have facilitated the study of the importance of individual amino acid residues in the mechanisms of substrate binding and translocation across the plasma membrane. Indeed, the replacement of individual amino acid residues in protein sequences is now a widely used technique for the dissection of reaction mechanisms at the molecular level. Investigation of the glucose transporters by site-directed mutagenesis is still at an early stage, with analysis of less than 5% of the 492 residues of GLUT1 reported in the literature. As a first step in the molecular dissection of the GLUT1 transporter, site-directed mutagenesis coupled with the use of heterologous expression systems provide the basis for the construction of a detailed mutational map and thus, an investigation of transporter structure and function. A residue of interest can be replaced by another residue to determine its functional importance. Loss of transport activity or a perturbation of ligand binding suggests that a particular residue is somehow involved in sugar transport. Residues that are targeted for mutational studies are usually highly conserved or are invariant among all of the transporter isoforms. The majority of such studies have been carried out on the GLUT1 isoform. However, recently, investigation of such residues have been extended to the other GLUT isoforms in an effort to address the generality of the proposed structure-function model and, to identify factors that govern isoform specific characteristics. The three main mutagenic strategies that have been employed are the generation of point mutations, deletion mutants and the construction of chimeric transporters, which have large sequences of one transporter replaced by the equivalent sequence of another.

3.2.2 Substitution of Conserved Polar Residues.

Hydropathy analysis of the deduced amino acid sequence of GLUT1 ((Mueckler, 1985)) predicts that transmembrane segments 3, 5, 7, 8 and 11 may form amphipathic α -helices. These contain several serine, threonine, glutamine and asparagine residues which have been predicted, using molecular modelling studies, to lie on the same face of the α -helices, directed toward the centre of the protein. It is possible that these helices bundle together to form a membrane channel through which the substrate can pass. Hydroxyl and amide groups of polar amino acids lining the channel are capable of forming specific interactions with D-glucose via hydrogen bonding during its translocation across the membrane.

Studies involving the use of photoactivatable transport inhibitors have provided some clues as to the location of the substrate binding sites. The bis-mannose derivative, ATB-BMPA, has been shown to specifically interact at the exofacial binding site of the transporter (section 1.7.3), which has been mapped to a region within helices 7 and 8 (Davies *et al.*, 1991). Helix 7 contains the highly conserved motif QXXSGXNXXYY, which is present in all of the mammalian transporters and also is highly conserved in the wider super family of glucose transporters. Helix 8 also contains a number of conserved polar residues. The first demonstration using mutagenic techniques that helix 7 constituted part of the exofacial ligand-binding site came from a study in which three conserved residues Gln²⁸² and Asn²⁸⁸ of helix 7, and Asn³¹⁷ of helix 8, were mutated to leucine, isoleucine and isoleucine respectively (Hashiramoto *et al.*, 1992). When expressed in CHO-K1 cells all mutants were detected by Western blotting at comparable levels to wild type GLUT1. Retention of high levels of 2-deoxy-D-glucose transport activity by all three mutants implies no absolute requirement of these residues for transport activity. The structural separation of the exo- and endofacial binding sites in these mutants was investigated using the site specific ligands ATB-BMPA and cytochalasin B. All mutants retained comparable levels of cytochalasin B labelling at the endofacial site and the Asn²⁸⁸Ile and Asn³¹⁷Ile mutants retained high levels of ATB-BMPA labelling at the exofacial site. However Gln²⁸², located in helix 7, is implicated in forming the outside specific ligand-binding site due to a striking 95% reduction

in the level of ATB-BMPA labelling of this mutant, and a 10-fold increase in the K_i determined for 4,6-*O*-ethylidene-D-glucose inhibited 2-deoxy-D-glucose transport.

As Gln²⁸² is predicted to be located in the centre of helix 7, it was postulated by Hashiramoto and co-workers that this helix moves up in the membrane to accept exofacial ligands, possibly involving some unfolding near the top of the helix. Indeed, protection against proteolysis by ATB-BMPA supports the occurrence of a large conformational change resulting in the upward movement of helix 7 rendering the bottom of the helix inaccessible to proteases (Hashiramoto *et al.*, 1992).

In a second study by Mueckler co-workers in 1994, the role of five highly conserved transmembrane polar residues Asn¹⁰⁰, Gln¹⁶¹, Gln²⁰⁰, Tyr²⁹² and Tyr²⁹³ were investigated by mutagenesis. The aim was to assess the importance of these residues in substrate binding by replacing them with hydrophobic amino acids lacking hydroxyl or amide side chains and, in the case of Asn¹⁰⁰ and Gln¹⁶¹, more conservative substitutions were also made i.e. to uncharged polar residues. Both Gln¹⁶¹ mutants exhibited reduced 2-deoxy-D-glucose transport activity in oocytes due to reduced intrinsic activity of the protein and not as a consequence of reduced affinity for substrate, since no elevation in K_m was observed. As reorientation of the unloaded transporter is assumed to be the rate limiting step (Lowe & Walmsley, 1986), then mutation of Gln¹⁶¹ is likely to affect this step which involves a substrate independent conformational change. In contrast, the mutation of Gln²⁸² is postulated to affect the substrate binding event only (Hashiramoto *et al.*, 1992), since a reduction in exofacial ligand binding was observed despite very little effect on transport activities. Both studies by Mueckler and Hashiramoto are consistent with the hypothesis that helices 5 and 7 are amphipathic and contribute to the formation of the aqueous pore. These helices contain side groups that can participate in transient hydrogen bond formation with the substrate during translocation.

Due to its high degree of conservation throughout the wider superfamily of glucose transporters, the sequence Q²⁸²QXSGXN²⁸⁸XXFY²⁹³, towards the endofacial end of helix 7 has been the target of much mutagenic interest in the context of its role in the transport mechanism. Site-directed mutagenic studies on residues Gln²⁸² and Asn²⁸⁸ have already been discussed above. Mutation of tyrosine residues at positions 292 and 293 to

either isoleucine or phenylalanine was the object of a further study by Mori and co-workers in 1994. Of the four mutants, decreased 2-deoxy-D-glucose transport activity was observed only with the Tyr²⁹³ to isoleucine mutation. Ligand binding studies revealed that this loss of transport was associated with complete abolition of cytochalasin B labelling at the endofacial site. The conserved FYY sequence is predicted to form part of a hydrophobic patch on the transporter, located close to the C-6 position of the sugar as it locates at the exofacial site. This hypothesis is based on D-glucose analogue studies (Barnett *et al.*, 1975; Barnett *et al.*, 1973). Thus, the sequence Q²⁸²QLSGINAVFYY²⁹³ in helix 7 of GLUT1 is hypothesised to have a dual role in both hydrogen bonding to D-glucose and closing of the exofacial binding site during translocation. The Gln²⁸²Leu mutation is consistent with this interpretation since ATB-BMPA binding is abolished. In contrast, mutation of Tyr²⁹³Ile results in decreased transport activity associated with complete loss of cytochalasin B binding at the endofacial site and retention of ATB-BMPA labelling. The transporter is therefore stabilised in an outward facing conformation as a result of a single point mutation within helix 7 that perturbs the conformational changes necessary for closing of the exofacial site. This is a somewhat striking observation when compared to the conclusions drawn from a study in which 37 of the 42 C-terminal amino acids of GLUT1 were deleted (Oka *et al.*, 1990). Although expressed at the plasma membrane of CHO cells, the truncated GLUT1 was functionally inactive, probably due to an inability to alternate between conformational states. As cytochalasin B labelling was retained with a corresponding abolition of high affinity ATB-BMPA labelling, it was concluded that this mutant was locked in an endofacial conformation. It was postulated that the C-terminal domain is not involved in substrate/ligand binding to the endofacial site *per se*, but is involved in the formation of the outward facing binding site.

There are four other conserved tyrosine residues within the GLUT isoforms located at positions 28, 143, 308 and 432 in GLUT1. These, along with Tyr²⁹² and Tyr²⁹³ were mutated to Phe in the rat GLUT4 isoform (Wandel *et al.*, 1994). Glucose transport activity was reduced in Tyr¹⁴³Phe and Tyr²⁹³Phe but was unaffected in the other mutants. Cytochalasin B binding was reduced in mutants Tyr¹⁴³Phe, Tyr²⁹²Phe and Tyr²⁹³Phe.

Tyrosines at positions 143 and 293 seem to be functionally important and Tyr²⁹² may represent an additional contact site for cytochalasin B.

Transmembrane helix 11 contains a highly conserved polar amino acid located at position 415. Mutation of this asparagine to aspartic acid, i.e. replacement of a positive charge with a negative charge, causes a 5-fold decrease in the turnover number and a 1.5-fold increase in K_m (Ishihara *et al.*, 1991). Cytochalasin B & 4,6-*O*-ethylidene-D-glucose data suggest modulation at the inner but not the outer binding site. Asn⁴¹⁵ is likely to reside close to the inner binding site and the presence of an ionic charge in this domain may have decreased the turnover number of the protein by affecting the rate of conformational changes between the inward and outward facing transporter.

3.2.3 Substitution of Conserved Tryptophan Residues.

In 1981, a model was proposed, based on kinetic studies, in which the transporter undergoes conformational changes allowing the protein to alternate between two conformational states (Baldwin *et al.*, 1981). Since then, much evidence has been accumulated to support the conclusion that a change in protein secondary structure occurs as a consequence of D-glucose binding (Chin *et al.*, 1987; Chin *et al.*, 1986). D-glucose binding increases the α -helical content and, on this basis, domain transfer of an aqueous-accessible segment into the membrane was proposed (Pawagi & Deber, 1987).

Tryptophan residues can be used to monitor the intrinsic fluorescence of proteins and this is a useful technique to obtain information regarding substrate binding and conformational changes in the absence of an overall tertiary structure. In addition, information regarding the relationship of the integral membrane protein with the cellular lipid bilayer can be obtained. Protein intrinsic fluorescence can be monitored in the presence of small hydrophilic quencher molecules such as acrylamide and potassium iodide. If a tryptophan residue is directly involved in substrate binding or, if it is located in a dynamic segment that undergoes a domain shift during ligand-binding/translocation, then alterations will occur in its emission wavelength or its susceptibility to quenching.

Such techniques were used to investigate conformational/positional changes occurring in GLUT1 in the presence and absence of D-glucose and in the presence of the inhibitors cytochalasin B and maltose (Pawagi & Deber, 1990). GLUT1 contains six highly conserved tryptophans, the majority of which are predicted to be located in inaccessible hydrophobic regions of the membrane. Results obtained in the presence of inhibitors are interpreted in terms of ligand activated movement of a protein segment containing a tryptophan from an initially aqueous located region into or toward the membrane. This relocation event opens the channel whereas maltose and cytochalasin B block this conformational change and thus inhibit D-glucose transport. Conformational and hydropathy analyses have suggested that the region encompassing Trp³⁸⁸ is a dynamic segment that could undergo ligand activated movement into the membrane and hence open a putative channel within the protein.

Upon exposure to ultra-violet irradiation, GLUT1 can be covalently labelled with cytochalasin B at a region close to the endofacial glucose binding site. Labelling is D-glucose inhibitable. The wavelength required for photolabelling and the cleavage of photolabelled transporter with various proteases (Cairns *et al.*, 1987; Holman & Rees, 1987) suggest that the cytochalasin B labelling site may involve Trp⁴¹² and/or Trp³⁸⁸ of GLUT1. Due to the high conservation of Trp⁴¹² in the other isoforms, this residue was implicated in glucose binding and/or other aspects of the transport mechanism. Mutation of this residue in rabbit GLUT1 to leucine (Katagiri *et al.*, 1991) reduced 2-deoxy-D-glucose transport to 15-30% of wild type levels of activity when expressed in CHO cells. A marked decrease in 2-deoxy-D-glucose transport was also observed when the corresponding tryptophan residue in GLUT3, Trp⁴¹⁰, was replaced by leucine (Burant & Bell, 1992b). Further analysis of 2-deoxy-D-glucose transport kinetics revealed that this dramatic decrease in transport activity was associated with a 2.5-fold increase in K_m and a 3-fold decrease in turnover number. In addition, cytochalasin B labelling was not abolished but decreased by 40% and cytochalasin B binding was also decreased. Side-specific glucose analogues used in conjunction with cytochalasin B binding show that this mutation does not affect the exofacial binding site, but alters the conformation at the endofacial site such that cytochalasin B binding and its inhibition by *n*-propyl- β -D-glucopyranoside were both affected. Thus it seems that Trp⁴¹²

is not the sole cytochalasin B labelling site but is located close to the inner binding site. Protease digestion studies of cytochalasin B-labelled GLUT1 indicate that the photolabelling site is located between residues 388-412 (Holman & Rees, 1987) and so Trp⁴¹² may be one of many labelling sites in this region.

This led to a study by Garcia and co-workers in 1992 to assess the possible role of all six tryptophan residues in transporter activity. When replaced by either glycine or leucine, only mutations at Trp³⁸⁸ (in helix 10) and Trp⁴¹² (in helix 11) affected 2-deoxy-D-glucose or 3-O-methyl-D-glucose transport activity when expressed in oocytes, CHO cells or COS-7 cells (Garcia *et al.*, 1992; Katagiri *et al.*, 1993; Shurman *et al.*, 1993). Decreased transport activity in the case of Trp⁴¹² mutants was associated with a dramatic reduction in the intrinsic activity of the mutant proteins. Whilst only a moderate reduction in intrinsic activity was detected for the Trp³⁸⁸ mutants, decreased transport activity can be accounted for by reduced level of protein detected in oocytes and decreased targeting to the plasma membrane. Double mutation of both Trp³⁸⁸ and Trp⁴¹² in GLUT1 results in total abolition of cytochalasin B labelling and reduced cytochalasin B binding or 2-deoxy-D-glucose transport. Thus, it was proposed that either tryptophan residue could be labelled by photoactivation (Inukai *et al.*, 1995).

3.2.4 Substitution of Proline Residues.

There are a number of highly conserved sequences among the GLUT isoforms that are rich in proline residues. Indeed, this observation can be extended to the wider family of membrane transporters. It is rather surprising that these residues exist in the membrane spanning domains since proline is known as a classic breaker of α -helical structure. Such considerations have prompted several groups to investigate the role of these residues in transporter function, particularly with regard to the conformational changes involved in substrate translocation. Such studies will be discussed in detail in section 3.3 and Chapter 4 of this thesis.

3.2.5 Mutation of Cysteine Residues of GLUT1.

Despite no absolute conservation amongst the mammalian GLUT isoforms, cysteine residues have been targeted for mutagenesis to examine their role in transport activity, protein conformational stability and oligomerisation. GLUT1 contains 6 cysteine residues and the individual replacement of these residues have no reported consequences on transporter function (Wellner, 1994). Double, triple and cysteine-less mutants retain wild type GLUT1 transport kinetics (Due *et al.*, 1995a; Wellner, 1995). Mutants lacking cysteine residues in either the N- or C-terminal domains and the cysteine-less mutant all exhibit asymmetric transport. In addition, K_m and V_{max} parameters for equilibrium exchange of 3-*O*-methyl-D-glucose were greater than those for zero-*trans* uptake, as is the case for the wild type transporter. With regard to cytochalasin B binding, mutation of cysteines in the N- and C-terminal domains results in increased affinity. The cysteine-less mutant exhibits an affinity for cytochalasin B that is at least 5-fold greater than the wild type (Wellner, 1994).

Mutagenic studies have confirmed the locations of Cys²⁰⁷ and Cys⁴²⁹ at the endofacial loop between transmembrane helices 6 and 7, and at the exofacial loop between transmembrane helices 11 and 12, respectively. Constructs in which these residues were individually replaced lost sensitivity to *p*-chloromercuribenzenesulphonate (pCMBS) when either injected intracellularly or applied externally to oocytes ((Wellner, 1994).

The observation that the cysteine-less mutant retains wild type transport kinetics questions the proposal made by Carruthers and co-workers in 1995 that a single intramolecular disulphide bridge between Cys³⁴⁷ and Cys⁴²¹ stabilises transporter oligomeric structure and accelerates transport function (section 1.10). The expression system used in this study (CHO-cells) however, is different from that used by Wellner and co-workers and this may affect the oligomeric states of the transporters. The fully functional cysteine-less mutant should also prove useful in further studies investigating the transmembrane topology and function of GLUT1. For example, it can be used as a template to substitute cysteines back into the transporter at serine residues likely to be exposed at extramembraneous regions or, at locations close to the channel or substrate binding site(s). This, in combination with cell-impermeant sulfhydryl reagents, should identify regions

necessary for transporter function. The mutant should also provide a useful template for the introduction of fluorescent groups in selected regions of the transporter allowing observation of transporter function via fluorimetric methods. That is, of course, providing that the transporter remains fully functional.

3.2.6 Point Mutations in the N-Terminus.

The effects of substitution of an N-terminal amino acid on both ligand binding and transport activity was discussed in section 1.7.4b. The only other residue (in addition to Gln¹⁶¹ in helix 5), located within the N-terminus that has been reported to affect transport activity is Val¹⁶⁵ in GLUT1 or Val¹⁹⁷ in GLUT2. Mutation of the aforementioned valines in both isoforms to isoleucine resulted in a severe reduction in transport activity (Mueckler *et al.*, 1994). Such an effect is most surprising, considering that the mutation represents replacement of one hydrophobic transmembrane residue for another, differing in structure by only one methyl-group. The Val¹⁹⁷Ile substitution of GLUT2 has been discovered in a single allele of a patient with non-insulin-dependent diabetes. Interestingly, the reverse mutation of this residue, i.e. Ile-Val, resulted in a complete restoration of functional activity when expressed in oocytes (Mueckler *et al.*, 1994b). Substitution of isoleucine for valine is one of the more common conservative substitutions observed at equivalent positions in homologous proteins (Schultz & Schirmer, 1979). A further point of interest is that Val¹⁶⁵ in GLUT1 is predicted to lie approximately one helical turn in distance from Glu¹⁶¹ which has been demonstrated to affect exofacial ligand binding (Mueckler *et al.*, 1994a). The valine side chain is thus predicted to lie close to the exofacial substrate binding site within the putative channel. The presence of a bulkier side chain at this crucial position may be sufficient to block binding or passage of substrate through the channel.

3.2.7 Substitution of Extramembraneous Residues.

The majority of mutational studies to date have been confined predominantly to those regions of the transporter that are highly conserved between the GLUT isoforms, i.e. the transmembrane domains. Another common feature exhibited by all GLUT isoforms is a potential *N*-linked glycosylation site located within the large extracellular loop linking transmembrane helices 1 and 2. This site has been identified as Asn⁴⁵ in GLUT1 and its high degree of conservation in the other isoforms may suggest an important role for *N*-linked glycosylation in transporter function. Indeed, this was the aim of a study carried out by Asano and co-workers in 1991. Mutation of Asn⁴⁵ to asparagine, tyrosine or glutamine abolished *N*-linked glycosylation and led to a 2-fold reduction in the transporter affinity for 2-deoxy-D-glucose. It was concluded that, although glycosylation of the transporter is not absolutely essential, it may play a role in maintaining a structure capable of high affinity substrate binding, thereby increasing transport activity (Asano *et al.*, 1991). This may account for some of the anomalies observed when comparing studies carried out in different heterologous expression systems, for example, the glycosylation pattern of a transporter expressed in *Xenopus* oocytes may be different from that observed in the native cell.

Other studies concerning residues that are not confined to transmembrane regions of the transporter have been discussed previously (section 1.7.4). For example, the cytoplasmic C-terminal tail has been shown to play a role in transport activity and formation of the exofacial binding site (section 1.7.4a).

3.2.8 Generation and Characterisation of Chimeric Transporter Proteins.

Comparative studies have revealed that the GLUT isoforms exhibit distinct kinetic parameters for glucose transport and therefore display different sugar transport characteristics in the tissues in which they are predominantly expressed (Colville *et al.*, 1993a; Colville *et al.*, 1993b; Gould *et al.*, 1991). It is the primary amino acid sequence of the transporter protein, and not the tissue in which it is expressed, that governs its affinity for glucose. In an effort to identify the structural determinants that account for these unique

functional characteristics, the effects of exchanging various domains between isoforms has been probed by the generation of chimeric transporters. This strategy makes use of site-specific oligonucleotide primers and recombinant PCR to generate the transporters, which can then be heterologously expressed in a range of cell systems for functional characterisation.

To date, a variety of constructs have been reported (reviewed in Saravolac & Holman, 1997). Chimeras in which the C-terminal tail is exchanged between human GLUT1 and rat GLUT4, or between human GLUT3 and GLUT4 exhibit 2-deoxy-D-glucose transport activity that is comparable to wild type levels (Burant & Bell, 1992; Pessino *et al.*, 1991). Thus, the role of the C-terminal region in transport catalysis appears to be identical between these pairs of isoforms. However, when the C-terminal 20 amino acids of the murine GLUT1 isoform are replaced with those of human GLUT4, significant alterations in transport kinetics are observed. The GLUT1/GLUT4 chimera does not appear to exhibit accelerated equilibrium exchange, a property characteristic of GLUT1. Accelerated exchange is not transferred to GLUT4 in the reverse chimera consisting of GLUT4 sequence with a GLUT1 C-terminus. This suggests rapid equilibrium exchange is a property unique to GLUT1 and it requires specific sequences in other regions of the protein in addition to the C-terminal region (Dauterive *et al.*, 1996).

GLUT2 has a very specific tissue distribution and is characterised by high K_m and V_{max} values compared to the other isoforms. GLUT2 is also unique among the GLUTs in that it can transport both D-fructose and D-glucose (Colville *et al.*, 1993a; Colville *et al.*, 1993b). Furthermore, this isoform exhibits distinct kinetics of cytochalasin B inhibition of glucose transport and is only very poorly photolabelled (Axelrod & Pilch, 1983). These distinct properties are likely to be attributable to the more divergent regions of the transporter sequence. There have been a number of studies involving the C-terminal cytoplasmic tail region of GLUT2. Replacement of the C-terminal residues of human GLUT1 with the corresponding 89 residues of the GLUT2 human isoform resulted in a 4-fold and 3.8-fold increase in K_m and V_{max} values for 2-deoxy-D-glucose transport, respectively. A decrease in the affinity for cytochalasin B was also observed compared to wild type GLUT1 (Katagiri *et al.*, 1992). Together these observations suggest that the C-terminus confers GLUT2-like

kinetics onto the GLUT1 transporter, but does not contribute to cytochalasin B binding. Similar results were obtained from a study in which C-terminal regions of GLUT2 and GLUT4 were exchanged. Replacement of the carboxy-terminus of GLUT4 with that of GLUT2 resulted in a 2-fold increase in the K_m for 3-O-methyl-D-glucose. However, replacement of the region encompassing the large intracellular loop and transmembrane helices 7 and 12 was necessary to increase the K_m to a value approaching that of wild type GLUT2 (Buchs *et al.*, 1995). Thus, in addition to the cytoplasmic C-terminal tail, transmembrane helices 7 and 12 are also important for the distinctive affinity exhibited by GLUT2.

In an attempt to address which regions of GLUT2 and GLUT3 are responsible for substrate specificity, a series of chimeras containing various portions of the N- and C-terminal domains of these isoforms were constructed. Chimeras containing N- and C-terminal regions of GLUT2 including transmembrane helix 7 exhibited low affinity 2-deoxy-D-glucose uptake and were capable of D-fructose transport. In contrast, chimeras containing helix 7 sequence derived from GLUT3 exhibited high affinity 2-deoxy-D-glucose transport and no detectable levels of D-fructose transport (Arbuckle *et al.*, 1996). It was concluded that helix 7 contributes to both high affinity 2-deoxy-D-glucose transport and substrate selectivity between GLUT2 and GLUT3 isoforms (discussed further in Chapter 6).

GLUT5 is the most divergent member of the mammalian GLUT family possessing only 40% identity with the other isoforms. An interesting but poorly understood property of this isoform is its ability to transport D-fructose and inability to transport D-glucose (Burant *et al.*, 1992). A chimeric study was designed to address the biochemical properties of GLUT5 and to investigate the domains responsible for fructose transport. Expression of GLUT5 in CHO cells resulted in transporters localised at the plasma membrane of oocytes that were capable of transporting D-fructose but not D-glucose. In addition, fructose transport was not inhibited by cytochalasin B and no detectable levels of photolabelling were recorded (Inukai *et al.*, 1995). Most GLUT1/GLUT5 chimeras expressed no measurable fructose or glucose transport . However, chimeras consisting of N-terminal GLUT5 sequence to the end of helix 6, or GLUT1 sequence containing only the C-terminal 44 residues derived from GLUT5, exhibited glucose transport and cytochalasin B binding.

These observations may support the hypothesis that transmembrane helix 7 is an important determinant for regulation of substrate specificity, since both chimeras that transport glucose contain the GLUT1 helix 7 sequence. GLUT5 on the other hand appears to have a more specific structural requirement for transport of D-fructose, involving regions of the transporter other than helix 7.

3.3 Role of Transmembrane Proline Residues in Membrane Transport Proteins.

3.3.1 Introduction.

There are several classes of protein that span the cell lipid bilayer that can be divided based on the structure and function of their transmembrane segments. Proteins such as the histocompatibility antigens, the immunoglobulin M heavy chain and the epidermal growth factor receptor contain a single transmembrane segment that serves to anchor these proteins to the membrane. Transport proteins such as the Ca^{2+} , Mg^{2+} -ATPase of the sarcoplasmic reticulum, the *lac* permease of *E.coli* and the mammalian facilitative glucose transporters are predicted to traverse the membrane several times. The transmembrane segments are conformationally ordered to create a specific transport channel. A high proportion of polar residues located within certain transmembrane segments impart the amphipathic characteristics required for the formation of a hydrophilic channel. Regulation of the channel itself must involve either the creation or accessibility of the channel.

Advances in recombinant DNA technology over the last 10-15 years have made available the sequences of many membrane proteins. However, the details of transporter function at the molecular level and the precise mechanism of regulation are poorly understood at present. Such advances are ultimately hindered by difficulties associated with obtaining high-resolution crystal structures for this class of protein. Molecular dynamics and molecular modelling, in combination with mutagenic studies, may provide some insights into the transport mechanism. Large conformational changes in protein structure are predicted to be necessary for substrate translocation across the lipid bilayer. Such

structural/positional changes would have to be both reversible and dynamic events, resulting in specific conformational consequences. The observation, made from a survey of the transmembrane segments of integral membrane proteins (Brandl and Deber, 1986), that membrane-buried proline residues were found in nearly all transport proteins examined, led to the proposal that they play a specific functional role. In fact, proline residues were found to be selectively included in membrane-spanning regions (Jones *et al.*, 1994) and it was noted that they are conserved at similar positions in transport proteins that have common functions (Brandl and Deber, 1986).

3.3.2 Characteristics of Proline Residues.

3.3.2a General Properties.

Membranous regions of proteins are largely comprised of hydrophobic residues that promote helical structure. Thus, the selective inclusion of proline residues within transmembrane α -helices is somewhat surprising, considering the relative rigid backbone angles of the imino acid and the fact that it lacks an amide proton for stabilisation of α -helical structure through hydrogen-bonding. Proline is thus known as a classical breaker of α -helical structure. In principle, proline residues create thermodynamically less stable structures when occurring within membranes. However, transmembrane helices are typically longer in length (~20 residues) and therefore are more stable due to increased hydrogen-bonding. Consequently, such helices are more capable of bearing the energetic cost of accommodating a membrane-buried proline residue.

There are however two specific properties of a proline-containing peptide bond that make it well suited for a functional role in substrate translocation across the membrane : (1) The tertiary amide character of the Xaa-Pro (where Xaa represents any amino acid) carbonyl group can participate in hydrogen-bonding, acting as a hydrogen-bond acceptor. It can also act as a transient liganding site for positively charged species. (2) *Cis* peptide bonds involving prolines are of comparable stability to the *trans* state when proline occurs at the carboxy-terminal side of the bond. Isomerisation of the Xaa-Pro peptide bond is a dynamic

and reversible event that could bring about the required structural changes resulting in the realignment of amphipathic transmembrane helices to initiate the formation or opening of a hydrophilic channel (Figure 3.1). Such observations initiated several studies investigating the role of transmembrane proline residues in various membrane transport proteins.

3.3.2b Transmembrane Proline Residues Cause Kinks in Helices.

From a structural point of view, the ability of a proline to break the hydrogen-bonding pattern of an α -helix causes deviations from the ideal backbone internal parameters. One structural consequence of this is the creation of a kink or bend in the helix backbone. In globular proteins, Pro-kinked helices orientate themselves with their convex sides towards the solvent. In contrast, those found in multiple membrane-spanning proteins tend to be orientated with their convex sides towards the protein interior, since there are no other molecules but other regions of the protein itself that can provide hydrogen-bonding groups to the unpaired amide and carbonyl groups of the kink (von Heijne, 1991). In this regard, kinked helices may participate structurally to form a pocket which can bury a charged residue or chromophore.

3.3.2c Accommodation of a *Cis*-Proline in Transmembrane Helices.

Studies on the conformational changes occurring in bacteriorhodopsin and rhodopsin that are associated with the function of these proteins indicate that the Xaa-Pro peptide bonds can act as hinges (Ganter *et al.*, 1989, Gerwert *et al.*, 1990, Rothschild *et al.*, 1990). Isomerisation about Xaa-Pro peptide bonds are also known to be associated with the conformational changes that occur during visual transduction (Shieh *et al.*, 1990). However, direct and conclusive evidence to reject or accept the involvement of *cis-trans* isomerisation of proline peptide bonds in membrane protein function can not be obtained from mutational studies that assay *only* for protein *activity* and *do not* detect *conformational changes*.

If *cis-trans* isomerisations were to take place during the functioning of membrane proteins, then one would expect that a *cis*-Pro could be accommodated in a transmembrane

α -helix. The isomerisation event depicted in Figure 3.1 would result in the introduction of a helix-turn-helix motif, consequently making it difficult for the helix to traverse the membrane, resulting in drastic alterations in protein structure. In order to maintain a near native structure, the isomerisation event would have to be accompanied by changes in the local parameters. Although ^1H and ^{13}C -NMR studies have demonstrated a good amount of main chain flexibility resulting from the presence of proline residues (Deber *et al.*, 1990), the presence of *cis*-Pro was not indicated in this study. Molecular dynamics simulation has been used to characterise the alternative conformation, flexibility and rigidity of transmembrane helices of bacteriorhodopsin and rhodopsin (Iyer & Vishveshwara, 1995). This technique has also been applied to hydrophobic peptides containing proline residues. It was concluded that *cis*-Pro can be accommodated in an α -helix, allowing access to multiple conformations from a helix-turn-helix-like motif to a straight helix. This is due to the introduction of local distortions *only*, such that the helical character and direction of propagation is maintained. These observations represent a plausible involvement for *cis-trans* isomerisation events in membrane protein function (and folding).

3.3.3 Mutation of Proline Residues in the *lac* Permease of *E.coli*.

The *lac* permease is a prototypic membrane transporter that catalyses co-transport of a β -galactoside molecule with a single H^+ (Kaback, 1983). Based on CD studies and hydropathy analysis of its primary structure (Foster *et al.*, 1983), it is predicted to adopt a similar transmembrane topology to that of the GLUT isoforms. This protein contains twelve proline residues, nine of which are membranous. In a study designed to determine whether *cis-trans* isomerisation of Xaa-Pro peptide bonds are important for transport function, each of the nine transmembrane prolines were individually mutated (Consler *et al.*, 1991). Since this isomerisation event is unique to proline, replacement should render the transporter inactive. Alanine or glycine substitutions at any proline, with the exception of Pro²⁸ (discussed below), resulted in significant retainment of lactose transport activity. Alanine or glycine substitutions at position 192 led to reduced steady state levels of lactose accumulation compared to wild type, which was attributed to partial uncoupling of the

transporter. It was concluded that the *cis-trans* isomerisation of Xaa-Pro peptide bonds is not an absolute requirement for transport activity. In the same study, the importance of any structural discontinuities resulting by replacement of proline with glycine, alanine or leucine was investigated. No correlation was found to exist between transport activity and the ability of a substituted amino acid to promote or break α -helical structure. Rather it is the hydrophobicity and/or the size of the substituted amino acid that dictates the levels of transport activity attained. Replacement of Pro²⁸ with either glycine, alanine or leucine leads to transporter inactivation. Substitution of serine at this position does not abolish substrate translocation or high affinity ligand binding. It was thus concluded that Pro²⁸ is important for substrate recognition and binding.

In the absence of a high-resolution structure and the lack of any detailed kinetic analyses of these mutants, it is difficult to define a precise role for transmembrane proline residues in this study.

3.3.4 Mutation of Proline Residues in the Phosphate-Specific Transporter of *E.coli*.

The Pst system is a periplasmic phosphate permease (Gerdes & Rosenberg, 1974). It comprises two hydrophobic proteins, PstA and PstC, that are likely to form the membrane-spanning portion of the Pst system, each consisting of five or six transmembrane helices. There are two proline residues located at approximately equivalent positions within the membrane in adjacent helices of the PstA and PstC proteins. Individual substitution of the two prolines in either PstA or PstC to alanine results in partial loss of phosphate uptake activity (Webb *et al.*, 1992). Transport activity is completely abolished in the double alanine mutants. In contrast, individual replacement with leucine renders the transporter inactive. Thus, the prolines appear to act cooperatively such that substitution of one with the more bulky residue, leucine prevents the remaining proline from carrying out its functional role. Unfortunately, mutation to inactivity does not distinguish between a structural or dynamic role for these residues, but does confirm their requirement for transporter function.

3.3.5 Role of Transmembrane Proline Residues in Bacteriorhodopsin.

Bacteriorhodopsin is present in the purple membrane of *Halobacterium halobium* (Stoeckenius & Bogomolni, 1982). Light activation leads to pumping of protons from the inside to the outside of the cell. There are three proline residues located within helices B, C and F at position 50, 91 and 186 respectively. Site-directed mutagenesis in combination with FTIR difference spectroscopy has been employed to probe the role of these prolines in the function of this protein (Braiman *et al.*, 1988; Gerwert *et al.*, 1990). It is well established that an isomerisation event around the C₁₃=C₁₄ double bond is crucial to proton pumping (Braiman & Mathies, 1980). Light-induced conformational changes of two prolines around the C-N bond have been detected in addition to the global movement of the polypeptide backbone during proton pumping, as deduced from strong difference bands in the amide I/amide II region. It was postulated that the higher degree of flexibility around the C-N amide bond of proline peptide bonds compared to that of other amino acids may be a hinge for functionally important conformational changes that facilitate the vectorial transport of a proton. Also, a full isomerisation event could establish a transient proton binding site ((Dunker, 1982)). Absorption bands were assigned to transmembrane Pro¹⁸⁶ which, interestingly, is located close to Tyr¹⁸⁵ in the retinal binding pocket which undergoes protonation changes upon photoactivation (Braiman & Rothschild, 1988). Tentative assignment of the other absorption bands have been made to Pro⁵⁰ and Pro⁹¹. Mutation of Pro¹⁸⁶ to alanine or glycine has an impact on the chromophore and the ability to pump protons. Mutation of Pro⁵⁰ or Pro⁹¹ to alanine or glycine led to reconstitution of the functional properties. Evidence from these studies suggest an involvement of Pro⁵⁰, in helix B, and Pro¹⁸⁶ in conformational changes of the protein. The Tyr¹⁸⁵-Pro¹⁸⁶ region of helix F acts as a hinge that links chromophore isomerisation with structural changes. All three prolines may be structurally active and may act cooperatively.

3.3.6 Mutation of Proline Residues in GLUT1.

Although there is much experimental evidence to suggest the occurrence of large conformational changes that result in the sequential exposure of the substrate binding site to the external and internal surfaces of the glucose transporter, the details of this dynamic event at the molecular level are still poorly understood. However, analysis of the amino acid sequence of the GLUT isoforms reveals the presence of a high proportion of membrane-buried proline residues, several of which are 100% conserved throughout the isoforms (Tables 3.1-3.2). Molecular modelling and dynamic studies have predicted that the highly conserved **G³⁸²PGPIP** sequence located within helix 10 (Figure 3.2) is important for facilitating the opening and closing of the external binding site (Hodgson *et al.*, 1992). Mutation of Pro³⁸⁵ in this sequence of GLUT1 to isoleucine (but not glycine or alanine) resulted in loss of transport activity associated with reduced ATB-BMPA labelling and retention of cytochalasin B labelling. These observations are consistent with the transporter adopting an endofacial conformation (Tamori *et al.*, 1994). In contrast, glycine substitution at this position resulted in retention of ligand binding at both inside and outside sites. Other transmembrane proline residues of potential interest are located within helix 6. There are 3 prolines located at positions 187, 196 and 205 that are conserved in all GLUT isoforms except for the low affinity GLUT2, where histidine, arginine and phenylalanine are present instead. In the case of individual mutation of these residues to alanine, wild-type transporter activity was retained, suggesting that the presence of proline at these positions is not an absolute requirement for transport. Individual mutation of proline residues within helix 10 also resulted in wild-type transport activity levels. Thus, despite the putative contribution of transmembrane proline residues to the structure and function of a protein, their individual replacement may not necessarily disrupt the transport mechanism. This is in line with the studies described for bacteriorhodopsin, *lac* permease and the Pst system. Substitution of proline residues to the neutral-polar amino acid glutamine considerably reduced transporter activity (Wellner, 1995). Since replacement with isoleucine also impairs transport activity (Tamori *et al.*, 1994), the polarity of the substituted residue cannot be the sole factor affecting catalytic activity. It may be that the specific chemical properties of the substituted

side chain cause structural changes in the protein that hinder the conformational changes required for substrate translocation, thus, one might predict that the greater the size of the substituted residue, the lower the transport activity (Consler *et al.*, 1991).

A putative mode of operation of the transporter was suggested. Conformational flexibility about the prolines of helix 10 enables the alternate packing of helices 11 and 12 against the outside substrate binding site comprising helices 7, 8 and 9, and the inner site located at the base of helix 10. The cytoplasmic tail at the base of helix 12 is also involved. Packing of this region against the base of helix 10 enables formation of the exofacial binding site. In the endofacial conformation, the cytoplasmic tail moves away from the base of helix 10 exposing the cytochalasin B binding site. Retention of transport activity by the mutants containing glycine substitutions in this region can be rationalised on the basis that this residue provides a non-hindered atomic environment for conformational flexing. However, since Wellner *et al* and Tamori *et al* performed *no detailed kinetic analyses* of these mutants, such models are purely based upon speculation. A more thorough analysis, for example, measurement of the kinetic parameters associated with the binding of site-specific ligands, may highlight a more subtle role for proline residues in transporter function.

3.3.7 Mutation of Proline Residues in GLUT3.

There are several proline residues that are conserved throughout the GLUT isoforms (Tables 3.1 and 3.2). Regions particularly rich in prolines include transmembrane helix 6, including the start of the large intracellular loop at the base of this helix, and helix 10. The putative role of helix 10 in providing conformational flexibility required for substrate translocation has already been discussed above. The function of the conserved proline-rich motif located at the base of helix 6 has not yet been investigated. A mutagenic study was thus undertaken in which the proline residues located within these and other regions were mutated to alanine (Figure 3.3). Mutations were made at positions 203, at the base of helix; 206 and 209, at the start of the large intracellular loop; 381, 383 and 385 within helix 10; 399, at the base of helix 11; and 451, at the base of helix 12.

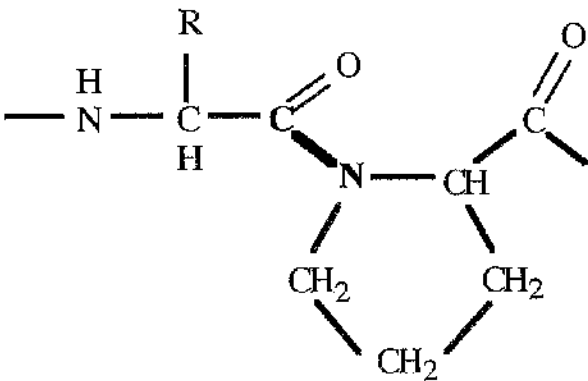
GLUT 3 was chosen in preference to GLUT1 and the other isoforms primarily due to the lack of information regarding the function of this transporter. In addition, there are distinct advantages of using GLUT3 for mutagenic studies. This isoform displays a relatively low K_m for zero-*trans* uptake of 2-deoxy-D-glucose into *Xenopus* oocytes, thus any alteration in transport kinetics is predicted to be more measurable with this isoform compared to, for example, GLUT2. In order to further investigate the effects of proline mutations on the ability of the transporter to adopt both the exofacial and endofacial conformations, site-specific ligands will be used. The inhibitory effects of cytochalasin B on 2-deoxy-D-glucose transport mediated by GLUT3 are much greater than by GLUT2, due to the higher affinity of GLUT3 for this ligand. In addition, photolabelling of GLUT2 by cytochalasin B has not been successful to date (Axelrod & Pilch, 1983), and immunoprecipitation of GLUT2 is reported to be rather problematic (Jordan & Holman, 1992). Quantification of mutant and wild-type transporters expressed at the oocyte plasma membrane by comparative immunoblotting is a requirement for thorough mutant characterisation. The availability of membrane fractions containing known quantities of GLUT3 favours the use of this isoform, since no such standards are available for GLUT2. An alternative strategy would be to perform equilibrium binding studies with [3 H]cytochalasin B, in the presence of various concentrations of non-labelled cytochalasin B, and in the presence or absence of D-glucose. The number of available D-glucose-sensitive cytochalasin B binding sites can be derived from a Scatchard analysis. Since cytochalasin B binds with a stoichiometry of 1:1, then the number of cytochalasin B binding sites is equivalent to the number of transporters at the plasma membrane. This would not be possible for GLUT2 since the K_d of this isoform for this ligand is so high ($1.7\mu\text{M}$ - (Axelrod & Pilch, 1988) that the concentrations required for equilibrium binding studies would exceed the solubility limit of cytochalasin B in aqueous solution (about $50\mu\text{M}$).

Figure 3.1

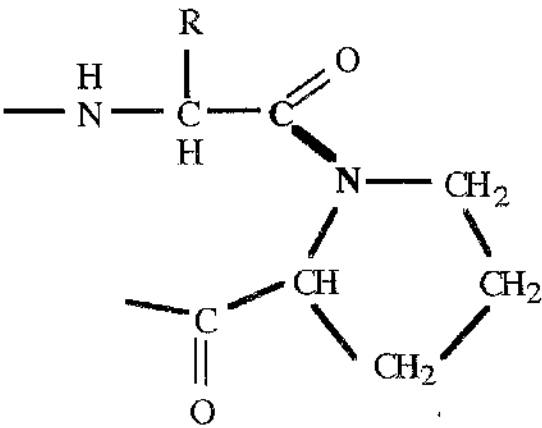
Structure and Isomerisation of a Xaa-Pro Peptide Bond.

This is a two-dimensional representation of the peptide bond formed between a proline and an N-terminal amino acid, denoted as Xaa. Most peptide bonds formed between two residues are in the *trans* configuration. This form is intrinsically favoured energetically due to fewer repulsions between non-bonded atoms. If the C-terminal residue is proline, however, the cyclic side chain diminishes the repulsions between atoms and the intrinsic stability of the *cis* isomer is of comparable stability to that of the *trans* form. Xaa-Pro peptide bonds can therefore undergo *cis-trans* isomerisation events, which would cause redirection of the local peptide chain.

Structure and Isomerisation of a Xaa-Pro Peptide Bond.



trans



cis

Figure 3.2

Comparison of Amino Acid Sequences in Putative Transmembrane Helices 6, 10 and 12 of the Human and Rat Facilitative Glucose Transporters.

This diagram shows a comparison of the amino acid sequences of the human GLUTs 1-5 and the rat GLUT7 isoforms in the region of helices 6, 10 and 12. Conserved residues are in bold and the consensus sequence is given. GLUT3 proline residues targeted for mutagenesis in this study are shown in red. Helix 12 contains a high proportion of phenylalanine residues (shown in blue), contributing to the highly hydrophobic nature of this segment..

Figure 3.2

Comparison of Amino Acid Sequences in Putative Transmembrane Helices 6, 10 and 12 of the Human and Rat Facilitative Glucose Transporters.

I-----TM6-----I

hGLUT1	WPL LLS I I F I P A L L Q C I V L P F C P E S P R.....
hGLUT2	W H I L L G L S G V R A I L Q S L L L F F C P E S P R.....
hGLUT3	W P L L L G F T I L P A I L Q S A A L P F C P E S P R.....
hGLUT4	W P L L L G L T V L P A L L Q L V L L P F C P E S P R.....
hGLUT5	W P I L L G L T G V P A A L Q L L L L P F F P E S P R.....
rGLUT7	W P H L L S L S R I P A A L Q P A I L P F P P E S P P.....

I-----TM6-----I

Consensus	W * L L * * * * * A * L Q * * * L * F * P E S P *.....
-----------	--

I-----TM10-----I

hGLUT1	I V A I F G F V A F F E V G P G P I P W E.....
hGLUT2	M I A I F L F V S F F E I G P G P I P W E.....
hGLUT3	I G A I L V F V A F F E I G P G P I P W E.....
hGLUT4	I V A I F G F V A F F E I G P G P I P W E.....
hGLUT5	I V C V I S Y V I G H A L G P S P I P A L.....
rGLUT7	M T A I F L F V S F F E I G P I P I P F E.....

I-----TM10-----I

Consensus	* * * * * V * * * * * G P * P I P * *.....
-----------	--

I-----TM12-----I

hGLUT1	G P Y V F I I F T V L L V L F F I F T Y F K V P E T K....
hGLUT2	G P Y V F F L F A G V L L A F T L F T F F K V P E T K....
hGLUT3	G A Y V F I I F T G F L I T F L A F T F F K V P E T R....
hGLUT4	G P Y V F L L F A V L L L G F F I F T F L R V P E T R....
hGLUT5	G P Y S F I V F A V I C L L T T I Y I F L I V P E T K....
rGLUT7	G P Y H F W A F H G V V I V W Y G N Y W F K V P E T K....

I-----TM12-----I

Consensus	G * Y * F * * F * * * * * * * * * * * V P E T *.....
-----------	--

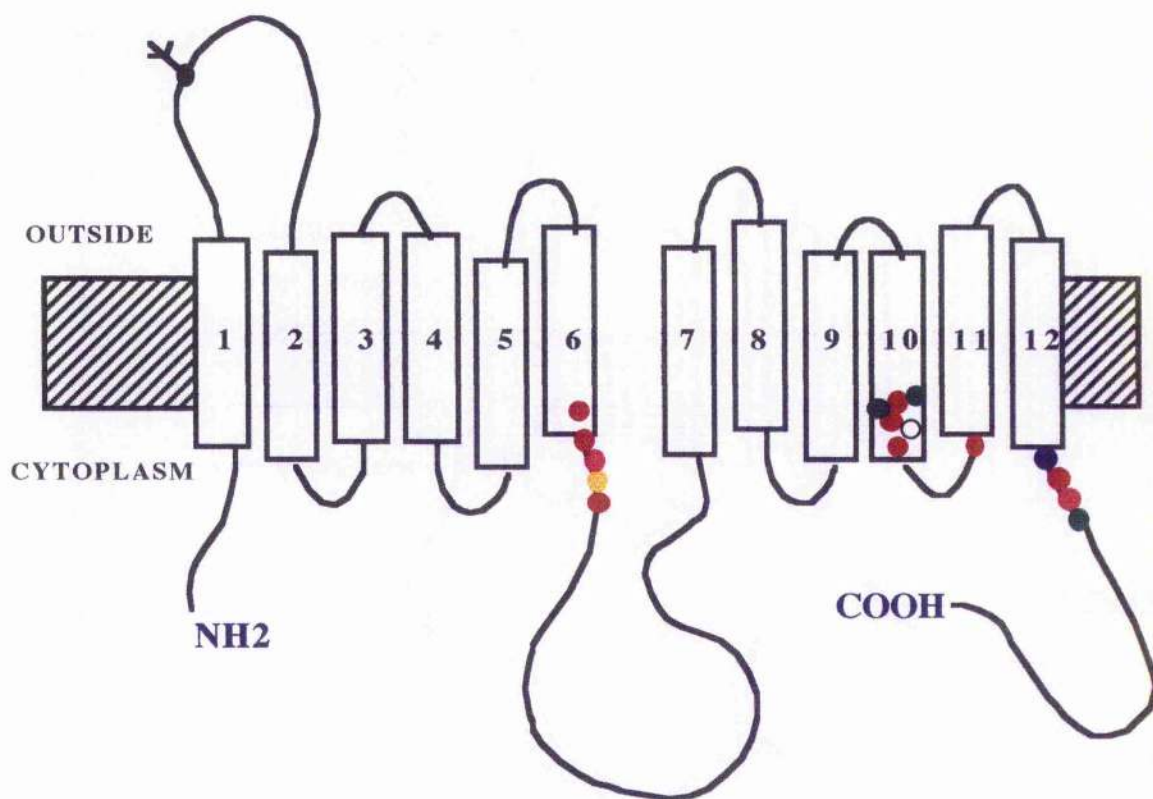
Figure 3.3

Location of Proline Residues Targeted for Mutagenesis.

This is a diagrammatic representation of the general topology of the GLUT3 isoform based on that proposed for GLUT1 by Mueckler and co-workers in 1985. The location of the proline residues targeted for mutagenesis in this study are shown in red, and their position within motifs that are conserved in the human GLUTs 1-5 and rat GLUT7 isoforms are shown, as revealed by sequence alignments.

Figure 3.3

Location of Proline Residues Targeted for Mutagenesis.



- Pro Residues To Be Mutated to Ala
- GPGPIP Motif Conserved in GLUTs 1,2,3,4,5 & 7
- VPET(K) Motif Conserved in GLUTs 1,2,3,4,5 & 7
- PESP(R) Motif Conserved in GLUTs 1,2,3,4,5 & 7

Table 3.1**Distribution of Proline Residues in Human GLUTs 1-5 and Rat GLUT7.**

Transporter Region	hGLUT1	hGLUT2	hGLUT3	hGLUT4	hGLUT5	rGLUT7
N-Terminal Tail	1	-	1	3	-	-
TM1	-	-	-	-	-	-
Extracellular Loop 1	2*	6*	3*	5*	2*	5*
TM2	-	-	-	-	2	-
Intracellular Loop 2	-	-	-	-	-	-
TM3	-	-	-	-	1	-
Extracellular Loop 3	-	1	-	-	-	1
TM4	1*	1*	1*	1*	1*	1*
Intracellular Loop 4	1*	1*	1*	1*	1*	1*
TM5	-	-	-	-	1	-
Extracellular Loop 5	-	-	-	-	-	-
TM6	3	-	3	3	3	3
Intracellular Loop 6	4**	3**	3**	5**	2**	4**
TM7	-	-	-	-	-	-
Extracellular Loop 7	1	1	1	1	1	1
TM8	-	-	-	-	-	-
Intracellular Loop 8	-	-	-	-	-	-
TM9	-	-	-	-	-	-
Extracellular Loop 9	1	-	-	1	1	-
TM10	3***	3***	3***	3***	3***	3***
Intracellular Loop 10	2*	2*	2*	2*	1*	1*
TM11	-	-	-	-	-	1
Extracellular Loop 11	-	-	1	-	1	-
TM12	1	1	-	1	1	1
C-Terminal Tail	3*	2*	2*	4*	4*	3*

* represents a proline residue that is conserved in all isoforms.

Table 3.2

Summary of the Distribution of Proline Residues in Human GLUTs 1-5 and Rat GLUT7.

	hGLUT1	hGLUT2	hGLUT3	hGLUT4	hGLUT5	rGLUT7
Total Proline Residues	23	21	21	30	25	25
TM Proline Residues	8	5	8	8	11	9
% TM Prolines	35%	24%	38%	27%	44%	36%

3.4 Mutagenesis, Subcloning and Sequencing of GLUT3 cDNAs.

3.4.1 Introduction.

The method used for generation of mutant GLUT3 cDNAs made use of site-directed oligonucleotide primers and recombinant polymerase chain reaction (PCR). Oligonucleotides were designed to be complementary in sequence to the wild type GLUT3 cDNA in the region of the residues of interest except for a single base change such that alanine is encoded in place of proline.

3.4.2 Vectors.

Several vectors are available that contain the cDNA encoding individual members of the human facilitative glucose transporters. These are described in section 2.3.1 and are used as templates for the synthesis of transporter mRNAs which can be subsequently injected into *Xenopus laevis* oocytes for heterologous expression and characterisation.

The construct used in this study, pSPGT3, comprises the GLUT3 cDNA ligated into the multiple cloning site of pSP64T (Kayano et al., 1990), Figure 3.4. In this construct the protein coding region of the GLUT3 cDNA is under the transcriptional control of the strong SP6 promoter. SP6 RNA polymerase is a commercially available enzyme.

3.4.3 Recombinant Polymerase Chain Reaction.

This is a modification of the method described by Katagiri and co-workers in 1992. Oligonucleotides, 15 bases in length, were designed to have complementary sequences to the sense strand of pSPGT3 in the region of the proline residue to be mutated. A single base change was incorporated such that the codon corresponding to the required proline residue encoded an alanine. A second series of oligonucleotide primers were designed that were complementary to the antisense strand of GLUT3, encompassing the same region as the sense strand oligonucleotide and incorporating the complementary base changes (Table 3.3).

In addition, two 37mer oligonucleotides were constructed that were identical to the untranslated regions of the GLUT3 cDNA at the 5' ends of the sense and antisense strands, termed G3-start and G3-end respectively (Table 3.3).

3.4.3a Primary PCR Reactions.

Two separate primary PCR reactions were performed. In the first reaction, G3-start, (corresponding to the 5' untranslated region of the GLUT3 sense strand) and the internal mutagenic primer, (corresponding to the antisense strand in the region encompassing the proline of interest), were incubated with pSPGT3 plasmid dsDNA. PCR under certain reaction conditions, (section 2.2), resulted in the production of primary PCR fragment-1 (Figure 3.5).

A second identical reaction was carried out using G3-end, (corresponding to the 5' untranslated region of the GLUT3 antisense strand) and the second internal mutagenic primer, (corresponding to the sense strand of GLUT3 in the region of the required mutation). Incubation under certain reaction conditions, again in the presence of pSPGT3, resulted in the production of primary PCR fragment-2 (Figure 3.5).

Both primary PCR fragments were separated by agarose gel electrophoresis and fragments of the correct size were identified and excised from the gel (Figure 3.6). Sizes of the primary products varied depending on which proline residue was mutated. DNA fragments were purified as described, (section 2.2.6), and used as templates for the secondary PCR reactions.

3.4.3b Secondary PCR Reactions.

The two PCR fragments generated in the primary reactions contain a complementary sequence of 20-24 bps and this forms the basis of the secondary PCR reaction. When incubated together under specific reaction conditions, (section 2.2), melting of the DNA double helix occurs and subsequent cooling enables the 3'end of PCR fragment-1 to anneal to the complementary 3'end of PCR fragment-2. Each strand can then act as a primer for the

3' extension of the opposite strand mediated by *Taq* or *Pfu* DNA polymerase, resulting in the generation of a full length GLUT3 cDNA sequence containing the specific point mutation. This then acts as a template for further amplification using the G3-start and G3-end external primers (Figure 3.5).

Final full length secondary PCR products were separated from non-specific products by agarose gel electrophoresis, excised from the gel and purified from the agarose as described in sections 2.2.6. Secondary fragments were then restricted with *BstXI* and *EcoRV* and ligated into pSPGT3 vector backbone also restricted with these enzymes (Figure 3.7). Constructs were transformed into competent or ultracompetent JM109 *E.coli* cells (section 2.3.8 and 2.3.9). Plasmid DNA was purified from colonies (section 2.3.12) and screened for the required point mutation and any non-desirable mutations by automated DNA sequencing of both strands (section 2.4).

3.4.3c Results using *Taq* DNA Polymerase.

This was the initial DNA polymerase chosen to carry out the PCR reactions. *Taq* DNA polymerase is a thermostable enzyme produced from *Thermus aquaticus*. It is the thermostability of *Taq* DNA polymerase that makes it ideal for use in PCR reactions since, after the initial primer extension step, the reaction mixture is heated to 95°C to allow the newly synthesised strands to detach from the templates (Figure 3.5). On cooling, more primers anneal at their respective positions, and as *Taq* DNA polymerase is unaffected by the heat treatment, a second round of DNA synthesis can take place. The reaction is continued through 30 cycles with DNA amplification proceeding in an exponential fashion.

After subcloning into the *BstXI*-*EcoRV* restricted pSPGT3 vector, screening of transformed *E.coli* colonies revealed that the frequency of mutant/wild-type colonies averaged at about 1:5, and this varied between mutants from 5:1 to approximately 1:40. Complete sequencing of the cDNAs revealed that, although the required mutation was often present, the error rate of *Taq* DNA polymerase was such that, on average 2 bps in every thousand was misincorporated into the final product. This is due to the absence of 3' to 5' exonuclease proof-reading activity of this enzyme. Therefore, upon identification of

sequence errors, the pSPGT3 sequence was scanned for the presence of suitable unique restriction sites located within the coding sequence. These sites must be located at a distant far enough away from the desired proline mutation to produce a restriction fragment long enough to be restricted and subcloned into wild type pSPGT3, free from any such misincorporations. This however was not possible in the majority of cases, since most of the misincorporations occurred within the original *BstXI-EcoRV* cloning fragment, usually in close proximity to the required proline mutation.

3.4.3d Results using *Pfu* DNA Polymerase.

In an effort to address the infidelity problem associated with the use of *Taq* DNA polymerase, *Pfu* DNA polymerase, isolated from *Pyrococcus furiosus*, was used to generate the PCR fragments. *Pfu* DNA polymerase has 3'-5' exonuclease proof-reading activity and therefore has a much higher fidelity than *Taq* DNA polymerase, incorporating errors 30-fold less frequently. Reaction conditions used for *Pfu* DNA polymerase were similar to those used for *Taq* DNA polymerase with some differences in the protocols (sections 2.2.2 to 2.2.5). The major difference is the step at which *Pfu* DNA polymerase is added to the PCR reaction mixture. *Pfu* DNA polymerase is much less stable than *Taq* DNA polymerase at high temperatures and is therefore added after the initial 95°C melting step. The yield of the PCR products generated by *Pfu* DNA polymerase was noticeably reduced, particularly with regard to the secondary products which were observed to be generally lower than the primary product yields. This observation was attributed to the thermo-instability of *Pfu* DNA polymerase relative to *Taq* DNA polymerase, and also due to the much lower extension rate of *Pfu* DNA polymerase (1kb/4mins and 1kb/min for *Pfu* and *Taq*, respectively)

The higher fidelity of *Pfu* DNA polymerase resulted in a higher ratio of mutant / wild-type clones that, upon sequencing, were found to contain no misincorporations.

3.4.4 Sequencing of Subclones.

Automated DNA sequencing was carried out as described in section 2.4. This method can be used to sequence up to 500 bps of ss or dsDNA from the site of primer binding, although only the first 300-350 bps are generally accurate. Sequencing Grade *Taq* DNA polymerase was used in all sequencing reactions. As this enzyme exhibits thermal stability at temperatures of up to 95°C, higher reaction temperatures can be used in the sequencing cycles. This decreases the secondary structure of the DNA template and therefore allows polymerisation through regions of the DNA containing strong secondary structure. High temperatures also increase the stringency of primer hybridisation. In the case of each mutant, both strands of the cDNA spanning the entire protein coding region was sequenced. This enabled confirmation of the required mutation and detection of any base misincorporations or errors that may have occurred during the PCR reactions and subcloning procedures. To facilitate this, a series of oligonucleotide primers were synthesised (Table 3.4) and their annealing sites were designed such that the sequence obtained from one primer overlapped with that obtained from another (Figure 3.8). Sequence alignments and comparisons were analysed using Biosoft GeneJockey II software on an Apple Macintosh Performa 400 computer. Representative ABI chromatograph traces are shown in Figures 3.9 and 3.10 for mutant wild type and GLUT3 sequences.

Figure 3.4

Diagrammatic Representation of pSPGT3 Showing the Binding Positions of the PCR Primers.

The GLUT3 cDNA was cloned into the pSP64T as a *Bgl* II/*Bam*HI fragment into the untranslated regions of the *Xenopus* β -globin gene, which had previously been cloned into the multiple cloning site of pSP64T (Krieg and Melton, 1984). Thus, the GLUT3 cDNA is flanked by 89bps of 5' untranslated region (UTR) and 141bps of the 3' untranslated region. This serves to stabilise the *in vitro* synthesised mRNA in *Xenopus* oocytes. In addition, there is an SP6 polymerase promoter located 5' to the GLUT3 cDNA and flanking sequences, and an ampicillin resistance gene for selection purposes.

Also indicated on the diagram are the oligonucleotide primers used for generation of the GLUT3 Pro-Ala mutants. The external primers are referred to as G3-start and G3-end and they are complementary in sequence to the 3' and 5' untranslated regions flanking the GLUT3 cDNA. The internal primers are mutagenic oligonucleotides and these are complementary in sequence to the GLUT3 cDNA in the region of the proline residue to be mutated, with the exception of a single base change such that the proline is replaced by an alanine.

Figure 3.4
Diagrammatic Representation of pSPGT3 Showing the Binding Positions of the PCR Primers.

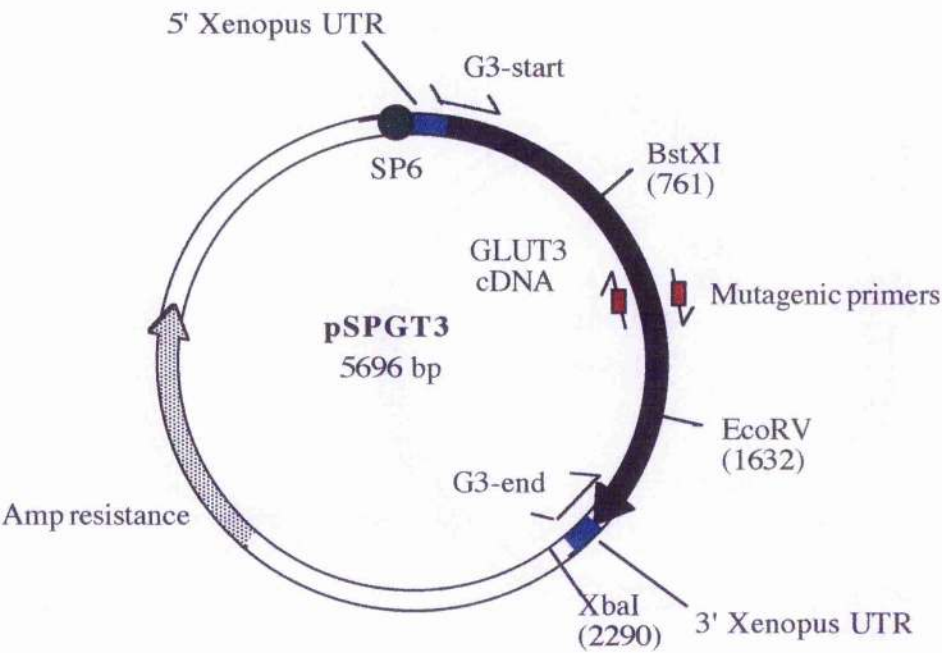


Table 3.3**Mutagenesis Oligonucleotides.**

	Sequence	Mutation
antisense strand	ACGGGTGTCT <u>GCG</u> ACTTTGAAGAA	Pro ⁴⁵¹ ->Ala
sense strand	TTCTTCAAAGTC <u>GCT</u> GAGACCCGT	Pro ⁴⁵¹ ->Ala
antisense strand	CATCGCAGCT <u>GCG</u> CGGGGGCCCTG	Pro ³⁹⁹ ->Ala
sense strand	CAGGGCCCCG <u>GCG</u> CAGCTGCGATG	Pro ³⁹⁹ ->Ala
antisense strand	AATAAACCAG <u>GCA</u> ATGGGGCCTGG	Pro ³⁸⁵ ->Ala
sense strand	CCAGGCCCCATT <u>GCT</u> TGGTTTATT	Pro ³⁸⁵ ->Ala
antisense strand	CCAGGGAAT <u>GGC</u> GCCTGGTCCAAT	Pro ³⁸³ ->Ala
sense strand	ATTGGACCAGGCG <u>GCC</u> ATTCCCTGG	Pro ³⁸³ ->Ala
antisense strand	AATGGGGCCT <u>GCT</u> TCCAATTTCAAA	Pro ³⁸¹ ->Ala
sense strand	TTTGAAATTGGAG <u>GCA</u> GGCCCCATT	Pro ³⁸¹ ->Ala
antisense strand	CAAAAATCT <u>GGC</u> ACTTTTCAGGGCA	Pro ²⁰⁹ ->Ala
sense strand	TGCCCTGAAAGT <u>GCC</u> CAGATTTTTG	Pro ²⁰⁹ ->Ala
antisense strand	GGGACTTTC <u>AGC</u> GCAAAATGGAAG	Pro ²⁰⁶ ->Ala
sense strand	CTTCATTTT <u>GCG</u> CTGAAAGTCCC	Pro ²⁰⁶ ->Ala
antisense strand	AGGGCAAAAT <u>TGC</u> AAGGGCTGCACT	Pro ²⁰³ ->Ala
sense strand	AGTGCAGCCCTT <u>GCA</u> TTTTGCCCT	Pro ²⁰³ ->Ala

Table 3.3 (cont.)

Complementary		
	Sequence	Sequence
G3-end (antisense strand)	GTCGACGTCGACGAGGGAGAGGT GGCTTTCCCATGCC	Binds to sense strand at 3'UTR
G3-start (sense strand)	GTCGACGTCGACTCACCCCTAGATC TTCTTGAAGAC	Binds to anti- sense strand at 3'UTR

Codons that contain the single base change such that alanine is encoded in place of proline are underlined.

Figure 3.5

Generation of GLUT3 Pro-Ala Mutant cDNAs by Recombinant PCR Reactions.

This diagram shows the binding positions of the reaction primers to the GLUT3 cDNA template, followed by the sequence of events in both the primary and secondary PCR reactions. Two separate primary reactions are carried out, each using a specific combination of PCR primers. In reaction 1, GLUT3 template (pSPGT3) is incubated in the presence of G3-start and the mutagenic primer corresponding to the antisense strand of the GLUT3 cDNA. Under certain reaction conditions, the GLUT3 template strands melt, allowing the annealing of the primers to the template strands. New strands are then extended from these primers in the 5' to 3' direction by *Taq* or *Pfu* DNA polymerase (dotted lines). Melting, reannealing and extension occurs a further 30 times producing primary PCR product-1 corresponding to the 5' portion of the GLUT3 cDNA with the Pro-Ala mutation located at the 3' end of the fragment (corresponding to the sense strand). In reaction 2, the second mutagenic primer in combination with G3-end are used, in essentially the same reaction as that described for reaction 1, to generate primary PCR product-2. This product corresponds to the 3' end of GLUT3 (sense strand), with the Pro-Ala mutation located at the 5' end of the fragment.

In the single secondary PCR reaction, equal quantities of the two primary PCR products are used as templates for a second round of reaction cycles using G3-start and G3-end primers. In the initial stages of the process the two templates melt and reanneal to form a single template. This is possible due to the presence of a short overlapping sequence of 18-24bps between the 3' end of the sense strand of primary PCR product-1 and the antisense strand of primary PCR product-2, corresponding to the region of the Pro-Ala mutation. In the initial few cycles, these strands anneal and are extended in the 5' to 3' direction (dotted lines) to form a full length secondary PCR product, which can then act as a template for the subsequent amplification with G3-start and G3-end. Only the sense strands of each of the primary PCR products can be extended after association, since binding of the antisense strand of product-1 and sense strand of product-2 leads to a complex which can not be extended in the 5' to 3' direction. In addition, the formation of product-1/product-2 complexes is relatively infrequent when compared to the frequency of self association of the primary product strands. Both these factors lead to lower secondary PCR yields than those obtained in the primary PCR reactions.

Figure 3.5
Generation of GLUT3 Pro-Ala Mutant cDNAs by Recombinant PCR Reactions.

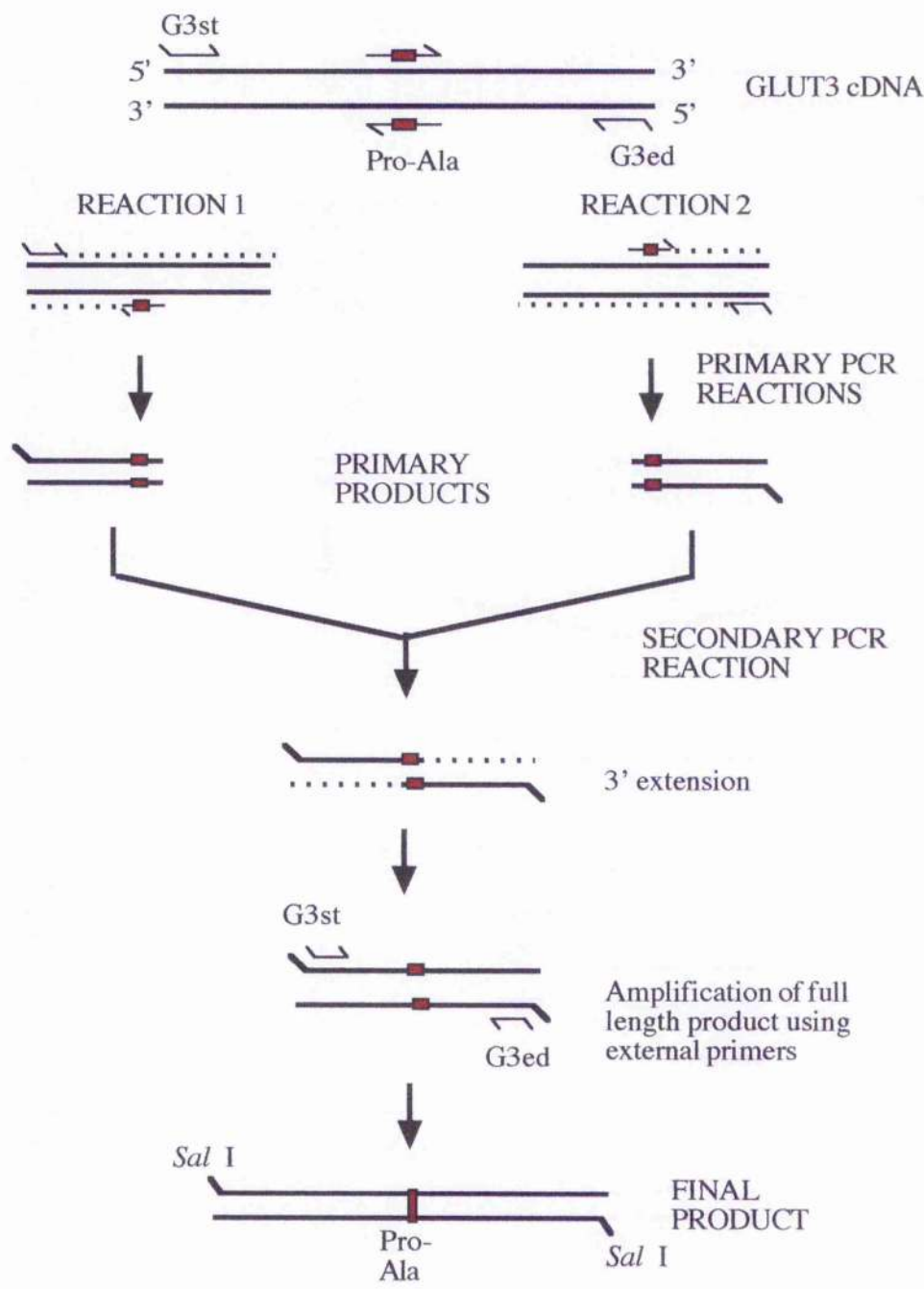


Figure 3.6

1% Agarose Gel of PCR Products and Vectors Used for Cloning of GLUT3 Pro-Ala Mutants.

This shows photographs of various PCR products and vector cDNAs which have been subjected to 1% agarose gel electrophoresis and stained with ethidium bromide. Gel 1, Lane 1 contains 0.625 μ g of *Bst*E II-digested lambda DNA; Lane 2, 5 μ l (from total of 60 μ l) of primary PCR product-1 generated using *Pfu* DNA polymerase; Lane 3, 5 μ l (from total of 60 μ l) of primary PCR product-2 generated using *Pfu* DNA polymerase; Lane 4, 5 μ l (from total of 20 μ l) of secondary PCR product generated using *Pfu* DNA polymerase; Gel 2, Lane 1, contains 0.625 μ g of *Bst*E II-digested lambda DNA; Lane 2, 3 μ l (from total of 20 μ l) purified *Bst*X I/*Eco*R V-digested pSPGT3 vector, Lane 3, 3 μ l (from total of 200 μ l of maxi-preparation of plasmid DNA) pSPGT3 containing the Pro²⁰⁶Ala mutation.

Figure 3.6
1% Agarose Gel of PCR Products and Vectors Used for Cloning of GLUT3
Pro-Ala Mutants.

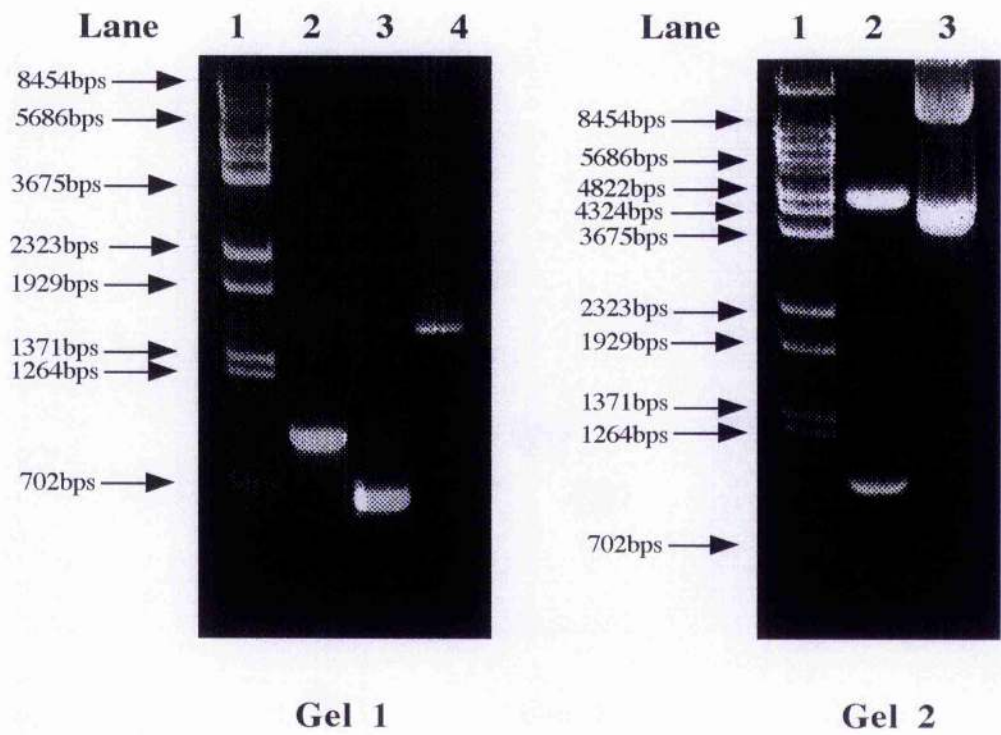


Figure 3.7

Subcloning of Secondary PCR Products into pSPGT3.

pSPGT3 was digested with *BstX* I and *EcoR* V to remove a 871bp fragment of GLUT3, and the backbone vector purified. Secondary PCR products were also digested with the same enzymes to yield a fragment of 871bps which was subsequently purified and ligated into the *BstX* I/*EcoR* V sites of the pSPGT3 backbone vector. This produced an intact pSPGT3 vector incorporating a Pro-Ala mutation.

Figure 3.7

Subcloning of Secondary PCR Products into pSPGT3.

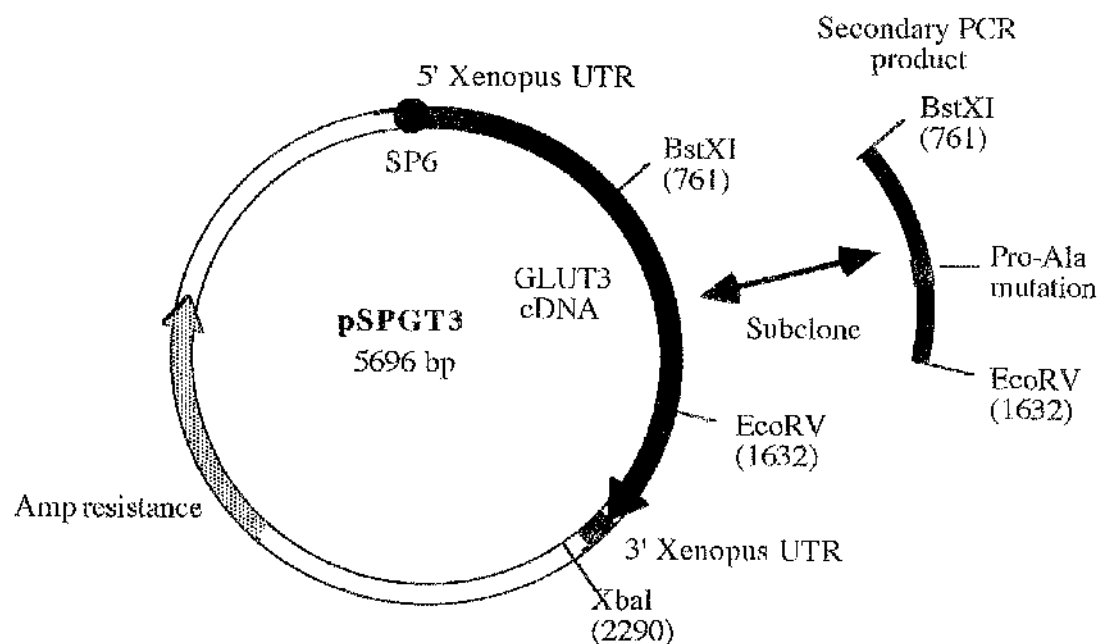


Table 3.4**Sequencing Oligonucleotides.**

G36T	GCTGTGATATTTGCC
G35T	CTGTGTAAAGTAGCT
G34T	CCTGAAAGTCCCAGA
G33T	ATCGGCGCGGGTGTG
G33T+	ATCTATGCCACCATC
G32T	ACTGGACCTCCAAC
G31B	GGGAGAGGTGGCTTT
G32B+	TAAATAGTGAGCAGC
1/535	ACAGTCATGAGCGTG
G33B	GTAGCTGGACACTCT
G34B	TGAGCAAAAATCTGG
G35B	AGCTACTTTACACAG
G36B	GGCAAATATCAGAG

Figure 3.8

Diagram of the Binding Positions of Sequencing Oligonucleotides in the GLUT3 cDNA.

This is a diagrammatic representation of the GLUT3 cDNA coding sequence from the 5'end of the sense strand to the 3'end. Position "0" corresponds to base "0" in pSPGT3. The GLUT3 open reading frame (ORF) begins at position 255 and ends (STOP) at position 1743. The approximate positions of the restriction enzymes used in the cloning procedures are shown, and the locations of the proline residues targeted for mutation are shown in red. The annealing positions of G3-Start and G3-End are shown in blue. Sequencing primers, shown in green, pointing from left to right and depicted above the GLUT3 cDNA bind the antisense strand and are used to generate 300-350bps of cDNA sequence to their right. Primers pointing from right to left and depicted below the GLUT3 sequence bind to the sense strand and are used to generate 300-350bps of cDNA sequence to their left. Comparison of the sequences generated by all the primers is sufficient to accurately describe the entire GLUT3 cDNA sequence. Initial screening for the required Pro-Ala point mutation was achieved by utilising either G32B+ or G33B, depending on the position of the mutation. These primers were found to yield accurate sequences in the regions of the mutations.

Figure 3.8
Diagram of the Binding Positions of Sequencing Oligonucleotides in the GLUT3 cDNA.

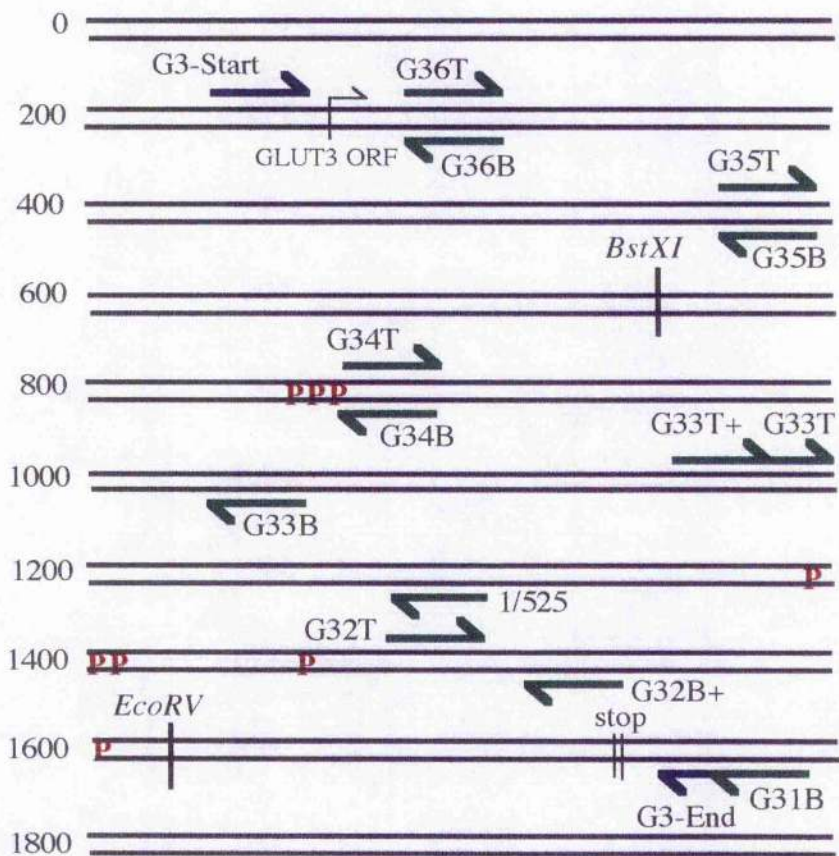


Figure 3.9

ABI Trace of GLUT3 Sequence Showing the Pro³⁸¹Ala Mutation.

The chromatograph shows part of the GLUT3 cDNA sequence in the region encompassing the Pro³⁸¹Ala mutation. The sequence of bases corresponding to each of the peaks is shown above the chromatograph and the single C-G mutation is indicated by the arrow. Data was generated by a 373A Automated DNA Sequencer, incorporated by an ABI Data Collection Program and analysed by an ABI Data Analysis Program.

Figure 3.9
ABI Trace of GLUT3 Sequence Showing the Pro³⁸¹Ala Mutation.

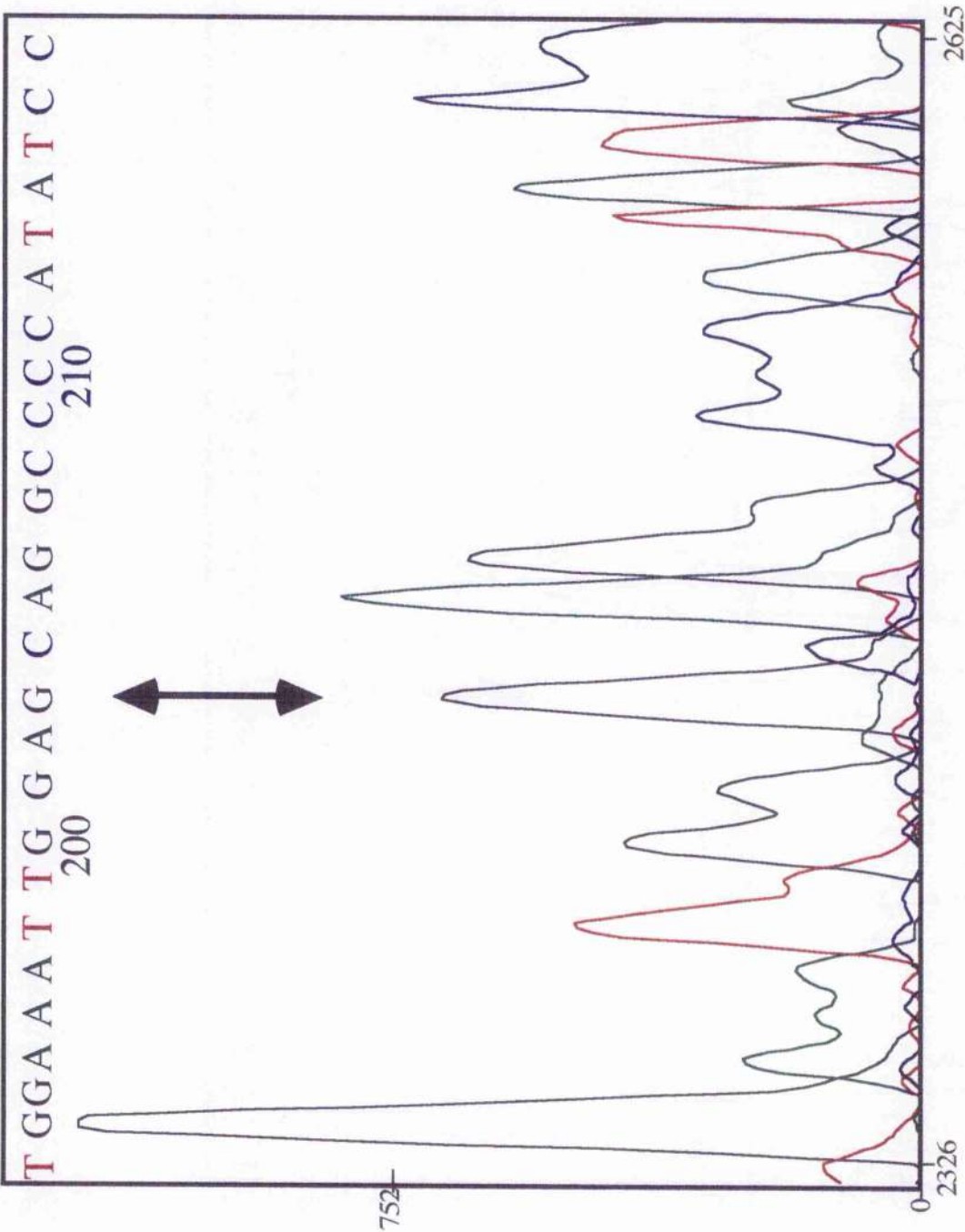


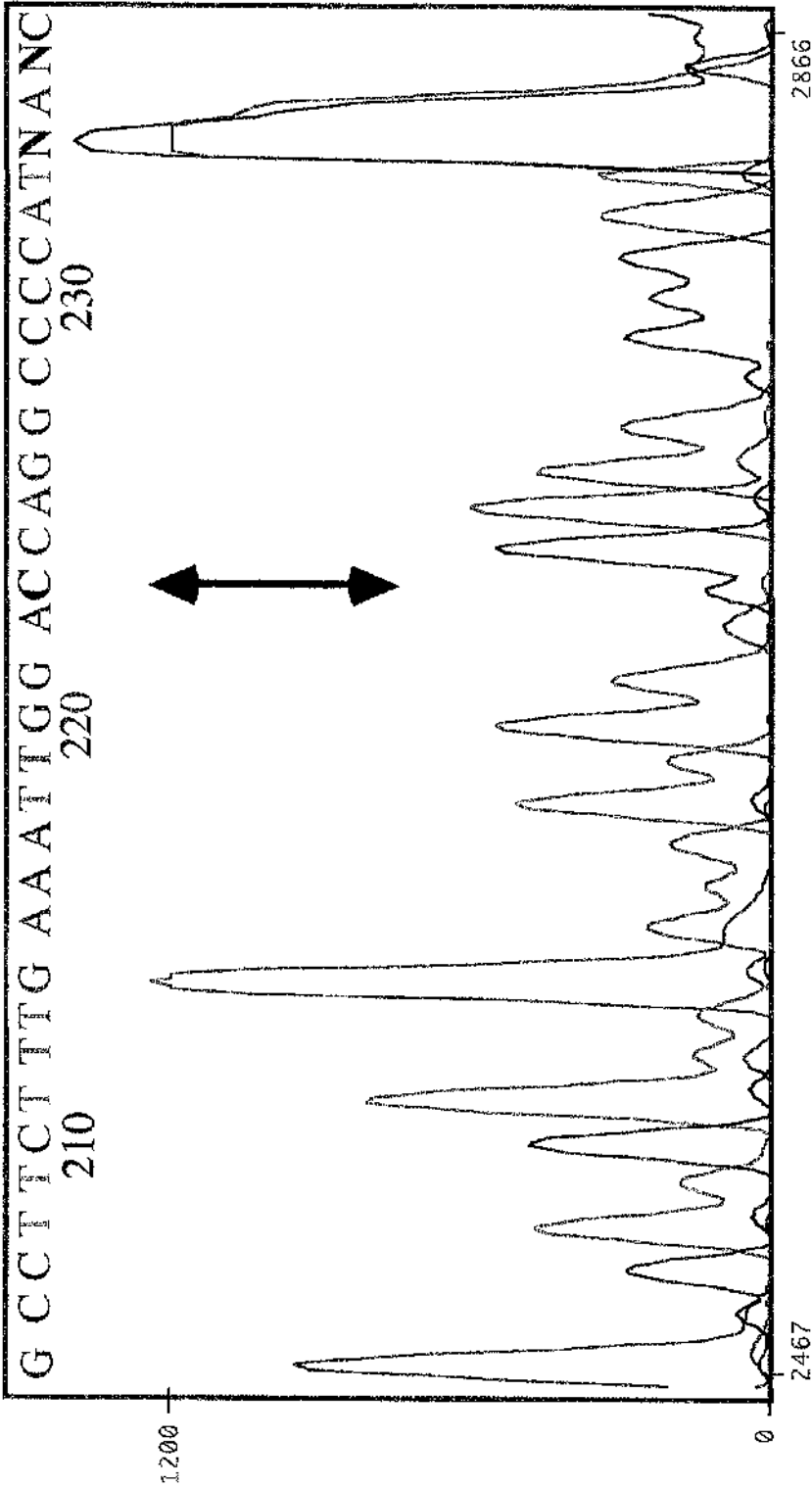
Figure 3.10

ABI Trace of Wild Type GLUT3 Sequence in the Region of Pro³⁸¹.

The chromatograph shows part of the wild type GLUT3 cDNA sequence in the region encompassing Pro³⁸¹. The sequence of bases corresponding to each of the peaks is shown above the chromatograph. The single base targetted for mutation such that alanine is encoded in place of proline in the Pro³⁸¹Ala mutant is indicated by the arrow. The data was generated by a 373A Automated DNA Sequencer, incorporated by an ABI Data Collection Program and analysed by an ABI Data Analysis Program.

Figure 3.10

ABI Trace of Wild Type GLUT3 Sequence in the Region of Pro³⁸¹.



3.5 Discussion.

Despite the complexity of the mutagenic data, a number of interesting features have emerged from these studies. Many of the highly conserved residues such as Trp⁶⁵, Asn¹⁰⁰, Asn²⁸⁸, Gln²⁸², Asn³¹⁷ and most of the tyrosine residues of GLUT1 can be mutated without any significant effect on transport activity. Thus, the selective pressure for maintaining these residues may be attributed to other essential functions such a protein folding rather than transporter activity. On the other hand, there are several point mutations that do severely diminish transporter function for example, Gln¹⁶¹, Val¹⁶⁵, Tyr²⁹³ and Pro³⁸⁵ of GLUT1. It may be that these residues are required to exist in a precise location such that they can participate in hydrogen bonding or hydrophobic interactions. Evidence emerging from chimeric studies suggest that much of the divergent transport kinetics exhibited by the different isoforms can be attributed to the more variant sequences.

This study investigates the role of conserved proline residues in the human GLUT3 isoform. A survey of the bilayer-spanning regions of integral membrane proteins revealed that nearly all transport proteins examined contained proline residues that were evenly distributed between aqueous and membranous domains (Brandl and Deber, 1986). This observation led to the proposal that membrane-buried proline residues have a specific function in transport proteins, possibly contributing to protein folding, membrane insertion and/or stability. They may also be directly involved in the transport process due to the unique *cis-trans* isomerisation property of the preceding peptide bond formed with proline residues.

Transmembrane proline residues have been the target of mutagenic investigation in a variety of membrane transport proteins. The *lac* permease of *E.coli* is one example of such a study. The importance of the *cis-trans* isomerisation of peptide bonds preceding nine transmembrane proline residues in the transport event was investigated by mutation of each residue to alanine and glycine (Consler *et al.*, 1991). Since *cis-trans* isomerisation is a property unique to proline peptide bonds, then replacement should render the transporter inactive. Although glycine and alanine substitutions at position 192 resulted in lower steady-state levels of lactose accumulation, it was concluded that the *cis-trans* isomerisation event is

not an absolute requirement for transport activity. In the same study, the importance of possible structural discontinuities arising as a consequence of prolyl replacement with either helix-breaking (glycine) or helix-promoting (alanine and leucine) residues was addressed. There appeared to be no correlation existing between activity and the ability of a substituted amino acid to make or break α -helical structure, although some substitutions led to partial uncoupling. In the absence of a high-resolution structure and the lack of any detailed kinetic analysis of the mutants, it is difficult to define a precise role for transmembrane proline residues in this study. Other studies have suggested structural and/or dynamic roles for transmembrane prolines for example, in the "channel gating" mechanism of the *E.coli* phosphate-specific transport system (Wellner *et al.*, 1992) and in the isomerisation events crucial to the proton pump mechanism of bacteriorhodopsin (Gerwert *et al.*, 1990; Tuzi *et al.*, 1994).

The human GLUT isoforms also contain a high proportion of transmembrane proline residues. GLUT1 for example, contains twenty three proline residues and of these, eight are harboured within membranous domains. Interestingly, helices 6 and 10 each contain three proline residues with the unique proline-rich domain **G³⁸²PGPIP** of helix 10 conserved in all mammalian facilitative glucose transporter isoforms (Figures 3.2 and 3.3). In fact, sequence alignment of the human isoforms, GLUTs 1-5, and the rat GLUT7 isoform reveal several interesting features, summarised in Table 3.2. Each isoform contains between 21 and 30 prolines of which ten are 100% conserved. A further six are more than 80% conserved i.e. present in five of the six isoforms. The large intracellular loop connecting helices 6 and 7 contains the **PESPR** motif which is located within one residue of the putative end of helix 6 (Figure 3.3). The large extramembraneous regions of the transporters including the extracellular loop connecting helices 1 and 2, the intracellular loop connecting helices 6 and 7 and the C-terminal cytoplasmic tail appear to be particularly rich in proline residues, at least 1 of which is 100% conserved implying a structural role.

The large body of experimental evidence in support of the existence of two distinct alternating conformational states (section 1.6 and 1.7), and the previously discussed proposals regarding a role for transmembrane prolines in membrane transport proteins prompted investigations into the functional importance of the highly conserved Pro-rich

sequences located within helices 6 and 10 of GLUT1. Molecular modelling and molecular dynamics studies suggested that prolines 383 and 385 could be particularly important in facilitating the alternate opening and closure of the exofacial binding site (Hodgson *et al.*, 1992). This hypothesis was directly investigated by the mutation of Pro³⁸⁵ to isoleucine which resulted in a loss of GLUT1 transport activity and labelling by ATB-BMPA, but retention of cytochalasin B labelling suggested that the transporter is locked in an endofacial conformation (Tamori *et al.*, 1994). Based on these observations, a putative model was proposed in which the prolines of helix 10 provide a point of conformational flexibility such that helices 11 and 12 can alternately pack against the exofacial binding site comprising helices 7, 8 and 9, or against the endofacial site at the base of helix 10. Retention of wild-type 2-deoxy-D-glucose transport rates were observed upon replacement of each of the proline residues located within helix 6 of GLUT1 with alanine. Thus, it was concluded that the presence of proline in any of these positions is not an absolute requirement for transport activity. Replacement with more bulky residues significantly reduced transport rates but this was attributed to reduced targeting of the protein to the plasma membrane. Whilst such conclusions question the role of transmembrane proline residues in GLUT1, no information regarding the kinetics of the transport event were provided. It is possible then that subtle alterations in the transporter structure and function may have been overlooked.

3.6 Summary.

Proline residues located at positions 203, 206 and 209 at the base of helix 6, 381, 383 and 385 within helix 10, 388 at the start of helix 11 and 451 at the base of helix 12 of GLUT3 were individually mutated to alanine. PCR technology was used to alter the base sequence of GLUT3 such that alanine was encoded in place of the prolines of interest. Mutated PCR fragments were subcloned into the pSPGT3 vector and the sequence of both strands were scanned for the presence of the required point mutation and any misincorporations that may have arisen during the PCR and cloning procedures.

CHAPTER 4

Functional Studies of Heterologously Expressed Pro-Ala Mutants in *Xenopus laevis* Oocytes.

4.1 Aims

1. Mutant (Pro-Ala) and wild type GLUT3 cDNAs will be used as templates for *in vitro* synthesis of mRNA. Subsequent injection of this mRNA into *Xenopus laevis* oocytes will allow kinetic characterisation of the heterologously expressed transporters.
2. To measure K_m values for zero-*trans* entry of 2-deoxy-D-glucose by each mutant. Parameters for the wild-type GLUT3 transporter will be determined in parallel.
3. To investigate the effects of the site-specific ligands maltose and cytochalasin B on the zero-*trans* uptake of 2-deoxy-D-glucose by GLUT3 and Pro-Ala mutants.
4. To discuss the results in terms of the proposed models for transporter structure.

4.2 Introduction.

4.2.1 General Information Regarding GLUT Tertiary Structure.

The major factor hindering the elucidation of the precise molecular mechanism of facilitative glucose transport across the cellular plasma membrane is the lack of a crystal structure defining the tertiary arrangement of the protein. In fact, the current knowledge regarding membrane transport protein structure and function is limited such that it is difficult to make accurate predictions in the absence of characterised models. However, a wealth of experimental data has been obtained to support the topological model of GLUT1 (and the other GLUT isoforms) predicted by Mueckler, based on amino acid sequence alignments and hydropathy analyses (Figure 1.2). According to this model, transmembrane helices 3, 5, 7, 8 and 11 are moderately amphipathic and, therefore, the protein is suggested to accommodate a water-filled glucose channel. Hydrogen-tritium and hydrogen-deuterium exchange data (Jung *et al.*, 1986) obtained from studies using purified GLUT1 is consistent with this prediction. Various spectroscopic techniques have been used to probe the secondary structural motifs of the protein, revealing a high helical content. The putative disposition of the hydrophilic loops connecting transmembrane helices and the N- and C-terminal segments have been confirmed, although the sizes of the loops and the precise helical boundaries are not irrefutable.

A prime area of interest is the relationship between transporter structure and the mechanism of substrate translocation. Extensive biophysical and biochemical data exists to support the occurrence of large conformational changes occurring during transport catalysis. Two distinct conformational states exist such that alternation between the two allows sequential exposure of substrate to either side of the membrane. Exofacial and endofacial D-glucose binding sites have been demonstrated to be structurally separate, and the regions of the transporter that interact with site-specific ligands have been mapped to distinct areas of the protein. Mutagenic studies have highlighted specific residues or sequences within the protein that are crucial for substrate binding or for conformational changes (Figure 1.6).

Glucose transport is a dynamic event that represents a reversible conformational process, dictated ultimately by the protein's amino acid sequence. The information regarding the actual amino acids involved in this process is minimal at present. Transmembrane helices are characterised by a preponderance of hydrophobic residues such as valine, leucine, isoleucine, alanine and phenylalanine. The somewhat surprising selective inclusion of proline, a classical breaker of α -helical structure, in transmembrane helices (discussed in section 3.3) has prompted a variety of studies, utilising mutagenesis and modelling of Pro-containing helices, to investigate their functional importance in membrane spanning regions of proteins. Two distinct roles have been suggested in the literature- proline can act in a structural capacity (section 3.3.2b) or can have a more dynamic role through *cis-trans* isomerisation of Xaa-Pro peptide bonds (section 3.3.2c).

4.2.2 Conclusions from Previously Investigated Proline Residues of GLUT1.

Highly conserved Pro-containing motifs have been identified in the GLUT isoforms (section 3.3.6) and several transmembrane proline residues of GLUT1 have been the target of mutagenic studies. One such study by Tamori and co-workers in 1994 investigated the relationship between conformational changes and the presence of proline and glycine residues in helix 10 (Tamori *et al.*, 1994). Pro³⁸⁵ was targeted since it is located within the conserved **GPGPIP** sequence that has been implicated in the opening/closing of the exofacial binding site (Hodgson *et al.*, 1992). Reduced zero-*trans* uptake of 2-deoxy-D-glucose into CHO cells was observed when this residue was replaced by isoleucine (but not alanine or glycine). Reduced transport, abolishment of exofacial ATB-BMPA photolabelling and normal levels of cytochalasin B photolabelling led the authors to suggest that the ability of the protein to adopt the exofacial binding site was impaired as a direct consequence of the mutation (Data summarised in Table 4.1). No such effects were observed when Pro³⁸⁵ was replaced by alanine in this study, which appears to have overlooked the fact that transport of 2-deoxy-D-glucose is a series of events involving substrate binding to the exofacial site, transporter reorientation to the endofacial conformation, dissociation of the substrate from

the endofacial binding site and reorientation of the unloaded transporter to the exofacial conformation. Thus, it is possible that the effects of mutation of a single proline residue to alanine are not manifested in an altered overall rate of transport. Other aspects of the translocation mechanism may well have been altered and these effects may not be detectable by single measurement of transport rates at a single substrate concentration. A more extensive kinetic analysis of the mutants would define a more precise role for the proline residue. Effects mediated at the exofacial substrate binding site can be investigated by determining K_m values for zero-*trans* influx of substrate using a range of external sugar concentrations. Subtle effects at either of the binding sites caused by the mutation are more likely to be detected by the use of non-transportable site-specific ligands.

A second study was undertaken in which the role of proline residues located within helices 6 and 10 were investigated, again using a mutagenic approach (Wellner, 1995). Individual replacement of prolines at positions 187, 196 and 205, within helix 6, to alanine resulted in retention of wild type transport activity, suggesting that the presence of prolines at each of these positions is not an absolute requirement for transport catalysis. The same substitutions, this time within helix 10, also resulted in retainment of wild type transport activity, however, the lack of a more extensive kinetic analysis of these mutants prevents detection of more subtle roles for these residues in transporter function.

4.2.3 Use of Site Specific Ligands as Transport Inhibitors.

Cytochalasin B is a non-competitive and competitive inhibitor of D-glucose influx and efflux, respectively, and thus, is proposed to interact with the endofacial side of the transporter. Since cytochalasin B competitively inhibits D-glucose binding at the endofacial binding site and *vice versa*, their sites of interaction with the transporter are proposed to be the same. In addition, the binding moiety of cytochalasin B has an arrangement of oxygen atoms that can be superimposed onto that of D-glucose. Therefore, the hydrogen bonding patterns formed between the transporter and cytochalasin B are predicted to be similar to those formed with D-glucose. Both GLUT1 and GLUT3 have similar affinities for cytochalasin B (K_i values of $\sim 2\mu\text{M}$ for both isoforms).

Measurement of K_i values for cytochalasin B inhibition of substrate transport gives an estimation of the relative affinity at the endofacial binding site, proposed to be in the region at the base of helix 10 (Figure 1.6).

Maltose is a disaccharide composed of two D-glucose molecules joined by an α -(1-4) glycosidic linkage (Figure 4.2). It is a competitive inhibitor of D-glucose influx, and is therefore proposed to interact at the exofacial D-glucose binding site. Maltose is not transported due to steric hindrance. Therefore, measurement of K_i values for maltose inhibition of D-glucose influx are independent of the transporter turnover number, representing an effect mediated at the exofacial binding site only. GLUT1 and GLUT3 have similar reported values for maltose inhibition of 2-deoxy-D-glucose influx (20-30mM).

4.3 Heterologous Expression of Proteins in *Xenopus laevis* Oocytes.

4.3.1 Use of *Xenopus laevis* Oocytes.

Since the demonstration by Gurdon and co-workers in 1971 that *Xenopus* oocytes could efficiently translate exogenous mRNAs injected into their cytoplasm, the oocyte has become a favoured system for the study of transcript processing and translation (Gurdon *et al.*, 1971). During oogenesis, the oocyte accumulates a vast cellular store of enzymes and organelles which are required for the early stages of development. Thus, an isolated oocyte can essentially be viewed as a miniature protein synthesis factory, containing ~200,000 more ribosomes and 10,000 more tRNAs than a typical somatic cell. The ability to rapidly and efficiently translate exogenous mRNA (or cRNA), coupled to the ability to correctly modify polypeptides by phosphorylation, glycosylation, cleavage of precursor proteins and assembly of multi-subunit proteins, has led to the extensive use of this system.

Oocytes that are ready for use, i.e. those that translate exogenous mRNA most efficiently, are at stage IV or V of development. They are the largest oocytes, and are characterised by a distinct sharp boundary between the animal (dark) and vegetal (pale green/yellow) poles. Healthy oocytes exhibit a uniform pigmentation of the animal pole.

They are isolated from the toad by surgery and dissected from the surrounding vascular network and connective tissue prior to use (section 2.6.4).

Heterologous expression of proteins can be achieved in two ways: by microinjection of *in vitro* transcribed mRNA into the oocyte cytoplasm, or by microinjection of plasmid DNA into the nucleus. Although both methods result in adequate levels of protein expression for functional studies, microinjection of mRNA into the cytoplasm is much less technically demanding and thus, is the most commonly used approach. Typically, 50nl of ~1mg/ml mRNA is injected into each oocyte. An incubation period of 48 hours in physiological medium (Barths - Table 2.1) results in sufficient levels of protein expression to allow accurate determination of transport activity in individual oocytes by quantitation of radiolabelled sugar accumulation.

4.3.2 Expression of Glucose Transporter Isoforms.

The low endogenous glucose transport rates exhibited by non-injected oocytes make them an ideal system in which to probe the structure-function relationship of glucose transporters utilising mutagenesis.

Translation and processing of injected GLUT mRNA (encoding a particular isoform) enables kinetic data to be obtained, essentially, for a single transporter isoform. Previously, it has been demonstrated that the rates of sugar transport for water-injected oocytes and non-injected oocytes are identical (Gould & Lienhard, 1989). This can be a problem in other cell types and thus, subtraction of water-injected values gives a value that represents that of the injected transporter only. Oocytes were initially used for a kinetic analysis of GLUT1 (Gould & Lienhard, 1989), and since then, many groups have utilised oocytes for expression and characterisation of other GLUT isoforms, in addition to various chimeric transporters and other mutant transporters. GLUT2 and GLUT3 exhibit high rates of 3-O-methyl-D-glucose transport in oocytes, typically 20-fold higher than rates observed for non-injected oocytes. GLUT4 expressing oocytes exhibited much lower rates of transport, consistent with the proposed intracellular localisation of this isoform. A variety of kinetic parameters have been measured for GLUTs 1, 2, 3 and 4 utilising this expression system

(Table 4.2), including K_m values for 2-deoxy-D-glucose zero-*trans* influx, 3-O-methyl-D-glucose transport (under both zero-*trans* influx and equilibrium exchange conditions) and alternative transported substrates. For example, GLUT2 has been demonstrated to be capable of D-fructose transport, whereas GLUT3 is capable of D-galactose transport to a greater extent than the other isoforms. These observations have formed the basis of other studies by this group in which the structural requirements of sugar binding to these isoforms were investigated using a variety of sugar analogues (Colville *et al.*, 1993a). A range of GLUT2/GLUT3 chimeric transporters were also generated, with a view to identifying the regions of GLUT2 and GLUT3 that are involved in substrate recognition and high affinity glucose binding (Arbuckle *et al.*, 1996).

The generation of specific point mutations within the transporters, coupled to the subsequent expression and analysis of the mutant proteins in oocytes or cultured cells, have provided important insights into the transport mechanism. Crucial residues that participate in various aspects of substrate translocation have been identified from such studies. Residues may interact directly with the transported sugar molecule or may act in a structural capacity to mediate the conformational changes requisite for translocation or formation of the binding sites. A putative role for proline residues in membrane protein function has already been discussed in Chapter 3 of this thesis.

Here a kinetic analysis of various mutant GLUT3 proteins heterologously expressed in *Xenopus* oocytes is presented to examine the role of conserved proline residues in GLUT3 function (Chapter 3 and Figure 3.3). K_m values for zero-*trans* entry of 2-deoxy-D-glucose have been determined for each Pro-Ala GLUT3 mutant and the wild type transporter, for comparison. To establish whether any effects caused by the mutations are manifested in the ability of the transporter to correctly adopt endofacial and exofacial conformations, the inhibitory effects of the site-specific ligands cytochalasin B and maltose on 2-deoxy-D-glucose zero-*trans* influx were measured. These results are discussed in terms of the proposed structural models for the transporters.

Table 4.1

Summary of the Kinetic Data Available for Human GLUT1 Proline Mutants.

Mutation	Expression System	Transport Activity	Km	Cytochalasin B Binding	ATB-BMPA Binding
P187A	Oocyte	wt	n.d		
P187H	"	wt	"		
P196A	"	wt	"		
P196R	"	↓	"	+	
P383A	"	wt	"		
P383Q	"	↓	"		
P385A	"	wt	"		
P385Q	"	↓	"		
P387A	"	wt	"		
P387Q	"	↓	"		
P383A +P385A	"	wt	"		
P385I	CHO	↓	"	wt	-
P385G	"	wt	"	↑	↓

wt indicates comparable or identical to wild type GLUT1.

↑↓ indicates parameter was significantly increased or reduced respectively relative to the wild type.

+

indicates activity was observed.

-

indicates no detectable activity (<5% wt).

n.d not determined.

Figure 4.1

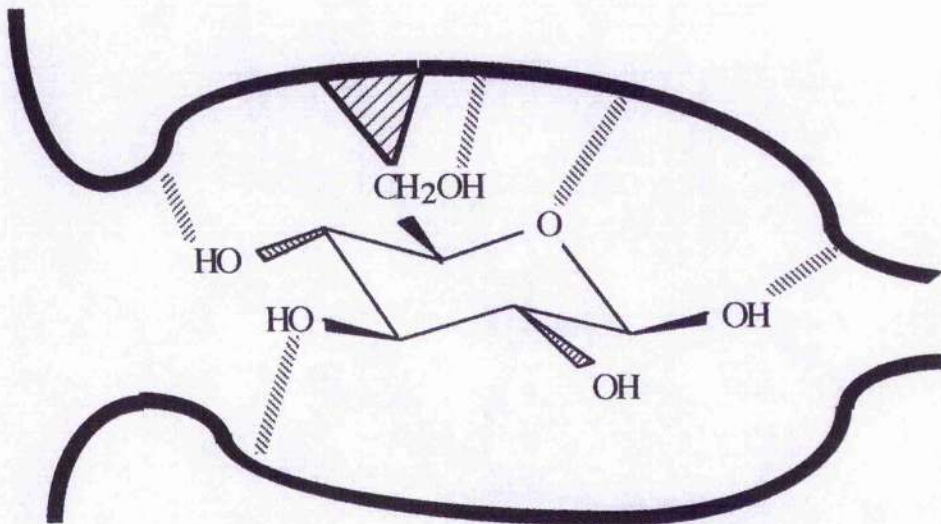
Models of the Interaction of β -D-Glucose with GLUTs 1 and 3.

These are generalised models showing the interactions formed between β -D-glucose and GLUT1 (a) and GLUT3 (b) at the exofacial binding site. Hydrogen bonds are illustrated by dashed lines and the C-6 hydrophobic interactions are shown by a dashed triangle. The hydrogen bond formed at the C-4 position of GLUT3 is likely to be less significant in substrate binding than with GLUT1 and the other isoforms, (shown in red), since GLUT3 binds D-galactose, the C-4 epimer of D-glucose.

Figure 4.1

Models of the Interaction of β -D-Glucose with GLUTs 1 and 3.

(a)



(b)

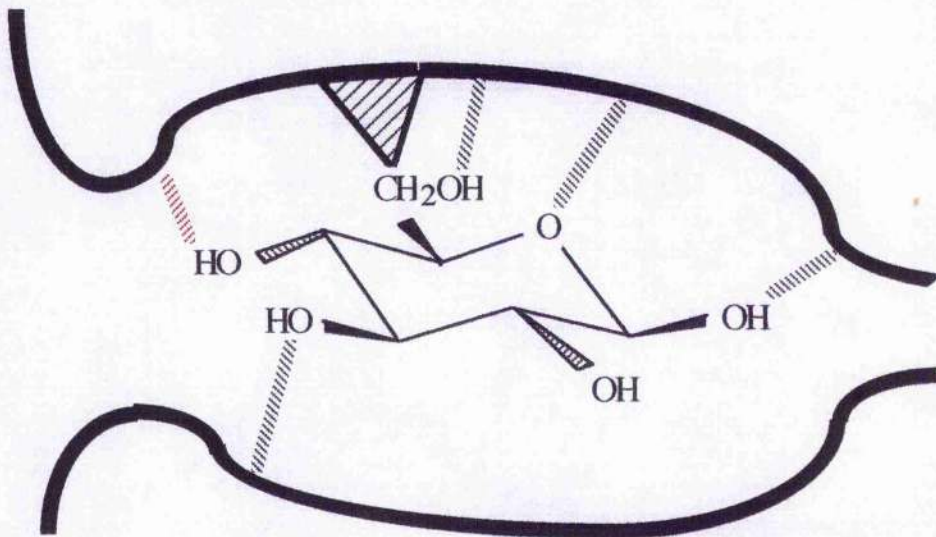


Figure 4.2

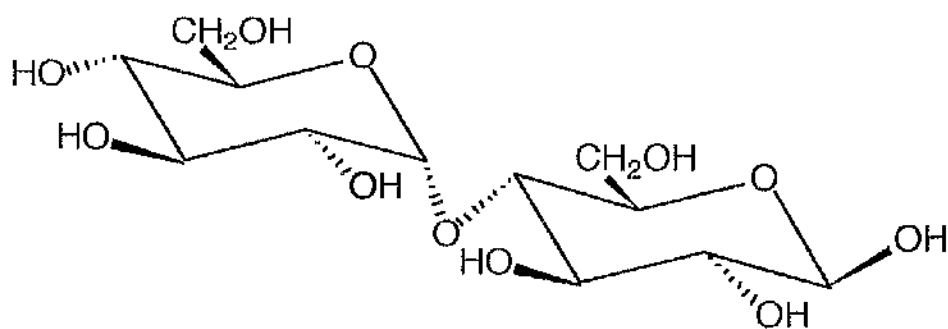
Structure of β -D-Glucose and β -D-Maltose.

This diagram shows the structures of β -D-glucose and β -D-maltose. Maltose is a disaccharide of D-glucose in a $\alpha(1-4)$ glycosidic linkage. Maltose is used as an inhibitor of sugar transport as it can bind to the transporter but is not transported.

The C-1 position of the first glucose "subunit" of maltose enters the exofacial binding pocket of the transporter in a "D-glucose-like" manner. The sugar hydroxyls at positions C-3 and C-6 are also analogous, so it is expected that these will interact with the binding site in a " β -D-glucose-like" manner. However, the bond with the C-4 hydroxyl will not be formed because this carbon is involved in the glycosidic linkage with the other glucose "subunit" of maltose. This other glucose unit effectively acts as a large bulky group at the C-4 position of the first glucose unit, which prevents closing of the transporter around the sugar molecule. It is possible that the interaction of the C-3 and C-6 carbons with the exofacial binding site may also be affected by the presence of the large bulky substituent at the C-4 position.

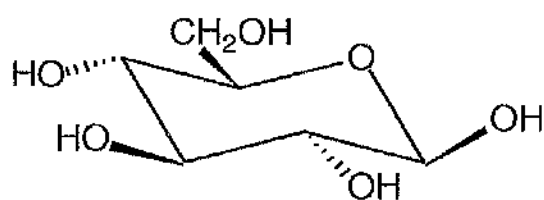
Figure 4.2

Structure of β -D-Glucose and β -D-Maltose.



β -D-MALTOSE

(Glucose- α (1-4)-glucose)



β -D-GLUCOSE

Table 4.2

Kinetic Parameters of the Glucose Transporter Isoforms Expressed in Oocytes.

Isoform	K_m (mM)	3-O-MG equilibrium exchange (mM)	Alternative substrates
	DeGlc zero- <i>trans</i> entry (mM)		
GLUT1	6.9 \pm 1.5	20.9 \pm 2.9	Galactose (K_m 17mM)
GLUT2	11.2 \pm 1.1	42.3 \pm 4.1	Fructose (K_m 66mM)
GLUT3	1.4 \pm 0.06	10.6 \pm 1.3	Galactose (K_m 8.5mM)
GLUT4	4.6 \pm 0.3	1.8	Not studied in oocytes
GLUT5	n.d.	n.d.	Fructose* (K_m 6mM)

The data from this table was taken from results published in a number of studies (reviewed in Gould & Holman 1993).

n.d. - no data, substrate not transported.

* Fructose is the preferred substrate of GLUT5, not the alternative substrate.

4.4 Results.

4.4.1 Transport of 2-Deoxy-D-Glucose by GLUT3 Pro-Ala Mutants into *Xenopus* Oocytes.

After construction and sequencing of each mutant, the cDNAs were linearised with *Xba* I (section 2.3.4) and used as templates for *in vitro* synthesis of mRNA (section 2.5). In addition, wild type GLUT3 mRNA was also synthesised. The relative mRNA concentrations were assessed by agarose gel electrophoresis (Figure 2.3) and adjusted to approximately 1mg/ml. 50nl of mRNA was injected into each oocyte, and, after an incubation period of 48 hours in sugar-free medium (Table 2.1), oocytes were assayed for uptake of [³H]2-deoxy-D-glucose over a period of 30 mins. Groups of 6-10 oocytes were assayed for 2-deoxy-D-glucose transport at each external sugar concentration. The radioactive tracer taken up by each oocyte was measured, and the mean for each group was calculated. By measuring the rates of *zero-trans* entry as a function of substrate concentration, the K_m value for transport of this substrate can be deduced from construction of a Lineweaver-Burk plot. Oocytes expressing the wild type GLUT3 transporter and non-injected oocytes were also assayed under identical conditions. Non-injected oocytes were used to measure non-specific endogenous transport levels at each substrate concentration used, and were subtracted from transport rates obtained for mutant and wild type injected oocytes to obtain specific rates of transport. It has been shown previously that the amount of label accumulating within the oocyte increases linearly over this time period, suggesting that transport of sugar is the rate-limiting step and not the subsequent phosphorylation mediated by hexokinase (Colville *et al.*, 1993b).

Three to four mutant mRNAs, in addition to wild type GLUT3 mRNA, were individually injected into oocytes isolated from a single toad. This is mainly due to the fact that the mutant cDNAs were generated over a period of time, and also to limit the size of the transport assays. K_m values obtained for 2-deoxy-D-glucose *zero-trans* entry by GLUT3 and Pro-Ala GLUT3 mutants expressed in *Xenopus* oocytes are shown in Table 4.3. The values represent the mean of at least three separate experiments for each mutant and those of

GLUT3 were determined in parallel at least once for each mutant. K_m values were calculated from Lineweaver-Burk plots in which $1/\text{rate}$ of transport is plotted against $1/\text{substrate}$ concentration, according to the equation:-

$$1/v = 1/V_{\max} + K_m/V_{\max}[S]$$

where v is the rate of transport measured, V_{\max} is the maximum rate of transport, K_m is the substrate concentration at which half-maximal transport activity is attained, and $[S]$ is the substrate concentration. Representative plots are shown in Figures 4.3 and 4.4 for the wild type transporter and the Pro⁴⁵¹Ala mutant, respectively

4.4.2 Determination of K_i Values for Cytochalasin B Inhibition of 2-Deoxy-D-Glucose Zero-*trans* Uptake.

Individual oocytes injected with either wild type or mutant mRNA, together with non-injected control oocytes were assayed for zero-*trans* uptake of [³H]2-deoxy-D-glucose over a range of external sugar concentrations as described above. The effects of cytochalasin B on zero-*trans* uptake was investigated in parallel by incubating oocytes, expressing either wild type, mutant GLUT3 or neither, in the presence of 2 μ M cytochalasin B in Barths medium (Table 2.2). Oocytes to be exposed to the inhibitor were treated with 2mg/ml collagenase solution for 30 mins (section 2.7.2) and then cytochalasin B for 15 min prior to assay. This serves to break down the follicular cells of the oocyte enabling the inhibitor to penetrate the cell plasma membrane more readily. This extra step does not alter the kinetics of 2-deoxy-D-glucose (Gould and Colville, unpublished data). Transport was initiated by addition of radiolabelled sugar, and terminated after a 30 min incubation period.

K_i values were determined from the construction of Lineweaver-Burk plots by application of the equation:-

$$\text{gradient of line (inhibitor)} = K_m / V_{\max} \cdot (1 + [I] / K_i)$$

where $[I]$ is the concentration of cytochalasin B and K_i is the concentration of inhibitor that causes a 50% reduction in the rate of transport. A summary of the K_i values determined for the non-competitive inhibition of 2-deoxy-D-glucose zero-*trans* influx by GLUT3 and Pro-Ala GLUT3 mutants is given in Table 4.3 and Lineweaver-Burk plots for P206A, P381A, P383A and P385A are shown in Figures 4.5-4.8.

4.4.3 Determination of K_i Values for Maltose Inhibition of 2-Deoxy-D-Glucose Zero-*trans* Uptake.

To investigate the inhibitory effects of the exofacial ligand maltose on 2-deoxy-D-glucose transport by GLUT3 and GLUT3 Pro-Ala mutants, transport rates were measured, as described above, in the presence and absence of 50mM maltose in Barths medium. Oocytes to be exposed to the inhibitor were pre-incubated in maltose solution for at least 15 mins prior to initiation of transport by the addition of radiolabelled sugar. Again, transport rates were measured over a range of external sugar concentrations and non-injected oocytes were assayed in parallel under identical conditions to obtain endogenous transport rates.

The effects of maltose on 2-deoxy-D-glucose transport by GLUT3 and Pro-Ala GLUT3 mutants are shown in Figures 4.9-4.14. K_i values were calculated from these graphs by the application of the equation quoted in section 4.4.2 and are summarised in Table 4.3.

4.5 Conclusions.

4.5.1 Expression of Pro-Ala GLUT3 Mutant Transporters and Their Ability to Transport 2-Deoxy-D-Glucose in *Xenopus* Oocytes.

All mutated GLUT3 cDNAs generated by recombinant PCR reactions were capable of acting as templates for *in vitro* synthesis of mRNA with efficiencies approaching that of wild type GLUT3. Upon injection into *Xenopus* oocytes, expression of the mutant transporter proteins resulted in increased rates of zero-*trans* uptake of 2-deoxy-D-glucose to

levels comparable to wild type GLUT3 (between 3-6 pmoles/min/oocyte), which were consistently several-fold higher than rates observed in non-injected oocytes (typically 0.3-0.6 pmoles/min/oocyte). Measurement of kinetic parameters for 2-deoxy-D-glucose transport mediated by Pro²⁰³Ala and Pro³⁹⁹Ala was not possible due to low levels of transport activity consistently observed for these transporters.

4.5.2 Kinetics of 2-Deoxy-D-Glucose Transport Mediated by Pro-Ala Mutants and Wild Type GLUT3.

Comparison of the K_m values measured for 2-deoxy-D-glucose zero-*trans* influx in oocytes for each of the mutants with that obtained for GLUT3 reveal that none of the mutations affected the ability of the protein to transport this substrate. In fact, no significant alterations were observed in the affinities of the mutants for substrate compared to wild type GLUT3. Mutants exhibited K_m values of 0.62 ± 0.3 - 1.7 ± 0.2 mM compared to 1.2 ± 0.03 mM determined for wild type GLUT3, which is in good agreement with previously reported GLUT3 K_m values (Colville *et al.*, 1993b).

4.5.3 Competitive Inhibition of 2-Deoxy-D-Glucose Zero-*trans* Influx by Maltose.

K_i values for maltose inhibition of transport are presented in Table 4.3. The value determined for wild type GLUT3 is in good agreement with values previously reported for GLUT3 expressed in oocytes (Colville *et al.*, 1993b). All Pro-Ala mutations resulted in an increase in the K_i value for maltose (to various extents) compared to GLUT3, indicating a decrease in the affinities of the mutant transporters for this exofacial ligand. Only values obtained for Pro²⁰⁶, Pro³⁸¹, Pro³⁸³ and Pro⁴⁵¹ were statistically significant, with values 2-3 fold higher than that obtained for the wild type transporter. Lineweaver-Burk plots for these mutants are shown in Figures 4.10-4.12 and 4.14.

4.5.4 Non-Competitive Inhibition of 2-Deoxy-D-Glucose Zero-trans Influx by Cytochalasin B.

K_i values for cytochalasin B inhibition of transport are presented in Table 4.3. Again, the value determined for the wild type transporter was comparable to that previously reported in this expression system (Colville *et al.*, 1993b). Only mutation of proline residues to alanine at the base of helix 10, Pro³⁸¹, Pro³⁸³ and Pro³⁸⁵, resulted in a significant increase in the K_i values (Figures 4.6-4.8), indicating a decrease in affinity for this inhibitor at the endofacial binding site of 3-4 fold compared to wild type. Mutation of prolines at positions 206, 209 and 451 to alanine did not significantly affect the K_i value, as determined by application of a Students t-test.

Table 4.3

Kinetic Parameters of GLUT3 Wild-Type and Pro-Ala Mutants Expressed in *Xenopus* Oocytes.

Mutant	K_m deGlc (mM)	K_i Maltose (mM)	K_i Cytochalasin B (μ M)
Wild type GLUT3	1.2\pm0.03	33\pm2	2.8\pm0.6
P203A	n.d.	n.d.	n.d.
P206A	1.7 \pm 0.2	76 \pm 17*	2.1 \pm 0.9
P209A	0.95 \pm 0.5	56 \pm 13	2.1 \pm 1.2
P381A	0.96 \pm 0.1	80 \pm 14*	0.5 \pm 0.4***
P383A	1.46 \pm 0.6	71 \pm 2**	1.0 \pm 0.5***
P385A	0.62 \pm 0.3	43 \pm 9	0.97 \pm 0.7***
P399A	n.d.	n.d.	n.d.
P451A	1.23 \pm 0.2	67 \pm 9**	1.76 \pm 0.5

Statistically significant changes from wild type are indicated by *(p=0.05), **(p<0.05), *** (p<0.02).n.d., not determined.

Figure 4.3

Lineweaver-Burk Plot of 2-Deoxy-D-Glucose Transport by GLUT3 Injected Oocytes.

Each point is the mean of the transport rate determined from groups of at least 7 oocytes (section 2.7). The rate of transport was determined by exposure of the oocytes to radiolabelled 2-deoxy-D-glucose for 30 mins and the counts per minute determined as described (section 2.7). For each experiment endogenous oocyte transport was measured by a parallel incubation of non-injected control oocytes in trace radiolabelled 2-deoxy-D-glucose. Values obtained for control oocytes were subtracted from the values obtained from the GLUT3 injected oocytes to obtain the heterologous transport rate. Transport rates measured for control oocytes were typically 10% of the rates obtained for injected oocytes. The data shown in this plot is representative of at least four separate experiments.

Figure 4.3
Lineweaver-Burk Plot of 2-Deoxy-D-Glucose Transport by GLUT3 Injected Oocytes.

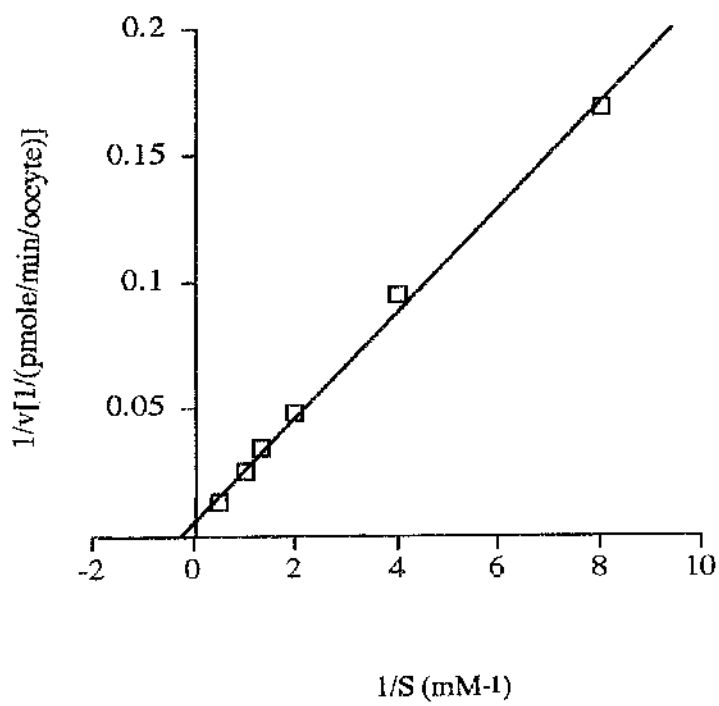


Figure 4.4

Lineweaver-Burk Plot of 2-Deoxy-D-Glucose Transport by P451A Injected Oocytes.

Each point is the mean of the transport rate determined from groups of at least 7 P451A-injected oocytes. Rates of transport were determined by exposure of the oocytes to radiolabelled 2-deoxy-D-glucose for 30 mins and the counts per minute determined. Values are corrected for endogenous rates of transport as described (Figure 4.3 legend). The range of errors were typically $\pm 10\%$ at each point. Error bars are omitted for clarity. This plot is representative of at least four separate experiments.

Figure 4.4

Lineweaver-Burk Plot of 2-Deoxy-D-Glucose Transport by P451A Injected Oocytes.

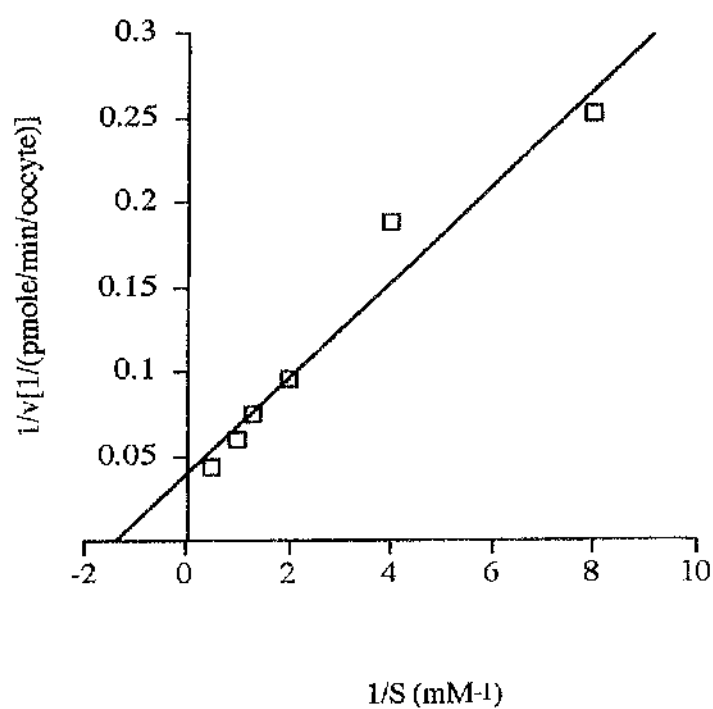


Figure 4.5

Lineweaver-Burk Plot of 2-Deoxy-D-Glucose Transport by P206A Injected Oocytes in the Presence and Absence of Cytochalasin B.

Transport rates of 2-deoxy-D-glucose into oocytes expressing P206A were determined as described. Each point is the mean of at least seven separate oocytes at each sugar concentration. Values are corrected for endogenous rates of transport (Figure 4.3 legend). Transport rates were measured in the presence and absence of 2 μ M cytochalasin B as indicated. The range of errors were typically $\pm 10\%$ at each point. Error bars are omitted for clarity. This plot is representative of at least four separate experiments.

Figure 4.5

Lineweaver-Burk Plot of 2-Deoxy-D-Glucose Transport by P206A Injected Oocytes in the Presence and Absence of Cytochalasin B.

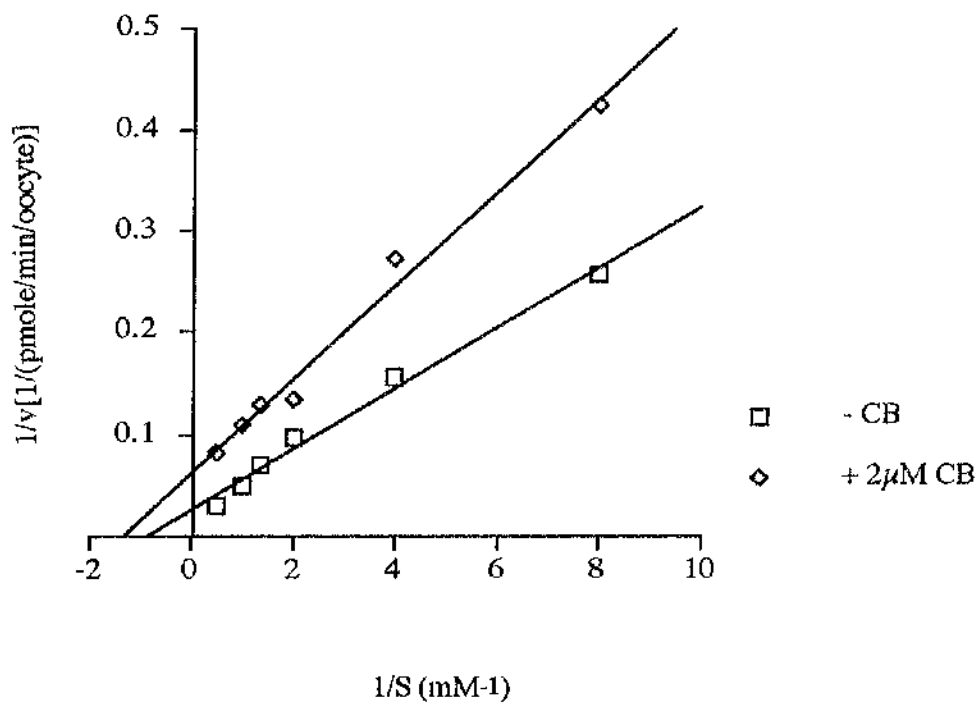


Figure 4.6

Lineweaver-Burk Plot of 2-Deoxy-D-Glucose Transport by P381A Injected Oocytes in the Presence and Absence of Cytochalasin B.

Transport rates of 2-deoxy-D-glucose into oocytes expressing P381A were determined as described. Each point is the mean of at least seven separate oocytes at each sugar concentration. Values are corrected for endogenous rates of transport (Figure 4.3 legend). Transport rates were measured in the presence and absence of 2 μ M cytochalasin B as indicated. The range of errors were typically $\pm 10\%$ at each point. Error bars are omitted for clarity. This plot is representative of at least four separate experiments.

Figure 4.6

Lineweaver-Burk Plot of 2-Deoxy-D-Glucose Transport by P381A Injected Oocytes in the Presence and Absence of Cytochalasin B.

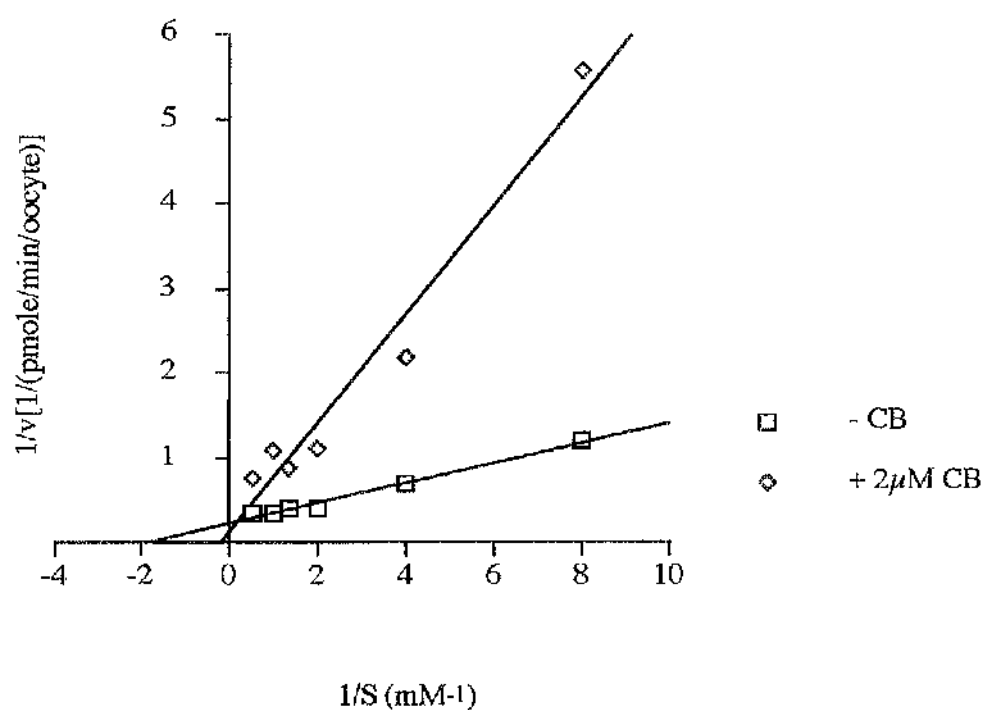


Figure 4.7

Lineweaver-Burk Plot of 2-Deoxy-D-Glucose Transport by P383A Injected Oocytes in the Presence and Absence of Cytochalasin B.

Transport rates of 2-deoxy-D-glucose into oocytes expressing P383A were determined as described. Each point is the mean of at least seven separate oocytes at each sugar concentration. Values are corrected for endogenous rates of transport (Figure 4.3 legend). Transport rates were measured in the presence and absence of 2 μ M cytochalasin B as indicated. The range of errors were typically $\pm 10\%$ at each point. Error bars are omitted for clarity. This plot is representative of at least four separate experiments.

Figure 4.7

Lineweaver-Burk Plot of 2-Deoxy-D-Glucose Transport by P383A Injected Oocytes in the Presence and Absence of Cytochalasin B.

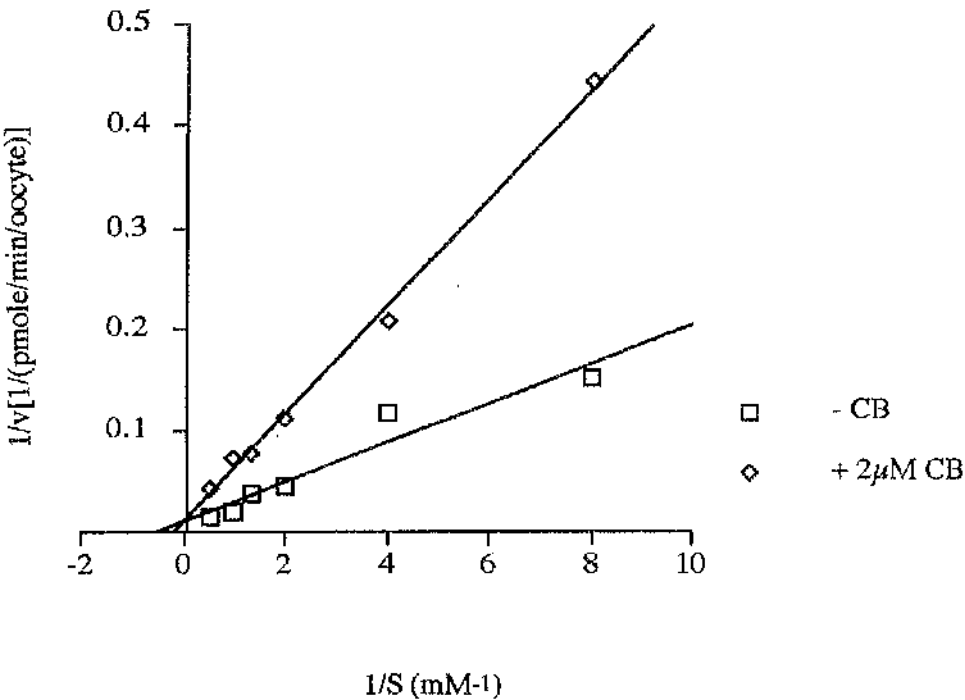


Figure 4.8

Lineweaver-Burk Plot of 2-Deoxy-D-Glucose Transport by P385A Injected Oocytes in the Presence and Absence of Cytochalasin B.

Transport rates of 2-deoxy-D-glucose into oocytes expressing P385A were determined as described. Each point is the mean of at least seven separate oocytes at each sugar concentration. Values are corrected for endogenous rates of transport (Figure 4.3 legend). Transport rates were measured in the presence and absence of 2 μ M cytochalasin B as indicated. The range of errors were typically $\pm 10\%$ at each point. Error bars are omitted for clarity. This plot is representative of at least four separate experiments.

Figure 4.8

Lineweaver-Burk Plot of 2-Deoxy-D-Glucose Transport by P385A Injected Oocytes in the Presence and Absence of Cytochalasin B.

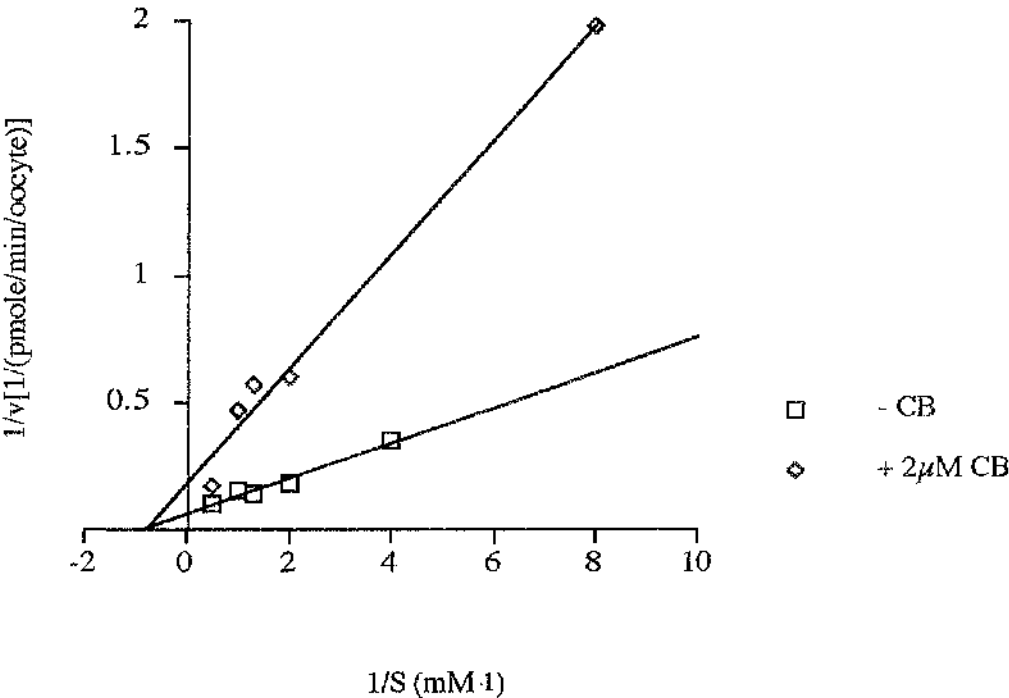


Figure 4.9

Lineweaver-Burk Plot of 2-Deoxy-D-Glucose Transport by GLUT3 Injected Oocytes in the Presence and Absence of Maltose.

Transport rates of 2-deoxy-D-glucose into oocytes expressing GLUT3 were determined as described. Each point is the mean of at least seven separate oocytes at each sugar concentration. Values are corrected for endogenous rates of transport (Figure 4.3 legend). Transport rates were measured in the presence and absence of 50mM maltose as indicated. The range of errors were typically $\pm 10\%$ at each point. Error bars are omitted for clarity. This plot is representative of at least four separate experiments.

Figure 4.9
Lineweaver-Burk Plot of 2-Deoxy-D-Glucose Transport by GLUT3 Injected Oocytes in the Presence and Absence of Maltose.

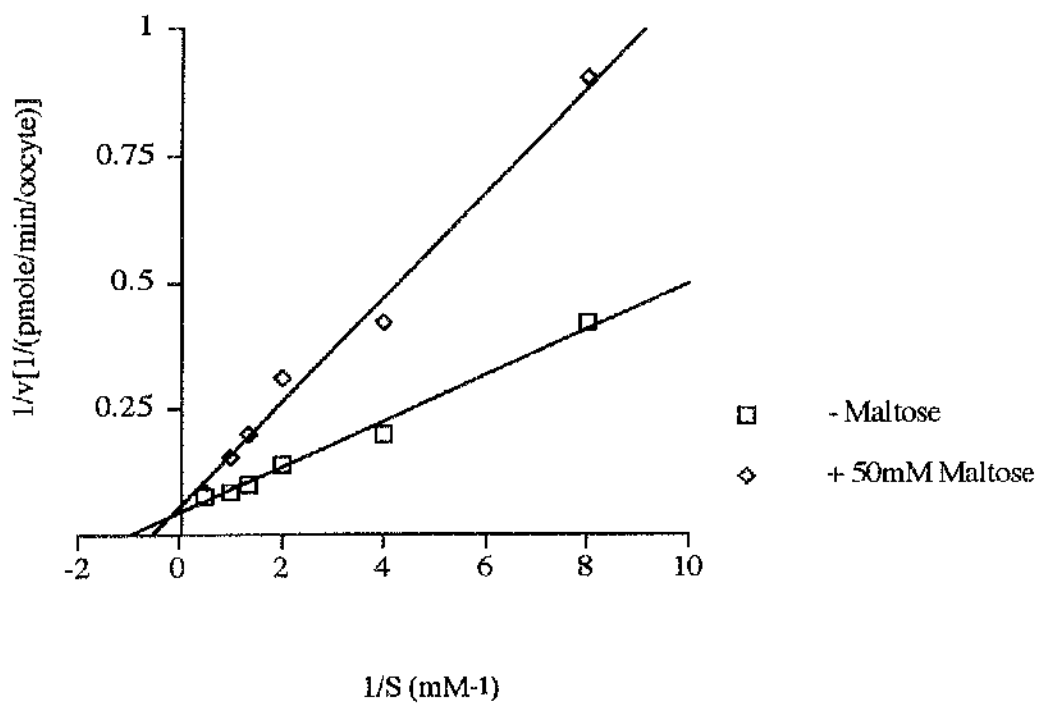


Figure 4.10

Lineweaver-Burk Plot of 2-Deoxy-D-Glucose Transport by P206A Injected Oocytes in the Presence and Absence of Maltose.

Transport rates of 2-deoxy-D-glucose into oocytes expressing P206A were determined as described. Each point is the mean of at least seven separate oocytes at each sugar concentration. Values are corrected for endogenous rates of transport (Figure 4.3 legend). Transport rates were measured in the presence and absence of 50mM maltose as indicated. The range of errors were typically $\pm 10\%$ at each point. Error bars are omitted for clarity. This plot is representative of at least four separate experiments.

Figure 4.10

Lineweaver-Burk Plot of 2-Deoxy-D-Glucose Transport by P206A Injected Oocytes in the Presence and Absence of Maltose.

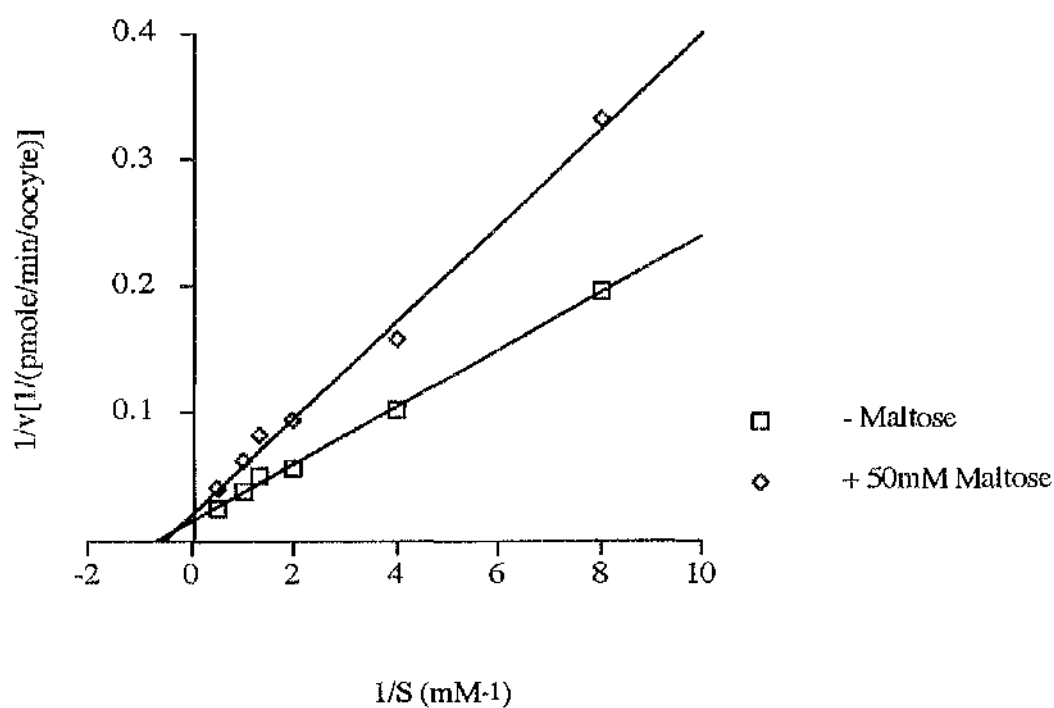


Figure 4.11

Lineweaver-Burk Plot of 2-Deoxy-D-Glucose Transport by P381A Injected Oocytes in the Presence and Absence of Maltose.

Transport rates of 2-deoxy-D-glucose into oocytes expressing P381A were determined as described. Each point is the mean of at least seven separate oocytes at each sugar concentration. Values are corrected for endogenous rates of transport (Figure 4.3 legend). Transport rates were measured in the presence and absence of 50mM maltose as indicated. The range of errors were typically $\pm 10\%$ at each point. Error bars are omitted for clarity. This plot is representative of at least four separate experiments.

Figure 4.11

Lineweaver-Burk Plot of 2-Deoxy-D-Glucose Transport by P381A Injected Oocytes in the Presence and Absence of Maltose.

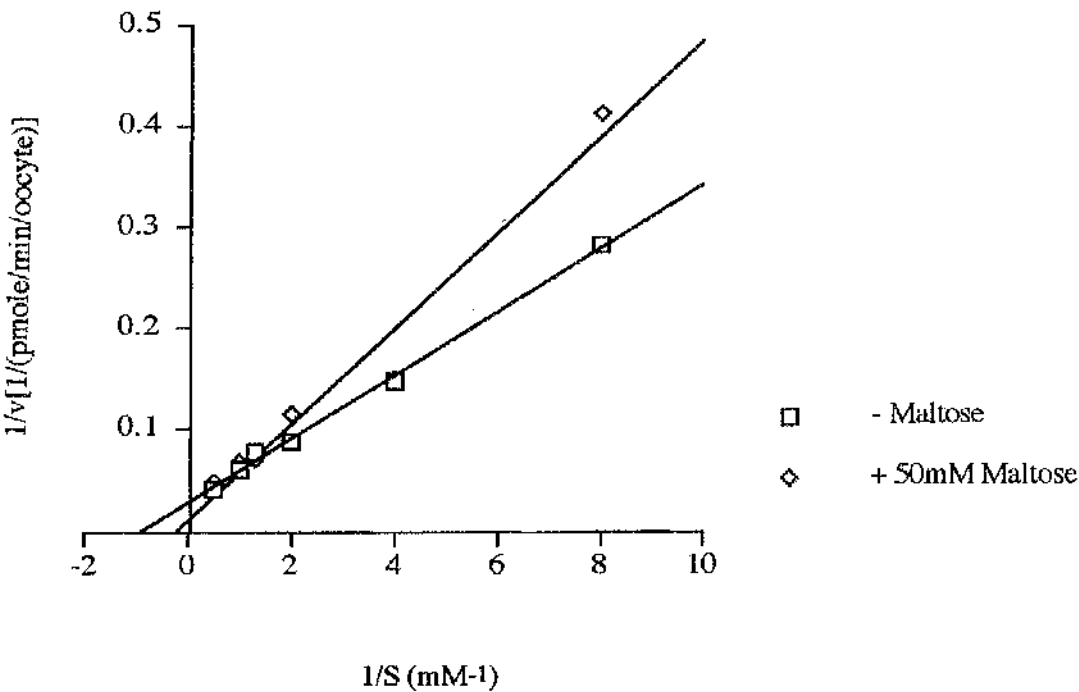


Figure 4.12

Lineweaver-Burk Plot of 2-Deoxy-D-Glucose Transport by P383A Injected Oocytes in the Presence and Absence of Maltose.

Transport rates of 2-deoxy-D-glucose into oocytes expressing P383A were determined as described. Each point is the mean of at least seven separate oocytes at each sugar concentration. Values are corrected for endogenous rates of transport (Figure 4.3 legend). Transport rates were measured in the presence and absence of 50mM maltose as indicated. The range of errors were typically $\pm 10\%$ at each point. Error bars are omitted for clarity. This plot is representative of at least four separate experiments.

Figure 4.12

Lineweaver-Burk Plot of 2-Deoxy-D-Glucose Transport by P383A Injected Oocytes in the Presence and Absence of Maltose.

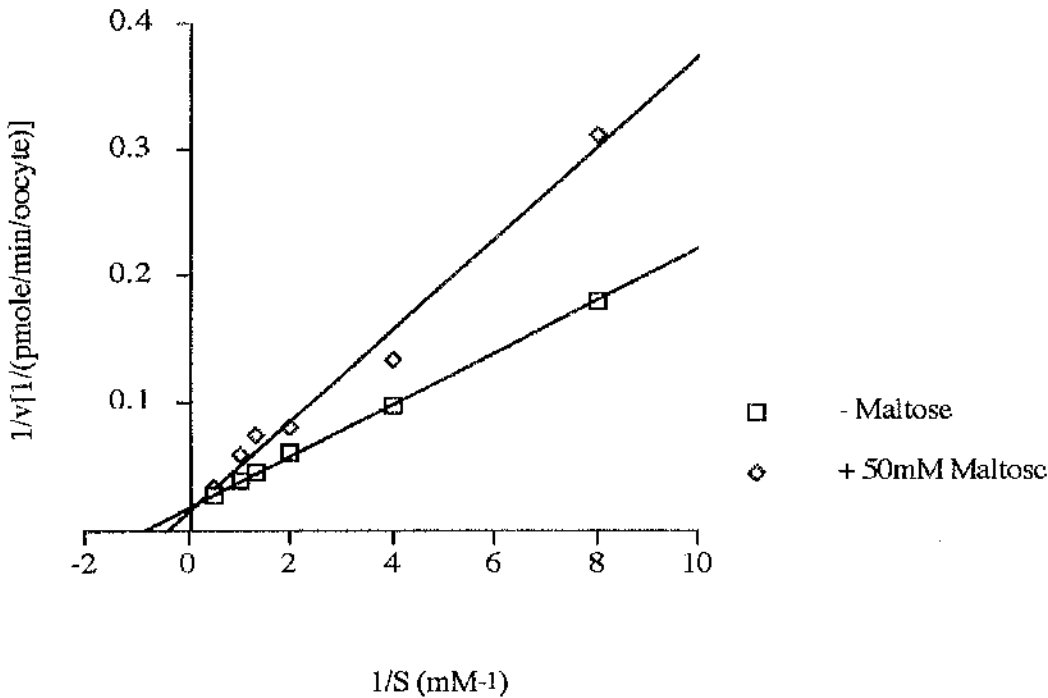


Figure 4.13

Lineweaver-Burk Plot of 2-Deoxy-D-Glucose Transport by P385A Injected Oocytes in the Presence and Absence of Maltose.

Transport rates of 2-deoxy-D-glucose into oocytes expressing P385A were determined as described. Each point is the mean of at least seven separate oocytes at each sugar concentration. Values are corrected for endogenous rates of transport (Figure 4.3 legend). Transport rates were measured in the presence and absence of 50mM maltose as indicated. The range of errors were typically $\pm 10\%$ at each point. Error bars are omitted for clarity. This plot is representative of at least four separate experiments.

Figure 4.13

Lineweaver-Burk Plot of 2-Deoxy-D-Glucose Transport by P385A Injected Oocytes in the Presence and Absence of Maltose.

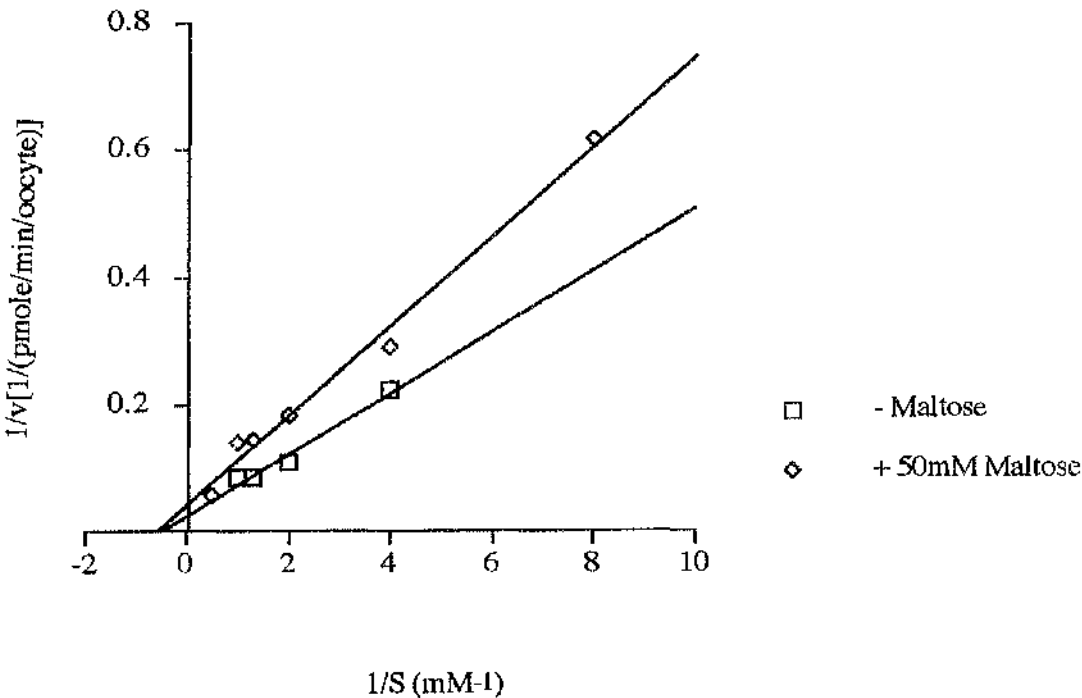
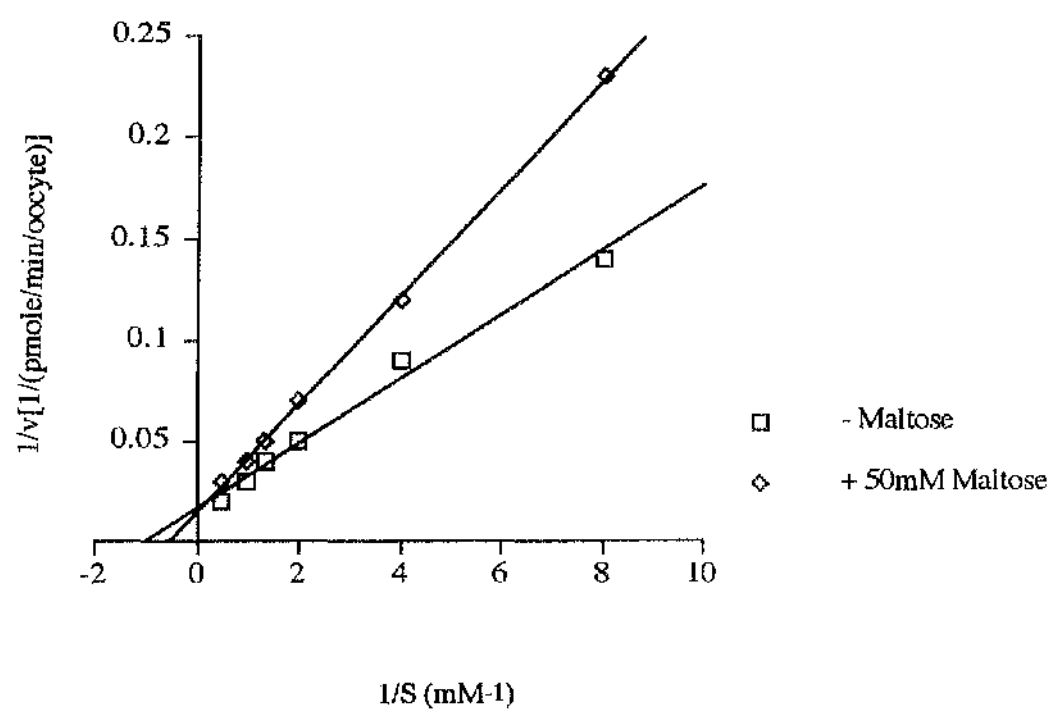


Figure 4.14

Lineweaver-Burk Plot of 2-Deoxy-D-Glucose Transport by P451A Injected Oocytes in the Presence and Absence of Maltose.

Transport rates of 2-deoxy-D-glucose into oocytes expressing P451A were determined as described. Each point is the mean of at least seven separate oocytes at each sugar concentration. Values are corrected for endogenous rates of transport (Figure 4.3 legend). Transport rates were measured in the presence and absence of 50mM maltose as indicated. The range of errors were typically $\pm 10\%$ at each point. Error bars are omitted for clarity. This plot is representative of at least four separate experiments.

Figure 4.14
Lineweaver-Burk Plot of 2-Deoxy-D-Glucose Transport by P451A Injected Oocytes in the Presence and Absence of Maltose.



4.6 Discussion.

4.6.1 Location of GLUT3 Proline Residues and Mutation to Alanine.

In the light of previous reports that proline residues may play a significant role in the structure and function of membrane proteins, a study was undertaken to investigate the role of several proline residues in transport mediated by GLUT3. The prolines targeted for mutation were located at the putative end of helix 6, (Pro²⁰³), the start of the large intracellular loop at the base of transmembrane helix 6, (Pro²⁰⁶ and Pro²⁰⁹), within transmembrane helix 10, (Pro³⁸¹, Pro³⁸³, and Pro³⁸⁵), the putative start of helix 11, (Pro³⁹⁹), and at the start of the cytoplasmic C-terminal tail near the base of helix 12 (Pro⁴⁵¹) (Figure 3.3). These residues were individually replaced with alanine. The basis for this substitution is two-fold. Firstly, as *cis-trans* isomerisation is unique to Xaa-Pro peptide bonds, replacement of a proline residue with alanine should remove flexibility around such a bond, if in fact Xaa-Pro isomerisation is crucial for transport. Secondly, alanine is a relatively small residue and is a good helix former. The substituted residue should not be so large as to potentially block transport of a substrate through the channel and, since some of the prolines targeted are within helices, should not disrupt the helical structure by introduction, for example, of a charged species. Replacement by alanine should, essentially, remove any flexibility around the peptide bond without significant disruption of the local protein structure.

Previous mutagenic studies have investigated the roles of proline residues within transmembrane helix 6 of GLUT1. These residues are conserved in all GLUT isoforms, except for GLUT2, and were concluded not to be crucial for transport. Proline residues investigated in this study included those contained within the highly conserved sequence **PESP(R)**, located at the base of helix 6. These residues have not previously been investigated, despite their high degree of conservation. This motif is mirrored by the conserved sequence **VPET(K)**, located at the base of helix 12, at the start of the cytoplasmic tail. Since this region has been implicated in correct formation of the exofacial binding site, the proline residue contained within this sequence was also mutated to alanine in this study.

Transmembrane helix 10 is predicted to be a highly mobile region of the transporter that is suggested to form a pivotal point for the conformational changes required for substrate translocation (Gould and Holman, 1993). The endofacial half of this helix contains the conserved sequence, **GPGPIP**. Since proline does not possess an amide hydrogen atom, the hydrogen bonding pattern of the helix is predicted to break down in this region. This, coupled to the presence of the small residue glycine, is predicted to create a non-hindered atomic environment for conformational flexing around this region. The ability of Xaa-Pro peptide bonds to undergo *cis-trans* isomerisation has also been suggested to contribute to conformational flexibility in membrane proteins (section 3.3.2a). The proline residues within helix 10 (at positions 381, 383 and 385) of GLUT3 were targeted for mutagenesis in this study, despite the publication of a recent study investigating the corresponding residues of GLUT1 (prolines 383, 385 and 387). The reasons for this are 2-fold- (1) mutation of the corresponding residues in GLUT3 will assess the generality of the results obtained from GLUT1, and (2) a more extensive kinetic analysis of the Pro-Ala mutant GLUT3 transporters expressed in oocytes, with the use of site-specific ligands, should reveal whether the effects of the mutations are manifested in the ability of the protein to expose groups that constitute the endofacial or exofacial binding sites. It is possible that such effects may have been overlooked in the absence of detailed kinetic analyses of previously reported mutants of GLUT1, particularly since individual replacement of proline residues may be compensated for by the presence of other prolines in the protein. In addition, the consequences of mutation of proline residues predicted to lie close to the endofacial side of the membrane at the start of the large central loop and the C-terminal tail were investigated.

4.6.2 Proline Residues and GLUT3 Function.

All Pro-Ala mutants generated and expressed in this study exhibited broadly comparable rates of 2-deoxy-D-glucose transport into oocytes relative to wild type GLUT3. Since no significant changes in the K_m for 2-deoxy-D-glucose influx was observed, it can be concluded that none of the proline residues are absolutely required for transport catalysis.

The results also infer that the mutations did not greatly perturb protein folding and targeting. After 2-deoxy-D-glucose influx, the substrate is rapidly phosphorylated (not rate-limiting) enforcing its retention inside the oocyte. The interaction of this substrate with the endofacial binding site is negligible and, therefore, measurement of the K_m value is a function of the affinity at the exofacial binding site. Use of this substrate is preferential to the use of D-glucose in this regard.

It is important to remember however, that the K_m is a function of substrate binding at the exofacial site, an exofacial to endofacial reorientation of the loaded carrier, substrate dissociation at the endofacial binding site and reorientation of the unloaded carrier. Therefore the K_m can be affected by the catalytic turnover of the transporter. In this study, measurement of K_m is used to assess the affinity of the exofacial binding site in each of the mutants relative to GLUT3. Since wild type transport levels were retained for all point mutants and no significant changes in K_m observed, it is unlikely that the catalytic turnover of the transporter has been affected. However, direct measurement of the turnover numbers for each mutant expressed in this system must be carried out in order to verify this (Chapter 5).

4.6.3 Effects of Pro-Ala Mutations Mediated at the Exofacial Binding Site.

As mentioned above, the K_m measured for 2-deoxy-D-glucose transport can be affected by the catalytic turnover of the transporter. However, the ability of maltose to inhibit 2-deoxy-D-glucose uptake can be used to further identify changes in the affinity of the mutants for substrate at the exofacial binding site. This is because maltose is a non-transportable sugar analogue, composed of two D-glucose molecules joined by an α -(1-4)-glycosidic linkage (Figure 4.2). It binds to the transporter in a D-glucose-like manner, forming similar hydrogen bonding patterns with the transporter (Figure 4.1). The rate constants that govern the binding of maltose to the transporter are not dependent on the movement of the loaded carrier to the endofacial conformation (k_2), dissociation of the substrate (K_{si}) or reorientation of the unloaded carrier (k_{-1}) (Figure 4.15). K_i values for

maltose inhibition of 2-deoxy-D-glucose influx therefore represent a true measure of events mediated at the exofacial binding site which is independent of transporter turnover number. It can also be considered as a measure of the affinity of the exofacial binding site for maltose.

Comparison of the K_i values determined for the Pro-Ala mutants with the wild type GLUT3 value has revealed some interesting changes in the phenotype of several of the mutants. Discussion of the data in terms of the putative tertiary arrangement of the helices has provided a further insight into the role of proline residues in transporter function.

Mutation of the first proline in the sequence, **P²⁰⁶ESP²⁰⁹(R)**, located at the base of transmembrane helix 6 at the start of the large intracellular loop, to alanine, resulted in a 2-3 fold reduction in the affinity of this transporter for maltose. Although the Pro²⁰⁹Ala mutation also resulted in a decrease in affinity, unlike Pro²⁰⁶Ala, this was not statistically significant. Two putative models for the tertiary arrangement of the transmembrane helices of GLUT1 have been proposed and are represented in Figure 1.7. A putative structural role for the large intracellular loop is proposed in model 2. It places helix 7 in close proximity to helices 1 and 2, on the far side of the protein relative to helix 6. Helix 7 contains the highly conserved sequence, **QQXS GXNXXXY**, and is predicted to move up in the membrane to accept exofacial ligands (Holman and Rees, 1987). Thus, it may be hypothesised that the **PESP(R)** motif at the start of the large intracellular loop plays a structural role in that it allows the upward movement of helix 7 in the membrane. Replacement of the proline residues in this sequence may have restricted this upward movement such that the groups that interact with maltose at the exofacial binding site are not sufficiently or correctly exposed, thus reducing the affinity. The upward movement of helix 7 in the membrane is based on the observation that the transporter becomes less susceptible to thermolysin cleavage at the base of this helix in the presence of exofacial ligands (Holman & Rees, 1987). If replacement of Pro²⁰⁶ (and to a lesser extent Pro²⁰⁹) with alanine has restricted this movement sufficiently, then it would be predicted that, in the presence of exofacial ligands, the protein may become more susceptible to thermolytic cleavage compared to wild type.

The fact that the reduced affinity at the exofacial binding site does not manifest itself in the K_m for 2-deoxy-D-glucose uptake can be rationalised in terms of the fact that this effect may be small in comparison to the other events that constitute transporter turnover.

The **PESP(R)** motif is paralleled by the sequence **VPET(K)**, located at the base of transmembrane helix 12, at the start of the C-terminal cytoplasmic tail. Interestingly, mutation of the proline residue within this motif, Pro⁴⁵¹Ala also resulted in a 2-3 fold decrease in the affinity for maltose at the exofacial binding site. The C-terminal cytoplasmic tail has been implicated as important for the correct formation of the exofacial binding site. Truncation analyses of GLUT1 have identified a minimum structural requirement of all but the last carboxy-terminal 24 amino acids for correct formation of the exofacial binding site. The current hypothesis for formation of the exofacial site is that the cytoplasmic tail packs against the base of helix 10, blocking the endofacial site. Helices 11 and 12 are predicted to move relative to helices 7, 8 and 9 by conformational flexing around the base of helix 10. Data obtained for the Pro⁴⁵¹Ala mutant suggests that the conserved **VPET(K)** sequence at the base of helix 12 may be involved in allowing the cytoplasmic tail to correctly pack against the base of helix 10, thus resulting in correct formation of the exofacial binding site.

Helix 12 is predicted to undergo positional changes during substrate translocation (See above). Analysis of the amino acid sequence of this helix reveals that it contains a high proportion of hydrophobic residues which appear to be clustered toward the endofacial end of the helix (Figure 4.16). In fact, this helix is the most hydrophobic helix in the transporter, with a hydrophobicity of 0.89 compared to 0.52 of helix 7 (Mueckler *et al.*, 1985). There are seven phenylalanine residues in this helix, compared to one to four found in other helices. Due to its high hydrophobic nature, it is unlikely that this segment moves up or down in the membrane. Instead, this helix could tilt in the membrane such that the cytoplasmic tail moves towards the base of helix 10 in the presence of exofacial ligands. The **VPET(K)** sequence contains strong helix-formers and thus would facilitate the movement of the base of helix 12 into or toward the membrane.

Pro-Ala substitutions at residues 381 and 383 within helix 10 also affected maltose binding, causing a 2-3 fold reduction in the affinity of the transporter for this ligand. The K_i value determined for Pro³⁸⁵Ala was not statistically different from wild type, suggesting that

this mutation did not significantly perturb exofacial ligand binding. Mutation of Pro³⁸⁵ in GLUT1 to isoleucine reduced transport activity and this was associated with reduced ATB-BMPA photolabelling (Tamori *et al.*, 1994). Replacement of this residue with glycine resulted in retainment of wild type transport levels but, interestingly, this mutant exhibited a 50% reduction in exofacial ligand photolabelling. It was concluded that this residue is important for the exofacial to endofacial conformational change. Perturbation of maltose binding caused by the Pro³⁸³Ala mutation in GLUT3 is consistent with this. This study also extends the hypothesis to include Pro³⁸¹. Although the mutation at Pro³⁸⁵ resulted in a slight decrease in the affinity of this transporter for maltose, it is concluded that this residue may not be as important as the prolines at positions 381 and 383. This may be explained in terms of the interaction of this proline with the immediate residues on either side. Pro³⁸¹ and Pro³⁸³ are flanked by glycine residues which are structurally important in proteins in that they allow unusual main chain conformations. It is postulated that they provide a non-hindered atomic environment for flexing around the prolines at positions 381 and 383, and that this is more restricted around position 385 due to the presence of the more bulky residues isoleucine and tryptophan which flank this residue.

4.6.4 Effects of Pro-Ala Mutations Mediated at the Endofacial Binding Site.

Measurement of K_i values for the inhibition of 2-deoxy-D-glucose transport by cytochalasin B are a reflection of the effects mediated at the endofacial binding site of the transporter. Individual mutation of all proline residues of helix 10 to alanine resulted in a 3-4 fold increase in the affinity for this ligand. These results are best considered in conjunction with the data obtained for the maltose inhibition studies, since measurement of K_i values for cytochalasin B inhibition of transport are performed under influx conditions in this study (see section 4.6.5). Tamori and co-workers have already suggested that Pro³⁸⁵ of GLUT1 plays an important role in allowing the exofacial to endofacial conformational change. Mutation of this residue to isoleucine stabilises the endofacial conformation such that retention of endofacial ligand photolabelling is associated with a corresponding decrease in

the level of exofacial ligand photolabelling. Data obtained for this residue of GLUT3, Pro³⁸³, is in good agreement for this role, since retainment of cytochalasin B inhibition of 2-deoxy-D-glucose influx was associated with a decrease in the affinity of the transporter for maltose. This observation can also be extended to include Pro³⁸¹. A role for this residue was not previously detected in the GLUT1 studies, as affinities at the substrate binding sites were not investigated. The reduction in the Pro³⁸⁵ K_i value for cytochalasin B was not associated with a significant effect at the exofacial binding site, as was the case for Pro³⁸¹ and Pro³⁸³ (see above). It may be that this residue is not as important for allowing the correct formation of the exofacial binding site through conformational flexing in this region, as it is predicted to lie in a more hindered atomic environment. The increase in affinity for cytochalasin B exhibited by all helix 10 mutants may be related to the close proximity of Trp³⁸⁶ (Figure 4.17). This residue of GLUT1 (Trp³⁸⁸), maybe a site of covalent attachment upon UV irradiation and therefore a possible site of contact for cytochalasin B. It is possible that mutation of any of the three prolines to alanine causes local structural alterations such that the tryptophan becomes more accessible for interaction with the ligand, thus resulting in an increase in affinity. Interestingly, the Pro³⁸⁵Gly mutation in GLUT1 exhibited increased levels of cytochalasin B photolabelling ($146 \pm 13.6\%$ of wild type levels).

Mutation of proline residues at the base of helices 6 and 12 had no significant effect on the ability of the transporter to bind endofacial ligands. This would be consistent with the suggestion that these residues are more important for determining the correct formation of the exofacial binding site through structural changes involving helix 7 and the cytoplasmic tail respectively. No perturbation of endofacial ligand binding would be predicted since this region involves the base of helices 10 and 11.

4.6.5 Problems with this Study.

This study has been successful in that it has provided further evidence for a functional role for proline residues in transport catalysis mediated by the facilitative glucose transporter isoforms. Molecular modelling and mutagenic studies have implicated a role for prolines in transport catalysis mediated by GLUT1, however, an extensive kinetic

characterisation of the mutants generated was not undertaken and so it was not possible to speculate on a more defined role for these residues. In this study, although individual mutation of several proline residues in GLUT3 to alanine did not alter the K_m for 2-deoxy-D-glucose transport, a more subtle role for these residues could be implicated on the basis of small but significant alterations in the affinity of the transporter for ligands at the exofacial binding site. Measurement of K_i values for maltose inhibition of substrate influx are a direct representation of effects mediated at the exofacial substrate binding site, since maltose and D-glucose are assumed to compete for the same site under these conditions. Direct measurements of any effects mediated at the endofacial binding site are more difficult to measure under zero-*trans* influx conditions of 2-deoxy-D-glucose transport since the nature of inhibition is non-competitive (unlike maltose inhibition which is competitive). Ideally, to obtain this information, measurement of K_i values for inhibition of transport should be performed under zero-*trans* efflux conditions such that the inhibitor and the substrate compete at the same side of the transporter. However, there are several problems associated with performing such experiments in oocytes. Firstly, the substrate must be capable of being transported out of the cell and therefore, 3-*O*-methyl-D-glucose would need to be used instead of 2-deoxy-D-glucose. This substrate is not ideal as it can be transported back into the oocyte and so, the time period within which the rate of sugar efflux remains linear, i.e. before sugar influx occurs, is of the order of a few minutes (~3 mins). A further complication in this regard is the fact that the oocytes would need to be pre-loaded with radiolabelled tracer. The extracellular medium is then rapidly removed and replaced with sugar-free medium and the initial rates of sugar exit are measured by testing the amount of radioactivity in the external medium. The high dilution factor of the radiolabel on the external medium and the short time period over which transport rates would need to be measured increase the error margin substantially.

Secondly, in order to fully characterise the mutants generated in this and other studies, it is necessary to determine the turnover number of the transporters. This is an important parameter which would more precisely define the effects of a particular mutation on the function of the transporter. Since the turnover number is dependent on the number of transporters at the cell surface, and because this will vary between oocyte preparations from

different animals, determination of this parameter requires an accurate and reproducible method for isolating plasma membranes from oocytes. However, as discussed in detail in Chapter 5, problems associated with obtaining a pure and reproducible plasma membrane fraction from oocytes precluded the measurement of turnover numbers in this study.

In addition, more general problems have been encountered whilst using the *Xenopus* oocyte system for heterologous expression. Seasonal variation of oocyte batches, animal housing problems and infection have impeded characterisation of the GLUT3 mutants in terms of photolabelling and more extensive inhibition studies. Subcloning and expression of these constructs in an alternative expression system, where the membrane fractionation procedures are simpler and more reproducible, will not only allow measurement of turnover numbers but also enable more detailed inhibition studies to be performed (Chapter 7).

Figure 4.15

King-Altman Diagram Showing the Competition of 2-Deoxy-D-Glucose and Maltose at the Exofacial Binding Site of the Transporter.

The model proposed in this diagram is based on kinetic data which has been established for GLUT1, although it is generally believed that this model also applies to the other GLUT isoforms. The diagram describes the cycling of the transporter from an exofacial conformation, T_o , to an endofacial conformation, T_i , and back again in the presence and absence ($\pm S$) of deGlc. K_{so} and K_{si} represent the dissociation constants at the exofacial and endofacial sites respectively, and k_1 , k_2 , k_{-1} and k_{-2} describe the rate constants of the steps indicated. This schematic also describes the competition between deGlc and maltose at the exofacial binding site. Maltose binds to the exofacial binding site (T_o) but is not transported to the other side of the membrane. Therefore the rate constants that govern this event are not dependent on the movement of the loaded carrier to the inward-facing conformation (k_2), dissociation of the sugar (K_{si}), or reorientation of the empty carrier (k_{-1}). The kinetics of deGlc transport are dependent on all these steps. Thus, while the interaction of deGlc at the exofacial substrate binding site is influenced by other steps in the transport cycle, the interaction of maltose is dependent only on the rate of association and dissociation of this sugar at the exofacial site. Hence, measurement of the ability of maltose to inhibit deGlc transport (K_i), is independent of the turnover number of the transporter.

Figure 4.15

King-Altman Diagram Showing the Competition of 2-Deoxy-D-Glucose and Maltose at the Exofacial Binding Site of the Transporter.

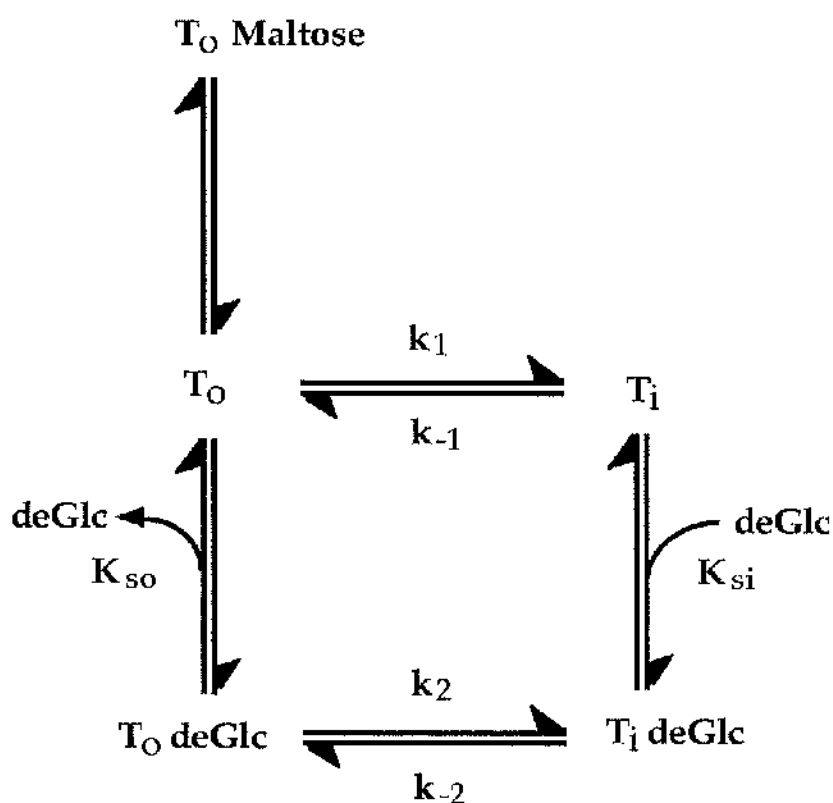


Figure 4.16

Predicted α -Helical Structure of GLUT3 Transmembrane Helix 12.

This shows the predicted secondary structure of GLUT3 putative transmembrane helix 12. The helix is viewed from the endofacial to exofacial direction with the amino acid sequence beginning at Gly⁴²⁸ at the "top" of the helix (numbered 1). The positions of the following residues rotate in a clockwise direction until residue, Phe⁴⁴⁸ is reached at the "bottom" of the helix (numbered 21). The diagram highlights the highly hydrophobic nature of this helix, due to a high proportion of phenylalanine residues.

Figure 4.16

Predicted α -Helical Structure of GLUT3 Transmembrane Helix 12.

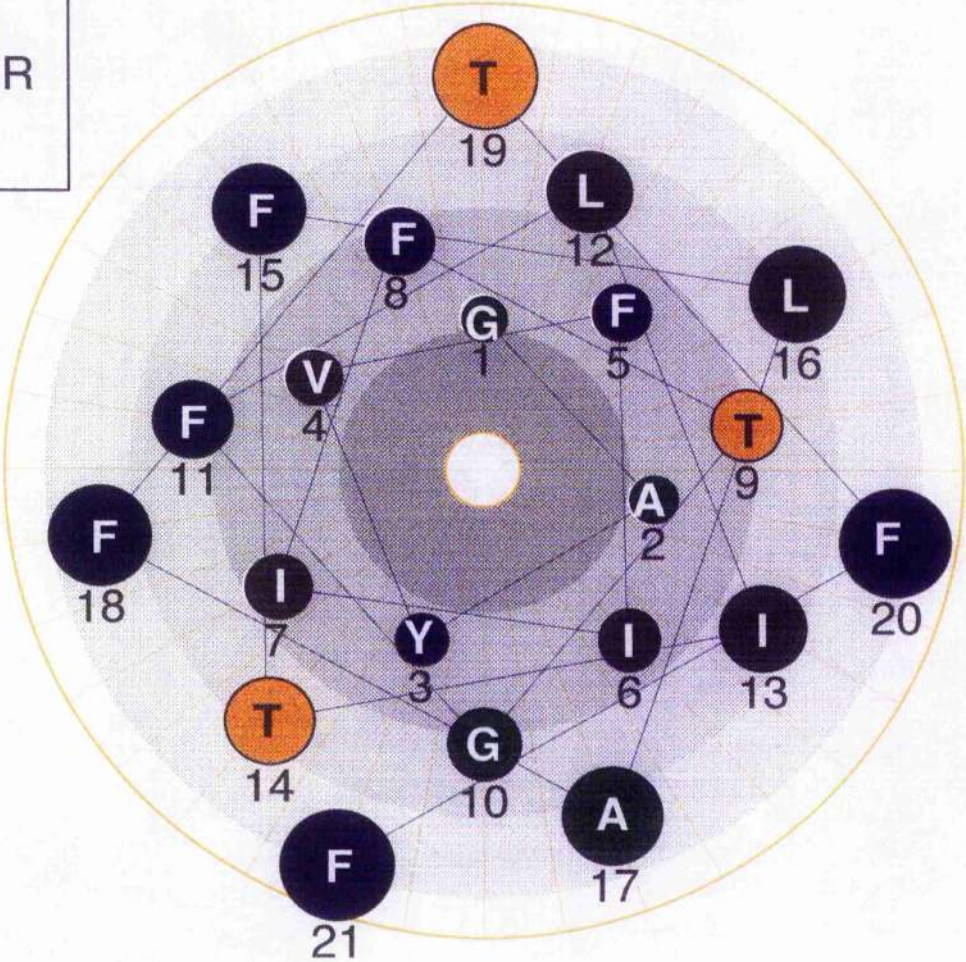
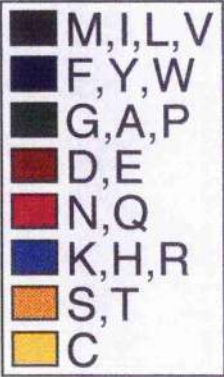


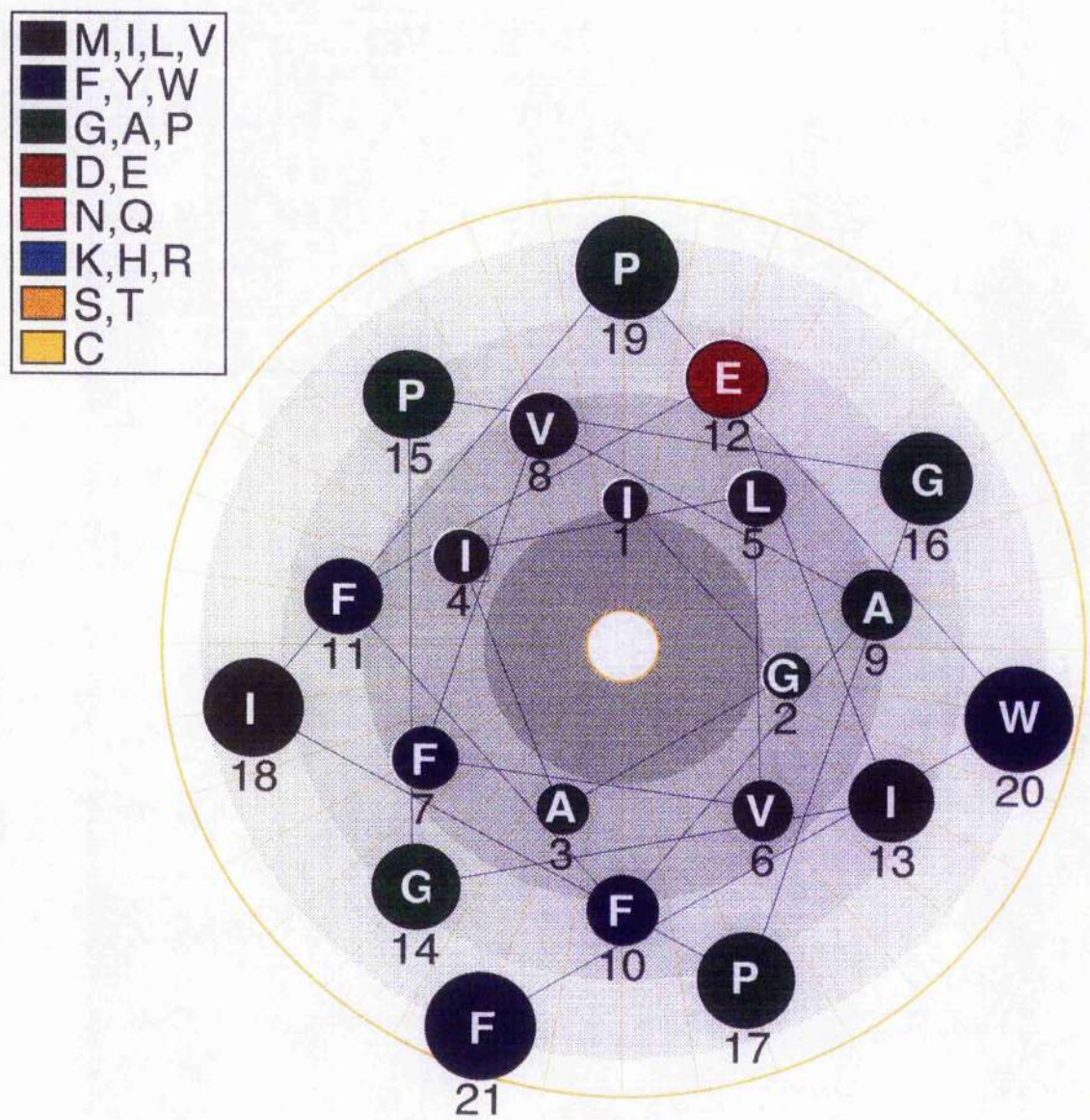
Figure 4.17

Predicted α -Helical Structure of GLUT3 Transmembrane Helix 10.

The predicted secondary structure of the putative transmembrane helix 10 of GLUT3 is shown. The helix is viewed from the endofacial end up through the helix such that the first residue, Ile³⁶⁸ (numbered 1) is at the "top" of the helix. The following residues rotate in a clockwise direction until Phe³⁸⁷ (numbered 21) is reached at the bottom of the helix. The diagram shows the relative orientation of the highly conserved **GP GPIP** motif and also the position of the single charged residue Glu³⁷⁹ which may be buried in a hydrophobic pocket.

Figure 4.17

Predicted α -Helical Structure of GLUT3 Transmembrane Helix 10.



4.7 Summary.

A collective role for proline residues in the global structure and function of GLUT3 is not yet clear in the absence of high resolution structural information. However, their selective inclusion within transmembrane domains together with a high degree of conservation of proline-containing sequences, suggests some important functionality. Based on the data obtained from other membrane proteins, e.g. bacteriorhodopsin and rhodopsin, and from the use of mutagenesis and molecular dynamics studies, proline residues have been implicated in providing conformational flexibility through their ability to cause kinks and by the *cis-trans* isomerisation of Xaa-Pro peptide bonds. Modelling studies have predicted that transmembrane helices are capable of accommodating *cis*-Pro and thus, the isomerisation events within helices can cause local structural changes without grossly affecting the overall propagation of the main chain. Such properties are consistent with a role for proline residues in the functionality of membrane proteins.

To date, several prolines of GLUT1 have been investigated by site-directed mutagenesis. The Pro-Gly rich region of helix 10 has been implicated in the conformational flexibility requisite for the alternate and subsequent exposure of substrate to either side of the transporter. These conclusions are based upon individual replacement of prolines with residues that either abolish or significantly reduce transport catalysis. However, in the light of other mutagenic studies, it should be remembered that protein inactivation by mutation does not distinguish between a structural or dynamic role for these residues. Additionally, it has been demonstrated that individual replacement of certain proline residues to alanine may not cause any detectable change in protein activity, probably due to the compensatory effects of other prolines. However, subtle structural perturbations may have gone undetected in these studies in the absence of more detailed kinetic analysis of the Pro-Ala mutants. It is possible that effects caused by these mutations are small in comparison to the overall turnover of the transporter.

A thorough kinetic analysis was undertaken in this study to investigate the role of conserved proline residues in the function of GLUT3. The data corroborates the finding that no individual proline is essential for transport catalysis. However, on the basis that small but

significant alterations in the nature of ligand binding at the exofacial binding site were observed, prolines are important for transporter function. In some cases, a reduction in exofacial ligand binding affinity was associated with an increased affinity for ligands at the endofacial site. Proline residues of helix 10 are suggested to contribute to the flexibility requisite for conformational changes. The **PESP(R)** motif at the base of helix 6 and the **VPET(K)** motif at the base of helix 12 may be important for allowing the structural changes required for correct formation of the exofacial substrate binding site.

CHAPTER 5

Isolation of Plasma Membrane Fractions from *Xenopus* Oocytes.

5.1 Aims.

- 1.** To devise a reliable and reproducible protocol for the isolation of a plasma membrane fraction from GLUT3-injected oocytes. The method should provide a clean fraction of plasma membranes, free from contaminating yolk protein and internal membranes.
- 2.** To determine the number of GLUT3 transporters expressed at the plasma membrane surface by quantitative Western blotting against GLUT3 standards.
- 3.** To use this system to measure turnover numbers for GLUT3 and each of the Pro-Ala mutants previously generated.

5.2 Introduction.

5.2.1 Use of *Xenopus* Oocytes for Kinetic Studies.

Xenopus oocytes have proved to be a useful and efficient system for the heterologous expression of mammalian facilitative glucose transporters (section 4.3). All of the human GLUT isoforms have been expressed in oocytes, and some of their kinetic properties accurately determined. This has proved difficult in their native cell environments, since there is often more than one glucose transporter isoform expressed in any given cell, and also due to the rapid equilibration of the cell water space which further complicates the analysis. Thus, it is difficult to know whether the measured kinetic parameters are truly representative of the heterologously expressed transporter unless k_{cat} values are also determined. In addition, a transporter heterologously expressed in CHO-cells for example, would need to be present at high enough levels to produce a substantial-fold increase in transport activity over endogenous levels of transport to enable accurate determination of kinetic parameters. The main advantage of the oocyte system over the native cell type is the low endogenous levels of transport. Oocytes also provide a useful system in which to explore the properties of mutant proteins and to determine the functional consequences of these mutations.

5.2.2 Measurement of Turnover Numbers.

In the experiments described in Chapter 4 of this thesis, measurement of K_m values for zero-*trans* uptake of substrate into oocytes represents a value that is essentially a reflection of the affinity of the transporter for this substrate at the exofacial binding site. As 2-deoxy-D-glucose is not transported back out of the oocyte, the interaction of the substrate at the endofacial site is assumed to be negligible. However, the K_m of 2-deoxy-D-glucose is a function not only of substrate association and dissociation events at the exofacial and endofacial sites, but also re-orientation of the transporter between the two conformational states. The K_m value can therefore be influenced by the catalytic turnover of the transporter

(i.e. the rate of transporter re-orientation). Since measurement of K_m and K_i values were used as a method of comparing the affinity at the exofacial binding site of the mutant transporters for substrate and ligand, the next stage in the kinetic analysis would be to determine the effects of the mutation on the catalytic turnover of the transporter proteins.

By analogy with enzyme systems, the steady-state flux is characterised in terms of K_m (the half saturation constant, which is a measure of the apparent affinity of the transport system for substrate) and V_{max} (the capacity for translocation when the transport system is saturated with glucose). V_{max} , which is dependent on the amount of transporter expressed at the plasma membrane of the oocyte, is given by:

$$V_{max} = k_{cat} [GT]$$

where $[GT]$ is the concentration of glucose transporters at the plasma membrane and k_{cat} is the number of times the transporter turns over per unit time. Therefore, unlike K_m values, the V_{max} will vary between oocyte preparations from different animals. As a result, use of this expression system is useless for determination of turnover numbers unless a reliable and reproducible method is available for quantitation of glucose transporters expressed at the plasma membrane.

For any vesicle, the first-order rate constant for equilibration (k_{obs}) at a substrate concentration below the K_m is given by:

$$k_{obs} = k (T)_t / K_m V_i$$

where k is the turnover number for equilibrium exchange, $(T)_t$ is the moles of transporter per vesicle, K_m is the half-saturation constant for equilibrium exchange, and V_i is the internal volume of the vesicle. All of these parameters are measurable in oocytes, with the exception of $(T)_t$ which requires a method for isolation of a purified plasma membrane fraction and a method for quantitating the number of transporters (e.g. immunoblotting against membrane fractions containing known amounts of transporter).

The main aim of this chapter is therefore to describe a method for the isolation of purified plasma membrane fractions from oocytes expressing GLUT3. This methodology should then prove useful in the further characterisation of the glucose transporter mutants generated in this study and others.

5.3 Subcellular Fractionation of *Xenopus* Oocytes.

There have been many published papers that describe methods for the isolation of plasma membrane fractions from oocytes. Most of these protocols have involved either manual dissection of plasma membrane "ghosts", produced by squeezing individual oocytes to expel the yolk and cellular contents into the incubation buffer, or the use of homogenisation and centrifugation procedures. Manual dissection of oocytes is a demanding and time-consuming task, and the homogenisation methods previously described have resulted in extensive fragmentation of the fragile plasma membrane sheets. A second major problem is that oocytes contain a large amount of intracellular yolk protein, comprising about 80% of the total cellular protein. As yolk protein is very glutinous, it is difficult to obtain plasma membrane fractions that are free from contaminating yolk protein and other intracellular components. This, coupled with the extremely fragile nature of the plasma membranes, has led to low and variable yields.

The development of a relatively simple procedure for the preparation of large plasma membrane complexes from oocytes was reported by Wall and Patel in 1989. The absence of any centrifugation steps and minimal homogenisation conditions resulted in little fragmentation. Good yields and enrichment of plasma membrane marker enzymes were reported (Wall & Patel, 1989). No individual dissection and rinsing procedures were required and the protocol was reported to be suitable for use with small numbers of cells as well as for large preparative procedures. This method formed the basis of the fractionation procedure used in this study.

5.4 Methods.

5.4.1 Cell Surface Labelling of Oocytes by Biotinylation.

Intact oocytes were incubated in the presence of either sulfo-NHS-biotin or NHS-LC-biotin (section 2.8.3b and 2.8.4b). Both reagents are analogues of NHS-biotin which reacts with primary amines (generally lysine groups) to form amide bonds. The reaction occurs via a nucleophilic attack of an amine towards the NHS ester (Figure 5.1), resulting in formation of a stable amide bond and the release of N-hydroxysuccinimide as a by-product. Incubation of oocytes in the presence of these reagents at 4°C results in cell surface labelling. Excess biotin is removed by the addition of a solution of L-lysine which quenches the biotin. Labelled oocytes were then rinsed in homogenisation buffer containing protease inhibitors (Table 2.2) and subjected to subcellular fractionation procedures (section 2.8.3 and 2.8.4). Levels of expressed GLUT3 were then quantitated by either dot blot analysis or Western immunoblotting.

5.4.2 Subcellular Fractionation Procedures.

Two methods are described for the isolation of plasma membrane complexes from oocytes, both of which are based on the method of Wall and Patel, 1989 with some minor modifications. Biotinylated oocytes (typically 100), were disrupted either by gentle homogenisation in a Dounce homogeniser (no more than 6-7 strokes) or using a P200 Gilson pipette (section 2.8.3c and 2.8.4c). The crude homogenate was allowed to settle by gravity for 10-30 mins, and the initial supernatant was removed which consisted mainly of yolk granules. Plasma membrane complexes were then subjected to a series of washes with gentle disruption using a pasteur pipette when necessary. Supernatants obtained after each wash were removed, pooled and subjected to centrifugation (1000 x g_{av}) to collect residual yolk protein. Three fractions were obtained, referred to as the Y (yolk), PM (plasma membrane) and S (supernatant) fractions. The protein concentration of each fraction was

determined by the Lowry microassay (section 2.8.3d) or the BCA Quantigold assay (section 2.8.4d).

5.4.3 Dot Blot Analysis.

After subcellular fractionation of the oocytes, equal amounts of protein from each fraction were transferred onto nitrocellulose membranes (section 2.8.4e). After blocking of non-specific sites, the nitrocellulose membranes were incubated with ^{125}I -streptavidin. Labelled membranes were then prepared for autoradiography and the amount of ^{125}I -streptavidin associated with each membrane fraction determined by γ -counting.

5.4.4 Quantitative Immunoblotting.

In addition to the dot blot analysis described above, oocyte fractions were also analysed by SDS PAGE and Western blotting (section 2.17.1-2.17.2). Plasma membrane standards obtained from cells engineered to stably express a known amount of GLUT3 protein were used for comparison purposes (Maher *et al.*, 1992). A rabbit polyclonal antiserum (1 in 250 dilution) raised against a synthetic peptide corresponding to the C-terminal 14 amino acids of human GLUT3 (Brant *et al.*, 1993) and ^{125}I -labelled goat anti-rabbit IgG were used for detection by autoradiography. Alternatively ECL methodology was used.

5.4.5 Plasma Membrane Marker Assay.

Each fraction was assayed for the plasma membrane marker enzyme 5'nucleotidase (section 2.8.5b). This enzyme activity was used to estimate the relative enrichment of plasma membranes obtained compared to the Y and S fractions. Oocyte fractions were incubated in the presence of the substrates, $[^3\text{H}]5'$ -AMP and $2',3'$ -AMP, and the rate of production of the product, adenosine, with time was determined by liquid scintillation spectrometry.

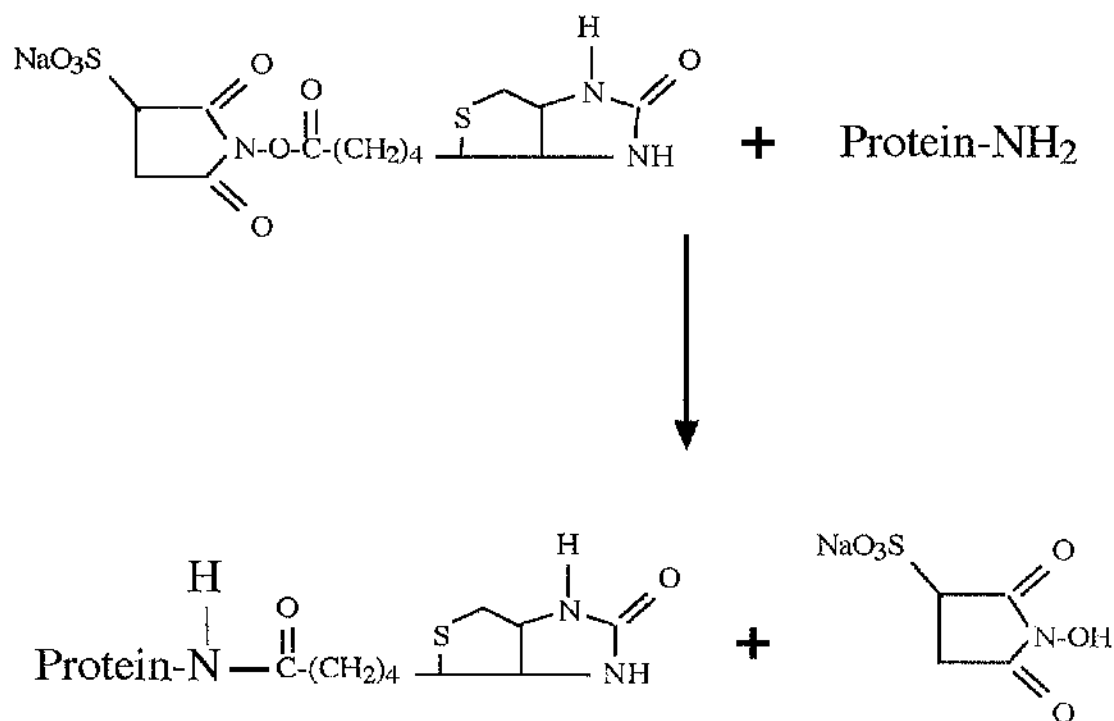
Figure 5.1

Reaction of NHS-Biotin and Sulfo-NHS-Biotin with Protein Amines.

N-hydroxysuccinimide esters react with primary amines to form amide bonds. The reaction occurs via a nucleophilic attack of an amine (generally lysine groups) towards the NHS ester, resulting in the formation of a stable amide bond and the release of N-hydroxysuccinimide as a by-product. In the experiments described here, biotin analogues are used to label the surface of intact oocytes which can be quantitated following subsequent fractionation procedures by reaction with ^{125}I -streptavidin.

Figure 5.1

Reaction of NHS-Biotin and Sulfo-NHS-Biotin with Protein Amines.



5.5 Results.

5.5.1 2-Deoxy-D-Glucose Zero-trans Influx Mediated by GLUT3 Expressing Oocytes.

Oocytes were isolated and injected with 50nl of 1mg/ml GLUT3 mRNA (section 2.6.4). After incubation for 48 hours at 18-20°C, groups of 10 injected and 5 non-injected oocytes were assayed for zero-trans uptake of 2-deoxy-D-glucose as described (section 2.7). Transport rates mediated by GLUT3 injected oocytes were typically between 2-5 pmols/min/oocyte, compared to between 0.2-0.7 pmols/min/oocyte for non-injected controls. Only oocytes exhibiting transport rates within or above this range expressed GLUT3 at sufficient levels and were subjected to subcellular fractionation procedures.

5.5.2 Surface Labelling and Fractionation of Oocytes.

Two biotin analogues were used for labelling of intact oocytes. Initially NHS-LC-biotin was used however since this analogue was not water soluble it was dissolved in the organic solvent, DMSO, before addition to the oocytes. To avoid any possible adverse effects caused by the DMSO during the following fractionation procedure, an alternative compound, sulfo-NHS-biotin, was subsequently used. This analogue was easily dissolved in aqueous buffers and therefore avoided the use of DMSO.

Biotinylated oocytes prepared as previously described, were then subjected to subcellular fractionation procedures. Initially, groups of 100 oocytes were gently disrupted with the use of a Dounce homogeniser and loose fitting pestle. The number of strokes required to disrupt the oocytes varied between oocyte preparations from different animals. Care was taken not to over-homogenise the oocytes, as this was found to cause extensive fragmentation of plasma membranes leading to decreased yields at the end of the procedure. The initial homogenate was allowed to settle by gravity, thus avoiding any centrifugation steps which also causes fragmentation. The large plasma membrane sheets settled to the bottom of the tube, with much of the yolk protein remaining in the initial supernatant. Any

remaining yolk protein, pigment granules and other intracellular contaminants were removed from the plasma membrane sheets by a series of washes, with gentle agitation using a glass pasteur pipette. All rinsing procedures were performed in the same tube, rather than transferring the plasma membrane sheets to a clean tube after each rinse, since the plasma membrane fractions adhered tightly to the sides of the tube resulting in the progressive loss of material. The same pipette was used throughout the procedure for the same reason. Again, the number of rinses required to remove contaminants varied between oocytes obtained from different animals. This procedure yielded three fractions, PM (containing enriched plasma membranes), Y (yolk protein and pigment granules), and S (intracellular components).

A second method used for oocyte fractionation was described (section 2.8.4) and was similar in many aspects. The major difference was the method used to initially disrupt the oocytes. The homogenisation procedure was often found to be too harsh resulting in very low recovery of plasma membranes, particularly when the oocytes were fragile. An alternative method was to use a P200 Gilson pipette fitted with a pipette tip cut to a suitable diameter such that passage of oocytes through the tip resulted in their disruption. Typically, 100 oocytes were disrupted in this way. Yolk and other intracellular contaminants were removed from the plasma membrane complexes by a series of washes, with gentle disruption using the same pipette when necessary. After each wash, the supernatant was removed and subjected to a slow speed centrifugation step ($1000 \times g$ for 5 mins), to collect residual yolk which was pooled. Each resulting supernatant was pooled and all fractions were pelleted at the end of the procedure to obtain three fractions PM, Y and S.

The protein concentration of each fraction was determined (Table 5.1). The Lowry protein microassay was used initially, but, due to the low amounts of protein recovered in the S and PM fractions, the more sensitive Quantigold protein assay was subsequently used, which was capable of detecting protein within the range of 5-200ng. The amount of protein recovered in the PM fraction varied considerably between oocyte preparations, with an average of $4.0 \pm 3.6 \mu\text{g}$ protein per oocyte ($n=6$).

5.5.3 Activity of Plasma Membrane 5'Nucleotidase in *Xenopus* Oocyte Fractions.

The amount of 5'nucleotidase activity was determined for each oocyte fraction, and the results of a typical assay are shown in Figure 5.2. The protein concentration used in the assay was adjusted such that the rate of adenosine release was linear with time. Comparison of these enzymic activities with those obtained for intact oocytes indicated average yields of 64% of the cell surface activity of this plasma membrane marker in the PM fraction, corresponding to a 20-fold enrichment. However, the PM fraction contained at least 80% of the total 5'nucleotidase activity recovered when activities were compared with total homogenate levels shown in Figure 5.3. This suggests some loss of activity during the fractionation procedure.

5.5.4 ¹²⁵I-Dot Blot Analysis of Oocyte Fractions.

The recovery of biotinylated plasma membranes was assessed by determining the level of ¹²⁵I-streptavidin associated with each fraction (Figure 5.4). The average results from five separate experiments are shown in Figure 5.5. Typically, only 30% of the total radioactivity was associated with the PM fraction and this value varied between oocyte preparations (Table 5.2). The level of radioactivity associated with the S and Y fractions was attributed either to non-specific binding, or to extensive fragmentation of the PM during the fractionation procedure, resulting in contamination of the other fractions with biotin.

5.5.5 Western Blot Analysis of Oocyte Fractions.

In an attempt to quantify the amount of GLUT3 protein in each fraction, equal amounts of protein were subjected to SDS PAGE alongside GLUT3 standard membranes. Proteins were transferred electrophoretically onto nitrocellulose membranes which were probed with polyclonal antiserum raised by immunising a rabbit with a synthetic peptide corresponding to the C-terminal 14 amino acid residues of GLUT3 (Shepherd, 1992a). A

representative immunoblot is shown in Figure 5.6. The GLUT3 protein was detected as a broad band migrating at an apparent molecular weight of approximately 40kDa. This band was not detected in non-injected control oocytes, but was present in all of the prepared oocyte fractions. In addition, two sharp bands of higher molecular weight which were not detected in the oocyte fractions but were present in the total membrane fraction of both injected and non-injected oocytes are likely to be associated with the yolk.

Unfortunately, an accurate quantitative determination of the GLUT3 protein associated with each fraction was not possible from any of the immunoblots obtained. This was due either to low levels of protein being resolved which were beyond the limits of detection of the antibody used, or to poor resolution of the GLUT3 standards making it difficult to draw conclusions from the immunoblots.

Table 5.1**Protein Yields of Oocyte Fractions.**

Oocyte Fraction	Protein Concentration * (mg/ml)	Protein Yield (μ g/oocyte)
PM	1.56 \pm 0.98	4.0 \pm 3.6
Y	20 \pm 12	163 \pm 102
S	7.4 \pm 5.6	26 \pm 22

* determined by Lowry protein microassay or Quantigold protein assay.

Figure 5.2

Measurement of the 5'Nucleotidase Activity of Oocyte Fractions.

An aliquot of the subcellular fractions prepared from 100 oocytes were incubated in the presence of 5mM 2',3'-AMP and 0.2mM [^3H]5'-AMP (1 $\mu\text{Ci/ml}$). At various time points (0-30 mins) duplicate samples were removed and added to 0.25M ZnSO_4 , followed by the addition of BaCl_2 . This serves to precipitate the phosphate produced during the reaction. The amount of radioactivity associated with the supernatants from these samples was determined by liquid scintillation spectrometry. The protein concentration was adjusted such that the rate of adenosine release was linear with time. A total oocyte fraction was prepared by extensive homogenisation of 20 oocytes and was assayed for 5'nucleotidase activity in the same way.

Figure 5.2

Measurement of the 5'Nucleotidase Activity of Oocyte Fractions.

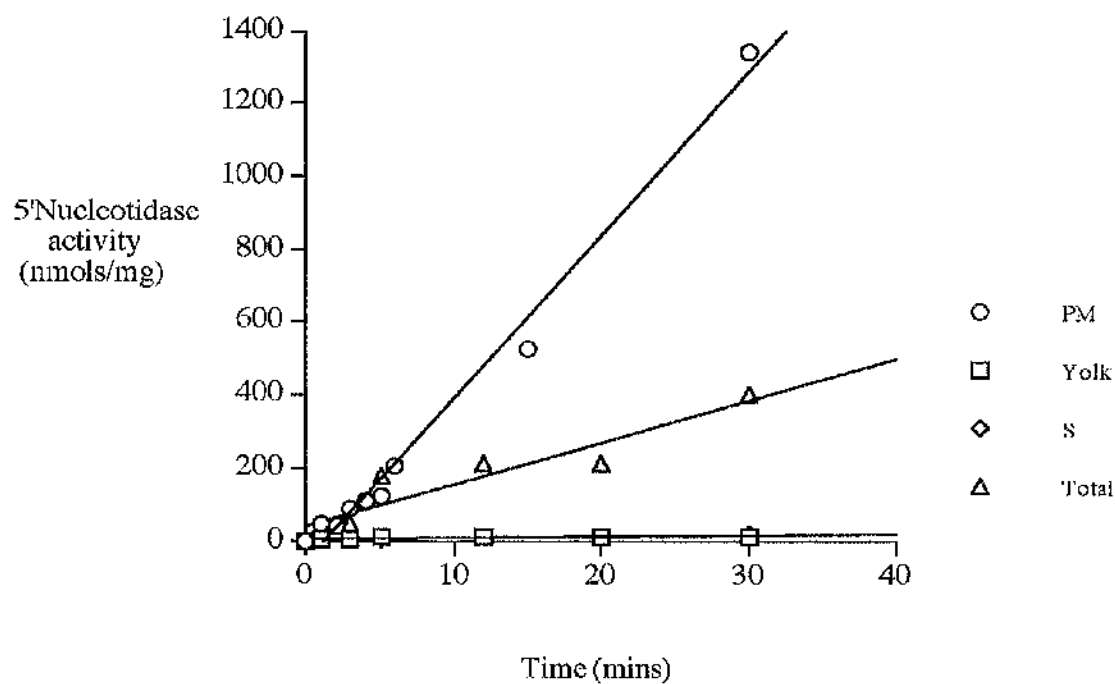


Figure 5.3

5'Nucleotidase Activities in Oocyte Membrane Fractions.

5'Nucleotidase activities were measured for oocyte fractions as described. Activities are expressed as a percentage of the total activity recovered and represent the mean (\pm S.D.) of six determinations from oocyte fractions obtained from different animals.

Figure 5.3

5'Nucleotidase Activities in Oocyte Membrane Fractions.

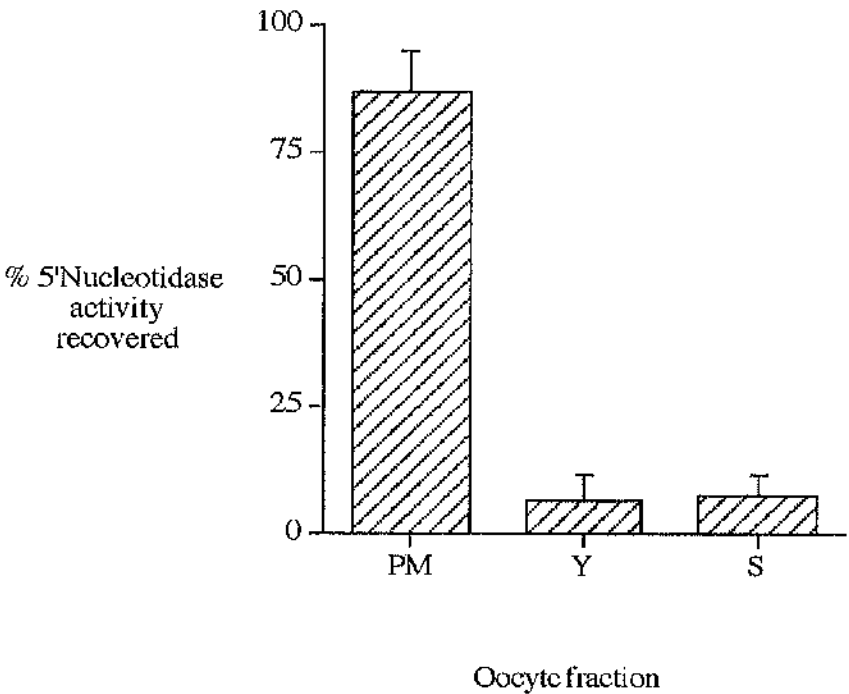


Figure 5.4

Specific Recovery of ^{125}I -Streptavidin Associated With Oocyte Fractions.

Intact oocytes were labelled with NHS-biotin and subsequently fractionated to obtain a purified plasma membrane fraction. Oocyte fractions were subjected to dot blot analysis and the recovery of the biotinylated plasma membranes was assessed by determining the level of ^{125}I -streptavidin associated with each fraction. This graph shows the results obtained from a typical experiment in which the ^{125}I -label associated with the plasma membrane fraction was enriched approximately 21-fold compared to that associated with the total oocyte sample.

Figure 5.4

Specific Recovery of ^{125}I -Streptavidin Associated With Oocyte Fractions.

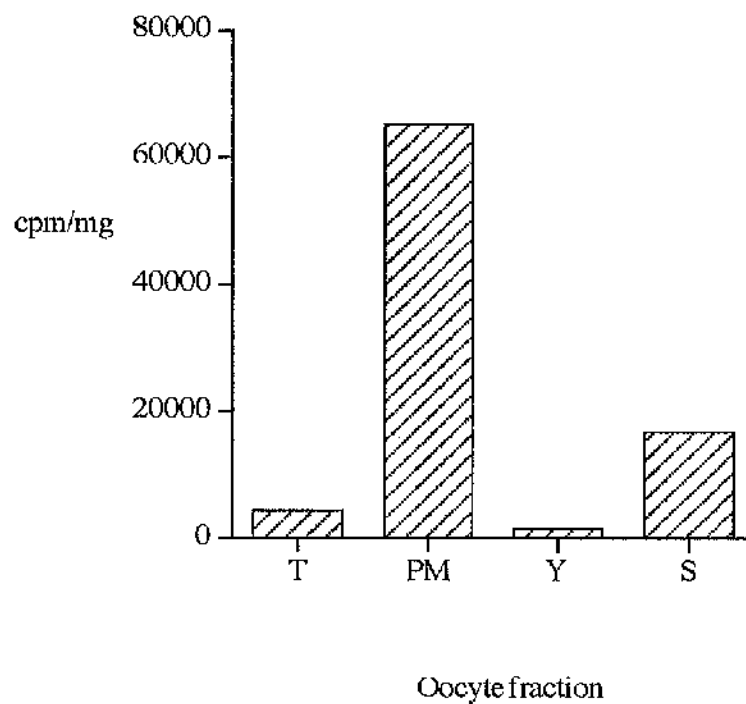


Figure 5.5

Recovery of ^{125}I -labelled Biotinylated Plasma Membranes from Oocytes.

Intact oocytes were labelled with NHS-biotin and subsequently fractionated to obtain a purified plasma membrane fraction. Oocyte fractions were subjected to dot blot analysis and the recovery of the biotinylated plasma membranes was assessed by determining the level of ^{125}I -streptavidin associated with each fraction. Results represent the mean (\pm S.D.) of five separate experiments using oocytes obtained from different animals.

Figure 5.5

Recovery of ^{125}I -labelled Biotinylated Plasma Membranes from Oocytes.

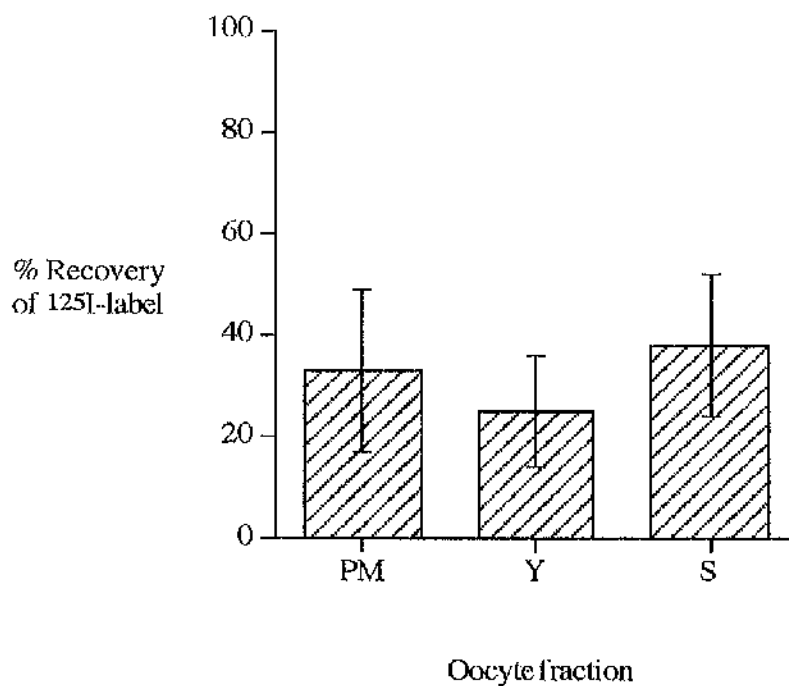


Table 5.2**Data obtained from a Typical Dot Blot Analysis.**

Oocyte Fraction	Total Protein (mg)*	Associated 125I-label (% cpm)	cpm	cpm/mg protein
PM	0.42	41%	27352	65124
Y	14.74	29%	18834	1278
S	1.2	30%	19838	16532
Total	16.36	100%	66024	4036

*determined by the Lowry protein microassay or the Quantigold protein assay.

Figure 5.6

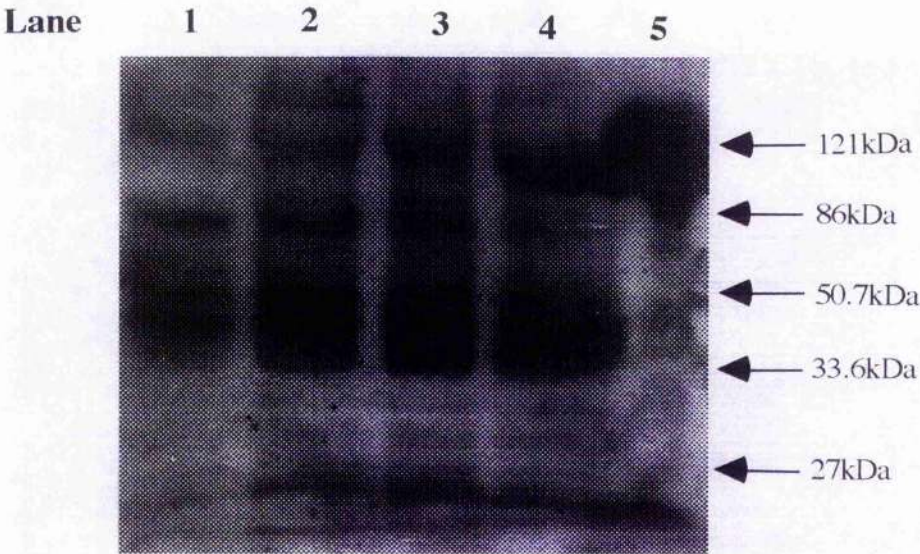
Western Blot Analysis of Oocyte Fractions Expressing GLUT3.

Oocytes expressing GLUT3 were subjected to subcellular fractionation. Total membrane fractions were prepared from GLUT3 expressing and non-injected oocytes. 30 μ g of each fraction was subjected to electrophoresis on 10% polyacrylamide gels and proteins were transferred to nitrocellulose membranes which were probed with a rabbit polyclonal antiserum (1 in 250 dilution) raised against a synthetic peptide corresponding to the C-terminal 14 amino acids of human GLUT3. ¹²⁵I-labelled goat anti-rabbit IgG (1 μ Ci/20ml) was used for detection by autoradiography. The GLUT3 protein is identified as a broad band migrating at an apparent molecular weight of approximately 40kDa.

Lane 1, total membranes prepared from non-injected oocytes; Lane 2, total membranes prepared from GLUT3-injected oocytes; Lane 3, Sinitial fraction prepared from GLUT3-injected oocytes; Lane 4, PM fraction prepared from GLUT3-injected oocytes; Lane 5, wash fraction prepared from GLUT3-injected oocytes. Positions of molecular weight markers are indicated to the right of the immunoblot.

Figure 5.6

Western Blot Analysis of Oocyte Fractions Expressing GLUT3.



5.6 Discussion.

The absence of a reliable method for the isolation of a pure plasma membrane fraction from *Xenopus* oocytes has precluded a more complete kinetic characterisation of wild type and mutant GLUT isoforms in this expression system. Transporter protein expression at the plasma membrane varies with different batches of cells, time after mRNA injection and also with the type of transporter introduced. Measurement of K_i and K_m values for transport of a substrate under the conditions described in this thesis are not dependent on the amount of transporter expressed at the plasma membrane surface. The oocyte system is therefore an ideal system in which to measure these parameters, which yield information regarding effects mediated at the substrate binding sites. However, in addition to measurement of K_m values, the transport process is also characterised by the V_{max} value which is related to the catalytic turnover over of the protein. V_{max} is dependent on the concentration of functional glucose transporters expressed at the plasma membrane and thus, varies between oocyte batches obtained from different animals. Therefore, in order to measure such parameters, it is necessary to have a method for estimating the actual amount of transporter expressed at the plasma membrane surface. This is further complicated by the fact that the oocyte plasma membrane contains only a small fraction of the total transporters synthesised from injected mRNA. Previous studies have reported that between 4-12% of GLUT1 is expressed at the cell surface in oocytes (Due *et al.*, 1995; Garcia *et al.*, 1992; Nishimura, 1993). Thus, any contamination of the plasma membrane fraction with intracellular membrane structures will cause an over-estimation of the transporter content at the plasma membrane.

Essentially pure plasma membrane "ghosts" can be prepared by manual dissection of oocytes (Garcia *et al.*, 1992; Geering *et al.*, 1989; Keller *et al.*, 1989), however, this methodology is time-consuming and involves individual rinsing of prepared plasma membrane sheets. Collagenase treatment for removal of oocytes from their follicular cell layer was not suitable due to weakening of the envelope structure, resulting in fragmentation of plasma membrane sheets during the rinsing process to remove intracellular yolk and membranes (Wall & Patel, 1989). Use of a homogeniser to disrupt the oocytes is a faster

method for the isolation of plasma membranes from large numbers of oocytes but, as was observed over a series of experiments, there were large variations in the final yields of plasma membranes obtained. This was attributed to extensive fragmentation of the fragile plasma membranes. Also, it was more difficult to separate the plasma membrane sheets from underlying yolk protein. Better separation was obtained if the oocytes were gently disrupted with a P200 Gilson pipette tip. The resulting plasma membrane sheets obtained in this way were much larger (clearly visible by eye) and generally sedimented at a faster rate than the yolk protein, the majority of which could be removed in the initial supernatant. Centrifugation of the plasma membrane-containing fractions was avoided at all stages of the fractionation procedure, as this was found to cause fragmentation resulting in low final yields. Plasma membranes were therefore allowed to settle by gravity after each rinse until the final fraction was obtained which could then be collected by centrifugation.

Although more than 80% of the plasma membrane marker activity was recovered in the PM fraction, the actual yield of plasma membranes was found to vary considerably between oocyte preparations, and this was attributed to the unavoidable fragmentation of plasma membrane sheets. Results from both dot blot and Western blot analyses indicated that preparation of a plasma membrane fraction free from other cellular contaminants was extremely problematic. It was therefore concluded that, for this expression system, the methodology was not suitable for a reliable determination of transporter turnover numbers.

Alternative methods for determination of k_{cat} values include the application of a Scatchard analysis to data generated by equilibrium binding of [3 H]cytochalasin B to isolated oocyte plasma membranes. Obviously, this methodology also requires a fractionation procedure for oocytes. The number of molecules at the cell surface of intact oocytes can be determined by equilibrium binding of [3 H]ATB-BMPA. This takes advantage of the fact that essentially all bound ATB-BMPA can be covalently attached to the transporter upon exposure to ultra-violet light to derive a value for the total binding sites, B_{max} . Unfortunately, this procedure is not convenient for use with the oocyte system due to the large numbers of mRNA injections. A more advantageous system in this respect would be, for example, heterologous expression in CHO cells. This approach will be discussed further in Chapter 6 of this thesis.

CHAPTER 6

Construction of GLUT2/GLUT3 Chimeric Glucose Transporters

6.1 Aims.

1. In a previous study, a series of GLUT3/GLUT2 chimeric transporters were generated and expressed in *Xenopus* oocytes to address the structural basis for the different substrate selectivities and distinct transport kinetics exhibited by these isoforms. Mirror image GLUT2/GLUT3 constructs were also constructed, however, functional expression of all chimeras in this series was not achieved. The aim of this chapter was therefore to use recombinant PCR reactions to reconstruct the two GLUT2/GLUT3 chimeric transporters that were not successfully expressed in oocytes.

1a. Resulting recombinant GLUT2/GLUT3 cDNAs will be purified and subcloned into a pSP64T derivative for subsequent expression in *Xenopus* oocytes.

1b. Both strands of the constructs will be fully sequenced using automated DNA sequencing to ensure that no sequence errors were incorporated during the PCR reactions and subcloning procedures.

2. The GLUT2/GLUT3 cDNAs will be used as templates for *in vitro* synthesis of mRNA which will be subsequently expressed in *Xenopus* oocytes. Individual oocytes will then be assayed for the ability to transport 2-deoxy-D-glucose, before a more extensive kinetic characterisation of the chimeras is undertaken.

6.2 Introduction.

The glucose transporter isoforms mediate transport catalysis by alternating between two distinct conformational states in which the substrate binding site is exposed to either side of the membrane (section 1.5.3). This mechanism has been well characterised and much of the work on GLUT1 has focused on mapping the exo- and endofacially exposed substrate binding sites. Site-specific ligands have proved useful in demonstrating that these sites are located in different regions of the protein. For example, ATB-BMPA, an exofacial-specific ligand, interacts with the GLUT1 transporter in the region of helices 7 to 9 (Hashiramoto *et al.*, 1992), whereas cytochalasin B interacts with the transporter in the endofacial conformation in the region of helices 10 and 11 (Holman & Rees, 1987). Structural separation of the binding sites has further been proposed on the basis of kinetic studies (section 1.7).

The six C-terminal helices are fundamental for the formation of the glucose binding sites. Ligand binding and proteolysis studies have demonstrated that the C-terminal half of GLUT1 contains sufficient information to bind both cytochalasin B and ATB-BMPA. However, in a study utilising the baculovirus Sf9 system to express separate N- and C-terminal halves of GLUT1, it was suggested that binding of these ligands to the C-terminal half of GLUT1 can only occur when both constructs encoding the N- and C-terminal halves are co-expressed (Cope *et al.*, 1994). Thus, although the C-terminus is directly involved in formation of the binding sites, the N-terminus may provide a packing surface which allows correct exposure of the ligand binding sites in the C-terminal half (section 1.7.4). Alternatively, it is possible that one of the initial steps in substrate binding may involve a transient association with groups from the N-terminal half, or both halves combined. Further support for the involvement of the C-terminal domain in substrate binding has come from site-directed mutagenesis studies. A summary of this work is given in Chapter 3. Several residues have been identified that are important for exofacial and endofacial sugar binding, and in the conformational changes occurring during the transport process. All but one of these residues are located in the C-terminal domain of the transporter (Figure 1.6).

Furthermore, the C-terminus is suggested to contribute three amphipathic helices to channel formation (section 1.9), as predicted from molecular modelling studies.

6.2.1 Regions Involved in Substrate Selectivity.

The membrane topology of GLUT1 has been well characterised (section 1.4.2), and much evidence exists in support of the alternating conformer model of transport (section 1.5.3b). In addition, regions of the transporter involved in substrate binding at the exofacial and endofacial sites have been defined and the various kinetic parameters governing sugar transport have been exhaustively measured (section 1.5.3c).

The high degree of sequence identity and the virtually superimposable hydropathy plots of the GLUT isoforms suggest that the topology and mechanism of transport predicted for GLUT1 will extend to the other members of the GLUT family. However, an interesting feature exhibited by the mammalian GLUT isoforms is their ability to transport different substrates with distinct kinetic parameters, despite their high degree of sequence homology (Table 4.1). At present however, there is little published work that investigates the structural determinants that govern isoform specific substrate selectivities and transport kinetics. Elucidation of these factors would, for example, explain why only GLUT2 and GLUT5 are capable of recognising and transporting D-fructose whereas, GLUT3 can bind and transport D-galactose with a high affinity. The few studies reported to date which have addressed this point have used a chimeric transporter approach to investigate the structural basis of substrate selectivity and isoform specific kinetics, reviewed in section 3.2.8. While this methodology has been successful in identifying regions of importance, it may not be possible to assume that the regions that dictate isoform specific substrate selectivity and kinetics are the same. Furthermore, the relative importance of these regions may vary between isoforms.

6.2.2 Expression and Characterisation of GLUT2/GLUT3 Chimeras.

It has previously been demonstrated in this laboratory that the liver-type transporter, GLUT2, is unique among the GLUT isoforms by virtue of its ability to transport both D-fructose and D-glucose. GLUT2 also has a high K_m for zero-*trans* entry of 2-deoxy-D-glucose into oocytes (11.2mM). In contrast, the brain-type isoform, GLUT3, exhibits a relatively low K_m for this transport event (1.4mM) and is a high affinity D-galactose transporter. The distinction between the two isoforms is also apparent in the K_m values for 3-O-methyl-D-glucose equilibrium exchange (42.3mM and 10.6mM for GLUT2 and GLUT3 respectively). Such distinct properties exhibited by these two isoforms formed the basis of a study in which the regions of the transporters involved in substrate selection and high affinity 2-deoxy-D-glucose transport were investigated (Arbuckle *et al.*, 1996). GLUT2 and GLUT3 were chosen as candidates for the generation of chimeric transporter, utilising a PCR based approach (chimeras were generated by Dr.M.Arbuckle, Glasgow University, UK.) Two series of chimeras were constructed (Figure 6.1). The GLUT2 series comprised GLUT2 transporters in which lengths of sequence from the start of helix 7, or another distinct point nearer the C-terminus, were replaced with the corresponding sequences of GLUT3. Characterisation of these mutants delineated important sequences for the property of D-fructose recognition by GLUT2. (In the context of this study, fructose "recognition" means that these transporters contain the sequence information which facilitates fructose binding.) Mirror image constructs were also produced, referred to as the GLUT3 series, comprising N-terminal GLUT3 sequence with various lengths of the C-terminal sequence replaced by that of GLUT2 (Figure 6.1). Characterisation of these mutants provided information regarding the "GLUT3-like" properties of high affinity 2-deoxy-D-glucose transport and D-galactose recognition.

Extensive characterisation of these constructs in *Xenopus* oocytes has been successful in identifying regions of importance for substrate selectivity and for determining the affinity of 2-deoxy-D-glucose transport. A summary of the data available to date is given in Table 6.1. The data shows that sufficient information is retained within the region of GLUT2 encompassing transmembrane helix 7 to the C-terminus to enable a chimeric

transporter containing this region, (G3(7St)), to transport D-fructose, and to exhibit a K_m for 2-deoxy-D-glucose approximating that of wild type GLUT2. In contrast, a chimera that contains the helix 7 sequence derived from wild type GLUT3, G3(7Ed), but which is otherwise identical to G3(7St), is not capable of transporting D-fructose and exhibits K_m values for both 2-deoxy-D-glucose and D-galactose that resemble those of GLUT3. On this basis, it is proposed that helix 7 contributes to the exofacial binding sites of both GLUT2 and GLUT3 in such a way as to define substrate recognition by GLUT2 (or lack of D-fructose recognition by GLUT3). This helix also plays a role in defining the kinetic behaviour of the transporters. This is consistent with the evidence provided by Hashiramoto and co-workers, showing that helix 7 constitutes part of the binding site for the exofacial ligand, ATB-BMPA (Hashiramoto *et al.*, 1992). Furthermore, a region lying between the end of helix 7 and the end of helix 10 also contributes to the affinity of the exofacial binding site for the ligand, maltose (as evidenced by measurement of K_i values for maltose inhibition of 2-deoxy-D-glucose influx). Data is also presented that implicates sequences in the N-terminal half of the protein that influence the kinetics of transport by GLUT2 and GLUT3.

Although this study has been successful in identifying these important regions, it remains somewhat incomplete for two reasons. Firstly, expression of the entire GLUT2 series in oocytes was not achieved, thus hindering a more comprehensive investigation of these chimeras. In an attempt to address this problem, the chimeras G2(7St) and G2(10Ed) were reconstructed by PCR, subcloned and sequenced to scan for errors. Secondly, general problems associated with the oocyte expression system impeded a detailed investigation of the GLUT3 series. Expression of these constructs in a mammalian cell line will enable further analysis of the constructs in terms of obtaining data regarding inhibition and competition studies, and also will permit determination of turnover numbers, measurement of which was also absent from the oocyte study.

Figure 6.1

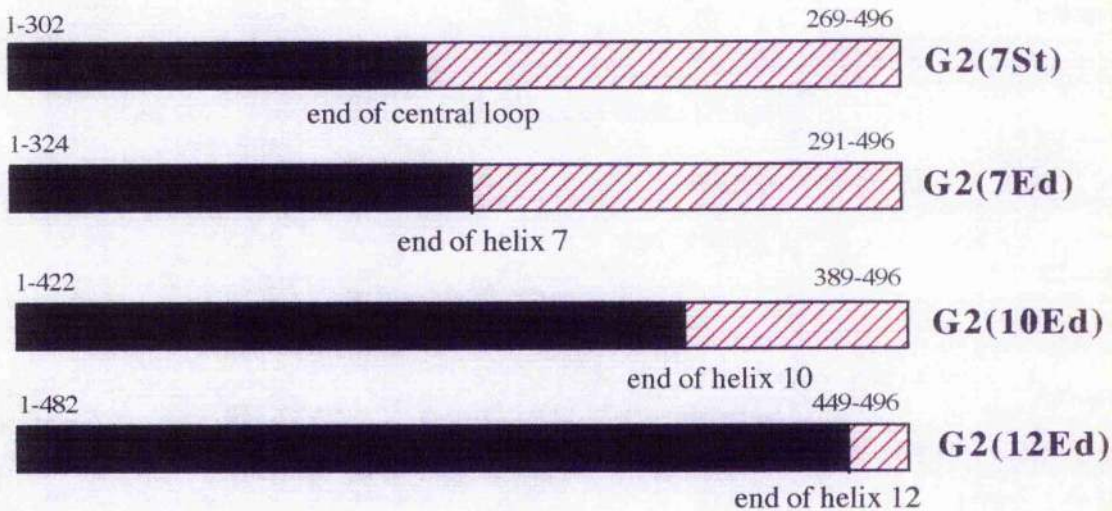
Junction Points of the GLUT2/GLUT3 Chimeric Transporters.

This diagram shows the junction points chosen for the generation of the GLUT2/GLUT3 chimeric transporters. GLUT2 sequence is shown in black and GLUT3 sequence in red. Amino acid numbers correspond to either GLUT2 or GLUT3 cDNA sequences and refer to the sequences above which they are positioned. The nomenclature is such that the N-terminal sequence is referred to followed by the junction site, given in brackets i.e. G2(7St) comprises N-terminal GLUT2 sequence up to the start of helix 7 and the corresponding GLUT3 sequence from this site to the end of the C-terminus.

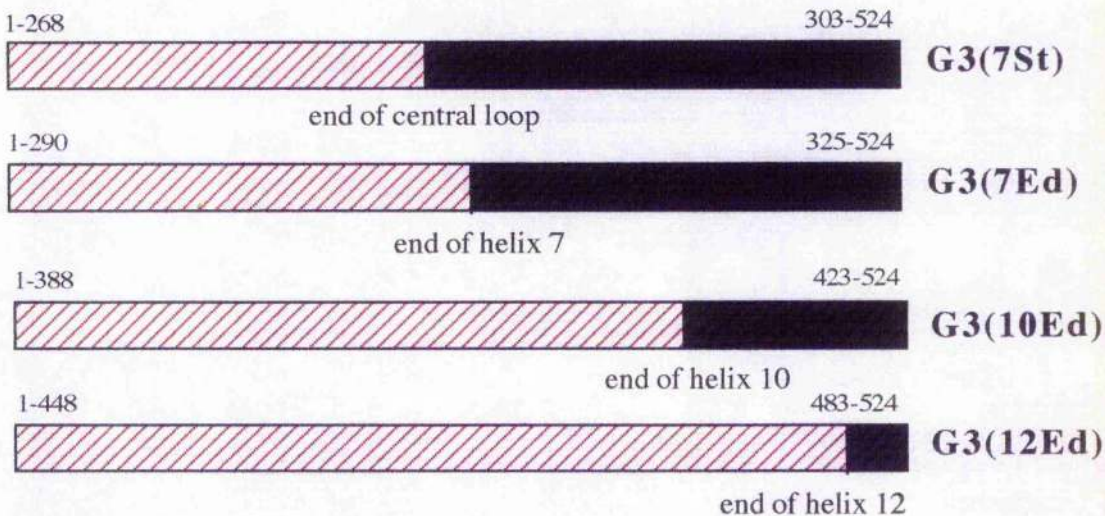
Figure 6.1


Junction Points of the GLUT2/GLUT3 Chimeric Transporters.

GLUT2 Series



GLUT3 Series



 **GLUT2 sequence**


 **GLUT3 sequence**

Table 6.1

Kinetic Parameters for Transport of Substrates by GLUT2/GLUT3 Chimeras.

Construct	K_m deGlc (mM)	K_i maltose (mM)	Fructose transport?	K_m fructose (mM)	K_m galactose (mM)
GLUT2	11.2±1.1	125±24	yes	76±11	92±8.4
GLUT3	1.4±0.06	28±2.5	no	n.d.	6.2±1.5
G2(7S)	-	-	-	-	-
G2(7Ed)	8.5±2.1		yes		
G2(10Ed)	-	-	-	-	-
G2(12Ed)	9.5±3.4	133±21	yes	139±21	-
G3(7S)	8.3±0.3	135±15	yes	365±21	25.4±2.1
G3(7Ed)	1.4±0.03	69±7	no	n.d.	2.55±0.4
G3(10Ed)	1.05±0.07	26±4	no	n.d.	2.8±0.9
G3(12Ed)	1.89±0.35	25±6.1	no	n.d.	4.8±0.88

Italics wild type values included for comparison.

n.d. no data.

6.3 Methodology Used to Generate GLUT2/GLUT3 Chimeric Transporters.

6.3.1 Recombinant PCR Reactions.

The GLUT2 and GLUT3 cDNAs have previously been cloned into the polylinker site of pSP64T to form the constructs pHTL217 and pSPGT3, as previously described in section 2.3.1. These constructs were used as templates in the recombinant PCR reactions described below.

Two series of oligonucleotide primers were designed for use in the PCR reactions, referred to as the internal and external primers. The external primers are 37'mers and correspond to the extreme 5' and 3' sequences of the sense strands of the GLUT2 and GLUT3 and are called G2st and G3ed, respectively. These primers encode *Sal* I restriction sites for subsequent cloning into pSP64T. The internal primers are 61 bases in length and are designed such that half of the oligonucleotide sequence corresponds to the GLUT2 sequence and the other half to the GLUT3 sequence either side of the junction site (at the start of helix 7 or the end of helix 10 for G2(7St) and G2(10Ed), respectively). The sequences of these primers are given in Table 6.2.

Two rounds of PCR reactions are carried out. In the two primary reactions, GLUT2 and GLUT3 wild type sequences are used as templates to amplify the appropriate N-terminal and C-terminal fragments, respectively (Figure 6.2). Thus, G2st is used in conjunction with GLUT2 template and the appropriate internal primer to amplify the N-terminal fragment in a single primary PCR reaction. In the second primary reaction, GLUT3 template is incubated in the presence of G3ed and the appropriate internal primer to amplify the C-terminal GLUT3 fragment. In a single secondary PCR reaction, the two primary products themselves act as the templates. Under certain reaction conditions, the strands of the primary fragments dissociate and re-anneal. The overlapping 3' tail regions bind and serve as primers for extension of the complementary strand. In the subsequent reaction cycles, G2st and G3ed then act to amplify the full length GLUT2/GLUT3 sequence to produce the final secondary

PCR reaction product. PCR reactions were carried out using Vent DNA polymerase and the reaction conditions were altered according to the manufacturers recommendations.

The PCR products were purified by agarose gel electrophoresis followed electroelution of the DNA and passage through a DEAE-Sephacel column (Elutip-D). Primary products were purified in this fashion before the subsequent overlap extension secondary PCR reaction.

6.3.2 Cloning Procedures.

Purified secondary PCR fragments contain sequences encoding *Sal* I restriction sites at the 5' and 3' ends, allowing subcloning into the pSP64T vector for subsequent expression in *Xenopus* oocytes. The backbone of this vector was obtained by digestion of pSPGT4 with *Sal* I (Figure 6.3). Three fragments were produced, corresponding to the backbone pSP64T vector containing the 5'UTR sequence, the GLUT4 protein coding sequence and a smaller fragment which is part of the 3'UTR sequence. The backbone vector was purified by electrophoretic extraction from agarose gel slices, followed by passage through a DEAE-Sephacel column (Elutip-D) and ethanol precipitation. The secondary PCR fragment was also digested with *Sal* I and purified using the same procedure before ligation into the vector backbone and transformation into competent *E.coli* cells. Plasmid DNA was prepared from several colonies to identify potential positive clones by restriction digestion analysis. Upon identification of positive clones, large scale plasmid preparations (section 2.3.12) were performed to obtain sufficient quantities of DNA for complete sequencing of the protein coding regions of the constructs. To facilitate this, a series of oligonucleotide primers were designed such that extension from their annealing sites resulted in the production of overlapping sequences.

6.3.3 Expression of GLUT2/GLUT3 Chimeras in *Xenopus* Oocytes.

The resulting chimeric constructs were linearised with *Xba* I and used as templates for *in vitro* synthesis of mRNA (section 2.5). Upon subsequent injection of mRNA, individual oocytes were assayed for the ability to transport 2-deoxy-D-glucose as described in section 2.7.

Table 6.2

Sequences of Oligonucleotide Primers Used to Generate GLUT2/GLUT3 Chimeric Transporters.

External Amplification Oligonucleotides:

GLUT2 Start	<i>gtgacgtagac</i> <u>TTCCGCACACAGACCTGGAATTGACA</u>
GLUT3 End	<i>gtgacgtagac</i> CGAGGGAGAGGTGGCTTTCCCATGCC

Internal Junction Oligonucleotides:

1505	GAGAGCTGGAGCACATGGAAATGATGATGGGCTGTCGGTAGCTGGAATTGGTGAAGAGC
1511	<u>CAGCTCTTACCAATTCCAGCTACCGACA</u> GCCCATCATCATTTGTGCTCCAGCTC
1507	GGGCGGGGCCCTGGCTGAAGAGTTGGGCC <u>ACCATGAACCAAGGGGATCGGGCTGGCCCA</u>
1509	<u>ATTGGCCAGGCCCGATCCCTGTTCATG</u> GTGGCCGAACCTCTTCAGCCAGGGCCCCCGC

Sequences corresponding to GLUT2 are underlined. Sequences which encode a *Sal*I restriction site used in subcloning of PCR fragments are written in lower case italics. All oligo's are written in the 5' to 3' direction.

Figure 6.2

Generation of GLUT2/GLUT3 Chimeras Using Recombinant PCR Reactions.

This diagram describes the PCR method used to construct G2(7St) and G2(10Ed), which comprise N-terminal GLUT2 sequence to the start of helix 7 and the end of helix 10, respectively, followed by C-terminal GLUT3 sequence to the end of the protein. The GLUT2 and GLUT3-based primary products are generated in two separate primary PCR reactions in which wild type GLUT2 and GLUT3 are incubated with the appropriate primers. The external primers anneal to the 3' regions of the antisense and sense strands of GLUT2 and GLUT3 respectively, and are referred to as G2Start and G3End. These primers also have tails which encode *Sal* I restriction sequences for use in the subsequent cloning procedures. The internal primers are designed to anneal in the region of the junction site and have tails that are complementary in sequence to the opposite primary PCR product. Thus, in a single secondary PCR reaction, the two primary PCR products act as templates, and under certain reaction conditions, undergo strand dissociation and re-anneal in the region of the overlapping sequences which are subsequently extended to produce a full length secondary PCR product. The external primers then act to amplify this product which is restricted with *Sal* I prior to ligation into *Sal* I restricted vector.

Figure 6.2
Generation of GLUT2/GLUT3 Chimeras Using Recombinant PCR Reactions.

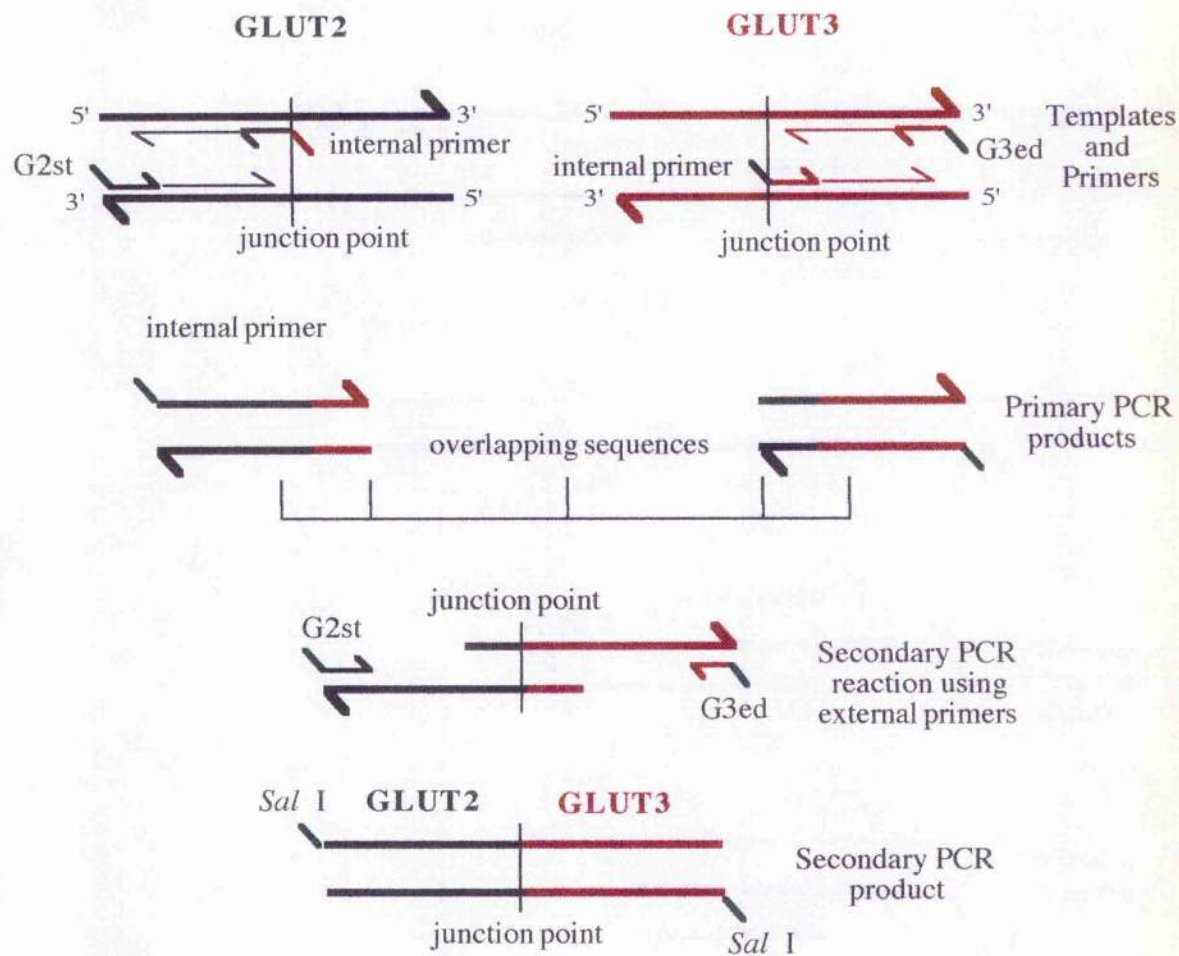
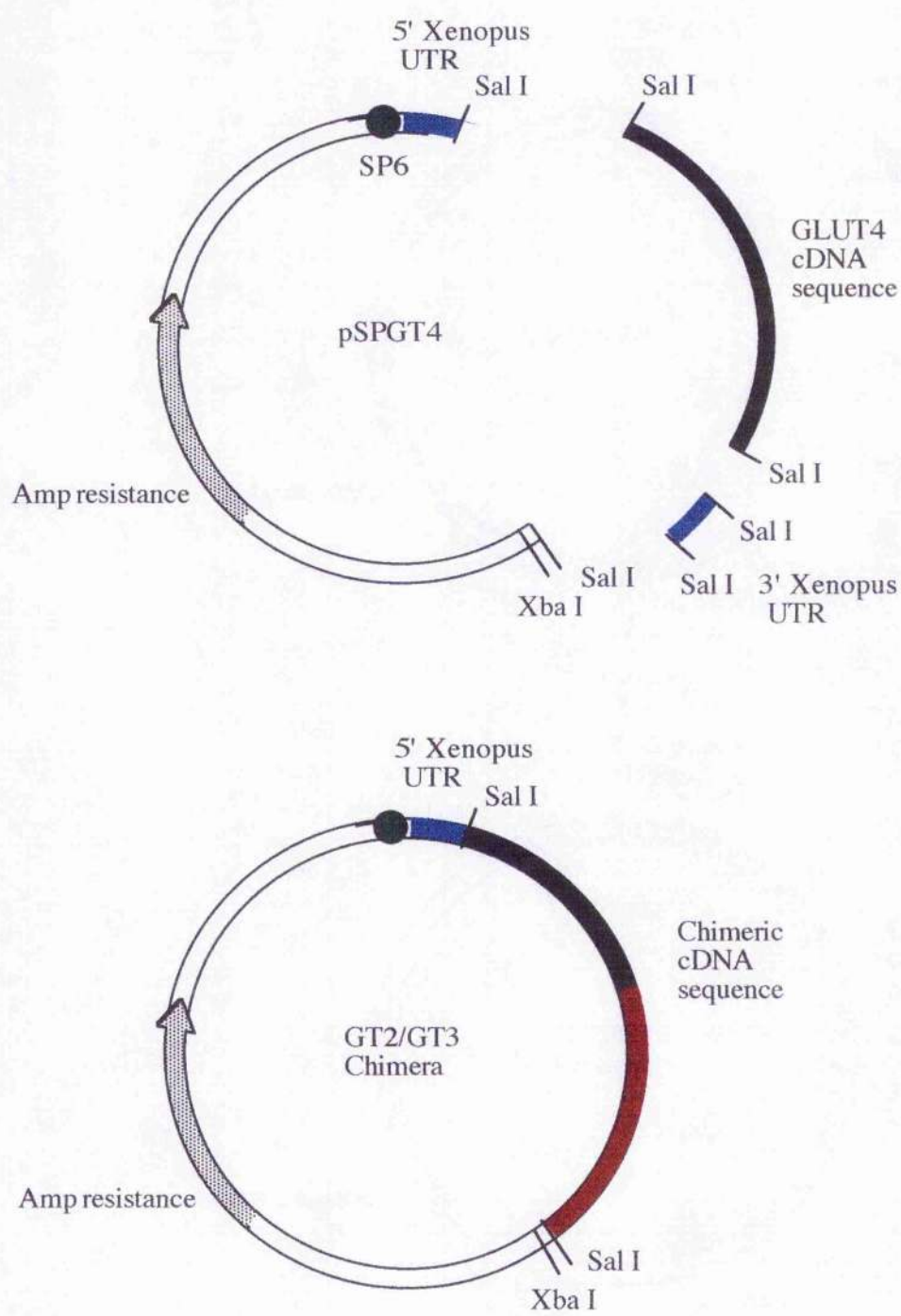


Figure 6.3

Restriction Digestion of pSPGT4 with *Sal* I and Cloning of GLUT2/GLUT3 Chimeric cDNAs.

The pSP64T vector backbone was obtained by restricting pSPGT4 with *Sal* I. Three fragments were produced corresponding to the backbone vector, the GLUT4 protein coding region, and a 200bp fragment corresponding to the 3' untranslated region of the *Xenopus* β -globin gene. The backbone vector was treated with alkaline phosphatase to prevent re-ligation, purified and ligated to the *Sal* I restricted GLUT2/GLUT3 cDNA. Transfected colonies were selected on the basis of resistance to ampicillin.

Figure 6.3
Restriction Digestion of pSPGT4 with *Sal* I and Cloning of GLUT2/GLUT3
Chimeric cDNAs.



6.4 Results.

6.4.1 PCR Using Vent Polymerase.

Previous attempts to generate G2(7St) and G2(10Ed) utilised *Taq* DNA polymerase to perform the PCR reactions. However, in an attempt to reduce the number of sequence errors, Vent DNA polymerase was used. This enzyme has 3' to 5' exonuclease proofreading activity and therefore is of higher fidelity than *Taq* DNA polymerase. Use of this enzyme resulted in high yields of secondary PCR products for both G2(7St) and G2(10Ed) (Figure 6.4) and also reduced the number of clones that were screened before identifying a clone that was completely free of sequence errors.

The parameters used in the PCR reactions with Vent DNA polymerase were similar to those used with *Pfu* DNA polymerase (section 2.2.4) with minor modifications. Hot start PCR was performed and extension times were strictly controlled to 1 min per kilobase of sequence. This prevents the exonuclease activity of the enzyme digesting the ends of the synthesised fragments and therefore destruction of the *Sal* I restriction sites and overlapping sequences. In addition, this enzyme required the presence of Mg^{2+} ions in the reaction mixture and a final concentration of 1mM was determined to be optimal for these reactions.

6.4.2 Subcloning of Chimeric Constructs.

Blunt ended secondary PCR products were digested with *Sal* I before ligation into the pSP64T backbone vector, also digested with *Sal* I. The resulting constructs were then transformed into competent *E.coli* cells for propagation and isolation of the plasmids. The correct orientation of the insert was determined by restriction digestion analysis with *Bgl* II and *Xba* I. Insert ligated in the correct orientation, i.e. for subsequent mRNA synthesis reactions, yielded two fragments of 4550 and 150bps (Figure 6.5), whereas insert ligated in the incorrect orientation yielded fragments of 3150 and 1550bps in length. The restriction and ligation stages of the subcloning procedure proved difficult as evidenced by the fact that a large fraction of the colonies screened by restriction digestion analysis contained religated

vector without insert. This is probably because the blunt ended PCR products generated by Vent DNA polymerase are difficult to digest with *Sal* I.

Upon identification of clones containing vector in the correct orientation, large scale plasmid preparations were performed and the constructs were sequenced fully to scan for sequence errors using an ABI Automated Sequencer (section 2.4). Suitable clones containing no sequence errors were identified for both G2(7St) and G2(10Ed).

6.4.3 *In Vitro* Synthesis of mRNA from G2(7St) and G2(10Ed) Constructs.

G2(7St) and G2(10Ed) constructs were linearised with *Xba* I and used as templates for *in vitro* mRNA synthesis reactions. Both chimeric cDNAs were transcribed into mRNAs of the correct predicted size, with efficiencies that were comparable to both wild type GLUT2 and GLUT3 cDNAs (Figure 6.6).

6.4.4 Measurement of 2-Deoxy-D-Glucose *Zero-Trans* Influx Mediated by G2(7St) and G2(10Ed) Expressing Oocytes.

Individual oocytes expressing either G2(7St), G2(10Ed) or the wild type GLUT2 or GLUT3 transporters were assayed for the ability to mediate 2-deoxy-D-glucose uptake. Non-injected control oocytes were also assayed in parallel under identical reaction conditions to obtain endogenous transport rates. The results of a typical transport assay are shown in Figure 6.7. The rates of transport obtained for G2(7St) and G2(10Ed) expressing oocytes were consistently much lower than those obtained for oocytes expressing the wild type transporters, with rates that were virtually indistinguishable from non-injected control oocytes.

Figure 6.4

GLUT2/GLUT3 PCR Products Generated Using Vent DNA Polymerase.

This diagram shows a 1% agarose gel of the various primary (Lanes 2 and 3), and secondary (Lane 1), PCR products generated by Vent DNA polymerase, pSPGT4 restricted with *Sal* I and CIP treated (Lane 4), and backbone pSP64T vector containing the secondary PCR fragment (Lane 5).

Transformed JM109 colonies which contained the cloned PCR product were screened by restriction digestion analysis of the plasmid DNA isolated from the clones, followed by agarose gel electrophoresis.

Figure 6.4

GLUT2/GLUT3 PCR Products Generated Using Vent DNA Polymerase.

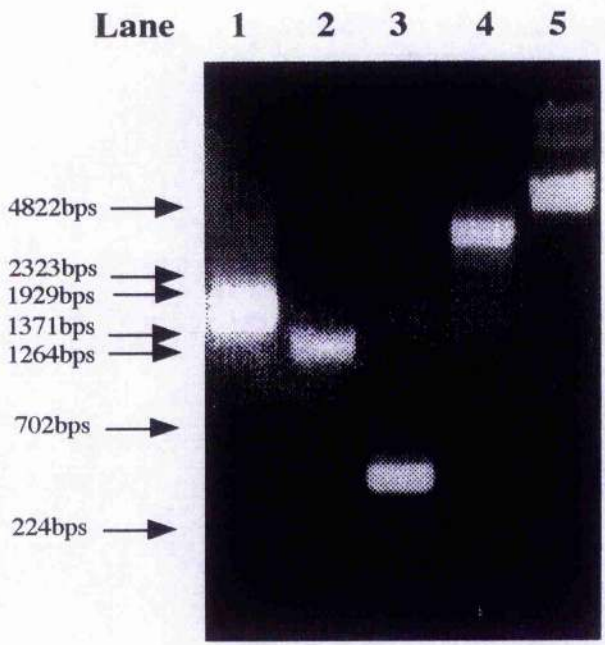


Figure 6.5

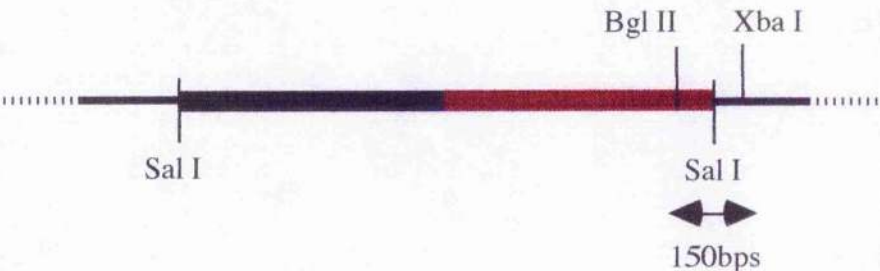
Restriction Digestion Analysis of GLUT2/GLUT3 Constructs.

This diagram shows the positions of the cleavage sites of the restriction enzymes used to determine the orientation of the GLUT2/GLUT3 cDNA in the vector. GLUT2 sequence is shown in black and GLUT3 sequence in red. The extreme C-terminal portion of GLUT3 contains a unique *Bgl* II restriction site which is not present in the GLUT2 sequence or the vector. A unique *Xba* I site is located 3' to the chimeric sequence in the vector. Therefore, restriction digestion with *Bgl* II and *Xba* I yields different sized fragments depending on the orientation of the ligated insert. Chimeric sequence inserted in the correct orientation i.e. for transcription driven by the SP6 promoter, yields two fragments of 4450 and 150bps. Insert ligated in the incorrect orientation results in the production of two fragments of 3150 and 1550bps in length. The fragments produced by restriction digestion were separated by agarose gel electrophoresis and the sizes were determined by comparison against molecular weight markers loaded onto the same gel.

Figure 6.5

Restriction Digestion Analysis of GLUT2/GLUT3 Constructs.

Correct Orientation



Incorrect Orientation

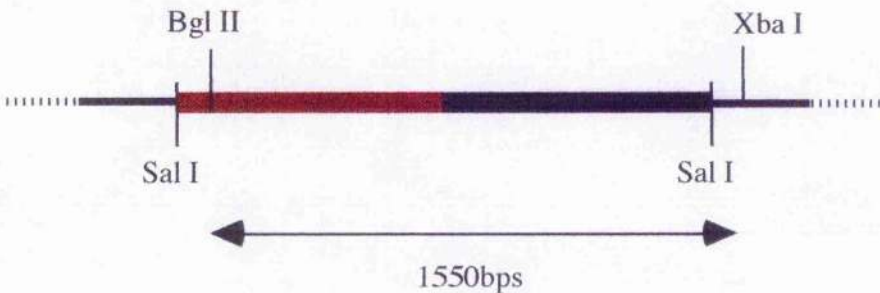


Figure 6.6

1% Agarose Gel of *In Vitro* Synthesised mRNA.

pSP64T vector containing the wild type GLUT3 cDNA or G2(7St), G2(7Ed), G2(10Ed) or G2(12Ed) chimeric cDNAs were linearised with *Xba* I and used as templates for the synthesis of mRNA. A 3 μ l aliquot (from a total of 40 μ l) of each reaction was analysed by 1% agarose gel electrophoresis. Molecular weight markers are loaded (Lane 1), followed by mRNA samples of GLUT3 (Lane 2), G2(7St) (Lane 3), G2(7Ed) (Lane 4), G2(10Ed) (Lane 5) and G2(12Ed) (Lane 6).

Figure 6.6
1% Agarose Gel of *In Vitro* Synthesised mRNA.

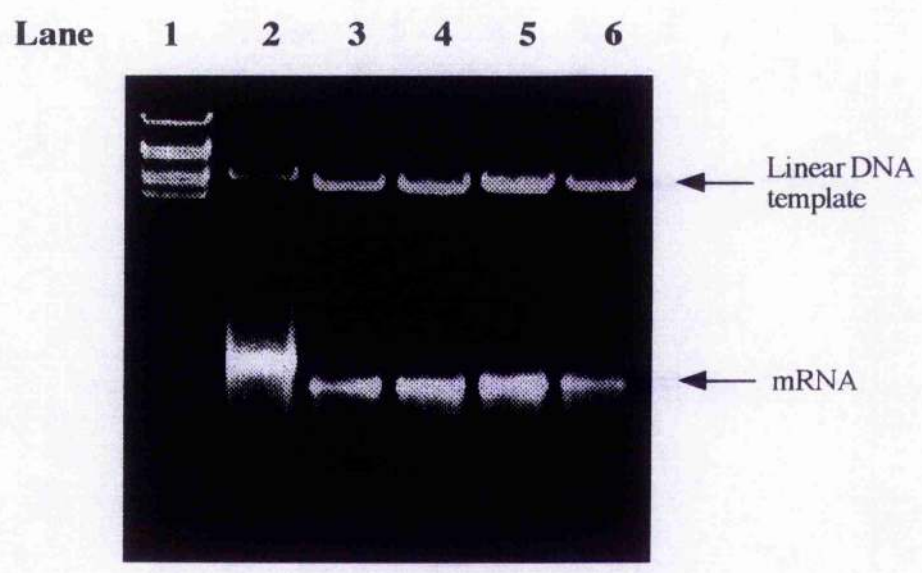
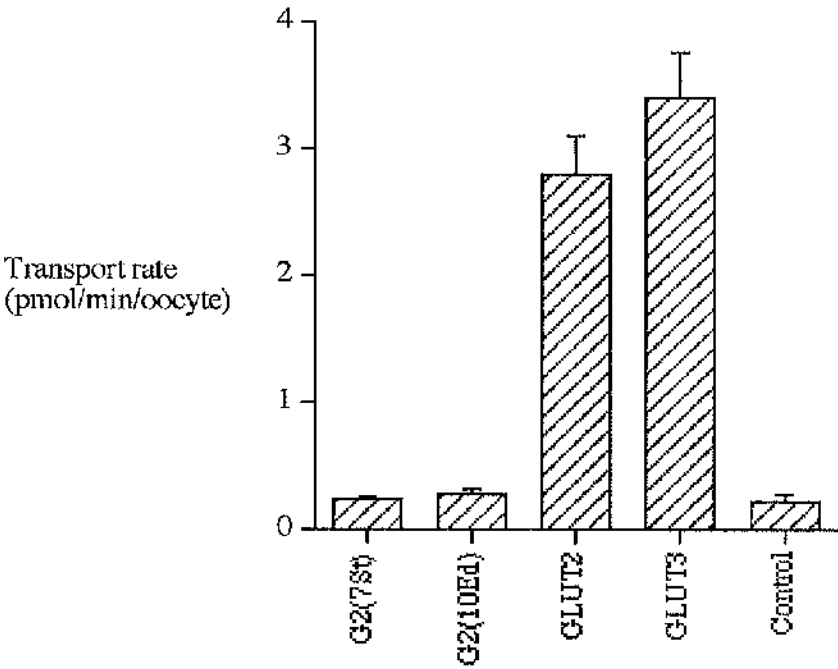


Figure 6.7

Measurement of 2-Deoxy-D-Glucose Uptake by Oocytes Expressing GLUT2, GLUT3, G2(7St) and G2(10Ed).

Oocytes were microinjected with 50ng of mRNA encoding wild type GLUT2 or GLUT3, or 50ng of mRNA encoding the G2(7St) or G2(10Ed) chimeric transporters. After incubation at 18-20°C for 48 hours, transport was determined by a 30 min incubation with 0.1mM 2-deoxy-D-glucose. Non-injected control oocytes were assayed in parallel under identical reaction conditions. The results presented are representative of a typical experiment, and are the mean \pm S.D. of seven oocytes.

Figure 6.7
Measurement of 2-Deoxy-D-Glucose Uptake by Oocytes Expressing GLUT2, GLUT3, G2(7St) and G2(10Ed).



6.5 Discussion.

In this initial attempt to resolve the expression problems encountered with the G2(7St) and G2(10Ed) transporters, these chimeras were reconstructed using recombinant PCR technology. Previously, PCR reactions were performed using *Taq* DNA polymerase which does not have 3' to 5' exonuclease proofreading activity. Thus, although the constructs were originally reported free of sequence errors, it is possible that misincorporations may have remained undetected. In order to reduce the number of incorporated errors Vent DNA polymerase was used in this attempt to reconstruct the chimeras. This enzyme does possess 3' to 5' exonuclease proofreading activity and thus has a higher fidelity compared to *Taq* DNA polymerase. Clones were identified for both chimeras that contained no sequence errors, and the chimeric cDNAs could be translated into a protein of the correct predicted size with efficiencies comparable to the wild type cDNAs. However, the low level of transport activity exhibited by these chimeras in oocytes precluded any functional or kinetic analysis. Thus, the lack of any measurable transport activity was concluded not to be due to sequence or cloning errors.

With regard to other previously generated GLUT2 series chimeras, low levels of functional expression were consistently observed for G2(7Ed) compared to wild type GLUT2. In fact, G2(12Ed) was the only transporter in the GLUT2 series that exhibited levels of functional expression approaching that obtained for wild type GLUT2. Some kinetic parameters were measured for these transporters, but the study remains incomplete in the absence of a functional and kinetic characterisation of the remaining chimeras in this series (Arbuckle *et al.*, 1996).

Expression of chimeric transporters which contain the GLUT2 amino-terminus have proved difficult not only in this study but also in those reported by other laboratories. Buchs and co-workers have obtained functional expression of a series of GLUT4/GLUT2 chimeras in oocytes, as evidenced by an increase in transport activity compared to non-injected oocytes. Interestingly, although chimeras containing N-terminal GLUT2 sequence could be efficiently translated into proteins of the correct size, an increase in transport activity was not detectable (Buchs *et al.*, 1995a). Similarly, chimeras of the rat GLUT2 and rat GLUT4

cDNAs have been demonstrated to be functionally inactive but were immunologically detected at comparable levels to GLUT4 protein in the total oocyte membrane fraction. Problems have also been reported expressing chimeras containing the GLUT2 amino-terminus in other cell types (Piper, 1993).

Possible reasons for the inactivity of certain chimeras containing N-terminal sequences derived from GLUT2 have not been pursued or discussed at any great length. Potential explanations include mistargeting of the chimeras to an intracellular location in the oocyte. Both GLUT2 and GLUT3 isoforms have previously been demonstrated to be expressed predominantly at the plasma membrane of oocytes (Gould & Holman, 1993). However, approximately 40% of GLUT2 was detected in an intracellular fraction compared to 15% of GLUT3. Thus, it may be that the relative distribution of the chimera at the plasma membrane is altered when certain N-terminal GLUT2 and C-terminal GLUT3 sequences are present in the same protein. Unfortunately, an accurate determination of plasma membrane associated chimeric transporters is precluded by the inability to reproducibly obtain pure plasma membrane fractions from oocytes (Chapter 5). Another handicap in this regard is the inability to determine the relative distribution of GLUT2 by a Scatchard analysis of equilibrium [^3H]cytochalasin B binding to membranes due to the low affinity of this isoform for this inhibitor (Axelrod & Pilch, 1983). A further complication is presented by the inability to directly compare the levels of expression of G2(7St) and G2(10Ed) with GLUT2 as these chimera contain the GLUT3 carboxy-terminus.

A further explanation is that the chimeras may be prematurely degraded due to alterations in the conformations of the proteins resulting from their chimeric nature. Whilst this is a possibility, it is more likely that the interactions that form between the N- and C-termini in the tertiary structure of the protein are sufficiently perturbed in the chimeras such that the transporters are functionally inactive. It has previously been suggested that the N-terminal domain exerts an influence on the ability of the protein to correctly form the ligand binding sites, by providing a surface for the structural packing of helices in the tertiary structure. This view is favoured over a direct involvement of N-terminal domain residues in the formation of the exofacial binding site. An investigation of the exact role of the N-terminus in formation of the substrate binding sites and the ability of the transporter to be

functionally active would require generation of chimeric transporters with junction sites located throughout this domain. In the light of the expression problems discussed above, an alternative approach would be to construct a series of transporters in which the regions that are important for substrate binding are exchanged between GLUT2 and GLUT3. For example, replacement of the GLUT2 helix 7 sequence, (and therefore the other individual helices), with that of GLUT3 would provide information regarding the nature and extent of the contribution made by the N-terminus. Such an approach may avoid the expression problems encountered when an entire domain, (or a large portion of a domain), of one transporter is replaced with that of another, since the foreign sequences are internal and are therefore predicted less likely to disrupt the global packing of the protein. Unfortunately, such attempts have been made by members of this laboratory, but the methodology has proved problematic (see Susan Kane, PhD Thesis, 1997, Glasgow University, U.K.). Nevertheless, in the absence of a protein structure, the use of the chimeric transporter approach in future studies will no doubt provide important information regarding the functional role of defined regions of the transporters.

CHAPTER 7

Expression of GLUT2 and GLUT3 **in CHO-Cells.**

7.1 Aims

1. To establish stable CHO-cell lines expressing the GLUT2 and GLUT3 isoforms, as an alternative to heterologous expression in *Xenopus* oocytes. Western blot analysis utilising anti-GLUT antibodies will be used to identify G418-resistant stable CHO-cell lines individually expressing GLUT2 and GLUT3.
2. To undertake a functional analysis of GLUT2 and GLUT3 expressed in CHO-cells by measurement of kinetic parameters for 2-deoxy-D-glucose, D-fructose and D-galactose transport. This will provide a basis for a more complete characterisation of the GLUT3 Pro-Ala mutants previously generated and studied in oocytes.
3. To subclone the GLUT3 series of chimeras into a suitable vector for high-level expression in mammalian cells. This will enable further characterisation of these mutants that have been previously studied in oocytes.

7.2 Introduction.

7.2.1 Heterologous Expression of Proteins in Mammalian Cell-Culture Lines.

A number of genes encoding either foreign or native membrane proteins have been expressed in cultured mammalian cells. This approach has been successfully used to investigate the properties of genes encoding transporters, channels and receptors, to study the trafficking of membrane proteins and membrane sorting events, and also to analyse the effects of introducing specific mutations into the cDNA of interest. For some proteins, expression in mammalian cells is necessary when post-translational modification is requisite for correct functional activity, e.g. if the membrane protein requires glycosylation, then expression in bacterial cells is not appropriate since such modifications can not be achieved.

There are generally two approaches used for heterologous expression in mammalian cell-culture lines. The first is to generate a transient expression system in which the cDNA of interest is introduced into a population of cells, but is not integrated into the host cell genome. The second method is the generation of stably transfected cell lines in which the cDNA of interest is integrated into the host cell genome. This latter method offers many advantages as an expression system. Once generated, stably transfected cell lines can be stored and propagated for long periods of time, often years, without the need to repeat the transfection/selection procedure. Thus, if a protein is being repeatedly studied then this methodology offers distinct advantages when compared to transient expression or, for example, the use of oocytes (Chapters 4 and 5).

7.2.2 Further Characterisation of GLUT3 Pro-Ala Mutants and the GLUT3 Series Chimeras in CHO-Cells.

In the light of the problems associated with the use of the *Xenopus* oocyte system for expression and characterisation of the GLUT3 Pro-Ala mutants generated in this study (section 4.6), stable expression in the Chinese Hamster Ovary (CHO-) cell line is a possible

alternative to complete these studies. The generation of CHO-cells that stably express the wild type GLUT3 isoform would provide a suitable base-line for comparison with cell lines expressing individual Pro-Ala mutants at comparable levels of expression to the wild type transporter. This system, although not as suitable for the kinetic studies already discussed utilising oocytes (section 4.2.3), is more convenient for use in photolabelling studies with both cytochalasin B and ATB-BMPA, avoiding the need for repeated oocyte injections. In addition, simple fractionation protocols exist for the isolation of plasma membrane fractions and therefore, measurement of the levels of GLUT3 wild type and mutant transporters at the cell surface would be possible, which, in turn would enable measurement of turnover numbers. Determination of this parameter was not possible using the oocyte system (Chapter 5).

Additionally, although the GLUT3 series of chimeras were successfully expressed in oocytes enabling some functional and kinetic characterisation, expression in an alternative system would facilitate a more detailed analysis such as the measurement of turnover numbers and the use photolabelling studies to further understand the relationship between the isoform-specific substrate binding requirements of GLUT2 and GLUT3.

7.3 Methods.

7.3.1 Expression Vectors.

Stable expression of a foreign gene in a eukaryotic cell can be achieved using plasmid constructs in which the cDNA of interest is inserted downstream of a eukaryotic RNA polymerase II promoter. There are several types of promoter available including the SV40 based promoters and promoters from the human cytomegalovirus, (CMV), which work well in most cell types, and are commercially available.

In addition to enhancer-promoter sequences to drive transcription of the cDNA, the vector must also possess polyadenylation and transcription termination sequences to enhance RNA stability. A selectable antibiotic resistance gene, e.g. the neomycin gene, is also required for isolation of resistant stable cell lines subsequent to transfection.

GLUT2 has previously been subcloned into the mammalian expression vector, pLK444 (Figure 7.1), and is under the transcriptional control of the human β -actin promoter and a simian virus (SV40) polyadenylation signal. This vector contains the neomycin resistance gene for selection purposes.

The GLUT3 cDNA has been cloned as a *Bam*HI-*Xba*I fragment from pSPGT3 into the *Bgl*II-*Xba*I sites of the pCMV-4 vector (Figure 7.2). The cDNA is under the transcriptional control of the enhancer-promoter sequences from the immediate early gene of the human cytomegalovirus (CMV). The polyadenylation signal and transcriptional termination sequences are derived from the bovine growth hormone (BGH) gene and enhance RNA stability. However, this vector does not have a selectable resistance gene.

7.3.2 Subcloning of GLUT3/GLUT2 Chimeras for Expression In CHO-Cells.

The GLUT3 series of chimeras have previously been cloned into the pSP64T plasmid for expression in *Xenopus* oocytes (Dr.M.Ar buckle, Glasgow University, U.K.) For expression in CHO-cells, these cDNAs were subcloned into the mammalian expression

vector, pcDNA3, thus placing the cDNAs under the transcriptional control of the CMV promoter. This vector also contains the BGH polyadenylation signal and a neomycin gene for selection (Figure 7.3).

7.3.3 Transfection of CHO-Cells and Selection of Stable Transfectants.

The method of transfection used was calcium phosphate precipitation, a procedure which is especially suitable for fibroblastic cell lines such as CHO-cells. DNA was mixed directly with a calcium chloride solution and phosphate buffer to form a fine precipitate which was dispersed over the cultured cells. This protocol is routinely used for stable transfection (section 2.13). A DMSO shock step was included in the protocol. Application of a 10-20% DMSO solution to the cells for a few minutes after DNA association serves to increase the efficiency of transfection. The exact mechanism of action is unknown, but the treatment may modify the cell membrane structure to enhance uptake of DNA.

The selection agent used for isolation of individual transfected colonies was the application of G418 (600 μ g/ml) to the growth medium. pL.K444 and pcDNA3 both possess a neomycin resistance gene for selection, however, the pCMV-GT3 construct does not possess the required selectable marker gene and therefore was co-transfected with pcDNA3. A 10:1 ratio of pCMV-GT3:pcDNA3 was used.

7.3.4 Western Blotting and Immunodetection of GLUT2 and GLUT3.

Upon selection and propagation of individual clones, several were screened for expression of either GLUT2 or GLUT3 by Western blotting and immunodetection. Cell lysates were prepared from a number of individual G418-resistant clones and subjected to SDS/PAGE (section 2.17.1). Proteins were transferred to nitrocellulose membranes which were subsequently probed with anti-GLUT2 or anti-GLUT3 antiserum (section 2.17.3). Nitrocellulose membranes were developed using the ECL detection system so that the presence of low levels of protein could be detected (section 2.17.5).

7.3.5 Functional Studies in CHO-Cells.

Transfected and non-transfected CHO-cells were grown as described (section 2.13.1) in preparation for measurement of transport activity. Cells were assayed for uptake of radiolabelled 2-deoxy-D-glucose and D-fructose in the presence and absence of cytochalasin B.

Figure 7.1

Schematic Representation of pLK444 Containing the Human GLUT2 cDNA.

The pLK444 is a mammalian expression vector which utilises the β -actin promoter to drive transcription of the cloned cDNA. The vector also contains three unique restriction sites for cloning purposes, a neomycin gene for selection purposes, and an SV40 polyadenylation signal. The GLUT2 cDNA was cloned as a *Bgl* II fragment (excised from pHTL-217, Kayano *et al.*, 1990) into the *Bam*H I site of pLK444.

Figure 7.1

Schematic Representation of pLK444 Containing the Human GLUT2 cDNA.

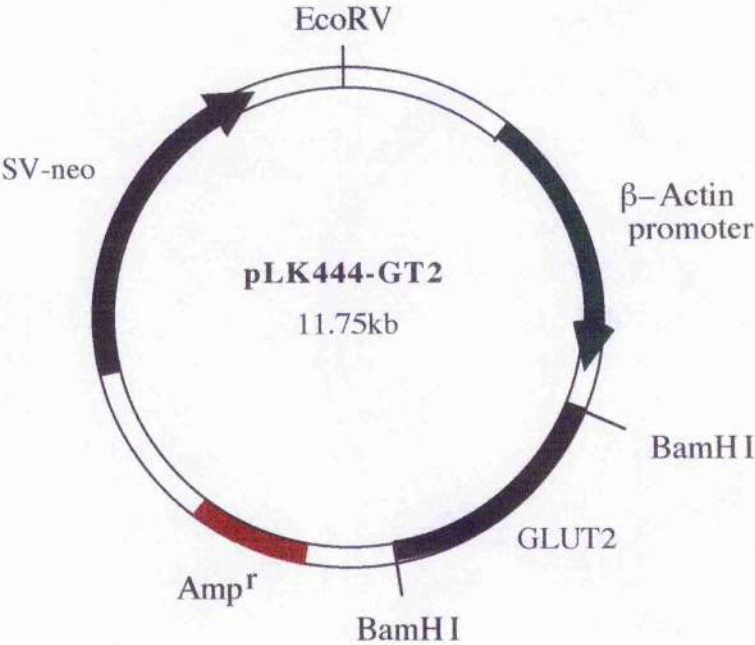


Figure 7.2

Schematic Representation of pCMV-4 Containing the Human GLUT3 cDNA.

This diagram shows the GLUT3 cDNA cloned as a *Bam*H I-*Xba* I fragment (excised from pSPGT3) into the *Bgl* II-*Xba* I sites of the pCMV-4 vector. The cDNA is under the transcriptional control of the enhancer-promoter sequences from the immediate early gene of the human cytomegalovirus (CMV). The polyadenylation signal and transcriptional termination sequences are derived from the bovine growth hormone (BGH) gene and enhance RNA stability. This vector does not contain a suitable selectable marker gene and therefore is co-transfected with another vector such as pcDNA3 which contains the neomycin resistance gene.

Figure 7.2

Schematic Representation of pCMV-4 Containing the Human GLUT3 cDNA.

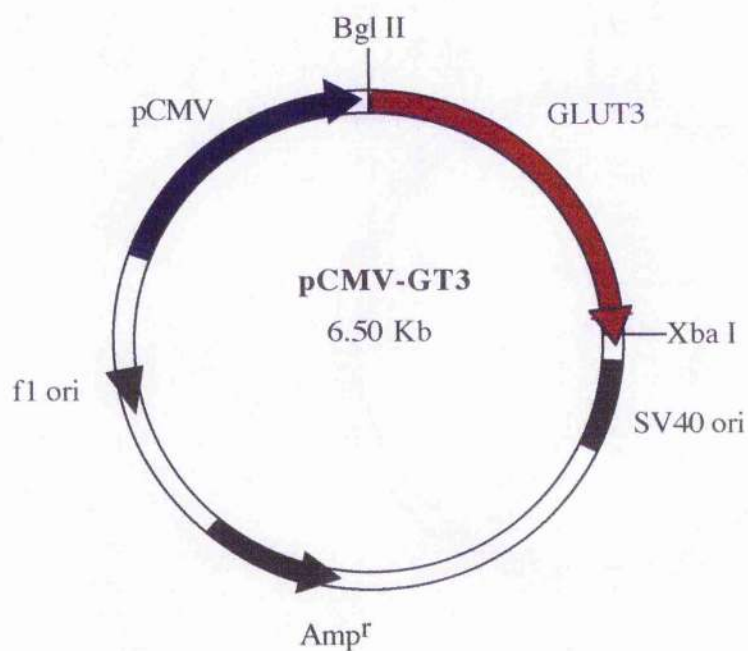
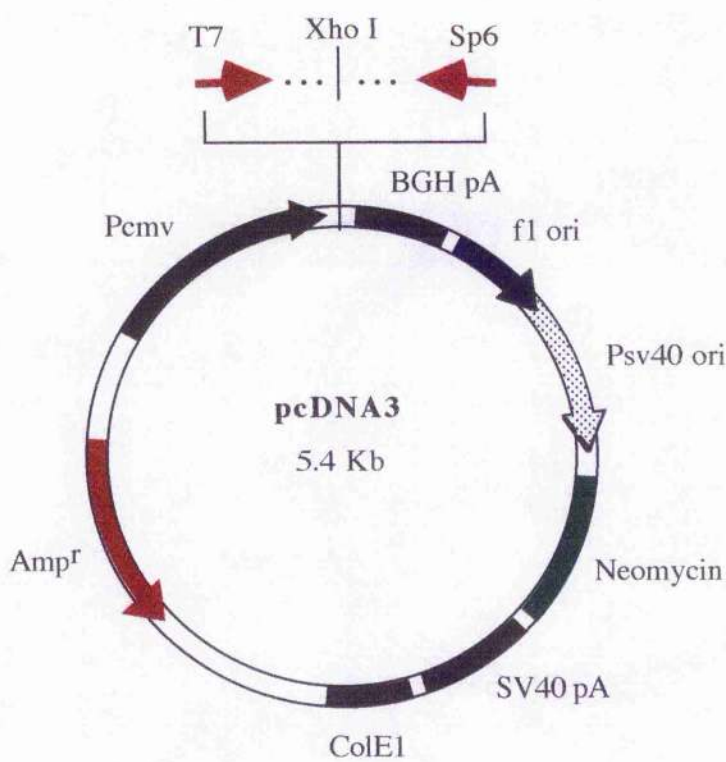


Figure 7.3

Schematic Representation of pcDNA3.

pcDNA3 is a mammalian expression vector designed for high-level expression of proteins. The cDNA of interest is placed under the transcriptional control of the enhancer-promoter sequences from the immediate early gene of the human cytomegalovirus (CMV). Polyadenylation signal and transcription termination sequences are derived from the bovine growth hormone (BGH) gene and serve to enhance RNA stability. There is a neomycin resistance gene for selection of G418 resistant stable cell lines.

Figure 7.3
Schematic Representation of pcDNA3.



7.4 Results.

7.4.1 Restriction Digestion Analysis of pcDNA3-G3/G2 Constructs.

All four chimeric cDNAs of the GLUT3 series were excised from the pSP64T vector as *Sal*I fragments of approximately 1.6kb in length. Fragments were subsequently purified and ligated into the *Xho*I site of the pcDNA3 polylinker sequence (Figure 7.4). The resulting constructs were successfully transformed into competent *E.coli* cells for large scale preparation of plasmid DNA and the DNA obtained from several individual transformed clones was screened for the presence of the G3/G2 insert by restriction digestion analysis. The orientation of the insert was determined from the size of the restriction fragments. Restriction with *Bst*XI yielded two fragments of approximately 0.5kb and 6.5kb or, approximately 1kb and 6kb, depending on the orientation (Figure 7.5).

7.4.2 Immunoblotting of Lysates Prepared from GLUT2-Transfected CHO-Cells.

Cell lysates were prepared from a number of GLUT2-transfected G418-resistant clones and were subjected to SDS/PAGE. Proteins were transferred to nitrocellulose membranes which were then probed with anti-GLUT2 antibodies (section 2.17.3). A representative immunoblot is shown in Figure 7.6. 25 μ g of rat liver membrane was included as a standard, and GLUT2 could be identified as a broad band migrating with an apparent molecular weight of approximately 50kDa. A band migrating at the same apparent molecular weight was identified in clone G2-2b.

7.4.3 Immunoblotting of Lysates Prepared from GLUT3-Transfected CHO-Cells.

Cell lysates were prepared from a number of GLUT3-transfected G418-resistant clones. After SDS/PAGE and transfer to nitrocellulose, the membranes were probed with

anti-GLUT3 antibodies. 25 μ g of rat brain was included as a standard and GLUT3 could be identified as a broad band migrating with an apparent molecular weight of approximately 40kDa. The level of GLUT3 expression in all GLUT3-transfected CHO-cell lines screened was below the limits of detection of the antibody used, with the exception of clone G3-1b. A faint band migrating with the same molecular weight as the GLUT3 standard was identified in this clone.

7.4.4 Immunoblotting of Lysates Prepared from GT3/GT2-Transfected CHO-Cells.

Cell lysates were prepared from a number of GT3/GT2 transfected G418-resistant clones and subjected to Western blotting. Since all chimeras in the GLUT3 series have C-terminal GLUT2 sequence, the immunoblots were probed with anti-GLUT2 antibodies targetted against the C-terminus. A band migrating with the same molecular weight as GLUT2 was identified in the cell lysate prepared from clone G3(7St)-C6 (Figure 7.6).

7.4.5 Transport Measurements in Transfected and Non-Transfected CHO-Cells.

CHO-cells were grown to confluency on 6-well plates and [3 H]2-deoxy-D-glucose and [14 C]D-fructose uptake (1 μ Ci/ml) was determined over a 3 min. period as described, (section 2.15.3). Uptake values were corrected for any non-specific association of sugar with the cells by subtracting uptake values measured in the presence of 10 μ M cytochalasin B. Assays were performed in triplicate for all incubation conditions and data from representative experiments for GLUT3 and GLUT2 transfected cells are shown in Figures 7.7 and 7.8, respectively. The values measured for transport activity mediated by clone G3-1b were determined to be significantly increased above non-transfected CHO-cells, ($P < 0.05$), by application of a Students t-test.

Figure 7.4

Subcloning of the GLUT3 Series of Chimeras into pcDNA3.

The GLUT3/GLUT2 recombinant cDNAs were excised as 1.6kb *Sal* I fragments from pSP64T. Fragments were purified and ligated into the *Xho* I site of pcDNA3, thus placing the cDNAs under the transcriptional control of the CMV promoter for expression in mammalian cells.

Figure 7.4
Subcloning of the GLUT3 Series of Chimeras into pcDNA3.

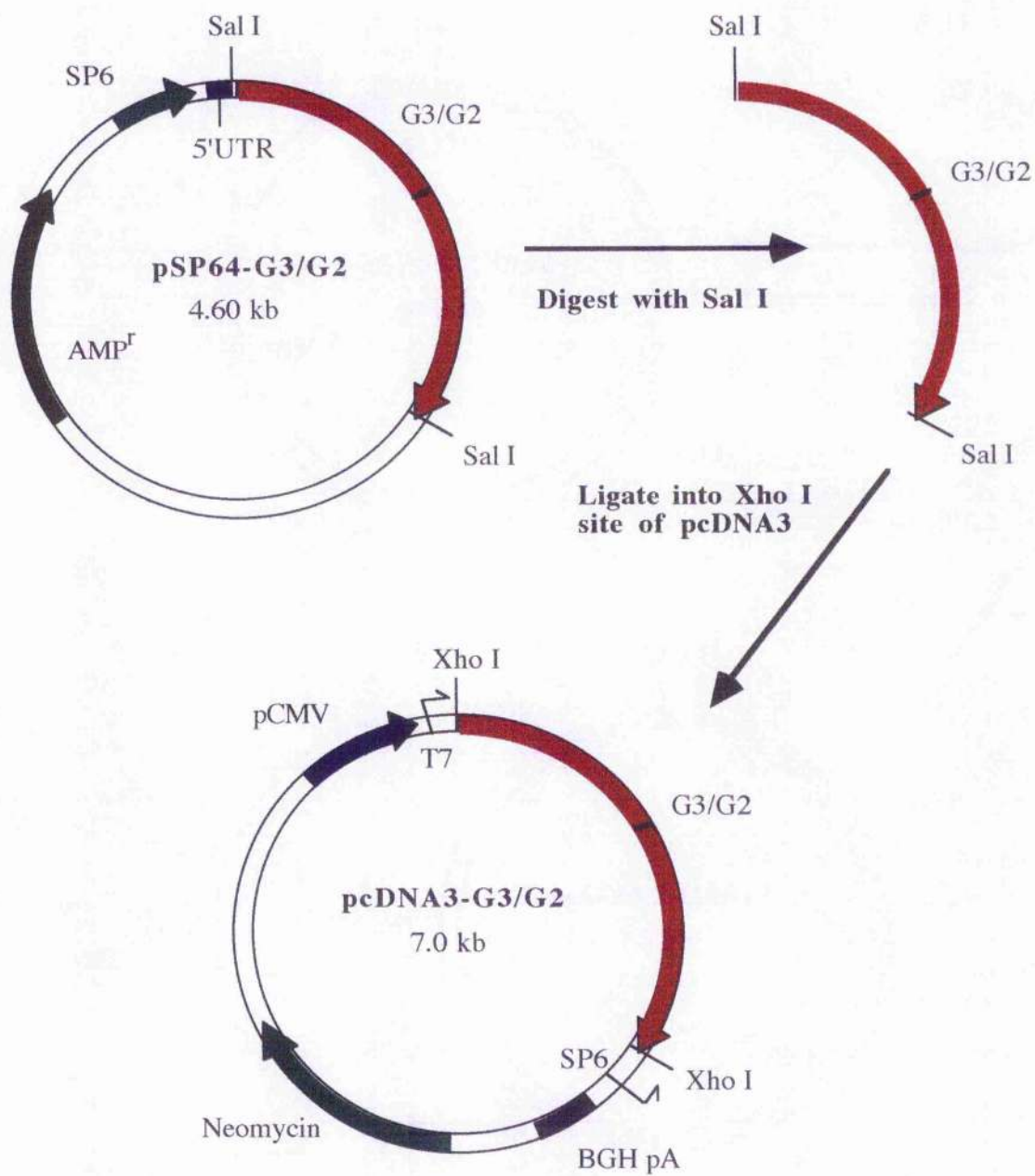


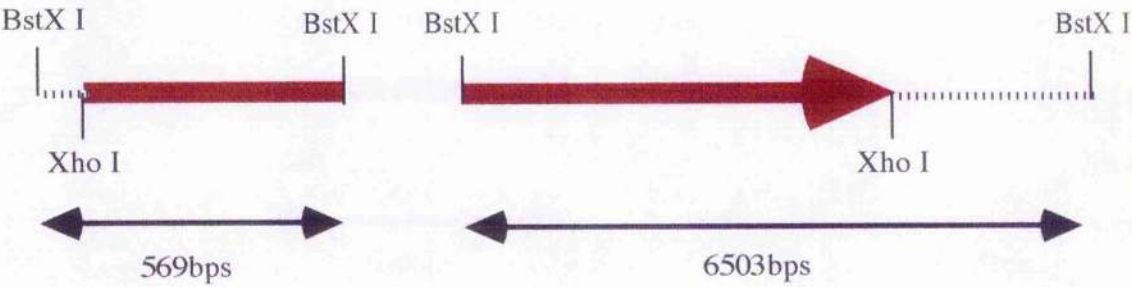
Figure 7.5

Restriction Digestion Analysis of pcDNA3-G3/G2 Constructs.

In order to detect the presence of the G3/G2 inserts, and to determine their orientation in the vector, plasmid DNA was prepared from a number of transformed *E.coli* cell colonies and subjected to restriction digestion analysis followed by 1% agarose gel electrophoresis. Restriction with *Bst*XI yields two fragments, the sizes of which depend on the orientation of the insert in the vector. Upon restriction of the vector containing the insert in the correct orientation, fragments of 569bps and 6503bps were generated. An insert cloned into the vector in the opposite direction yields fragments of 5949bps and 1123bps.

Figure 7.5
Restriction Digestion Analysis of pcDNA3-G3/G2 Constructs.

Correct Orientation



Incorrect Orientation

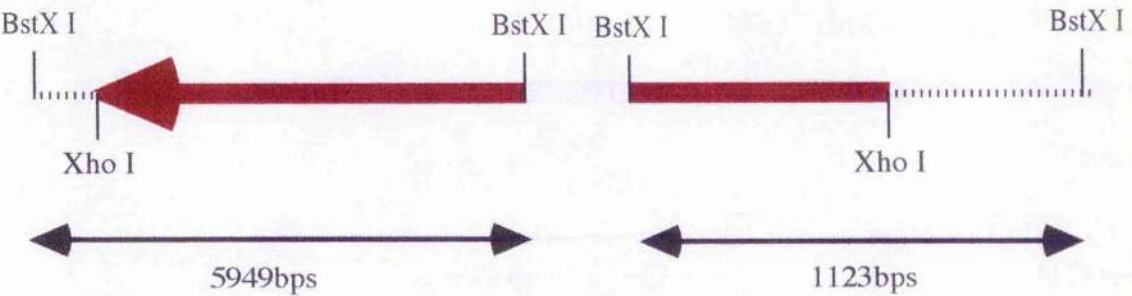


Figure 7.6

Immunological Detection of GLUT2 and G3(7St) in Lysates Prepared from CHO-Cells Individually Transfected with GLUT2 and G3(7St).

Cell lysates were prepared from a number of G418-resistant CHO-cell clones transfected with either GLUT2 or G3(7St). 60 μ l volumes of each sample (from a total of 1ml/6cm plate) were subjected to electrophoresis using 10% polyacrylamide gels and proteins were transferred to nitrocellulose membranes (section 2.17.2). The nitrocellulose membranes were then probed with anti-GLUT2 antibodies, and the blots were developed using the ECL detection system. Positions of the molecular weight markers in kilodaltons are indicated on the left hand side of the immunoblot.

Samples contain untransfected CHO-cell lysate (Lane 1), clone G2-3b (Lane 2), clone G2-2b (Lane 3), clone G2-8 (Lane 4), clone G2-10 (Lane 5), clone G3(7St)-6 (Lane 6), 25 μ g rat liver membranes (Lane 7).

Figure 7.6

Immunological Detection of GLUT2 and G3(7St) in Lysates Prepared from CHO-Cells Individually Transfected with GLUT2 and G3(7St).

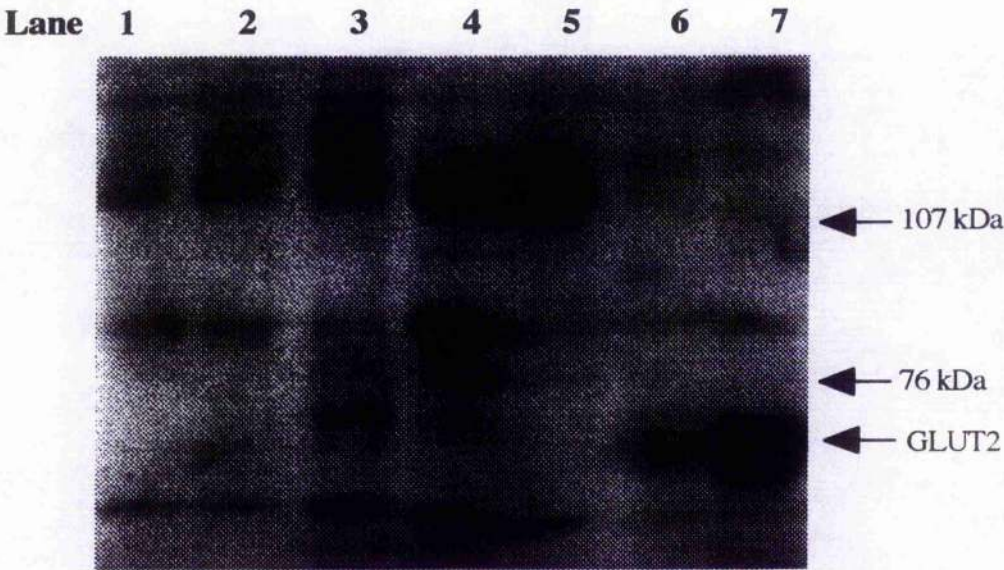


Figure 7.7

Measurement of 2-Deoxy-D-Glucose Transport in GLUT3-Transfected CHO-Cells.

[³H]2-Deoxy-D-glucose uptake was measured in non-transfected and GLUT3-transfected CHO-cells. Cells were grown on 6-well plates and glucose uptake was initiated by the addition of 0.1mM, 1 μ Ci/ml [³H]2-deoxy-D-glucose (final concentration). Uptake was measured over a period of 3 mins. Non-specific [³H]2-deoxy-D-glucose transport was corrected for by subtracting uptake measured in the presence of 10 μ M cytochalasin B. Results represent the mean (\pm S.D.) of two separate experiments, * indicates a significant difference from control values, (P<0.05).

Figure 7.7
Measurement of 2-Deoxy-D-Glucose Transport by GLUT3-Transfected CHO-Cells.

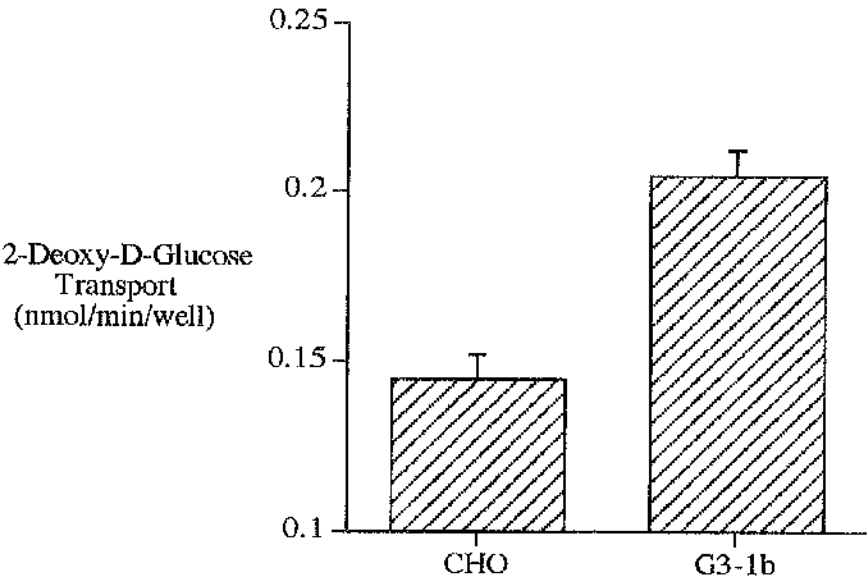


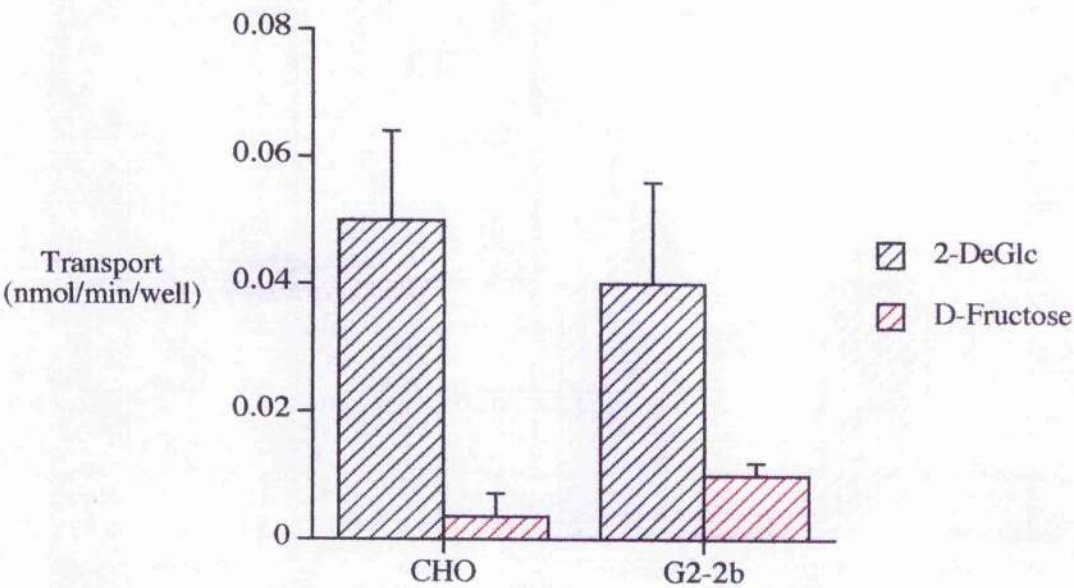
Figure 7.8

Measurement of 2-Deoxy-D-Glucose and D-Fructose Transport in GLUT2-Transfected CHO-Cells.

[³H]2-Deoxy-D-glucose and [¹⁴C]D-fructose uptake was measured in non-transfected and GLUT2-transfected CHO-cells. Cells were grown on 6-well plates and sugar uptake was initiated by the addition of 0.1mM sugar, (final concentrations) containing 1 μ Ci/ml . Uptake was measured over a period of 3 mins. Non-specific sugar transport was corrected for by subtracting uptake measured in the presence of 10 μ M cytochalasin B. Results represent the mean (\pm S.D.) of two separate experiments.

Figure 7.8

Measurement of 2-Deoxy-D-Glucose and D-Fructose Transport in GLUT2-Transfected CHO-Cells.



7.5 Discussion.

Although the *Xenopus* oocyte expression system has proved a valuable tool for the functional and kinetic characterisation of the GLUT3 Pro-Ala point mutations generated in this study, the GLUT3 series chimeras and a variety of other mutants constructed previously in this laboratory, several problems were encountered that impeded a more thorough investigation (section 4.6.5 and Chapter 5). Heterologous expression in the Chinese Hamster Ovary (CHO-) cell line was therefore considered as a possible alternative to the oocyte system, with the view that simple and reproducible fractionation protocols available for this cell line would facilitate a more accurate measurement of cell surface transporters and hence, determination of turnover numbers. In addition, the establishment of stable cell lines expressing a particular transporter, (either wild type or a mutant), would avoid the need for repeated oocyte injections which is both tedious and time consuming. In this regard, CHO-cells provide a more convenient system in which to perform photolabelling and other inhibition studies. However, CHO-cells, like many other cell types, express endogenous facilitative glucose transporters (GLUT1 in the case of CHO-cells), and therefore are not as suitable as the oocyte system for measurement of the various kinetic parameters already described (Chapter 4). Thus, use of the CHO-cell system also presents limitations but can be used to further complement and extend the data obtained in oocytes.

An attempt was therefore made to generate stable CHO-cell lines expressing either wild type GLUT2 or GLUT3. Expression of the wild type transporters is necessary to establish base-line parameters against which the mutants can be compared. Additionally, the GLUT3 series of chimeras were successfully subcloned into a suitable vector for expression in this system. Unfortunately, within the restricted time available to establish stable transfectants, none of the G418-resistant clones that were screened expressed the heterologous transporters at levels sufficient to undertake any functional or kinetic characterisations. There are several potential reasons for the low levels of expression observed in these cells. An alternative method of transfection, e.g., the lipid based DOTAP method, may increase the efficiency of DNA uptake by the cells, although the calcium phosphate method employed is routinely and successfully used for transfection of

fibroblastic cells including CHO-cells. Another consideration is the choice of promoter used to drive transcription of the cDNA of interest. GLUT2, in the pLK444 vector, is under the transcriptional control of the β -actin promoter. Although the β -actin gene is common to all cell types it has a relatively weak promoter. Thus, the use of a stronger promoter to drive transcription of the GLUT2 cDNA may elevate the level of expression attained. For example, the commercially available SV40, CMV and MTH promoters have all previously been successfully used for expression in CHO-cells. With regard to the GLUT3 construct, the cDNA is under the transcriptional control of the strong CMV promoter. However, a possible reason for the low levels of expression observed may be related to a low efficiency of uptake of this plasmid which does not possess the neomycin resistance gene for selection. It was therefore necessary to co-transfect this plasmid with one that does contain the selectable marker, on the basis that the cells that take up this plasmid are resistant to the selection agent and also are likely to carry the plasmid containing the cDNA of interest. Expression levels of the GLUT3 series chimeras were below the level of detection of the antibody used, but this may be because insufficient numbers of clones were screened due to time constraints.

Other, more general considerations include further optimisation of the transfection conditions used for this cell type. For example, the DNA to be transfected must be of high purity and free from protein, RNA and chemical contamination. The transfection procedure should be carried out at 22-25°C at a pH of 7.1. Furthermore, the cells should be healthy and in an exponential growth phase at the time of transfection. Also, the time of exposure to DMSO after DNA association and the concentration used may require careful optimisation for different cell types, since this reagent is toxic to cells.

This attempt to establish stably transfected CHO-cell lines expressing wild type and mutant glucose transporters has been unsuccessful. However, achievement of these objectives in future work will provide a useful system whereby a more comprehensive understanding of the kinetic behaviour and ligand binding properties of these transporters can be obtained.

CHAPTER 8

Discussion

Glucose occupies a central position in mammalian cellular homeostasis and metabolism. A prime example of this is the fact that the brain exhibits a requirement for glucose as its major energy source. Other mammalian cells are capable of utilising glucose as an immediate source of energy or, alternatively, can convert glucose into glycogen for storage in the liver and muscle, to be released when the body's demand for glucose is high. Cellular mechanisms have thus evolved to facilitate the sensing, uptake and release of this important metabolite which are essential for the maintenance of whole body glucose homeostasis. The tissue-specific expression of the mammalian facilitative glucose transporters is a key component of this system, and the structural and functional diversity exhibited by this family of proteins reflects the differing needs of tissues for glucose.

Transport of glucose into certain tissues is under both acute and chronic control by circulating hormones, insulin for example, is the primary effector of sugar transport in mammals. The mechanisms by which hormones are able to regulate the rate of glucose transport into cells, in addition to abnormal expression and/or dysfunctionality of the various isoforms may underlie certain diseased states. For example, peripheral insulin resistance may be caused by GLUT4 depletion or inactivation of this transporter in muscle and fat, leading to a condition known as non-insulin dependent diabetes mellitus (NIDDM). Expression of GLUT5 is also abnormal in insulin responsive tissues. In addition, due to its localisation to the insulin secreting pancreatic β -cells, GLUT2 is predicted to play an important role in the glucose sensing mechanism. Clearly then, the elucidation of the mechanisms by which these membrane proteins mediate glucose transport in non-diseased states will contribute to an understanding of transporter dysfunction in a variety of diseased states.

GLUT1 is the most extensively investigated isoform of this transporter family, due to its abundance in erythrocytes and the ability to reconstitute this protein in a purified and functional form. Kinetic, biochemical and biophysical studies have led to the construction of a topological model for GLUT1, and also to the characterisation of the transport mechanism. The protein is proposed to adopt a structure comprising twelve transmembrane helices which cluster together in such a way as to form an aqueous channel through which glucose can pass. Specific conformational changes in the protein structure are predicted to occur such

that a substrate binding site is alternately and sequentially exposed to the extracellular and cytoplasmic surfaces of the transporter, and these events can occur in the presence or absence of sugar. The sites at which glucose can associate and dissociate are structurally distinct and have been mapped to specific regions of the transporter on the basis of both kinetics and inhibitor selectivity. Thus, exposure of these binding sites represents distinct conformational states of the transporter. This model for the mechanism of transport is known as the single site alternating conformation model, and it is supported by the majority of the existing kinetic, biochemical and biophysical data.

In the absence of a high resolution crystal structure for GLUT1, the precise molecular mechanism of transporter function has not been elucidated. Thus, in the advent of recombinant molecular biology techniques and the availability of the transporter cDNAs, mutagenesis has provided the main strategy for probing the mechanism of action of these proteins. This approach has been successful in the identification of specific residues and stretches of sequence within the transporter that are involved in the substrate binding events or the conformational changes requisite for transport catalysis. Sequence alignments have revealed that the GLUT isoforms possess a number of highly conserved proline residues. Furthermore, the somewhat surprising selective inclusion of this classical helix breaker in the transmembrane regions, and the extension of this observation to the wider family of membrane transporters, predicts that these residues have specific functionality. Molecular dynamics and modelling studies predict that the highly conserved Pro-Gly rich sequence located within transmembrane helix 10 of the GLUT isoforms is important for facilitating the opening and closing of the external binding site. Further evidence in support of this hypothesis was provided by mutagenic studies in which the proline residues of this sequence were individually replaced with certain amino acids, resulting in a variety of phenotypic changes that affected both transport activity and ligand binding. This led to the suggestion of a putative mode of transporter operation in which conformational flexibility about the proline residues of helix 10 enables the alternate packing of helices 11 and 12 against the exofacial and endofacial substrate binding sites localised to helices 7, 8 and 9, and the base of helix 10 respectively. However, these predictions were based purely on simple measurement of transport rates, in the absence of any detailed kinetic measurements. Thus, a series of

GLUT3 mutant cDNAs were generated in which specific proline residues, located within helix 10 and in other highly conserved motifs present in the cytoplasmic loops, were individually replaced with alanine, with a view to determining the generality of the results obtained with GLUT1. Although individual mutation of the targeted proline residues had no significant effect on the K_m value for 2-deoxy-D-glucose uptake, the use of site-specific ligands to probe any effects mediated at the exofacial and endofacial substrate binding sites revealed some interesting phenotypic changes which were not previously detected in the GLUT1 studies. Furthermore, these effects not only apply to the specific proline residues identified in GLUT1, i.e. those of helices 6 and 10, but are extended to those that are located in highly conserved motifs which were not previously investigated. Mutation of the proline residues of helix 10 resulted in a significant perturbation of exofacial ligand binding, with an associated increase in affinity for endofacial ligands. In contrast, mutation of proline residues located in the highly conserved motifs at the base of helices 6 and 12 appeared to affect the ability of the transporter to correctly form the exofacial ligand binding site, with no associated effects detected at the endofacial site. No individual proline residue was found to be absolutely crucial for transport catalysis. It is however likely that they play a collective role in providing the local flexibility required for the conformational changes and the correct exposure of the exofacial substrate binding site. Obviously, conclusions drawn from such studies can only be confirmed by the generation of a high resolution crystal structure.

Measurement of the kinetic parameters for substrate transport under the conditions described are not dependent on the amount of transporter expressed at the plasma membrane. However, in addition to the K_m value, the transport cycle is also characterised by the V_{max} value which is related to the catalytic turnover of the protein. Since V_{max} is dependent on the concentration of functional transporters expressed at the cell surface, and the fact that this is variable between oocyte batches, the absence of a reliable method for isolating pure plasma membrane fractions from *Xenopus* oocytes has precluded a more complete kinetic characterisation of these mutants. There are a variety of alternative heterologous expression systems that are available for the study of protein structure and function. Generation of stably transfected cultured mammalian cells expressing the wild type transporter isoforms would provide a useful base-line for further investigation of the effects of mutations on

protein function. These systems are not completely ideal for measurement of the kinetic parameters that govern transport catalysis, due to higher levels of endogenous transport. However, the ease with which cell surface transporters can be quantitated and the reproducibility of the subcellular fractionation procedures makes them more convenient for use in photolabelling studies and the determination of transporter turnover numbers. In addition, use of such systems would avoid other extreme drawbacks such as seasonal variation of oocyte batches, which restricted the measurement of reliable data to a very limited time period within the year. This restriction was further compounded by animal housing problems, since *Xenopus laevis* are extremely sensitive to their environment which has a direct effect on the viability of the oocytes that are produced.

Although the isoforms exhibit similarities with regard to their general topology and mode of action, previous work in this lab has demonstrated that they differ not only in substrate selectivity, but, they also exhibit distinct kinetic profiles. Thus, subtle structural differences must exist which define isoform-specific behaviour. GLUT2, for example, is unique among the GLUT family by virtue of its ability to transport D-fructose in addition to D-glucose. In contrast, GLUT3 is capable of high affinity D-glucose and D-galactose transport, but can not mediate D-fructose transport. Thus, in an effort to address the structural basis for substrate recognition and glucose binding to these isoforms, a range of chimeric glucose transporters were generated in which regions of GLUT3 were replaced with the corresponding regions of GLUT2 and vice versa. Characterisation of the GLUT3 series of chimeras, comprising N-terminal GLUT3 sequence and various C-terminal portions of the GLUT2 isoform, was previously successful in oocytes. This study revealed that the structural information which allows GLUT2 to transport fructose is localised to helix 7. Furthermore, this region is an important requirement for high affinity transport of glucose and galactose mediated by GLUT3. Other regions that influence the kinetics of fructose transport by GLUT2 are not clear from the existing data, due to the inability of certain chimeras containing N-terminal GLUT2 sequence to elevate the transport capacity of oocytes sufficiently to undertake any functional or kinetic analyses. Reconstruction of these chimeric cDNAs in this study failed to rectify the problems associated with attaining their functional expression, and the potential reasons for this were not pursued due to time constraints.

However, on the basis that helix 7 is essential for fructose recognition, the generation of new GLUT2 and GLUT3 mutants is currently underway in this laboratory in which the QLS motif located within helix 7 (of GLUTs 1, 3 and 4) has been replaced with the HVA motif of the GLUT2 helix 7. Initial analysis of these mutants suggest that the QLS motif is the sole determinant for the ability of GLUT2 to accept fructose and for high affinity 2-deoxy-D-glucose transport mediated by GLUT3. Further progression of this study will involve the use of sugar analogues to study the interaction of individual sugar hydroxyls with the existing chimeric transporters and the generation of other GLUT2 and GLUT3 mutants in which individual helices are sequentially swapped throughout the transporter structure.

Dissection of the molecular mechanism of glucose transport mediated by the GLUT isoforms is still in its infancy. However, the future application of molecular biology techniques coupled to the use of appropriate heterologous expression systems will no doubt contribute to a more comprehensive insight into the function of this important class of membrane proteins.

References

- Allard, W. J., & Lienhard, G. E. (1985) *J.Biol.Chem.* **260**, 8668-8675.
- Alvarez, J., Lee, D. C., Baldwin, S. A. and Chapman, D. (1987) *J. Biol. Chem.* **261**, 7101-7104.
- Appleman, J. E., & Lienhard, G. E. (1989) *Biochemistry* **28**, 8221-8227.
- Arbuckle, M. I., Kane, S., Porter, L. M., Seatter, M. J., & Gould, G. W. (1996) *Biochemistry* **35**, 16519-16527.
- Asano, A., Katagiri, H., Takata, K., Lin, J.-L., Ishihara, H., Inukai, K., Tsukuda, K., Kikuchi, M., Hirano, H., Yazaki, Y., & Oka, Y. (1991) *J. Biol. Chem.* **266**, 24632-24636.
- Asano, T., Shibasaki, Y., Kasuga, M., Kanazawa, Y., Takaku, F., Akanuma, Y., & Oka, Y. (1988) *Biochem. Biophys. Res. Comm.* **154**, 1204-1211.
- Axelrod, J. D., & Pilch, P. F. (1983) *Biochemistry* **22**, 2222-2227.
- Baker, G. F., & Widdas, W. F. (1973) *J. Physiology* **231**, 143-165.
- Baldwin, J. M., Gorga, J. C., & Lienhard, G. E. (1981) *J.Biol.Chem.* **256**, 3685-3689.
- Baldwin, S. A. (1993) *Biochim. Biophys. Acta.* **1154**, 17-49.
- Baldwin, S. A., Baldwin, J. M., Gorga, F. R., & Lienhard, G. E. (1979) *Biochim. Biophys. Acta* **552**, 183-188.
- Baldwin, S. A., Baldwin, J. M., & Lienhard, G. E. (1982) *Biochemistry* **21**, 3836-3842.
- Baldwin, S. A., & Henderson, P. J. F. (1989) *Annu. Rev. Physiol.* **51**, 459-471.
- Baldwin, S. A., & Lienhard, G. E. (1989) *Methods Enzymol.* **174**, 39-50.
- Barnett, J. E. G., Holman, G. D., Chalkley, R. A., & Munday, K. A. (1975) *Biochem. J.* **145**, 417-429.
- Barnett, J. E. G., Holman, G. D., & Munday, K. A. (1973) *Biochem.J.* **131**, 211-221.

- Basketter, D. A., & Widdas, W. F. (1978) *J. Physiol.* **278**, 389-401.
- Bell, G., Kayano, T., Buse, J., Burant, C., Takeda, J., Lin, D., Fukumoto, H., & Seino, S. (1990) *Diabetes Care.* **13**, 198-206.
- Birnbaum, M. J. (1989) *Cell* **57**, 305-315.
- Birnbaum, M. J., Haspel, H. C., & Rosen, O. M. (1986) *Proc. Natl. Acad. Sci. USA* **83**, 5784-5788.
- Bloch, R. (1973) *Biochemistry* **12**, 4799-4801.
- Braiman, M., & Mathies, R. (1980) *Biochemistry* **11**, 5421-5428.
- Braiman, M. S., Mogi, T., Marti, T., Stern, L. J., Khorana, M. G., & Rothschild, K. J. (1988) *Biochemistry* **27**, 8516-8520.
- Braiman, M. S., & Rothschild, K. J. (1988) *Annu. Rev. Biophys. Chem.* **17**, 541-570.
- Brandl, C. Y., and Deber, C.M. (1986) *Proc. Natl. Acad. Sci. U.S.A.* **83**, 917-921.
- Brant, A. M., Jess, T. J., Milligan, G., Brown, C. M., & Gould, G. W. (1993) *Biochem. Biophys. Res. Comm.* **192**, 1297-1302.
- Buchs, A., Lu, L., Morita, H., Whitesell, R. R., & Powers, A. C. (1995a) *Endocrinology* **136**, 4224-4230.
- Burant, C. F., & Bell, G. I. (1992) *Biochemistry* **31**, 10414-10420.
- Burant, C. F., & Bell, G. I. (1992b) *Biochemistry* **31**, 10412-10420.
- Burant, C. F., Takeda, J., Brot-Laroche, E., Bell, G. I., & Davidson, N. O. (1992) *J. Biol. Chem.* **267**, 14523-14526.
- Cairns, M. T., Alvarez, J., Panico, M., Gibbs, A. F., Morris, H. R., Chapman, D., & Baldwin, S. A. (1987) *Biochim. Biophys. Acta.* **905**, 295-310.
- Cairns, M. T., Elliot, D. A., Scudder, P. R., & Baldwin, S. A. (1984) *Biochem. J.* **221**, 179-188.

- Carruthers, A. (1986) *J. Biol. Chem.* **261**, 11028-11037.
- Carruthers, A. (1991) *Biochemistry* **30**, 3898-3906.
- Carruthers, A., & Helgerson, A. L. (1991) *Biochemistry* **30**, 3907-3915.
- Charron, M. J., Brosius III, F. C., Alper, S. L., & Lodish, H. F. (1989) *Proc. Natl. Acad. Sci. USA* **86**, 2535-2539.
- Chin, J. J., Jhun, B. H., & Jung, C. Y. (1992) *Biochemistry* **31**, 1945-1951.
- Chin, J. J., Jung, E. K. Y., Chen, V., & Jung, C. Y. (1987) *Proc. Natl. Acad. Sci. U.S.A.* **84**, 4113-4116.
- Chin, J. J., Jung, E. K. Y., & Jung, C. Y. (1986) *J. Biol. Chem.* **261**, 7101-7104.
- Ciaraldi, T. P., Horuk, R., & Matthaei, S. (1986) *Biochem. J.* **240**, 115-123.
- Clark, A. E., & Holman, G. D. (1990) *Biochem. J.* **269**, 615-622.
- Colville, C. A., Seatter, M. J., & Gould, G. W. (1993a) *Biochem. J.* **194**, 753-760.
- Colville, C. A., Seatter, M. J., Jess, T. J., Gould, G. W., & Thomas, H. M. (1993b) *Biochem. J.* **290**, 701-706.
- Connolly, T. J., Carruthers, A., & Melchoir, D. L. (1985) *J. Biol. Chem.* **260**, 2617-2620.
- Consler, T. G., Tsolas, O., & Kaback, H. R. (1991) *Biochemistry* **30**, 1291-1298.
- Cope, D. L., Holman, G. D., Baldwin, S. A., & Wolstenholme, A. J. (1994) *Biochem. J.* **300**, 291-294.
- Corpe, C. P., Baseleh, M. M., Affleck, J., Gould, G. W., Jess, T. J., & Kellet, G. L. (1996) *Eur. J. Physiol.* **432**, 192-201.
- Craik, J. D., & Elliott, K. R. F. (1979) *Biochem. J.* **182**, 503-508.
- Cushman, S. W., & Wardzala, L. J. (1980) *J. Biol. Chem.* **255**, 4758-4762.

- Dauterive, R., Laroux, S., Bunn, S. C., Chaisson, A., Sanson, T., & Reed, B. C. (1996) *J. Biol. Chem.* **271**, 11414-11421.
- Davidson, N. O., Hausman, A. M. L., Ifkovits, C. A., Buse, J. B., Gould, G. W., Burant, C. F., & Bell, G. I. (1992) *Am. J. Physiol.* **262**, C795-C800.
- Davies, A., Meeran, K., Cairns, M. T., & Baldwin, S. A. (1987) *J. Biol. Chem.* **262**, 9347-9352.
- Davies, A. F., Davies, A., Preston, R. A. J., Clark, A. E., Holman, G. D., & Baldwin, S. A. (1991) *Molecular Basis of Biological membrane Function, SERC, U.K.*
- Deber, C. M., Glibowicka, M., & Wooley, G. A. (1990) *Biopolymers* **29**, 149-157.
- Diamond, D. L., & Carruthers, A. (1993) *J. Biol. Chem.* **268**, 6437-6444.
- Dohm, G. L., Tapscott, E. B., Pories, W. J., Flickinger, E. G., Meelheim, D., Fushiki, T., Atkinson, S. M., Elton, C. W., & Caro, J. F. (1988) *J. Clin. Invest.* **82**, 486-494.
- Due, A. D., Cook, J. A., & Fletcher, S. J. (1995a) *Biochem. Biophys. Res. Comm.* **208**, 590-596.
- Due, A. D., ZhiChao, Q., Thomas, J. M., Buchs, A., Powers, A. C., & May, J. M. (1995) *Biochemistry* **34**, 5462-5471.
- Dunker, A. K. (1982) *J. Theor. Biol.* **97**, 95-127.
- Edwards, P. A. W. (1973) *Biochem. Biophys. Acta.* **307**, 415-418.
- Elliott, K. R. F., & Craik, J. D. (1983) *Biochem. Soc. Trans.* **10**, 12-13.
- Flier, J. S., Mueckler, M., McCall, A. L., & Lodish, H. F. (1987a) *J. Clin. Invest.* **79**, 657-661.
- Flier, J. S., Mueckler, M. M., Usher, P., & Lodish, H. F. (1987b) *Science* **235**, 1492-1495.
- Foster, D. L., Boublik, M., & Kaback, H. R. (1983) *J. Biol. Chem.* **258**, 31.

Fukumoto, H., Kayano, T., Buse, J. B., Edwards, Y., Pilch, P. F., Bell, G. I., & Seino, S. (1989) *J. Biol. Chem.* **264**, 7776-7779.

Fukumoto, H., Seino, S., Imura, H., Seino, Y., Eddy, R. L., Fukushima, Y., Byers, M. G., Shows, T. B., & G.I., B. (1988) *Proc. Natl. Acad. Sci. USA* **85**, 5434-5438.

Ganter, U. M., Schmid, E. D., Perez-Sala, D., Rando, R. R., & Siebert, F. (1989) *Biochemistry* **28**, 5954-5962.

Garcia, J. C., Strube, M., Leingang, K., Keller, K., & Mueckler, M. M. (1992) *J. Biol. Chem.* **267**, 7770-7776.

Geering, K., Thiculaz, F., Verrey, M. R., Hauptle, M. T., & Rossier, B. C. (1989) *Am. J. Physiol.* **257**, C851-C858.

Gerdes, R. G., & Rosenberg, H. (1974) *Biochim. Biophys. Acta.* **351**, 77-86.

Gerwert, K., Hess, B., & Engelhard, M. (1990) *FEBS* **261**, 449-454.

Gibbs, A. F., Chapman, D., & Baldwin, S. A. (1988) *Biochem. J.* **256**, 421-427.

Gorga, F. R., & Lienhard, G. E. (1982) *Biochemistry* **21**, 1905-1908.

Gould, G. W., & Holman, G. D. (1993) *Biochem. J.* **295**, 329-341.

Gould, G. W., & Lienhard, G. E. (1989) *Biochemistry* **28**, 9447-9452.

Gould, G. W., Thomas, H. M., Jess, T. J., & Bell, G. I. (1991) *Biochemistry* **30**, 5139-5145.

Gurdon, J. B., Lane, C. D., Woodland, H. R., & Marbaix, G. (1971) *Nature* **233**, 177-182.

Hashiramoto, M., Kadowaki, T., Clark, A. E., Muraoka, A., Momomura, K., Sakura, H., Tobe, K., Akanuma, Y., Yazaki, Y., Holman, G. D., & Kasuga, M. (1992) *J. Biol. Chem.* **267**, 17502-17507.

Haspel, H. C., Rosenfeld, M. G., & Rosen, O. M. (1988) *J. Biol. Chem.* **263**, 398-403.

Hediger, M. A., Coady, M. J., Ikeda, T. S., & Wright, E. M. (1987) *Nature* **330**, 379-381.

Helgerson, A. L., & Carruthers, A. (1987) *J. Biol. Chem.* **262**, 5464-5475.

Hellwig, B., & Brown, F. M. (1992) *Biochem. Biophys. Acta.* **1111**, 178-184.

Henderson, P. J. F., Baldwin, S. A., Cairns, M. T., Charalambous, B. M., Dent, H. C., Liang, W. J., Lucas, V. A., Martin, G. E., McDonald, T. P., McKeown, B. J., Muir, J. A. R., Petro, K. R., Roberts, P. E., Shatwell, K. P., Smith, G., & Tate, C. G. (1992) *Int. Rev. Cytol.* **137**, 149-208.

Herbert, D. N., & Carruthers, A. (1991) *Curr. Opin. Cell biol.* **3**, 702-709.

Herbert, D. N., & Carruthers, A. (1992) *J. Biol. Chem.* **267**, 23829-23838.

Hirshman, M. F., Goodyear, L. J., Wardzala, L. J., Horton, E. D., & Horton, E. S. (1990) *J. Biol. Chem.* **265**, 987-991.

Hodgson, P. A., Osguthorpe, D. J., & Holman, G. D. (1992) *11th Annual Molecular Graphics Meeting, Abstract.*

Holman, G. D., & Karim, B. (1988) *Biochem. Biophys. Acta.* **946**, 75-84.

Holman, G. D., Kozka, I. J., Clark, A. E., Flower, A. F., Saltis, J., Habberfield, A. D., Simpson, I. A., & Cushman, S. W. (1990) *J. Biol. Chem.* **265**, 18172-18179.

Holman, G. D., Parker, B. A., & Midgley, P. J. W. (1986) *Biochem. Biophys. Acta.* **855**, 115-126.

Holman, G. D., & Rees, W. D. (1987) *Biochim. Biophys. Acta.* **897**, 395-405.

Inukai, K., Katagiri, H., Takata, K., Asano, T., Anai, M., Ishihara, H., Nakazaki, M., Kikuchi, M., Yazaki, Y., & Oka, Y. (1995) *Endocrinology* **136**, 4850-4857.

Ishihara, H., Asano, T., Katagiri, H., Lin, J. L., Tsukuda, K., Shibasaki, Y., & Oka, Y. (1991) *Biochem. Biophys. Res. Commun.* **176**, 922-930.

Iyer, L. K., & Vishveshwara, S. (1995) *FEBS Letters* **374**, 21-24.

Jacquez, J. A. (1984) *Am.J.Physiol.* **246**, R289-298.

- James, D. E., Brown, R., Navarro, J., & Pilch, P. F. (1988) *Nature* **333**, 183-185.
- James, D. E., Strube, M., & Mueckler, M. (1989) *Nature* **338**, 83-87.
- Jones, D. T., Taylor, W., & Thornton, J. M. (1994) *FEBS Letters* **339**, 269-275.
- Jordan, N. J., & Holman, G. D. (1992) *Biochem. J.* **286**, 649-656.
- Jung, C. Y. (1971) *J. Membr. Biol.* **5**, 200-214.
- Jung, E. K. Y., Chin, J. J., & Jung, C. Y. (1986) *J. Biol. Chem.* **261**, 9155-9160.
- Kaback, H. R. (1983) *J. Membr. Biol.* **76**, 95.
- Kaestner, K. H., Christy, R. J., McLenithan, J. C., Braiterman, L. T., Cornelius, P., Pekla, P. H., & Lane, M. D. (1989) *Proc. Natl. Acad. Sci. USA* **86**, 3150-3154.
- Kahlenberg, A., & Dolansky, D. (1972) *Canadian Journal of Biochemistry* **50**, 638-643.
- Karim, A. R., Rees, W. D., & Holman, G. D. (1987) *Biochem. Biophys. Acta* **902**, 402-405.
- Kasahara, M., & Hinkle, P. C. (1977) *J. Biol. Chem.* **252**, 7384-7390.
- Katagiri, H., Asano, T., Ishihara, H., Tsukuda, K., Lin, J.-L., Inukai, K., Kikuchi, M., Yazaki, Y., & Oka, Y. (1992) *J. Biol. Chem.* **267**, 22550-22555.
- Katagiri, H., Asano, T., & Ishihara, H. e. a. (1993) *Biochem. J.* **291**, 861-867.
- Katagiri, H., Asano, T., Shibasaki, Y., Lin, J.-L., Tsukuda, K., Ishihara, H., Akanuma, Y., Takaku, F., & Oka, Y. (1991) *J. Biol. Chem.* **266**, 7769-7773.
- Kayano, T., Barrant, C. F., Fukumoto, H., Gould, G. W., Fan, Y.-S., Eddy, R. L., Byers, M. G., Shows, T. B., Seino, S., & Bell, G. I. (1990) *J. Biol. Chem.* **265**, 13276-13282.
- Kayano, T., Fukumoto, H., Eddy, R. L., Fan, Y.-S., Byers, M. G., Shows, T. B., & Bell, G. I. (1988) *J. Biol. Chem.* **263**, 15245-15248.

- Keller, K., Strube, M., & Mueckler, M. (1989) *J. Biol. Chem.* **264**, 18884-18889.
- King, A. P. J., Tai, P.-K. K., & Carter-Su, C. (1991) *Biochemistry* **30**, 11546-11553.
- Klip, A., Ramlal, T., Young, D. A., & Holloszy, J. O. (1987) *FEBS letts.* **224**, 224-230.
- Krieg, P. A., & Melton, D. A. (1984) *Nucleic Acid Research* **12**, 7057-7070.
- Krupka, R. M. (1971) *Biochemistry* **10**, 1143-1153.
- Krupka, R. M., & Deves, R. (1986) *Biochem. Cell. Biol.* **64**, 1099-1107.
- Lachaal, M., Rampal, A. L., Lee, W., Shi, Y.-W., & Jung, C. Y. (1996) *J. Biol. Chem.* **271**, 5225-5230.
- LeFevre, P. G. (1961) *Pharmacol. Rev* **13**, 39-70.
- Li, J., & Tooth, P. (1987) *Biochemistry* **26**, 4816-4823.
- Lin, J.-L., Asano, T., Katagiri, H., Tsukuda, K., Ishihara, H., Inukai, K., Yazaki, Y., & Oka, Y. (1992) *Biochem. Biophys. Res. Commun.* **184**, 865-870.
- Lowe, A. G., & Walmsley, A. R. (1986) *Biochim. Biophys. Acta.* **857**, 146-154.
- Lowe, A. G., & Walmsley, A. R. (1987) *Biochim Biophys. Acta.* **903**, 547-550.
- Maher, F., Vannucci, S. J., Takeda, J., & Simpson, I. A. (1992) *Biochem. Biophys. Res. Comm.* **182**, 703-711.
- Maiden, M. C. J., Davis, E. O., Baldwin, S. A., Moore, D. C. M., & Henderson, P. J. F. (1987) *Nature* **325**, 641-643.
- May, J. M. (1988) *J. Biol. Chem.* **263**, 13635-13640.
- May, J. M. (1989) *J. Biol. Chem.* **263**, 875-881.
- May, J. M., Buchs, A., & Carter-Su, C. (1990) *Biochemistry* **29**, 10393-10398.
- May, J. M., & Mikulecky, D. C. (1982) *J. Biol. Chem.* **257**, 11601-11608.

- Miyazaki, J., Araki, K., Yamato, E., Ikegami, H., Asano, T., Shibasaki, Y., Oka, Y., & Yamamura, K. (1990) *Endocrinology* **127**, 126-132.
- Mori, H., Hashiramoto, M., Clark, A. E., Yang, J., Muraoka, A., Tamori, Y., Kasuga, M., & Holman, G. D. (1994) *J. Biol. Chem.* **269**, 11578-11583.
- Morris, D. I., Robbins, J. D., & Ruoho, A. E. (1991) *J. Biol. Chem.* **266**, 13377-13384.
- Mueckler, M., Caruso, C., Badlwin, S.A., Panico, M., Blench, I., Morris, H.R., Allard, W.J., Leinhardt, G.E., Lodish, H.F. (1985) *Science* **229**, 941-945.
- Mueckler, M., Weng, W., Kruse, M. (1994a) *J.Biol.Chem.* **269**, 10533-10538.
- Mueckler, M., Kruse, M., Strube, M., Riggs, A.C., Chiu, K.C., Permutt, M.A. (1994b) *J.Biol.Chem.* **269**, 17765-17767.
- Muraoka, A., Hashiramoto, M., Clark, A.E., Edwards, L.C., Sakura, H., Kadowaki, T., Holman, G.D., Kasuga, M. (1995) *Biochem. J.* **311**, 699-704.
- Nagamatsu, S., Kornhauser, J.M., Burant, C.F., Seino, S. Mayo, K.E., Bell, G.I. (1992) *J. Biol. Chem.* **267**, 467-472.
- Nishimura, H., Pallardo, F.V., Seidner, G.A., Vannucci, S., Simpson, I.A., Birnbaum, M.J. (1993) *J. Biol. Chem.* **268**, 8514-8520.
- Oka, Y., Asano, T., Shibasaki, Y., Lin, J-L., Tsukuda, K., Katagiri, H., Akanuma, Y., Takaku, F. (1990) *Nature* **345**, 550-553.
- Orci, L., Thorens, B., Ravazzola, M., Lodish, H.F. (1989) *Science* **245**, 295-297.
- Pawagi, A. B., & Deber, C. M. (1987) *Biochem Biophys. Res. Commun.* **145**, 1087-1091.
- Pawagi, A. B., & Deber, C. M. (1990) *Biochemistry* **29**, 950-955.
- Pederson, O., & Gliemann, J. (1981) *Diabetologia* **20**, 630-635.

- Pessino, A., Hebert, D. N., Woon, C. W., Harrison, S. A., Clancy, B. M., Buxton, J. M., Carruthers, A., & Czech, M. P. (1991) *J. Biol. Chem.* **266**, 20213-20217.
- Piper, R. C., Tai, C., Kulesza, P., Pang, S., Warnock, D., Baenziger, J., Slow, J.W., Geuze, H.J., Puri, C., James, D.E. (1993) *J.Cell.Biol.* **121**, 1221-1232.
- Ploug, T., Galbo, H., Vinten, J., Jorgensen, M. & Richter, E.A. (1987) *Am. J. Physiol. (Endocrinol. Metab.)* **253** (16), E12-E20.
- Rothschild, K. J., He, Y. N., Gray, D., Roepe, P. D., Peltien, S. L., Brown, R. S., & Herzfeld, J. (1990) *Proc. Natl. Acad. Sci.* **29**, 5954-5960.
- Santalucia, S., Camps, M., Castello, A., Munoz, P., Nucl, A., Testar, X., Palacin, M., & Zorzano, A. (1992) *Endocrinology* **130**, 837-846.
- Saravolac, E. G., & Holman, G. D. (1997) in *Facilitative glucose transporters* (Gould, G. W., Ed.) pp 39-61, R.G.Landes and Co., Georgetown, Texas.
- Schultz, G. E., & Schirmer, P. H. (1979) *Principles of Protein Structure*, Springer-Verlag, New York.
- Sergeant, S., & Kim, H. D. (1985) *J. Biol. Chem.* **260**, 14677-14682.
- Shanahan, M. F., Morris, D. P., & Edwards, B. M. (1987) *J. Biol. Chem.* **262**, 5978-5984.
- Shepherd, P. R., Gould, G.W., Colville, C.A., McCoid, S.C., Gibbs, E.M., Kahn, B.B. (1992a) *Biochem. Biophys. Res. Comm.* **188**, 149-154.
- Shepherd, P. R., Gibbs, E.M., Waslau, C., Gould, G.W., Kahn, B.B. (1992b) *Diabetes* **41**, 1360-1365.
- Shieh, B.-H., Stammes, M. A., Seavello, S., Harris, G. L., & Zuker, C. S. (1990) *Nature* **338**, 67-70.
- Shurman, A., Keller, K. I. M., & Monden, e. a. (1993) *Biochem. J.* **290**, 497-501.
- Simpson, I. A., & Cushman, S. W. (1986) *Annu. Rev. Biochem.* **55**, 1059-1089.

- Slepek, V. Z., Quick, M. W., Davidson, N., Lester, H. A., & Simon, M. I. (1993) *J. Biol. Chem.* **168**, 21889-21894.
- Stoeckenius, W., & Bogomolni, R. (1982) *Annu. Rev. Biochem.* **52**, 589-616.
- Suzuki, K., & Kono, T. (1980) *Proc. Natl. Acad. Sci. (USA)* **77**, 2542-2545.
- Tamori, Y., Hashiramoto, M., Clark, A. E., Morei, H., Muraoka, A., Kadowaki, T., Holman, G. D., & Kasuga, M. (1994) *J. Biol. Chem.* **269**, 2982-2986.
- Taylor, L. P., & Holman, G. D. (1981) *Biochem. Biophys. Acta.* **642**, 325-335.
- Thorens, B., Sarkar, H.K., Kaback, H.R., Lodish, H.F. (1988) *Cell* **55**, 281-290.
- Tuzi, S., Naito, A., & Saito, H. (1994) *Biochemistry* **33**, 15046-15052.
- von Heijne, G. (1991) *J. Mol. Biol.* **218**, 499-503.
- Waddell, I. D., Zomerschoe, A.G., Voice, M.W. & Burchell, A. (1992) *Biochem. J.* **286**, 173-177.
- Waddell, I. D., Scott, H., Grant, A., & Burchell, A. (1991) *Biochem. J* **275**, 363-369.
- Wadzinski, B. E., Shanahan, M. F., & A.E.Ruoho(1987) *J. Biol. Chem.* **262**, 17683-17689.
- Wadzinski, B. E., Shanahan, M. F., & Clark, R. B., . (1988) *Biochem. J.* **255**, 983-990.
- Wadzinski, B. E., Shanahan, M. F., Seamon, K. B., & Ruoho, A. E. (1990) *Biochem. J.* **272**, 151-158.
- Wall, D. A., & Patel, S. (1989) *J. memb. Biol.* **107**, 189-201.
- Walmsley, A. R., Lowe, A.G. (1987) *Biochim. Biophys. Acta.* **901**, 229-238.
- Wandel, S., Schurmann, A., Becker, W., Summers, S. A., Shanahan, M. F., & Joost, H. G. (1994) *FEBS Letters* **348**, 114-118.
- Wang, J.-F., Falke, J.J., Chan, S.I. (1986) *Proc. Natl. Acad. Sci. (USA)* **83**, 3277-3281.

- Webb, D. C., Rosenberg, H., & Cox, G. B. (1992) *J. Biol. Chem.* **267**, 24661-24668.
- Weiler-Guttler, H., Zinke, H., Mockel, B., Frey, A., & Gassen, H. G. (1989) *Biol.Chem.Hoppe-Seyler* **370**, 467-473.
- Wellner, M., Monden, I., Keller, K. (1994) *Biochem. J.* **299**, 813-817.
- Wellner, M., Monden, I., & Keller, K. (1992) *FEBS Lett.* **309**, 293-296.
- Wellner, M. M., Mueckler, MM;Keller, K. (1995) *European Journal of Biochemistry* **227**, 454-458.
- Wheeler, T. J., Hinkle, P.C. (1981) *J. Biol. Chem.* **256**, 8907-8914.
- Whitesell, R. R., & Gliemann, J. (1979) *J. Biol. Chem.* **254**, 5276-5283.
- Widdas, W. F. (1952) *J. Physiology* **118**, 23-39.
- Widdas, W. F. (1955) *J.Physiol. (lon)*. **127**, 318-327.
- Williams, S. A., & Birnbaum, M. J. (1988) *J. Biol. Chem.* **263**, 19513-19518.
- Yano, H., Seino, Y., Inagaki, N., Hinokio, Y., Yamamoto, T., Yasuda, K., Masuda, K., Someya, Y. & Imura, H. (1991) *Biochem. Biophys. Res. Commun.* **174**, 470-477.
- Zeng, H., Parthasarathy, P., Rampal, A. L., & Jung, C. Y. (1996) *Biophys. J.* **70**, 14-21.
- Zoccoli, M. A., Baldwin, S. A., & Lienhard, G. E. (1978) *J. Biol. Chem.* **253**, 6923-6930.
- Zottola, R. J., Cloherty, E. K., Coderre, P. E., Hansen, A., Hebert, D. N., & Carruthers, A. (1995) *Biochemistry* **34**, 9734-9747.